

**An Investigation of Inorganic Background
Soil Constituents with a Focus on Arsenic
Species**

**A Thesis submitted for the degree of
Doctor of Philosophy**

By

Costa J. Diomides

Victoria University

School of Molecular Sciences

September 2005

Preface

I, Costa Jeremy Diomides, declare that the PhD thesis entitled “An Investigation of Inorganic Background Soil Constituents with a Focus on Arsenic Species” is no more than 100,000 words in length, exclusive of tables, figures, appendices, references and footnotes. This thesis contains no material that has been submitted previously, in whole or in part, for the award of any other academic degree or diploma. Except where otherwise indicated, this thesis is my own work.

Signature

Date

Conference Presentations Relevant to the Scope of this Thesis

- (1) Diomides, C., Correll, R. and Naidu, R. Assessment of aberrant levels, Fifth National Workshop on the Assessment of Site Contamination, Environment Protection & Heritage Council (EPHC) & National Environment Protection Council (NEPC), Adelaide, South Australia, 13 – 15 May 2002.
- (2) Diomides, C., Bigger, S. W. and Orbell, J. D. Speciation and bioavailability of naturally elevated soil constituents (esp. arsenic), Victorian Arsenic Forum, Environment Protection Authority – Victoria (EPAV), Melbourne, Victoria, 27 November, 2002.

Publications Relevant to the Scope of this Thesis

- (1) Diomides, C., Correll, R. and Naidu, R. Assessment of aberrant levels, Proceedings of the Fifth National Workshop on the Assessment of Site Contamination, Environment Protection & Heritage Council (EPHC) & National Environment Protection Council (NEPC), Adelaide, South Australia, pp 225-233.

Abstract

A database was developed for the storage and convenient analysis of inorganic background soil constituent data within specific geological groups in Victoria, Australia. A statistical analysis of the data revealed the relative abundances of metals and, in particular, arsenic within soils of various geological units. These units included the Quaternary Aeolian (Qpw) (highest concentration of zinc, lowest concentration of chromium) the Quaternary Fluvial (Qrc) (highest chromium and nickel, equal highest copper, lowest lead and equal lowest arsenic); the Quaternary Newer Volcanics (Qvn) (equal lowest arsenic concentration); Silurian Anderson Creek Formation (Sla) (highest arsenic); Silurian Dargile Formation (Sud) (highest lead, equal highest copper); Tertiary Brighton Group (Tpb) (lowest nickel) and Older Volcanics (Tvo) (lowest copper and zinc). The identification of arsenic as a significant background constituent prompted a formal study of this element with respect to the nature of its sorption onto different kinds of soils, its bioavailability and speciation.

Arsenic soil sorption analyses were conducted in the laboratory on clay loam, light clay, sand and silt loam soils. These experiments demonstrated that the sorption of arsenic was dependent on soil type and time of soil exposure to the arsenic solution. The bioavailability of arsenic from soil was also investigated using a relative bioavailability test method referred to as the “geophagy gut simulation” extraction method. The adaptation of this method to these investigations showed it to be a viable, fast and simple technique. The experimental results indicated that the relative bioavailability of sorbed total arsenic was dependent on soil type. Given that the toxicity of arsenic is dependent on its speciation, techniques were also evaluated to assess arsenic speciation in soil extracts. To this end, the utility of electrospray mass spectrometry (ESI-MS) for the qualitative and quantitative assessment of arsenic and phosphorus speciation in solution was explored. Although this technique yielded interesting qualitative outcomes it was deemed not to be suitable for quantification. From the qualitative data, various postulates were formulated for the interaction between different species that were subsequently tested by quantum chemical calculations. A technique, based on extraction into chloroform, for quantifying the amount of As^{III} in a sample was adapted to these investigations and was found to be highly accurate and discriminating, albeit time consuming. All phosphorus and arsenic species found to coexist in the ESI-MS

experiments were modelled using high-level density functional theory (DFT). From these calculations, the relative energies of the species could be determined as well as reaction energies for their inter-conversion. This allowed hypotheses to be proposed for the distribution of such species in solution and how they might be taken up into clay structure. The DFT calculations also yielded geometrical information on a wide range of species as well as their electrostatic potential energy maps.

Acknowledgements

Sincere thanks are extended to Associate Prof. Stephen W. Bigger, principle supervisor, and Prof. John D. Orbell, co-supervisor, for their expert supervision and guidance. The following people are also thanked for assistance in this project:

Ms Jean Meaklim, external co-supervisor (EPAV)

Mr Vince Murone (Analytical Consulting Services)

Mr Stephen Geytenbeek (Victoria University)

Associate Prof. Neil Barnett (Victoria University)

Dr Saman Buddhadasa (NMI)

Dr Mala Santhakumar (NMI)

Mr Paul Adorno (NMI)

Mr Stavros Tzardis (NMI)

Dr Nunzio Limongiello (NMI)

Mr Leo Demel (NMI)

Mr Sebastian Barone (NMI)

All the staff at NMI for their assistance

Dr Frank Antolasic (RMIT)

Lastly, a big thankyou to my parents, sister and brother-in-law for their continued support and encouragement.

Abbreviations and Terms

AAS	Atomic absorption spectrometry
AASHTO	American Association of State Highway and Transportation Officials
AB	Activated Bauxsol
AFS	Atomic fluorescence spectrometry
AMG	Australian map grid
ANZECC	Australian and New Zealand Environmental and Conservation Council
As ^{III}	Trivalent arsenic species
As ^V	Pentavalent arsenic species
As ^{Adj}	Adjusted arsenic sample concentration
As ^{Ave}	Average total arsenic concentration
AsB	Arsenobetain
As ^{Bioavailability}	Arsenic bioavailability
As ^{Non-bioavailability}	Arsenic non-bioavailability
As ^{Blk}	Arsenic blank sample concentration
AsC	Arsenocholine
ASTM	American Society of Testing and materials
As ^{St. Dev.}	Standard deviation of arsenic concentration
As ^{Tot}	Total arsenic
As ^{Tot} (sorb)	Total arsenic sorbed
C _∞	Maximum sorption concentration
CE	Capillary electrophoresis
CEC	cation exchange capacity
DFT	Density functional theory
DGT	Diffusive gradients in thin films
DMA	Dimethylarsinic acid
DTPA	Diethylenetriaminepentaacetate acid
E°	Standard electrode potential
EC	Electrical conductivity
EDTA	Ethylenediaminetetraacetic acid
EPAV	Environment Protection Authority Victoria

ESI-MS	Electrospray Mass Spectrometry
EXAFS	Extended X-ray Absorption Fine Structure
FAA	Federal Aviation Administration
FAAS	Flame atomic absorption spectrometry
Fe ^{III}	Trivalent iron species
ΔG°	Gibbs free energy of formation
GC	Gas Chromatography
GFAAS	Graphite furnace atomic absorption spectrometry
HG	Hydride generation
HGAFS	Hydride generation atomic fluorescence spectrometry
HOMO	Highest occupied molecular orbital
HPLC	High performance liquid chromatography
ICP-AES	Inductively coupled plasma atomic emission spectrometry
ICP-MS	Inductively coupled plasma-mass spectrometry
IQR	Interquartile range
ISSS	International Soil Science Society
IUPAC	International Union of Pure and Applied Chemistry
IVG	<i>In vitro</i> gastrointestinal
IVG-AB	<i>In vitro</i> gastrointestinal - Absorption
LC	Liquid chromatography
LUMO	Lowest unoccupied molecular orbital
Min	minutes
MIT	Massachusetts Institute of Technology
MMA	Monomethylarsonic acid
MS	Mass Spectrometry
m/z	Mass to Charge Ratios
MW	Molecular weight
NATA	National Association of Testing Authorities
NEPM	National Environment Protection Measure
NHMRC	National Health and Medical Research Council
NMI	National Measurement Institute
NZVI	Nanoscale zero-valent iron
PBET	Physiologically-based extraction test
pzc	Point of zero surface charge

Q1	First quartile
Q3	Third quartile
Qpw	Quaternary Aeolian
Qrc	Quaternary Fluvial
Qvn	Quaternary Newer Volcanics
rpm	Revolutions per minute
S1	Clay loam
S2	Light clay
S3	Sand
S4	Silt loam
SBET	Simple bioaccessibility extraction test
SEP	Sequential extraction procedure
SFC	Supercritical fluid chromatography
SHIME	Simulator of human intestinal microbial ecosystems
Sla	Silurian Anderson Creek Formation
Sud	Silurian Dargile Formation
TEA	Triethylamine
THF	Tetrahydrofuran
TMAO	Trimethylarsine oxide
TOC	Total organic carbon
Tpb	Tertiary Brighton Group
Tvo	Older Volcanics
USCS	Unified Soil Classification Scheme
USDA	United States Department of Agriculture
USEPA	United States Environment Protection Agency
UV	Ultraviolet
XAFS	X-ray absorption fluorescence spectrometry
XANES	X-ray absorption near edge structure

Table of Contents

Preface	ii
Conference Presentations Relevant to the Scope of this Thesis	iii
Publications Relevant to the Scope of this Thesis	iii
Abstract.....	iv
Acknowledgements.....	vi
Abbreviations and Terms.....	vii
1.0 Introduction	1
1.1 General Overview	1
1.2 Aim of Study	5
2.0 Literature Review	6
2.1 Inorganic Background Soil Data.....	6
<i>2.1.1 Overseas Data</i>	<i>6</i>
<i>2.1.2 Australian Data</i>	<i>7</i>
<i>2.1.3 Implications of Inorganic Background Soil Data</i>	<i>9</i>
2.2 Factors Affecting Arsenic Sorption.....	11
2.2.1 Soil Particle Size and Soil Classification Systems.....	11
<i>2.2.1.1 Soil Classification Systems</i>	<i>11</i>
<i>2.2.1.2 Particle Size of the Soil.....</i>	<i>13</i>
2.2.2 Time of Contact with Soil	15
2.2.3 Temperature	16
2.2.4 Rate of Agitation	16
2.2.5 The Effect of pH	17
2.2.6 Sorption Materials	18

2.3 Bioavailability of Arsenic in Soil.....	20
2.4 Speciation of Arsenic in Soil.....	25
2.4.1 General Background Information Relating to Speciation Analyses.....	25
2.4.1.1 Separation Methods used in Arsenic Speciation Analyses	35
2.4.1.2 Detection Methods Used in Arsenic Speciation Analyses	36
2.4.2 Methods Utilised for the Speciation of Arsenic in Soils	38
3.0 Materials and Methods	43
3.1 Inorganic Background Soil Database.....	43
3.1.1 Development of Database	43
3.1.2 Statistical Analysis of Data	45
3.2 Arsenic Sorption	47
3.2.1 Effect of Soil Type on the Sorption of Arsenic	47
3.2.2 Temporal Studies of the Sorption of Arsenic.....	50
3.3 Bioavailability using Geophagy Method	51
3.4 Speciation Investigations	52
3.4.1 Electrospray Mass Spectrometry of Phosphorus and Arsenic Species.....	53
3.4.2 Computer Modelling of ESI-MS Identified Phosphorus and Arsenic Species	53
3.4.3 Selective Organic Phase Extraction of As ^{III} from Soil	54
3.4.3.1 Method for the Standardisation of Arsenite Sample	55
3.4.3.2 Method for Arsenite Sorbed onto Soil at Different pH Values.....	55

4.0 Results and Discussion	58
4.1 Inorganic Background Soil Data.....	58
4.1.1 Arsenic	58
4.1.2 Chromium	60
4.1.3 Copper.....	60
4.1.4 Lead.....	61
4.1.5 Nickel	62
4.1.6 Zinc	64
4.2 Arsenic Sorption	65
4.2.1 The Effect of Soil Type on As ₂ O ₃ Sorption	67
4.2.1.1 <i>Preliminary Study on the Effect of Soil Type on As₂O₃ Sorption</i>	67
4.2.1.2 <i>Further Analysis on the Effect of Soil Type on As₂O₃ Sorption</i>	72
4.2.2 Time Dependency of As ₂ O ₃ Sorption on Soil.....	74
4.3 Bioavailability of Arsenic.....	78
4.4 Speciation Investigations	82
4.4.1 Electrospray Mass Spectrometry	82
4.4.1.1 <i>Phosphate Speciation</i>	82
4.4.1.2 <i>Arsenic Speciation</i>	84
4.4.2 Computer Modelling of Phosphate, Arsenate and Arsenite.....	88
4.4.2.1 <i>Energies of Species and Reaction Energies</i>	88
4.4.2.2 <i>Geometries</i>	91
4.4.2.3 <i>Electrostatic potential energy calculations</i>	95
4.4.3 Extraction of Arsenite from Soil.....	106
4.4.3.1 <i>Standardisation of Arsenite Sample</i>	106

4.4.3.2 Arsenite Sorbed onto Soil at Different pH Values.....	108
---	-----

5.0 Conclusions & Future Directions 116

5.1 Conclusions.....	116
----------------------	-----

5.2 Future Directions.....	121
----------------------------	-----

6.0 References 122

Appendix A 162

Appendix B..... 164

Appendix C 172

List of Tables

2.1 Inorganic background soil data from overseas literature	7
2.2 Inorganic background soil data from Australian literature	9
2.3 Ranges of particle size for several soil classification systems	14
2.4 Methods used to determine the bioavailability of arsenic in soils	26
3.1 Spiked levels of As ₂ O ₃ used in S1, S2, S3 and S4 for total arsenic extraction	49
3.2 Spiked levels of As ₂ O ₃ used in S1, S2, S3 and S4 for bioavailable arsenic extraction	52
4.1 Soil type characterisation	66
4.2 Effect of soil type on As ₂ O ₃ sorption	68
4.3 Bioavailability results	80
4.4 Table of estimated partition coefficients	81
4.5 Phosphorus and arsenic species identified in the ESI-MS spectra together with their relative abundance	84
4.6 Water/hydronium clusters identified in the ESI-MS spectra	86
4.7 Geometries and further information for phosphorus and arsenic species	96
4.8 Purity of Arsenite sample	108
4.9 Amount of As ^{III} sorbed onto soil at different pH values	112

List of Figures

2.1	Log world average constituent concentration versus Log constituent concentration of various countries	8
2.2	Log of the NEPM background constituent concentration versus log of constituent concentration in various Australian capital cities	9
4.1	Summary statistics for arsenic in various geological units of Melbourne, Australia	59
4.2	Summary statistics for chromium in various geological units of Melbourne, Australia	61
4.3	Summary statistics for copper in various geological units of Melbourne, Australia	62
4.4	Summary statistics for lead in various geological units of Melbourne, Australia	63
4.5	Summary statistics for nickel in various geological units of Melbourne, Australia	64
4.6	Summary statistics for zinc in various geological units of Melbourne, Australia	65
4.7	Recoverable As^{Tot} in: (a) blank and (b) soil type S1 versus the spiked As_2O_3 concentration	69
4.8	Recoverable As^{Tot} in: (a) blank and (b) soil type S2 versus the spiked As_2O_3 concentration	70
4.9	Recoverable As^{Tot} in: (a) blank and (b) soil type S3 versus the spiked As_2O_3 concentration	71
4.10	Recoverable As^{Tot} in: (a) blank and (b) soil type S4 versus the spiked As_2O_3 concentration	71
4.11	Average As_2O_3 sorbed in soil type S1, S2, S3 and S4 at pH 2.3 and 20.3°C	73
4.12	Plot of the sorbed As_2O_3 versus time showing: (a) the rapid first-step sorption process and (b) the slower second-step sorption process	74
4.13	Plot of the As_2O_3 sorbed in the second-step sorption process versus time	75
4.14	A plot of $\ln(C_\infty - C_t)$ for the second-step sorption process versus time	76
4.15	A plot of % $As^{Bioavailability}$ versus the spiked As_2O_3 concentration	81

4.16	The ESI-MS difference spectrum obtained between anhydrous di-sodium hydrogen orthophosphate (Na_2HPO_4) in water and the background THF/water	83
4.17	The ESI-MS spectrum of anhydrous di-sodium hydrogen orthophosphate (Na_2HPO_4) in water showing the water/hydronium ion clusters that form in electrospray positive mode	85
4.18	The ESI-MS difference spectrum obtained between di-sodium hydrogen arsenate heptahydrate ($\text{Na}_2\text{HAsO}_4 \cdot 7\text{H}_2\text{O}$) in water and the background THF/water	87
4.19	The ESI-MS difference spectrum obtained between sodium arsenite (NaAsO_2) in water (pH 7.5) and the background THF/water	89
4.20	Relative computed E_{HOMO} values	104
4.21	Relative computed E_{LUOMO} values	104
4.22	A plot of % As^{III} extracted from S2 versus pH: (a) As^{III} as NaAsO_2 species, (b) As^{V} as Na_2HAsO_4 species and (c) 50% v/v mixture of As^{III} and As^{V} stock solutions	113
4.23	A plot of % As^{V} extracted from S2 versus pH: (a) As^{III} as NaAsO_2 species, (b) As^{V} as Na_2HAsO_4 species and (c) 50% v/v mixture of As^{III} and As^{V} stock solutions	113

List of Charts

4.1	Electrostatic potential energy structures for PO_3^- , HPO_4^{2-} and H_2PO_4^- species	99
4.2	Electrostatic potential energy structures for AsO_3^- , HAsO_4^{2-} and H_2AsO_4^- species	100
4.3	H_2PO_4^- and H_2AsO_4^- conformers	101
4.4	Electrostatic potential energy structures for AsO_2^- , pyramidal H_2AsO_3^- and tetrahedral H_2AsO_3^- species	102
4.5	Electrostatic potential energy structures for <i>cis</i> and <i>trans</i> H_2AsO_3^- species	103

1.0 Introduction

1.1 General Overview

It is commonly known that inorganic constituents (i.e. metals/metalloids) occur naturally in soils, usually at very low concentrations. These constituent concentrations are often referred to as “natural background concentrations”. A suitable definition for the term “background concentration” can be described as the concentration of a substance consistently present in the environment that has not been influenced by localised human activities [1]. Bedrock formed from natural geological processes undergoes weathering and ultimately releases inorganic constituents into the soil [2-3]. Metals such as chromium, manganese, nickel and vanadium comprise the list of some of the chemical constituents that are referred to in inorganic background soil data [4]. However, many other metals/metalloids can also be found in naturally occurring soil which can include: arsenic, barium, copper, mercury, lead and zinc. The Australian and New Zealand Guidelines for the Assessment and Management of Contaminated Sites [5] define “background” levels as the ambient levels of substances or chemicals typically found in the vicinity of a local area, but away from a specific activity or site. In many regards, the two definitions of background concentration are comparable, however, the first has more regard to natural substances that form by natural processes whereas the second does not distinguish between human activities and natural processes. Nonetheless, both definitions are relevant since, in many cases, it is extremely difficult to determine whether or not natural processes alone influence background soil quality.

In some cases inorganic background soil constituents can occur, outside of mineralised areas, at elevated levels that can be above nationally developed guidelines. In cases where elevated inorganic background constituents are present, an understanding of the levels that are present and the effect the constituents have on the surrounding environment, including human health, is vital. Inorganic background soil constituents are of interest for several reasons: (i) they can be used to characterise soil; (ii) they are part of the nutritional food chain from soil to plants to animals (including man); and, (iii) they are essential to the assessment of anthropogenically contaminated soil [6] in order to compare contaminated soil levels to that of background soil constituent levels.

In more recent time, arsenic has become an inorganic background soil constituent of particular interest. Arsenic has been shown to be a commonly occurring toxic metalloid that is present in various natural ecosystems, including the terrestrial soil environment [7]. The main source of arsenic in soil is its geological parent material with the most elevated arsenic concentrations occurring in magmatic sulfides and iron ores. Some of these ores include arsenic pyrites or mispickel, realgar and orpiment [7]. It has been shown [8] that in well-oxidized and alkaline soils, $\text{Ca}_3(\text{AsO}_4)_2$ is the most stable arsenic mineral, followed by $\text{Mn}_3(\text{AsO}_4)_2$. The order of increasing mineral stability is $\text{Cd}_3(\text{AsO}_4)_2 < \text{Pb}_3(\text{AsO}_4)_2 < \text{Cu}_3(\text{AsO}_4)_2 < \text{AlAsO}_4 < \text{FeAsO}_4 < \text{Zn}_3(\text{AsO}_4)_2 < \text{Ni}(\text{AsO}_4)_2$. In reduced and acidic soils, trivalent arsenic oxides and arsenic sulfides are most stable. It has been reported that arsenic sorbed by iron, aluminium and calcium, has a positive correlation with clay particles, in spite of the difference in texture and organic matter content, and total nitrogen [9]. Arsenic bound to aluminium has been shown to be more common than arsenic bound to calcium in soil samples [10]. Moreover, arsenic bound to iron in soils is the most common, however, in volcanic ash arsenic was found to be bound to aluminium to a greater extent [11].

The main factors that affect the sorption of different forms of arsenic in soil are the type (i.e. iron, aluminium, magnesium) and amounts of sorbing components in the soil, the pH, the redox potential [7], the cation exchange capacity [12-13] and the clay particle size [14]. It has been shown that soluble arsenic in soil increases with a decrease in pH and redox potential and that the water-soluble fraction of arsenic is highest in soils that have the lowest clay content [15]. The importance of determining the sorption qualities of soils is two fold: (i) it provides information relating to soil-arsenic chemistry; and, (ii) the information gained from arsenic sorption studies can be applied to the treatment of arsenic in “real-world” environmental situations.

A notable chemical property of arsenic is its ability to form two different oxidation states in the natural environment, namely, the pentavalent (As^{V}) and trivalent (As^{III}) states [16]. Both of these oxidation states are subject to chemically and microbiologically mediated oxidation, reduction and methylation [17-19]. It has been shown that the presence of Fe^{III} in soils oxidizes As^{III} into As^{V} , however, the rate of this reaction is relatively slow [20]. Manganese dioxide or birnessite has also been shown to be a good oxidant of As^{III} species [20]. The reduction of As^{V} can also take place in

certain environments, typically in anoxic environments, in soils that contain sulfides or in soils that contain certain microbial species [21]. Typically, As^{III} is present in anoxic conditions, while As^{V} is the dominant form of arsenic in oxic soils. Trivalent arsenic may occur as uncharged $\text{As}(\text{OH})_3$ in acidic soils and as an anion, AsO_3^{3-} , in alkaline soils [22]. On the other hand, As^{V} is present as an anion, H_2AsO_4^- or HAsO_4^{2-} , in the natural pH range of soils (pH = 4-8) [23]. The presence of arsenic as an anionic species causes it to be quite mobile in soils when it occurs in a soluble form.

The toxicity, biological availability and transport mechanisms associated with arsenic are highly dependent on its physicochemical form [24]. Inorganic arsenic species are known to be more toxic than organic arsenic species [24]. With regards to inorganic species, As^{III} (arsenious acid) is more toxic, more soluble and more mobile than As^{V} (arsenic acid) [25-27] whereas the organic species are generally less toxic as a result of methylation. It has been reported that monomethylarsonic acid (MMA) is more toxic than dimethylarsinic acid (DMA) [28]. In soils, arsenic is known to exist primarily in inorganic forms, but MMA and DMA have also been found in some soil extracts [29-34].

A means of determining the toxicity and biological availability of arsenic to humans is of particular interest in order to assess the potential health implications associated with the ingestion of arsenic, especially by children. In most cases this can only be achieved by performing bioavailability experiments. There are a number of definitions that can be found in the literature for the word “bioavailability”. These definitions vary according to the field of study and reflect the importance of the chemical and biological processes in a particular scientific discipline [35]. A general definition that is commonly used defines bioavailability as “the degree to which a substance in a potential source is free for uptake (movement into or onto an organism)” [36-37]. An environmental definition states: “bioavailability is a physicochemically driven desorption process” [38]. A suitable definition of “oral bioavailability” is “the fraction of an administered dose that reaches the central (blood) compartment from the gastrointestinal tract” [39]. Bioavailability defined in this manner is commonly referred to as the “absolute bioavailability” and is equal to the oral absorption fraction [39]. In contrast to the “absolute bioavailability” the “relative bioavailability” refers to comparative bioavailabilities of different forms of a substance or of different exposure

media containing the substance (e.g. the bioavailability of a metal from soil relative to its bioavailability from water) [39]. A distinction should also be made between the term “bioavailability” and the term “bioaccessibility”. The latter refers to the fraction that is soluble in the gastrointestinal environment and is available for absorption [16,39].

Bioavailability experiments can be conducted in two ways involving either *in vivo* experiments or *in vitro* experiments. The former involves using test animals to determine how much arsenic is sorbed by the animal’s gastrointestinal tract. From these experiments an estimation of the bioavailability of arsenic can be calculated for the human situation. In the case of *in vitro* experiments, simple extraction tests have been used for several years to assess the degree of metals/metalloids dissolution in a simulated human gastrointestinal tract environment [16,40-41]. Historically, relative bioavailability estimates for metal/metalloid constituents in soil have been based on *in vivo* studies in laboratory animals [39]. However, given the costs and time constraints associated with such studies, it is clear that a more efficient alternative is desirable. The most promising option involves the development and validation of *in vitro* extraction tests that are predictive of oral metals/metalloids bioavailability from soil. Such tests would provide a rapid and inexpensive method for developing more accurate exposure estimates for use in human health risk assessments [39].

The bioavailability of metal/metalloid constituents is of great importance in determining the toxicological effects of various constituents on human health as discussed above. However, an indication of these toxicological effects can also be ascertained by determining the chemical species of the constituents present [42]. In the past, natural and anthropogenic soil constituents were measured based on the total content of a specific element present in an analysed soil sample. However, the necessity to advance our knowledge of the mobility of chemicals in soils and the physiological activity of the inorganic elements makes necessary not only the determination of the total amount of these elements, but also the exact determination of the concentration of their different chemical forms [43-44]. It has been shown through biochemical and toxicological investigations that the chemical form of a specific element, or the oxidation state in which that element exists, is crucial in relation to its effect on living organisms [45]. To gain information on the activity of specific elements, it is necessary to establish not only the total content of the element but also to gain an indication of its individual chemical

and physical forms [45]. This approach is described as “speciation analysis”, i.e. the quantitative estimation of the content of the different species present under those conditions. According to the official International Union of Pure and Applied Chemistry definition [46], speciation analysis is “the process leading to the identification and determination of different chemical and physical forms of an element existing in a sample”.

1.2 Aim of Study

The objective of the current study is to contribute to the knowledge of inorganic background soil constituent levels, particularly in soils of Melbourne, Australia, by developing a background soil constituent database. The purpose of the database is to provide site-specific data for this region that will allow comparisons to be made against data from known or suspected contaminated sites. Using the database the significance of arsenic as a background soil constituent will be probed with a view to investigating the nature of its sorption onto different kinds of soils, its bioavailability and its speciation.

In particular, this study aims to: (i) identify the main factors that affect the sorption of arsenic onto soil particles of four different soil types consisting of a clay loam, light clay, sand and silt loam; (ii) estimate the proportion of total arsenic that is potentially made available (i.e. bioavailable) to the human body from each of the soil types using a simple *in vitro* procedure; (iii) investigate both qualitatively and quantitatively, the speciation of arsenic in environmental samples; (iv) assess the applicability and the potential use of ESI-MS to identify and characterise phosphorus (as a benchmark) and arsenic species that originate from aqueous solutions of dissolved salts; (v) explore a method for the quantification of arsenite in soil that involves a chloroform extraction technique that is first used to quantify the purity of an arsenite sample utilized in experimental work and then used to determine the amount of As^{III} sorbed onto soil at different pH values; and, (vi) assess the use of high-level density functional calculations to provide supporting evidence for the reaction mechanisms proposed for both phosphorus and arsenic species.

2.0 Literature Review

2.1 Inorganic Background Soil Data

In this section inorganic background soil data have been reviewed and compiled from the literature. The data obtained from this review have been discussed in the following three sections. Section 2.1.1 includes a discussion on inorganic background soil data found in overseas literature whereas Section 2.1.2 reviews information pertaining to Australian inorganic background soil data. The implications of inorganic background soil data are discussed in Section 2.1.3.

2.1.1 Overseas Data

A summary of information in the literature relating to inorganic background soil constituents in various countries and/or regions around the world is presented in Table 2.1. The countries and/or regions that have been included are: Canada [6], England & Wales [47-52], France [53], Hong Kong [54], Italy [55], Netherlands [56], Spain [56-57] and U.S.A. [1,58]. Figure 2.1 is a plot of the data for concentrations of particular chemical constituents in various countries and/or regions around the world that compares these to world average inorganic background values [59].

Figure 2.1 is a plot of the logarithmic concentration of literature values for some typical inorganic background chemical constituents at various international locations versus the logarithmic concentration of the world average inorganic background values. Clearly, the points that lie near the line of unit gradient are ones where the overseas literature values are in close agreement with the world average inorganic background values. Whereas, points that lie some distance from the line indicate cases where there is a significant difference between the values. It can be seen in Figure 2.1 that for each of the particular selected countries and/or regions the background level of chromium is below the world average background value. However, the levels of mercury, lead, and to a certain extent, zinc, in each of these countries and/or regions are above the respective world average background values. Furthermore, cadmium, copper and nickel have concentrations that are quite close to world background values. This analysis clearly shows that the inorganic background values reported in the literature for

different countries and/or regions differ significantly from the world average inorganic background levels. For this reason, it would be appropriate for each country and/or regions to develop specific data pertaining to its unique geological regions and soil. Such a database would be capable of providing the most useful information on inorganic background soil data.

Table 2.1. Inorganic background soil data from overseas literature.

Metal/ Country	As / mg kg ⁻¹	Cd / mg kg ⁻¹	Cr / mg kg ⁻¹	Cu / mg kg ⁻¹	Pb / mg kg ⁻¹	Hg / mg kg ⁻¹	Ni / mg kg ⁻¹	Zn / mg kg ⁻¹
Canada	-	-	43	22	20	0.059	20	74
England & Wales	17.5	0.7	44	15.6	48.7	0.25	22.1	78.2
France	-	0.74	29	13	30	0.04	35	16
Hong Kong	16.5	0.95	-	16.1	89.9	-	-	58.8
Italy	41	0.44	95	24	26	-	50	68
Netherlands	-	1.76	25.4	18.6	60.2	-	15.6	72.5
Spain	-	1.7	38	14	35	0.2	28	59
U.S.A.	-	0.50	53	25	20	0.071	20	54
Washington, U.S.A.	7	1	42	36	17	0.07	38	86
World Avg.	-	0.5	200	20	10	0.01	40	50

Note: It is assumed that all the (overseas) values are taken from the upper layer. However, in some cases authors do not make it clear where samples have been taken.

2.1.2 Australian Data

A review of the information in the literature relating to inorganic background soil constituents in Australia has been summarised and referenced in Table 2.2. Four Australian states have been considered and whose capital cities are: Adelaide [60-62], Hobart [62], Melbourne [62-63] and Sydney [62,64-65]. Figure 2.2 gives a comparison of the referenced literature data for concentrations of particular chemical constituents in these cities and compares these to the National Environment Protection Measure (NEPM) background ranges [4].

In particular, Figure 2.2 a plot of the logarithmic concentration of typical inorganic background chemical constituents found in particular Australian capital cities versus the

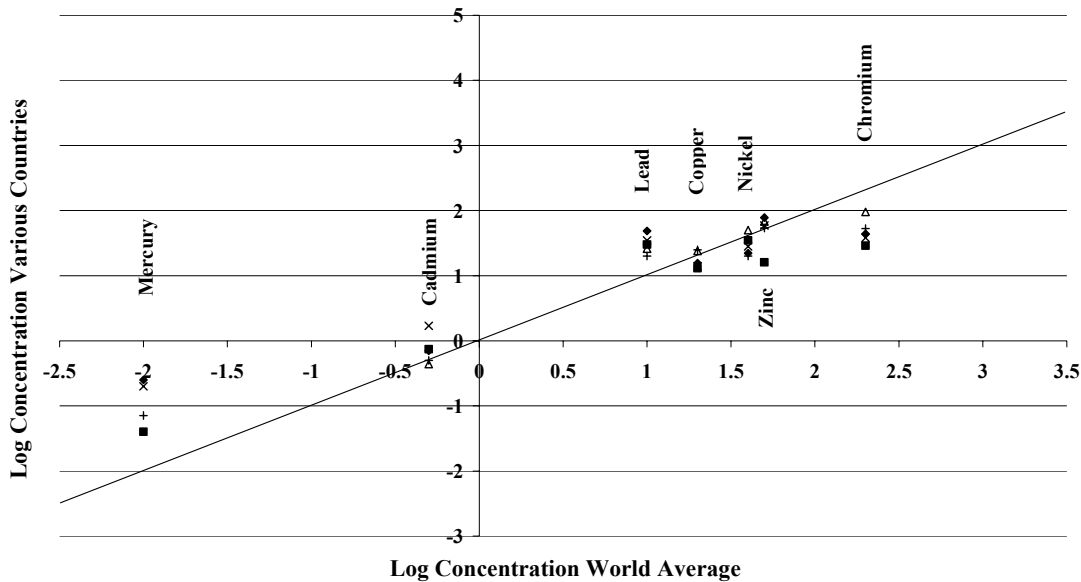


Figure 2.1. Log world average constituent concentration versus Log constituent concentration of various countries. Symbols represent: \diamond , England & Wales; \blacksquare , France; Δ , Italy; \times , Spain and $+$, U.S.A.

logarithmic concentration of the corresponding NEPM background values. In Figure 2.2, it can be seen that arsenic, nickel and chromium in the Australian capital cities studied are below the NEPM background values. However, mercury, cadmium, copper and zinc in both Hobart and Adelaide have background concentrations above the NEPM values. Additionally, in Hobart, the background concentration of lead is also above the corresponding NEMP value. Clearly, if the Australian background values reported in the literature are assumed to be correct, then the data in Figure 2.2 show that each of the capital cities studied has significantly different inorganic background constituent levels compared to NEPM background values. General national inorganic background values can provide useful information to an extent, however, they do not give a good indication of typical inorganic background concentrations in a particular region, local area or specific site [65-67]. In some groups of soil, it is supposed that soils within a given series would have a similar chemical composition [67]. Bini *et al.* [55] have indicated that the grouping of soil samples derived from the same parent material indicates that the nature of the rock is the most important soil-forming factor. Thus, a database that has its data categorised by parent material (i.e. geological regions) would be a most useful resource.

Table 2.2. Inorganic background soil data from Australian literature.

Metal/ Capital City in Australia	As / mg kg ⁻¹	Cd / mg kg ⁻¹	Cr / mg kg ⁻¹	Cu / mg kg ⁻¹	Pb / mg kg ⁻¹	Hg / mg kg ⁻¹	Ni / mg kg ⁻¹	Zn / mg kg ⁻¹
Adelaide	0.2-16	0.1-4.7	2-31	4-128	16-185	0.01-2.3	3-41	12-420
Hobart	2-45	<0.5- 164	2-94	1-571	<1-2220	0.02-3.9	2-130	18 - 22100
Melbourne	<0.2-8.2	-	3-43	<1-38	<0.4-39	-	1.9-50	<2-42
Sydney	2.5	0.03	18.7	11.3	21.3	0.03	8.6	30.1
NEPM	1-50	1	5-1000	2-100	2-200	0.03	5-500	10-300

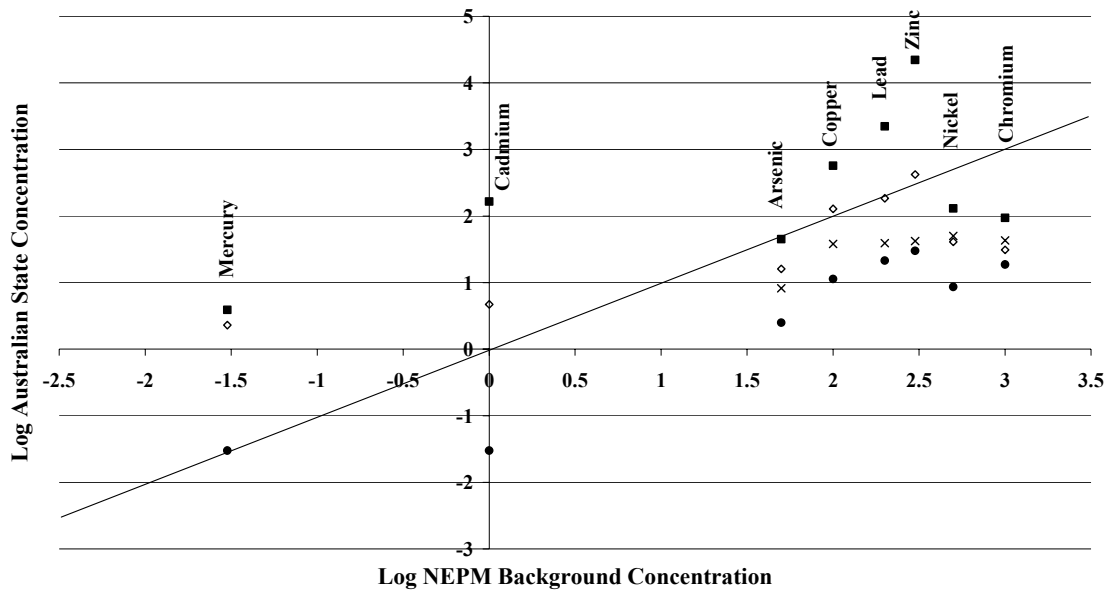


Figure 2.2. Log of the NEPM background constituent concentration versus log of constituent concentration in various Australian capital cities. Symbols represent: \diamond , Adelaide; \blacksquare , Hobart; \times , Melbourne and \bullet , Sydney.

2.1.3 Implications of Inorganic Background Soil Data

Although comparisons of literature data in this way provide useful information about inorganic background soil constituents, there are a number of limitations in conducting such comparisons. Firstly, one must consider that each study has been conducted

independently and issues associated with sampling strategies may not be standardised. Such issues include whether single samples are used or multiple samples are bulked/composited together, varying sampling depths, differing soil sampling intensities and sampling location strategies which vary randomly or systematically (e.g. targeted within a certain type of geological group) [62,67]. Very few literature studies present inorganic background soil data based on targeted samples located within geological regions. It also appears that targeting samples in this manner will produce extremely useful information on inorganic soil constituents since the soil is, to an extent, related to the parent geology [52,68-69]. It is evident that studies using a random sampling strategy, that are not targeted within geological groups, provide information that does not represent properly the actual background inorganic soil constituent results since different soil groups could be mistakenly grouped together.

In a similar manner, data obtained using different analytical techniques may also be compared inappropriately. There is no universal method of determining the total concentration of a particular element in soil. Although there are many accepted standard analytical methods, it is important to note that method efficiencies, sensitivity and detection limits change with each method and will continue to change over time [69]. In most cases it is clear that such comparisons should be avoided, however, in some cases study constraints do not allow the ideal comparisons to be made. In cases where different analytical techniques have been used care should be taken when comparing the data and it should be made clear to the reader that the comparison has this limitation.

An additional limitation with many inorganic background soil constituent studies is that they present data for chemical constituents as a total concentration and this provides limited information about chemical species present and the bioavailability of those species [62]. This can be problematic because one oxidation state of a metal can be extremely toxic, whereas the metal in a different oxidation state may be non-toxic. For example, chromium (VI) is very toxic compared to chromium (III), which is relatively harmless in low concentrations [70]. In cases where the total chromium concentration is reported it does not reveal whether chromium (VI) or chromium (III) is present. This, in turn, means that the background soil data does not give enough detail to establish the presence of toxic or non-toxic chemical constituents. This is the case with many other

metal/metalloid species. For example, arsenite is considered more toxic than arsenate [31,71] and methyl mercury is also considered to be more toxic than other inorganic species [72]. To a large extent, it is believed [62] that naturally elevated chemical constituents exist naturally as species that are relatively non-toxic, however, there has been very little work done to validate this belief. It is clear that inorganic background soil constituent data need to be scrutinised in terms of the individual chemical species present and not just as the total concentration of chemical constituents.

2.2 Factors Affecting Arsenic Sorption

Many factors play a role in the amount of metal/metalloid concentrations that are able to sorb onto various soil particles. In the following review, the factors controlling the sorption of arsenic species are considered with the intent of determining which factors are most significant. Some of the factors considered include the effect of soil particle size, contact time, temperature, rate of agitation, pH and sorption material.

2.2.1 Soil Particle Size and Soil Classification Systems

Before the effect of soil particle size can be discussed with respect to arsenic sorption, definitions of particle size need to be considered with respect to the various soil type classification systems. A review of common soil classification systems is presented in Section 2.2.1.1 that defines soil particles size for a number of soil classification systems. This is followed in Section 2.2.1.2 by a review of information relating the effect of soil particle size to the sorption of arsenic.

2.2.1.1 Soil Classification Systems

Many soil classification systems have been developed and used for specific purposes. However, because different professions are interested in different soil properties, a single descriptive soil classification system does not exist [69]. A simple method of soil classification is based on textural properties that classify soils by particle size distributions, taking into account the percentage sand, silt and clay content. Common textural classification systems have been developed by the United States Department of Agriculture (USDA) [73] and the Unified Soil Classification Scheme (USCS) [74-75].

These classification systems are generally used by engineers, geologists and agriculturalists.

Other textural soil classification systems have also been developed that use different particle size ranges. The American Association of State Highway and Transportation Officials (AASHTO) [76] and the Federal Aviation Administration (FAA) [77] have developed soil classification systems specifically used for road and runway construction. A number of other soil classification systems have also been developed: the American Society of Testing and materials (ASTM) [78], International Soil Science Society (ISSS) [69] and Massachusetts Institute of Technology (MIT) [79].

Most of the soil classification systems discussed above have been developed in America based on American soil properties. These systems have been extensively used in Australia, however, they do not necessarily provide the most appropriate soil classification for Australian soils. For this reason, the soil classification system used in the current study has been based on an Australian system called the Northcote bolus manipulation [80] that is an agronomical soil classification system. The Northcote bolus manipulation method used in this study defines soil particles less than 0.002 mm in diameter as “clays”, particles between 0.002 and 0.02 mm in diameter as “silts” and particles ranging between 0.02 and 2 mm in diameter as “sand” with an arbitrary separation of “coarse” and “fine” sand at 0.2 mm in particle diameter [80]. The definitions for clay, silt and sand are similar, but not identical, to other soil classification techniques. For example, the USDA defines soil particles in the following manner: (i) total clay, <0.002 mm; (ii) total silt, range between 0.002 to 0.05 mm; and, (iii) total sand, ranging between 0.05 to 2.00 mm. The USDA method has various other sub-classifications within these groups for coarse, medium and fine silts and sands [73].

The other soil classification systems: AASHTO, FAA and USCS, all have similar particle size definitions to the Northcote bolus manipulation system but, nonetheless, are still slightly different [69]. It is evident that the classification of soils in environmental studies is problematic because a standard technique has not been adopted. Various professional groups like engineers, geologists and agriculturalists require specific classification techniques for their own purpose. However, due to the overlap between environmental disciplines, one soil classification system may not

service the requirements of all involved and would require a system that best suits the given situation.

A table defining the soil particle sizes for each of the soil classification systems discussed above has been presented in Table 2.3. On close examination of the information summarized in Table 2.3 it can be seen that the soil particle sizes for most of the classification systems are similar. Interestingly, a comparison between the ISSS and the BOLUS system indicate that the two systems are almost identical in soil particle size distribution, suggesting that perhaps the BOLUS system is based on the internationally developed ISSS system.

2.2.1.2 Particle Size of the Soil

A review of information relating to the effect of particle size on the sorption of arsenic species was conducted. It has been shown by Singh *et al.* [81-82] that with the decrease in sorbent-particle size the extent of As^V removal increases for both hematite and feldspar. This has been explained on the basis of surface area per unit mass available for the sorption of As^V , where the surface area will be greater for smaller particles. The extent and rate of sorption both increase with a decrease in particle size and can be attributed to the following: (i) the increased surface area of the hematite/feldspar due to a smaller particle size will attract more As^V species on its surface as the number of active sites increases; (ii) when the diffusive path-length into the interior of the hematite/feldspar particles is reduced, the As^V species require less energy to jump from one active site to another active site and thus the rate-of-jump and finally the sorption increases; and, (iii) small particles move faster in solution than large ones and hence there will be a greater shearing effect due to collections and intraparticle effects on their surface [81-82].

In contrast to the findings of Singh *et al.* [81-82], Genc-Fuhrman *et al.* [83] have indicated that the larger particle size of activated seawater-neutralized red mud or activated Bauxsol (AB) is able to sorb/remove more As^V than AB with smaller particle size. The increased removal efficiency for the larger particles was reported as surprising because the efficiency of surface sorption processes would normally be expected to

Table 2.3. Ranges of particle size for several soil classification systems.

	AASHTO	ASTM	FAA	ISSS	MIT	USCS	USDA	BOLUS
	/ mm	/ mm	/ mm	/ mm	/ mm	/ mm	/ mm	/ mm
Colloids		0.0001- 0.0009						
Clay	0.0001- 0.002	0.0009- 0.0035	0.0001- 0.0035	0.0001- 0.002	0.0001- 0.002	0.0001- 0.075	0.0001- 0.002	0.0001- 0.002
Silt	0.002- 0.075	0.0035- 0.075	0.0035- 0.04	0.002- 0.02			0.002- 0.05	0.002- 0.02
Fine Silt					0.002- 0.006		0.002- 0.02	
Medium Silt					0.006- 0.02			
Coarse Silt					0.02- 0.06		0.02- 0.05	
Very fine Sand							0.05- 0.1	
Fine Sand	0.075- 0.35	0.075- 0.35	0.04- 0.25	0.02- 0.2	0.06- 0.2	0.075- 0.35	0.1- 0.25	0.02- 0.2
Medium Sand					0.2- 0.65	0.35- 2.0	0.25- 0.5	
Coarse Sand	0.35- 2.0	0.35- 2.0	0.25- 2.0	0.2- 2.0	0.65- 2.0		0.5- 1.0	0.2- 2.0
Very Coarse Sand							1.0- 2.0	

increase as the surface area-to-volume ratio of the particles increases. The explanation provided for this observation is that the surface area slightly increases with increasing particle size. The larger and the finer particles were examined by electron microscopy that indicated the larger particles are highly porous aggregates of much finer particles and that it is possible they have more sorption sites available than the smaller, well-crystalline particles.

In another interesting study [84] it has been suggested that the particle size varies with pH which influences the concentration of As^{V} sorption onto goethite. At pH = 3 goethite particles present much smaller diameters, hence showing higher surface areas, important for the effective sorption of metal ions, while at pH = 5 larger goethite particles can be observed, decreasing the removal efficiency of this sorbent towards As^{V} .

It is evident that the particle size of soil has a significant effect on the sorption of arsenic, however, it appears that the particle size is influenced by the sorption material that is present within a given system [81]. When comparing the particle size within the same sorption material it would appear that the smaller particles are able to sorb arsenic better. However, this may not be the case when comparing the arsenic sorption qualities of different sorbing materials as shown in the activated Bauxsol example [83].

2.2.2 Time of Contact with Soil

In a number of studies, the effect of the time of contact on the sorption of various arsenic species (commonly As^{V} and As^{III}) has been reviewed for different soil sorption materials. In a study performed by Genc-Fuhrman *et al.* [83], the time to reach equilibrium for the sorption of As^{V} onto an activated seawater-neutralized red mud, commonly referred to as an activated Bauxsol, is reported as 3 h [85]. The equilibrium process reported for As^{III} on AB was shown to remove arsenic shortly after the initial shaking commenced and increased over time until a steady state was reached after approximately 6 h. The results for both As^{V} and As^{III} indicate the first-order nature of the adsorption process and suggest that the process depends on both the solution concentration and the number of available adsorption sites.

In an alternative study [81], the sorption of As^{V} by hematite and feldspar as a function of the time of contact for different initial concentrations at optimum pH and temperature was investigated. It was found, in that study, that sorption is rapid during the initial stages and then approaches equilibrium after 35 min for hematite and 60 min for feldspar at each concentration. The results indicate the independent nature of the equilibrium period for the solute concentration. Similar observations were noted at different temperatures and pH. It was also noted that the adsorption of As^{V} increases

more for hematite than it does for feldspar when the solute concentration increases. There is an approximate ten-fold increase at optimum pH and temperature.

Similar to the studies reviewed to this point, Zeng [86] also investigated the effect of the time of contact on arsenic sorption using several sorbents, including a silica-containing iron (III) oxide sorbent. The results of the arsenic sorption tests show that the contact time over the tested range of 1–7 days has a trivial influence on the arsenic sorption.

From the reviewed studies it can be concluded that the time of contact varies greatly depending on the solute concentration and sorbent material. It appears the composition of the sorbent material has a significant effect on the time required for arsenic absorption. For example, in sorbent materials that contain more iron (hydr)oxides the time of contact required for arsenic sorption is far less than in sorbent materials that contain little or no iron (hydr)oxides. The effects of other sorbent materials, including iron (hydr)oxides, are reviewed in more detail in Section 2.2.6.

2.2.3 Temperature

The results of certain studies [81,87] suggest that the sorption of As^{V} increases (i.e. removal decreases) for both hematite and feldspar upon increasing the temperature from 20 to 40°C indicating the process to be exothermic. This may be attributed to the relative increase in the tendency of the solute to escape from the solid phase to the bulk phase with the rise in the temperature of the solution. This is in agreement with work conducted by Genc-Fuhrman *et al.* [83] who suggest that the increase in sorption with temperature in activated Bauxsol is due to the increased rate of diffusion of sorbate molecules into the pores of the material.

2.2.4 Rate of Agitation

The rate of agitation has a significant effect on the sorption of arsenic species as reported by Singh *et al.* [81]. In that study, the extent of As^{V} sorption was found to increase with an increase in the rate of agitation up to 125 rpm. Beyond an agitation rate of 125 rpm the extent of As^{V} sorption stays almost constant. This was found to be in good agreement with the findings of earlier workers [88-89]. It is evident that the

rate of adsorption is controlled by the degree of agitation to a certain extent as the increasing agitation reduces the boundary-layer resistance to mass transfer and increases the mobility of the system [88]. It seems that for agitation rates below 125 rpm, film transport is important, whereas at speeds of 125 rpm and above, the intraparticle diffusion becomes important [89].

2.2.5 The Effect of pH

In a study [83] using an activated Bauxsol it was suggested that the sorption process is pH dependent, favouring As^V sorption at pH values below 7.0 and As^{III} sorption at a pH of 8.5. It was suggested that arsenate sorption on AB is a ligand-based adsorption. It was also suggested that the pH dependence of arsenic sorption onto AB can be further understood by investigating the point of zero surface charge (pHpzc). The pHpzc is where the surface charge switches from negative (at higher pH) through zero to positive (at lower pH values). When the pH is below the pHpzc the solid surface is positively charged and favours the adsorption of As^V anions (e.g. H₂AsO₄⁻, HAsO₄²⁻), but when the pH is above the pHpzc the surface of the solid is negatively charged and anion adsorption must compete with Coulombic repulsion. The composition of Bauxsol has a complex mixture of different minerals, with each mineral having different pHpzc values [90]. These minerals can have different surface charges at a given pH that gives AB the capacity to remove arsenic over a wide pH range. The fact that AB sorbs As^V more efficiently at pH < 7.0 and decreases rapidly for pH > 7.0 may reflect the importance of hematite and maghemite in the sorption process [91]. Similar findings have been reported by others [92] who have shown that the adsorption of As^V on metal oxides and oxyhydroxides increases at lower pH values and gradually decreases at higher pH values. It has also been shown that the maximum sorption occurs for As^{III} at pH values between 7.0 and 8.5 for red mud and amorphous oxides [91,93].

In another study [94] it has been suggested that As^V typically exhibits pH dependent adsorption onto Fe oxides [95]. Similar findings have also been suggested in other studies [81,96] indicating that the removal of As^V by hematite and feldspar is pH dependent. In these studies the amount of As^V adsorbed increases with rising pH and reaches a maximum concentration at pH = 4.2 and pH = 6.2 for hematite and feldspar respectively. Among the different species of As^V, the H₂AsO₄⁻ species is predominant

within the pH range 2.0 to 7.0 and above this range the HAsO_4^{2-} species is dominant up to pH 11.0 [87]. The adsorption of arsenate is favoured electrostatically up to the pHpzc of the adsorbents but beyond this point specific adsorption plays an important role [96]. The decrease in the extent of adsorption below pH = 4.2 in the case of hematite and below pH = 6.2 in the case of feldspar may be attributed to the dissolution of the adsorbents and a consequent decrease in the number of adsorption sites [97]. The maximum removal around pH = 4.2 and pH = 6.2 with different adsorbents used, is attributed to surface complexation [97].

In solution, it has been suggested [28] that the arsenic species present depend on the pH and the redox activity of the system and a Pourbaix diagram (See Appendix A) has been constructed [28] for various As^{III} and As^{V} species that exist at different pH values. The Pourbaix diagram indicates that under oxidizing conditions As^{V} species are present at the following pH values: (i) at pH < 2 the H_3AsO_4 species is present; (ii) between pH = 2 and pH = 7 H_2AsO_4^- is present; (iii) between pH = 7 and pH = 11.5 HAsO_4^{2-} is present; and, (iv) at pH > 11.5 the AsO_4^{3-} species is present. Under reducing conditions As^{III} species are present at the following pH values: (i) pH < 7.5 H_3AsO_3 is present; (ii) between pH = 7.5 and pH = 12 the H_2AsO_3^- species is present; and, (iii) at pH > 12 the HAsO_3^{2-} species is present. From that study it is clear that pH and redox activity play an important role in determining the species of arsenic that are present, and this, in turn, affects the species of arsenic that are able to sorb onto a sorption material such as soil.

2.2.6 Sorption Materials

In a study completed by Yang *et al.* [94] it was determined that the Fe oxide content of the soil is the major factor governing the initial adsorption of As^{V} by the soil. It was shown that the percentage of As^{V} adsorbed increases sharply as the Fe oxide content increases, indicating the important role of Fe oxide in providing binding sites for As^{V} . Of the eight soils in that study with less than 5 g kg^{-1} of Fe oxides, none adsorbed more than 60% of the added As^{V} . When the Fe oxide concentration was above 5 g kg^{-1} , 27 of 28 soils adsorbed greater than 80% of the dissolved arsenic. Zhang and Stanforth [98] also reported similar results and indicated that iron oxides and oxyhydroxides (ferric(hydr)oxide), which are present in soils, sediments, and aquatic environments, have a strong affinity for arsenic species [99-101]. Goethite ($\alpha\text{-FeOOH}$) has been

widely used as a representative iron oxide in adsorption studies because it is widespread in nature, can be synthesized readily in the laboratory, and has a well characterized structure [102]. Adsorption of arsenate on hydrous iron oxides has been shown to initially occur rapidly followed by a slow sorption stage thereafter [95,103-105]. Other studies [106-107] have suggested that iron and aluminium oxides adsorb anionic arsenic species well in acidic soils, whereas calcium oxides in alkaline soils adsorb anionic arsenic species to a lesser extent.

In an alternative investigation, two types of reference materials, a hydrous ferric oxide (FeOOH) and a SiO₂ gel, were tested for adsorption of As^V and As^{III} following a batch adsorption procedure [86]. The experiments showed that arsenic removal by FeOOH was 100% for As^V (at pH = 6.5) and 99.5% for As^{III} (at pH = 7.3), whereas arsenic removal by SiO₂ was only 6.8% for As^V and 0% for As^{III} (both at pH = 6.9). The high capacity of FeOOH for absorbing each of the As^V and As^{III} species has also been reported by other researchers [95,108-109]. By contrast, SiO₂ gel can adsorb very little As^V and As^{III}. It was however, suggested that the addition of SiO₂ can influence arsenic adsorption in two ways: (i) the co-precipitated silica has no arsenic adsorption qualities, but may cover some active sites on FeOOH. When a high silica content is present, the coverage of SiO₂ on the FeOOH surface is likely to become significant, leading to a lowering of arsenic adsorption; and, (ii) dissolved silica species may compete with arsenic for adsorption sites on FeOOH since the silica has a relatively higher solubility compared to FeOOH. It has been shown that the dissolved silica species can significantly inhibit the adsorption of arsenic and some other trace metals in aqueous solutions [110-111].

It has been suggested in a number of other investigations that a wide range of possible adsorbents are responsible for arsenic removal including goethite and gibbsite [112-113], ferrihydrite and hydrous ferric oxides [103,114-115], hematite [116], activated red mud [91], and Bauxsol and activated Bauxsol [85,117]. Many of these sorbents may be used for arsenic removal in water systems, however, arsenic removal in large-scale water treatment plants usually involves coagulation with Fe or Al salts [83,118-119]. Processes based on adsorption and coprecipitation methods are significant because they can be used in small scale treatment plants and household systems, are easy to operate, may provide largely sludge-free operation, and may have a regeneration capability [120].

In research reported by Kanel *et al.* [121], a synthetically prepared nanoscale zero-valent iron (NZVI) was tested for the removal of As^{III}. The adsorption kinetics of the system were rapid, occurring in only minutes. Batch experiments were performed to determine the feasibility of NZVI as an adsorbent for As^{III} treatment in groundwater as affected by initial As^{III} concentration and pH (pH = 3-12). The investigation confirmed that NZVI and As^{III} form inner-sphere surface complexes. The effects of competing anions showed HCO³⁻, H₄SiO₄ and H₂PO₄²⁻ are potential interferences in the As^{III} adsorption reactions. The results suggest that NZVI is suitable for both *in-situ* and *ex-situ* groundwater treatment due to its high reactivity.

The literature indicates that there are many different materials that show good physical and chemical properties for the sorption of arsenic species. A family of substances that has been extensively mentioned in the literature as most suitable sorption materials for arsenic are the iron (hydr)oxides. Many of these iron (hydr)oxides are used in their mineral (natural) forms, like goethite, gibbsite, hematite and maghemite, whereas others may be modified or synthetically prepared to maximise the arsenic sorption qualities. It is clear that the material substrate plays a vital role in the sorption of arsenic and also has an influence over the particle size distribution. The pH of the system also plays a significant role in determining the amount of arsenic that is sorbed and, more importantly, the actual arsenic species that is present is of most importance in determining the toxicity of this metalloid and its availability to living organisms.

2.3 Bioavailability of Arsenic in Soil

Many studies have been performed to investigate bioavailability with a view to determining the availability of particular constituents to living organisms in order to determine their associated toxicities. However, the review presented here focuses on the methods used to determine the bioavailability of arsenic in soil.

In the past, the oral toxicity values obtained for arsenic have been derived from epidemiological studies of arsenic in water [16,122]. In these studies it has been suggested that the absorption of soluble arsenic ingested by humans is close to 100% and that absorption occurs in the gastrointestinal tract [16,40,123]. However, in

contrast to arsenic in water, arsenic in soil generally exists as mineral forms or as soil-arsenic complexes that will be incompletely solubilised during transit through the gastrointestinal tract. Consequently, arsenic in soil will be absorbed less than arsenic in water given that arsenic must be dissolved in order for it to be absorbed [16,124]. Experimental work using arsenic-contaminated soil [40] has confirmed that post-ingestion absorption of arsenic from most solid-phase compounds is likely to be substantially lower. In studies that assume 100% absorption of arsenic, the bioavailability is significantly over-estimated [39-40,94,125].

It has been suggested that the bioavailability of arsenic in soil can be divided into two kinetic steps; (i) dissolution of arsenic in gastrointestinal fluids; and, (ii) absorption across the gastrointestinal epithelium into the bloodstream [126]. The biological and chemical processes that take place in the gastrointestinal tract are extremely complex which means they are difficult to simulate in the laboratory [126]. For this reason many arsenic bioavailability studies are performed using controlled dosing studies involving animals, in order to estimate arsenic bioavailability in humans. Studies of this nature are referred to as *in vivo* bioavailability studies.

In a study [127] where the absolute arsenic bioavailability was determined in a contaminated residential soil and house dust, the bioavailabilities were determined to be between 20% and 28% (expressed relative to soluble arsenic in urine) when ingested by *Cynomolgus* monkeys [124]. In that study [127] it was suggested that in the event of ingestion of soils containing smelter waste, arsenic bioavailability will be constrained by encapsulation in insoluble matrices (e.g., enargite in quartz), formation of insoluble precipitates (e.g., iron hydroxide and silicate precipitating on arsenic phosphate grains), and formation of iron-arsenic oxide and arsenic phosphate cements that reduce the arsenic bearing surface area available for dissolution [94,124,127-128]. These geochemical and physical limitations together with kinetic limitations associated with dissolution of these phases during the short transit time through the gastrointestinal tract help explain the reduced bioavailability noted in other investigations using these materials [124,127].

Using a rat model [42], in an alternative study, the absolute bioavailability of arsenical pesticide-contaminated soils relative to As^{III} or As^V ranged from 1.02 to 9.87% and 0.26

to 2.98%, respectively (as determined using urinary arsenic measurements). In this particular study it was attempted to develop a suitable leachate test as an index of bioavailability. However, the results indicated that there is no significant correlation between the bioavailability and leachates using neutral pH water or 1 M HCl. The results also indicated that speciation is highly significant for the interpretation of bioavailability and risk assessment data. The bioavailable fractions of arsenic in these contaminated soils were shown to be low, suggesting a limited health impact to the environment and humans.

Numerous researchers have attempted to correlate *in vivo* experiments with *in vitro* experiments in order to develop relative bioavailability tests that are simple, convenient and reproducible [39,42,129]. A comparison of a physiologically-based extraction test (PBET) with *in vivo* studies for both rabbits and *Cynomolgus* monkeys was conducted to determine how well the *in vivo* experiments correlate to the PBET [16]. It was determined that the relative arsenic bioavailability in a residential soil sample was 48% in the *in vivo* rabbit experiment [130] versus 57% in PBET. The relative arsenic bioavailability in the *in vivo* monkey experiment was 20% [131] versus 31% in PBET. In both cases the PBET relative arsenic bioavailability conservatively overestimates the relative arsenic bioavailability compared to the two animal models, however, the results of the PBET indicate good predictive ability for arsenic bioavailability from soil. In another study [128], excellent agreement was found between the *in vivo* and *in vitro* availability of arsenic (11% versus 12%) which suggests that the *in vitro* dissolution methodology (based on a simulated gastrointestinal tract of a rabbit) replicates arsenic dissolution in the New Zealand White rabbit gastrointestinal tract.

In a study completed by Rodriguez *et al.* [129] an *in vitro* gastrointestinal (IVG) method based on a human model was developed to estimate the bioavailability of arsenic in contaminated soil from mining/smelter sites. In this method, the arsenic was extracted from the soil using simulated gastric and intestinal solutions. A variation to this method was also made, where iron hydroxide gel was used, in a second method, referred to as IVG-AB, to simulate the absorption of arsenic in a process analogous to that of food absorption in the gastrointestinal tract. In this study the *in vitro* arsenic bioavailability results were compared to *in vivo* results determined from dosing trials using immature swine and the results ranged from 2.7 to 42.8% arsenic bioavailability. The study

indicated that arsenic extracted by the IVG and IVG-AB methods were not statistically different to arsenic measured using the *in vivo* method. The study indicated that all IVG methods extract similar amounts of arsenic and thereby provide reliable estimates of bioavailable arsenic in a contaminated soil. In the same study a comparison was also made with the PBET method. The results indicated that the PBET stomach phase does not correlate well with the *in vivo* swine model, while the PBET intestinal phase does produce a positive correlation.

The estimated arsenic bioavailability using the IVG method in soils contaminated with arsenical pesticides was also completed by Sarkar and Datta [132]. In their study the IVG method was slightly modified to increase its accuracy in estimating the bioavailability of arsenic. In addition to simulating arsenic dissolution in gastric and intestinal solutions, absorption by the intestinal membrane was mimicked using iron-oxide coated filter paper strips inserted in nylon bags. In this method the intestinal lining is better physically simulated using iron-oxide coated filter paper strips compared to the iron hydroxide gel used by Rodriguez *et al.* [129] without adding to the total volume of the digestive solution. The *in vitro* experiments were sequentially performed in two phases, namely, the stomach phase and the absorbed-intestinal phase. Arsenic extraction in the *in vitro* absorbed intestinal phase increased, thereby making it more comparable to a potential *in vivo* arsenic method.

A study describing a multi-laboratory comparison and evaluation of five *in vitro* digestion models was conducted [133]. The five methods compared in this study were as follows: (i) the simple bioaccessibility extraction test (SBET method) that simulates mobilisation of contaminants in the acid conditions of the stomach and does not employ an intestinal compartment. The SBET method was first described by Ruby *et al.* [16,41] who validated it against *in vivo* swine studies; (ii) the German E DIN 19738 (DIN) method is based on an *in vitro* digestion model. It is a static *in vitro* gastrointestinal model that uses synthetic gastric and intestinal digestive juices that can be used with or without the influence of food in the presence of milk powder; (iii) the Netherlands *in vitro* digestive model, referred to as the RIVM method, is also based on a static *in vitro* gastrointestinal model that allows the soil to be subjected to a number of stages simulating the human digestive process; (iv) the “simulator of human intestinal microbial ecosystems of infants” (SHIME) method utilises a static gastrointestinal

system wherein the different digestive juices are added to the same reactor; and, (v) the TNO gastrointestinal model, referred to as the “TIM method”, is a dynamic model that simulates the transit through the gastrointestinal tract, the gastric and intestinal pH profiles and the secretion of digestive juice over time. The comparison of the five *in vitro* bioavailability methods revealed that for arsenic bioaccessibility, the simplest, SBET method, produces results similar to those of the more complicated TIM method. The three soils, that were used in the study [133], indicated: (i) for soil “Flanders” SBET bioaccessibility was 50% versus 52% for the TIM method; (ii) for soil “Oker 11” SBET bioaccessibility was 11% versus 15 % for TIM; and, (iii) for soil “Montana 2711” SBET 59% versus 50 % for TIM. These results suggest that the bioaccessibility of arsenic in the acidic environment of the stomach is the rate determining step in controlling arsenic sorption as opposed to sorption across the intestinal epithelium as reported by Ruby *et al.* [39].

An extremely simple relative bioavailability method has been described by certain researchers [134-135] who have used the ‘geophagy’ (gut simulation) method to estimate the proportion of mineral nutrients available to the human body. The method simulates mobilisation of mineral nutrients in the acid conditions of the stomach and does not employ an intestinal compartment. In a study undertaken by Ruby *et al.* [39] it was concluded that the extent of arsenic dissolution in the acidic environment of the stomach is predictive of relative oral bioavailability of arsenic in the animal models. Although arsenic is sorbed through the intestinal epithelium, the results suggest that the rate-controlling step in arsenic sorption is dissolution in the stomach rather than sorption across the intestinal epithelium. This suggests that using a simple gastric digestion model to estimate the relative bioavailability can provide meaningful results that would cost significantly less in comparison to performing *in vivo* experiments. Rodriguez *et al.* [129] also found that the simpler gastrointestinal models appear to correlate better with *in vivo* studies. In that study it was concluded that no *in vitro* model will exactly replicate *in vivo* bioavailability because the human digestive system is too complex and dynamic to simulate in the laboratory. It was suggested that perhaps the best way forward would involve developing an *in vitro* method that is based upon human gastrophysiology that correlates well with an *in vivo* method. From this correlation, mathematical relationships can be developed that will be useful in making risk estimates.

A summary of the methods that can be used to determine the bioavailability of arsenic in soils is presented in Table 2.4.

2.4 Speciation of Arsenic in Soil

A review of the literature relating to the speciation of arsenic in soil has been performed. The first part of this review, Section 2.4.1, considers general background information relating to speciation. This is followed by Section 2.4.2, a review of the methods that are specifically utilised to identify the speciation of arsenic in soils.

2.4.1 General Background Information Relating to Speciation Analyses

Many studies have been completed which utilise the technique of chemical speciation analysis to identify the chemical and physical forms of a constituent in a particular sample. However, much of the published work on metal speciation has dealt with the determination of metal species in natural waters, with papers on metal speciation in solid matrices scattered in the literature [43]. This is particularly the case for arsenic speciation in soils.

Many of the studies that appear in the literature concentrate on developing improved methods for speciation analysis that aim to solve existing problems. One of the main difficulties encountered in speciation analyses of soil samples is extracting the required constituent(s) from the solid state. In most cases the nature of the analytical equipment that must be used requires that the sample be dissolved. However, soils and sediments are resistant to complete dissolution [28] and the dissolution of soils may alter the species that were initially present. Using a chemical extractant is usually the most common form of extracting the chemical constituent of interest, however, careful selection of the chemical extractant is required. The chemical extraction reagents may themselves alter the indigenous speciation of elements [43,136]. It should also be noted that extractants that are less powerful leaching solutions are probably more selective for specific fractions than are more severe reagents but the overall efficiency of extraction may be lower [43,136].

It is, therefore, important that the extraction methods are efficient and minimize the destruction of the arsenic species present in the solid materials [137]. For example, the

Table 2.4. Methods used to determine the bioavailability of arsenic in soils.

Technique Used	General Comments & Notes	Advantages	Disadvantages	Reference
Diffusive gradients in thin films (DGT)	DGT measures labile metal species in soils <i>in situ</i> by immobilizing them in a layer of resin after diffusion through a polyacrylamide gel. The mass that accumulates per unit area in a known time can be used to calculate an <i>in situ</i> flux from the soil to the resin. This technique allows the relative bioavailability to be determined.	<ul style="list-style-type: none"> • Can be used <i>in situ</i> which overcomes analytical and contamination problems. • Can measure a wide variety of metals in soils. • Calibration is not necessary because the geometry and the diffusion layer thickness are well defined. • Consistent results for a given geometry and deployment time allows for good comparisons with other studies using the same set-up. 	<ul style="list-style-type: none"> • Results can be affected by soils that have very low moisture content. However, moisture can be controlled artificially. • The relation between moisture content and gel layer thickness is complex and requires further studies. • Can only give a relative bioavailability estimate in the case of humans. 	[138-141]
Simple bioaccessibility extraction test (SBET) method	The SBET is a static <i>in vitro</i> method that simulates mobilisation of contaminants in the acid conditions of the stomach and does not employ an intestinal compartment.	<ul style="list-style-type: none"> • Relative to an <i>in vivo</i> method the SBET offers a simple relative bioavailability estimate. • The method is cheap, cost-effective and amenable to the analysis of a large number of samples. • SBET avoids the physiological constraints and social barriers associated with <i>in vivo</i> experiments. • The method has been validated against <i>in vivo</i> swine studies. 	<ul style="list-style-type: none"> • Can only give a relative bioavailability estimate in the case of humans. • Failure of the method to account for the influence of food and other stomach/intestinal contents may contribute to an over-estimation of bioavailability. • Does not simulate the oral cavity or intestinal tract. 	[16,41, 133]

Table 2.4 (Cont...). Methods used to determine the bioavailability of arsenic in soils.

Technique Used	General Comments & Notes	Advantages	Disadvantages	Reference
The German method E DIN 19738 (DIN) method	The DIN method is based on a static <i>in vitro</i> gastrointestinal model that uses synthetic gastric and intestinal digestive juices that can be used with or without the influence of food.	<ul style="list-style-type: none"> • Relative to an <i>in vivo</i> method the DIN offers a simple relative bioavailability estimate. • The method is cheap, cost-effective and amenable to the analysis of a large number of samples. • DIN avoids the physiological constraints and social barriers associated with <i>in vivo</i> experiments. • The influence of food and other stomach/intestinal contents can be included in the model. 	<ul style="list-style-type: none"> • Can only give a relative bioavailability estimate in the case of humans. • Does not simulate the oral cavity. 	[133]
The Netherlands <i>in vitro</i> digestive model (referred to as RIVM) method	The RIVM method is based on a static <i>in vitro</i> gastrointestinal model that allows the soil to be subjected to a number of stages simulating the human digestive process.	<ul style="list-style-type: none"> • Relative to an <i>in vivo</i> method the RIVM offers a simple relative bioavailability estimate. • The method is cheap, cost-effective and amenable to the analysis of a large number of samples. • RIVM avoids the physiological constraints and social barriers associated with <i>in vivo</i> experiments. • Simulates the oral cavity. 	<ul style="list-style-type: none"> • Can only give a relative bioavailability estimate in the case of humans. • Failure of the method to account for the influence of food and other stomach/ intestinal contents may contribute to an over-estimation of bioavailability. 	[133]

Table 2.4 (Cont...). Methods used to determine the bioavailability of arsenic in soils.

Technique Used	General Comments & Notes	Advantages	Disadvantages	Reference
The simulator of human intestinal microbial ecosystems of infants (SHIME) method	The SHIME method utilises a static <i>in vitro</i> gastrointestinal system wherein the different digestive juices are added to the same reactor.	<ul style="list-style-type: none"> • Relative to an <i>in vivo</i> method the SHIME offers a simple relative bioavailability estimate. • The method is cheap, cost-effective and amenable to the analysis of a large number of samples. • SHIME avoids the physiological constraints and social barriers associated with <i>in vivo</i> experiments. • The influence of food and other stomach/intestinal contents can be included in the model. • The system can be extended to more reactors, in which case a dynamic system can be obtained. 	<ul style="list-style-type: none"> • Can only give a relative bioavailability estimate in the case of humans. • Does not simulate the oral cavity. 	[133]
The TNO gastrointestinal model (referred to as TIM) method	The TIM method is a dynamic <i>in vitro</i> model that simulates the transit through the gastrointestinal tract, the gastric and intestinal pH profiles and the secretion of digestive juice over time.	<ul style="list-style-type: none"> • Relative to an <i>in vivo</i> method the TIM offers a simple relative bioavailability estimate. • The method is cheap, cost-effective and amenable to the analysis of a large number of sample numbers. • TIM avoids the physiological constraints and social barriers associated with <i>in vivo</i> experiments. • This method has been validated by comparing the dissolution profiles of drugs <i>in vivo</i> and <i>in vitro</i>, and with food compartments. 	<ul style="list-style-type: none"> • Can only give a relative bioavailability estimate in the case of humans. • Failure of the method to account for the influence of food and other stomach/ intestinal contents may contribute to an over-estimation of bioavailability 	[133]

Table 2.4 (Cont...). Methods used to determine the bioavailability of arsenic in soils.

Technique Used	General Comments & Notes	Advantages	Disadvantages	Reference
Partition Coefficients	<p>The technique works on the premise that octanol, an alcohol, behaves in a manner similar to biological lipids such as fatty acid esters and derivatives of cholesterol, that are the main structural components of cell membranes. When a chemical is introduced to a system containing water and octanol, some of the chemical will dissolve in the octanol and some will dissolve in the water. When the system reaches equilibrium, the chemical will be partitioned between the two phases in amounts that minimise the energy of the system. The octanol-water partition coefficient is the equilibrium constant for the distribution of a chemical being investigated between these two phases.</p>	<ul style="list-style-type: none"> • Can be used for various types of environmental samples. • The partition coefficient is simply calculated by dividing the concentration of chemical X in the octanol phase with the concentration of chemical X in the water phase. The log of the partition coefficient ($\log K_{ow}$) is then calculated to give a relative bioconcentration value. 	<ul style="list-style-type: none"> • The technique relies on a mathematical approximation for the uptake and concentration of chemicals in living organisms (bioconcentration) that may not be a true indication of bioconcentration. • Requires further validation with <i>in vivo</i> studies. 	[142-159]
Exchange resin	<p>Exchange resins are used as a tool to better understand the dynamics and behaviour of heavy metals, as affected by soil properties and contamination levels, to estimate the viability of trace metals in soil.</p>	<ul style="list-style-type: none"> • The ability of the exchange process to distinguish between labile and non-labile solution forms of the metal. • The transfer to exchange resins may simulate natural processes (e.g. uptake by organisms) more closely than direct chemical attack. • Can measure a wide variety of metals in soil. 	<ul style="list-style-type: none"> • Can only give a relative bioavailability estimate in the case of humans. 	[160-161]

Table 2.4 (Cont...). Methods used to determine the bioavailability of arsenic in soils.

Technique Used	General Comments & Notes	Advantages	Disadvantages	Reference
Physiologically-based Extraction Test (PBET)	The PBET is an <i>in vitro</i> test system for predicting the bioavailability of metals from a solid matrix and incorporates gastrointestinal tract parameters representative of a human (including stomach and small intestinal pH and chemistry, soil-to-solution ratio, stomach mixing, and stomach emptying rates).	<ul style="list-style-type: none"> • Relative to an <i>in vivo</i> method the PBET offers a simple relative bioavailability estimate. • Replicates the gastrointestinal tract of a 2-3 year old infant that provides a direct basis for assessment of arsenic bioavailability following juvenile hand-mouth ingestion. • The method is cheap, cost-effective and amenable to the analysis of a large number of samples. • PBET avoids the physiological constraints and social barriers associated with <i>in vivo</i> experiments. 	<ul style="list-style-type: none"> • Can only give a relative bioavailability estimate in the case of humans. • For arsenic the PBET over-predicts bioavailability compared to rabbit and primate models (2-11% difference between <i>in vitro</i> and <i>in vivo</i> results). • Failure of the method to account for the influence of food and other stomach/intestinal contents may contribute to an over-estimation of bioavailability. • The PBET method underestimated bioavailable arsenic for calcine materials. 	[16,40,94, 129]
<i>In vitro</i> gastrointestinal (IVG) model	The IVG method is based on a human gastrointestinal model developed to estimate the bioavailability of arsenic in soil or solid media. In this method the arsenic is extracted from the soil using simulated gastric and intestinal solutions with or without an iron hydroxide gel present.	<ul style="list-style-type: none"> • Relative to an <i>in vivo</i> method the IVG method offers a simple relative bioavailability estimate. • Replicates the human gastrointestinal tract. • The method is cheap, cost-effective and amenable to the analysis of a large number of samples. • IVG avoids the physiological constraints and social barriers associated with <i>in vivo</i> experiments. • The IVG method incorporates a type of food into the gastric solution. 	<ul style="list-style-type: none"> • Can only give a relative bioavailability estimate in the case of humans. • The IVG method underestimates bioavailable arsenic for calcine materials. 	[39,129]

Table 2.4 (Cont...). Methods used to determine the bioavailability of arsenic in soils.

Technique Used	General Comments & Notes	Advantages	Disadvantages	Reference
<i>In vivo</i> studies	Controlled dosing studies using animals to determine the arsenic bioavailability in soils. In the <i>in vivo</i> dosing trials, soil arsenic bioavailability is evaluated by measuring arsenic in urine, blood, faeces and/or storage tissues (e.g. bone, skin, nails and hair).	<ul style="list-style-type: none"> • Gives the absolute bioavailability or the amount of arsenic that reaches the central (blood) compartment from the gastrointestinal track of the animal under investigation. • <i>In vivo</i> studies in various animals (e.g. rats, juvenile swine, earthworms, rabbits, guinea pigs, monkeys and pigs) can be used to estimate the relative bioavailability in humans. 	<ul style="list-style-type: none"> • Many animal models used for bioavailability assessments involve animals that have substantial anatomical and physiological differences from humans. Most of these models have not been validated against estimates of arsenic absorption in either children or adults. • Ethical considerations using animals in this manner. • Difficult to develop, expensive to run and time-prohibitive. • Require specialised facilities and personnel. 	[39,42,124, 127-128,130-131,162]
Whole cell- and protein-based biosensors	Biosensor technologies can be used for the determination of bioavailable heavy metals. The first is a whole-cell bacterial biosensor that emits a bioluminescent or fluorescent signal in the presence of a biologically available heavy metal. The second sensor is based on the direct interaction between metal-binding proteins and heavy metal ions.	<ul style="list-style-type: none"> • Can potentially be used for the detection of bioavailable heavy metals in environmental samples. • The whole cell-sensor is able to react only to the bioavailable fraction of metal ions. • The protein-based sensor has a high sensitivity towards metal ions. 	<ul style="list-style-type: none"> • Requires more research and needs to be tested on real environmental samples. 	[163]

Table 2.4 (Cont...). Methods used to determine the bioavailability of arsenic in soils.

Technique Used	General Comments & Notes	Advantages	Disadvantages	Reference
Geophagy 'gut simulation' extraction	The 'geophagy' method is an extremely simple <i>in vitro</i> method that simulates mobilisation of nutrients in the acid conditions of the stomach and does not employ an intestinal compartment.	<ul style="list-style-type: none"> • Relative to an <i>in vivo</i> method the 'geophagy' method offers an extremely simple relative bioavailability estimate. • The method is cheap, cost-effective and amenable to the analysis of a large number of samples. • The method avoids the physiological constraints and social barriers associated with <i>in vivo</i> experiments. • Has been used in the past to estimate the proportion of mineral nutrients available to the human body. 	<ul style="list-style-type: none"> • Can only give a relative bioavailable estimate to humans. • Failure of the method to account for the influence of food and other stomach/intestinal contents may contribute to an over-estimation of bioavailability. • Does not simulate the oral cavity or intestinal tract. • Has not been validated against <i>in vivo</i> bioavailability studies. 	[134-135]

application of an extractant such as hydrofluoric acid could prove to be unsuitable for soil speciation analysis because it is likely to destroy the silicate soil lattice and liberate all of the constituent elements present in the sample [164-165]. This extraction technique may be suitable for a total metal extraction but would probably not be specific enough for speciation analyses.

Many researchers [43,165-177] have conducted experiments to determine appropriate metal extractants for the determination of metals/metalloids in soil samples. The extraction procedures have included either single leaching steps or combined sequential extraction schemes, with the latter being more suitable for the speciation of metals/metalloids in soils [43]. Extractants such as neutral electrolytes, e.g. CaCl_2 or MgCl_2 , buffers of weak acids, e.g. acetic acid or oxalic acid, chelating agents, e.g. ethylenediaminetetraacetic acid (EDTA) or diethylenetriaminepentaacetate acid (DTPA), redox agents, e.g. NH_2OH , strong acids, e.g. HCl , HNO_3 , HClO_4 or HF , or bases, e.g. NaOH or Na_2CO_3 have been considered [43] and the advantages and disadvantages of each have been discussed. It has been suggested [43] that the ability of various extractants to release metal ions depends on their association with particular soil fractions. Extractants such as electrolytes, weak acids and chelating agents release metals from coordination sites, while strong acids and other redox agents are capable of releasing additional quantities of metals as a result of the decomposition of the solid matrix.

The number of papers reporting extractants specifically developed for the extraction of arsenic from soils is limited within the literature [178]. In a study conducted by Wenzel *et al.* [179-180], a sequential extraction procedure (SEP) was developed for arsenic by choosing extraction reagents commonly used for the sequential extraction of selenium and phosphorus. The reliability of this method has been discussed by its proponents [179]. The SEP for arsenic includes the following five extraction steps: (i) 0.05 M $(\text{NH}_4)_2\text{SO}_4$, 20°C, 4 h; (ii) 0.05 M $\text{NH}_4\text{H}_2\text{PO}_4$, 20°C, 16 h; (iii) 0.2 M ammonium oxalate buffer in the dark, pH = 3.25, 20°C, 4 h; (iv) 0.2 M ammonium oxalate buffer and ascorbic acid, pH = 3.25, 96°C, 0.5 h; (v) $\text{HNO}_3/\text{H}_2\text{O}_2$ microwave digestion. Within the inherent limitations of chemical fractionation, these arsenic fractions appear to be primarily associated with: (i) non-specifically sorbed; (ii) specifically-sorbed; (iii) amorphous and poorly-crystalline hydrous oxides of Fe and Al; (iv) well-crystallized hydrous oxides of Fe and Al; and (v) residual phases [179].

The results of another study [181] revealed the arsenic extraction efficiencies of 14 reagents increases in the following order: deionized water \sim 1 M NH_4Cl \sim 0.5 M NH_4Ac \sim 0.5 M NH_4NO_3 \sim 0.5 M $(\text{NH}_4)_2\text{SO}_4$ $<$ 0.5 M NH_4F $<$ 0.5 M NaHCO_4 $<$ 0.5 M $(\text{NH}_4\text{N})_2\text{CO}_3$ $<$ 0.05 M HCl $<$ 0.025 M H_2SO_4 $<$ 0.5 M HCl $<$ 0.5 M Na_2CO_3 $<$ 0.5 M KH_2PO_4 $<$ 0.5 M H_2SO_4 \sim 0.1 M NaOH . A four step sequential extraction procedure was also developed by Polyak and Hlavay [182] for the extraction of the nine metals/metalloids including arsenic. The four sequential extraction steps included the following extractants: (i) CH_3COOH at pH = 2.8, adjusted by HNO_3 to determine the exchangeable metals and metals bound to carbonate; (ii) NH_2OH at pH = 2, adjusted by HCl to determine the metals bound to Fe/Mn oxide; (iii) H_2O_2 , at pH 2–3 to determine the metals bound to organic matter and sulfides; and, (iv) HNO_3 and HClO_4 to determine the acid soluble metal content.

The extraction of both arsenic and zinc from a contaminated soil was reported [183] using various extraction methods to determine which method was most efficient. The extraction methods were tested and validated using a reference soil sample. The three extractive agents tested were: (i) 0.0625 M EDTA disodium salt; (ii) 0.005 M DPTA with 0.01 M CaCl_2 and 0.1 M triethylamine (TEA); and, (iii) 0.005 M DPTA in a single extraction. It was found that 0.005 M DPTA extracts the highest quantity of arsenic and was subsequently chosen for further assays using sonication. It was found that the sonication time reached a plateau after 9 min and increasing the sonication frequency increases arsenic extraction. It was concluded that in the extraction of arsenic and zinc sonication can be used to replace extraction with mechanical shaking in order to simplify analytical procedures when many samples need to be tested.

Once the metals have been extracted from the soil using a suitable extraction medium, the solution can be analyzed using instrumental techniques that have sufficient selectivity and sensitivity. The rapid analysis of samples to prevent species conversion is also important [137]. Instrumental techniques used for speciation analyses generally have two components: (i) a selective separation component; and, (ii) a sensitive detection component. Often techniques are combined to achieve both selectivity and sensitivity. The direct coupling of a separation device to various detection instruments enables improved specificity and detection for individual arsenic species [137]. These kinds of techniques are referred to as “hyphenated techniques”.

2.4.1.1 Separation Methods used in Arsenic Speciation Analyses

A number of different kinds of separation devices can be used in hyphenated techniques for the speciation of arsenic. One of the more common separation techniques is high performance liquid chromatography (HPLC) [184-190]. Other such separation techniques include capillary electrophoresis (CE) [191-193], supercritical fluid chromatography (SFC) [193] and gas chromatography (GC), the last having been applied to arsenic speciation analysis in fewer cases.

The main forms of HPLC separation techniques used for the speciation of arsenic include: (i) anion-exchange HPLC with either isocratic elution [194-202] or gradient step elution [203-206]; (ii) cation-exchange HPLC with isocratic elution [196,198,201]; and (iii) reversed-phase ion-pair HPLC used in conjunction with appropriate counter ions in the mobile phase and incorporating isocratic [207-211] or gradient elution [201]. In order to separate arsenic anions and cations in a single run, a column-switching system involving a combination of anion-exchange and reversed-phase HPLC has also been developed [212].

Both anion- and cation- exchange HPLC techniques have been used for arsenic speciation analysis in the literature discussed above. Depending on the ionic characteristics of the arsenic compounds, anion exchange is the most commonly used technique used to analyze As^{III} , As^{V} , MMA^{V} and DMA^{V} , whereas cation exchange is used to separate arsenobetain, arsenocholine, trimethylarsine oxide and Me_4As^+ species. The arsenic species separated using ion exchange HPLC are summarized in a review paper prepared by Gong *et al.* [137]. In a similar manner to ion exchange HPLC, ion-pair HPLC techniques have also been developed for the separation of arsenic species. Tetrabutylammonium (both hydroxide and phosphate) is the common pairing cation for separating As^{III} , As^{V} , MMA^{V} and DMA^{V} . The resolutions of these arsenic species depend on the concentration of the ion-pair reagent, the flow rate, ionic strength, and pH of the mobile phase [213-214]. The optimum pH range for separating the four arsenic species is between 5.0 and 7.0 [137].

The use of CE as a separation device has also been reported in a number of studies [186,191,193]. Some of the advantages of CE include its ability to separate complex mixtures of ionic species very quickly and efficiently and its ability to discriminate the

speciation pattern of redox-sensitive elements and organometallics, including arsenic species. In addition, CE has good tolerance to complex sample mixtures, requires very little sample, and minimal sample pre-treatment is required [186]. The limitation of CE is its lack of compatibility with several of the more sensitive methods of detection. However, further research on this issue may overcome this problem in the future.

2.4.1.2 Detection Methods Used in Arsenic Speciation Analyses

The separation techniques, mentioned above in Section 2.4.1.2, are often coupled to sensitive detection devices. This section discusses the devices used in some of these hyphenated techniques for the sensitive detection of arsenic species.

In the past, a common detection device used was flame atomic absorption spectrometry (FAAS) [194-195,206]. However, because FAAS suffers from low sensitivity and high background noise for arsenic determination, most recent applications of atomic absorption spectrometry (AAS) are combined with hydride generation (HG) [184,197,200,215-219]. HGAAS allows for extremely low detection limits. However, not all arsenic species form hydrides, and decomposition techniques are usually required. Graphite furnace atomic absorption spectrometry (GFAAS) has also been used as a detection device applied to arsenic speciation. Nonetheless, a direct coupling of HPLC to GFAAS has proven to be difficult [137,214,220]. A novel hyphenated technique utilizes thermospray nebulization of the HPLC effluent followed by thermochemical hydride generation in combination with AAS [221]. Electrothermal AAS has also been used as an off-line detector of the separated arsenic species [201,210,222].

Inductively coupled plasma atomic emission spectrometry (ICP-AES) has been successfully coupled to HPLC for use in arsenic speciation [194,196,202,204-205,211-212,220,223-224]. The coupling is straightforward because the usual flow rate under which an HPLC operates is compatible with the uptake flow rate of an ICP-AES system [137]. A number of applications have been demonstrated, primarily for samples containing high levels of arsenic. For systems containing lower levels of arsenic, HPLC-ICP-AES does not provide sufficient sensitivity for arsenic speciation. Several studies incorporating HG between HPLC and ICP-AES to enhance the sensitivity [225-228] have also been reported.

Inductively coupled plasma-mass spectrometry (ICP-MS) has become a favoured detection technique in arsenic analysis [184,207-208,229-234]. It provides ultra-sensitivity, multi-element capability and can be combined with most separation techniques for speciation analysis. The multi-element capability allows for the simultaneous determination of different elements in addition to arsenic [137]. ICP-MS has also been coupled with CE detection however the method has shown mixed levels of success [235-237]. Two major problems are the mismatch of sample volume between CE and ICP-MS and the suction generated by nebulization. To solve these problems, several interfaces between CE and ICP-MS have been developed. Although some progress has been made using this technique, the matrix effect and poor sensitivity limit CE-ICP-MS to standard solutions and simple systems.

Another hyphenated technique that has been used to detect arsenic species is hydride generation atomic fluorescence spectrometry (HGAFS) coupled to HPLC. The advantages of this technique are its powerful ability to selectively separate and sensitively detect arsenic species. Detection limits in the order of sub-microgram per liter have been achieved for arsenic speciation [238-240]. These are comparable to those achieved by HPLC-ICP-MS using pneumatic nebulization. The HPLC-HGAFS techniques have been applied to the speciation of arsenic in various environmental and biological samples [238-241].

In more recent time, electrospray ionization mass spectrometry (ESI-MS) has been repeatedly shown to be well suited for arsenic speciation, either used alone or in combination with HPLC [242-248]. Unlike ICP-MS, ICP-AES, AAS, and AFS, where elemental arsenic is detected, ESI-MS can provide molecular information of arsenic compounds for positive identification. Due to the availability of the structural information provided by ESI-MS, a number of studies have focused on the characterization and identification of organoarsenicals, such as arsenosugars and new arsenic species [242,245,249-254]. Corr and Larsen [242] first demonstrated the use of positive-ion ESI-MS for determining dimethylated arsenosugars at trace levels.

Others have coupled supercritical fluid extraction with AAS [255] and CE with ICP-AES [256] in order to perform arsenic analyses. Other methods utilise the coupling of ion exchange chromatography with ICP-MS [257-260]. Most of these researchers

discuss the benefits and drawbacks of their particular arrangement while some suggest how further improvements can be made to existing equipment.

Overall, it can be seen that some of the HPLC-atomic spectrometry techniques mentioned above require either costly equipment, such as ICP instrumentation, or systems developed “in-house” that are not readily available to many laboratories. These factors limit the use of these technologies at present. It is hoped that these technologies will become more affordable and more accessible in the future. The appropriate use of such technical equipment is also a limiting factor. In most cases specially trained personnel are required to maintain and operate such equipment to prevent misuse and misinterpretation of results.

2.4.2 Methods Utilised for the Speciation of Arsenic in Soils

One of the earliest known methods used for the speciation of arsenic in soils was reported by Forehand *et al.* [261] in 1976. The method used in this work is based on a method reported some years earlier [262] that utilized benzene as a highly selective and sensitive extractant for As^{III} (from a HCl medium) to separate arsenic from antimony and bismuth. In the Forehand *et al.* [261] method the soil sample is digested in HCl and this is followed by the reduction of As^V to As^{III} using SnCl₂ and KI. Benzene is used to extract the As^{III} which is then back extracted into water and analysed using AAS. The method relies on the premise that As^{III} is selectively extracted into an organic phase (i.e. benzene) from a strongly acidic phase that can then be back extracted into water for analysis. In the presence of excess HCl, chlorination of the arsenic will occur, resulting in arsenic trichloride and arsenic pentachloride. It has been shown that the arsenic trichloride is a covalent molecule while arsenic pentachloride most likely exists as ion complexes [263]. The arsenic trichloride is extracted selectively into the organic phase while arsenic pentachloride is excluded due its ionic properties. The arsenic trichloride contained in the organic phase can be recovered by back extraction with water, since arsenic is most stable in solution in its hydrolysed form [264-265].

Takamatsu *et al.* [29] in 1982 used almost the same method as Forehand *et al.* [261] to determine arsenic species in a contaminated soil. In that study, an analytical technique that consists of a sequential extraction using HCl, HCl/KI, benzene and H₂O/H₂O₂ followed by anion-exchange chromatography and final determination of arsenic by

flameless AAS is reported. Studies have been completed by others [32,42] who have utilized a similar speciation method to that of Forehand *et al.* [261] and Takamatsu *et al.* [29] however in some cases the solvent benzene has been substituted with chloroform.

In 1984, Maher [266] reported a speciation method to determine the arsenic species in a marine sediment. The method involves extracting the arsenic from the solid phase using HCl and NaOH/NaCl solution. The extracted arsenic species are then separated by solvent extraction and ion exchange chromatography and determined by AAS. The sediment extract has been found to contain 45-90% inorganic arsenic (i.e. As^{III} and As^V), 4-39% monomethyl arsenic species and 4-22% as dimethyl arsenic species. However, the method does not enable the elucidation of whether the methylated species were due to material entering the sediments in this form (i.e. from anthropogenic inputs or from natural marine plankton or other organic remains) or whether they were produced by chemical reactions within the sediment [28].

In a study conducted in 1992 [267], arsenic speciation analyses were conducted on soil samples that had been contaminated with an arsenic wood preservation material. A portion of each soil sample was extracted with water using ultrasonic treatment for a duration of 60 min. The establishment of the treatment was not stated in the reference. The mixture was filtered under pressure and then injected without further purification into a HPLC system for separation. Seven arsenic species were separated isocratically by anion- and cation- exchange HPLC in less than 4 min. Arsenic detection was carried out using an arsenic-specific FAAS detector with a hydrogen-argon flame that was optimized and modified for best achievable detection limits, and was interfaced on-line to the HPLC system. The advantage of this particular set-up is its simplicity and the common, moderately-priced equipment of which it is comprised. The detection limits obtained with the HPLC-FAAS system are sufficiently low for selected applications, including arsenic speciation in contaminated soils. The arsenic speciation results obtained using the HPLC-FAAS were compared with results obtained from the same HPLC separation system, this time, interfaced to the more powerful ICP-MS detector. The comparison confirmed the data obtained with the HPLC-FAAS system, but also emphasized that the latter system can only be applied to certain practical arsenic speciation problems.

In some cases the analysis of solid extraction residues by X-ray absorption fluorescence spectrometry (XAFS) has also been used for arsenic speciation analysis [268]. The XAFS technique has also been used to determine arsenic oxidation states, local coordination, and the relative proportion of different arsenic species in three California mine wastes [269]. X-ray absorption near edge structure (XANES) analysis indicated that As^V was the dominant oxidation state in the mine samples, but mixed oxidation states (nominally As⁰ and As^V) were observed in one of the three wastes [269].

In the late 1990s, a reported procedure for the extraction and separation of alkylarsenic species from Buffalo River Sediment standard reference material was developed [230]. The sample was sonicated in methanol-hydrochloric acid-water mixture (50:10:40% v/v) and filtered. The arsenic species in the extract were separated by anion exchange HPLC, using phosphate (pH = 6.0) and citrate (pH = 6.0) buffers as eluents, and detected by direct aspiration into an ICP-MS. Helgesen and Larsen [21] also used HPLC coupled with on-line ICP-MS to separate and selectively detect arsenic species in food and environmental samples (including soil samples) at their naturally occurring concentrations [270]. However, in this study, the soil samples were extracted using a calcium nitrate solution in which the samples were soaked for 1 h with gentle mechanical shaking at room temperature. The supernatant was separated from the soil solids by centrifugation prior to injection into the HPLC-ICP-MS system for arsenic speciation determination. The anion-exchange HPLC column was eluted isocratically using an ammonium carbonate solution containing 97% v/v water and 3% v/v methanol (at pH = 10.3) as the mobile phase. The eluate from the HPLC system was continuously introduced into the ICP-MS instrument that enabled the determination of As^{III}, As^V, MMA and DMA.

In a more recent study completed by Bissen and Frimmel [24] the speciation of As^{III}, As^V, MMA and DMA were reported by extracting the arsenic species from soil samples. The samples were sequentially extracted with 0.3 M ammonium oxalate (pH = 3, adjusted with 0.3 M oxalic acid), milli-Q water (pH = 5.8), 0.3 M sodium bicarbonate (pH = 8) and 0.3 M sodium carbonate (pH = 11). After the extraction procedure, the samples were filtered, diluted if necessary, and analyzed immediately by HPLC-ICP-MS. The separation of arsenic species was performed by an anionic exchange HPLC system containing a microporous resin bed consisting of ethylvinylbenzene crosslinked with 55% divinylbenzene having alkanol quaternary ammonium groups on latex

particles. The HPLC system was coupled with an ICP-MS detector (using NaOH as the mobile phase).

In 2001, a study [271] was conducted to determine the As^{III} , As^{V} , MMA and DMA concentrations in three reference materials, namely river sediment, agricultural soil, sewage sludge, that had been certified for their total arsenic content. The analytical method included an ion exchange liquid chromatography separating device coupled on-line to a HGAFS detector. Prior to analysis, the arsenic species were extracted from the soils using orthophosphoric acid that was chosen as a “soft” extractant able to dissolve arsenic species without modifying them [272]. The efficiency of this extraction procedure was studied in detail and was found to be more dependent upon the nature of the material analysed than on the acid concentration. Recoveries of 90–100% of total arsenic were obtained for the sediment and sludge reference materials whereas a 62% recovery was obtained for the soil reference materials. It was found that the method provides very low detection limits and has a high sensitivity for both the analysis of arsenic-poor samples and the dilution of arsenic-rich extracts. It was concluded that the proposed method has very good potential as a routine speciation analysis procedure for arsenic speciation studies in environmental solids. In a slightly earlier study, Thomas *et al.* [273] also used a phosphoric acid extraction method to speciate arsenic in soil and sediment samples. The extracts were then analysed using HPLC coupled to ICP-MS.

Another method reported for the speciation of arsenic in soils is based on the extraction of arsenic using phosphoric acid and ascorbic acid [274]. The arsenic extract is then analysed using a multiple hyphenated technique that includes the coupling of liquid chromatography (LC), ultraviolet (UV) irradiation, HG and ICP-MS. This speciation method has been applied to several contaminated soils. It showed that As^{V} is the main species in the soils and that in some samples As^{III} and methylated species could also be detected. The same study also compared results obtained using the LC-UV-HG-ICP-MS speciation technique with those obtained using a varied speciation technique, LC-UV-HG-AFS. The findings revealed that LC-UV-HG-AFS is adequate for arsenic speciation in soils to detect both inorganic and organic species. However, the findings also indicated that the ICP-MS coupled detection system is much more sensitive.

In 2003, an alternative study [275] was reported that utilized HPLC coupled to ICP-MS. In this study the efficiency of consecutive extractions using several individual

extractants or solvent mixtures was evaluated. The extractants included: water, methanol/water and phosphoric acid for arsenic species extracted from rice, fish, chicken tissue and soil samples. The analysis revealed the presence of As^{III} , As^{V} , MMA and DMA in the soil samples and that 1 M phosphoric acid was found to be the most efficient extractant. It was also revealed that MMA and DMA are stable in 1 M phosphoric acid extracts from soils whereas As^{III} gradually oxidizes to As^{V} .

Overall, it is evident that most speciation analyses are limited by the soil extraction procedure. The soil extractants used are not necessarily capable of extracting all the arsenic specifically from the soil and, even more importantly, there can be no certainty that the arsenic species remain in their indigenous form (i.e. extractants most likely alter the natural species in the soil upon extraction). More research is required for many of these extractants to validate their use in arsenic speciation analyses.

It would also be of great value to adopt a (validated) standard arsenic extraction method that can be used nationally or, possibly, globally for soil analyses. Currently, there are numerous extraction methods being used that have not been appropriately validated and so the results obtained may not be entirely reliable. It is clear from the review that, in terms of analytical instrumentation, the current technology is adequate for the speciation of arsenic extracts from soil samples (i.e. there is sufficient sensitivity and acceptable detection limits) however this may not be the case for water samples and other food samples. Even though current instrumentation provides sufficient sensitivity and detection levels for soil arsenic extract analyses, most of the reviewed analytical instruments are expensive to purchase, maintain and run.

3.0 Materials and Methods

3.1 Inorganic Background Soil Database

The experimental design for this part of the work does not include the collection and analysis of soil samples. Instead, inorganic background soil data were extracted from Environmental Audit (Contaminated Land) Reports prepared by independent environmental auditors, in accordance with section 57A of the Environment Protection Act 1970, which were submitted to the Environment Protection Authority Victoria (EPAV) between the years of approximately 1992 to 2000. This method of data collection provides valuable information since Environmental Audit Reports contain large amounts of site-specific information that in the past have only been used internally by staff at EPAV in a very limited manner, especially in the case of inorganic background soil constituents. The current study not only gained access to this large and valuable source of information, it also provided a summary of the information in a manner that allows quick and easy access to inorganic background soil data.

3.1.1 Development of Database

The data extracted from the Environmental Audit Reports were entered into a database that was previously designed and constructed [276]. Data entered into the database were subject to quality control processes that were developed as indicated below:

- Inorganic constituents elevated due to soil contamination were avoided. Contaminated inorganic constituents were identified from the site history and conclusions of the contaminated site audit report;
- A geology description was entered into the database for a particular site, based on the site geology (section of audit report), which allows each soil sample to be related to its parent geology;
- Any background soil sampling conducted as part of the audit report was entered directly into the database;

- In cases where normal assessment soil samples were used, borehole/test-pit logs were checked to determine whether sampling was conducted in natural soil or in fill material. Only samples that were taken from natural soil profiles were entered into the database;
- Soil samples that were recovered from the surface (i.e. from approximately the top 20 cm) of the soil profile were not entered into the database. This was done in order to ensure that natural soils were not affected by anthropogenic contaminants so that data entered into the database pertained to unaffected natural soils only. Surface soils may be contaminated by atmospheric fallout (e.g. lead fallout from automobile emissions) and surface runoff contaminants that accumulate in highly organic surface soils;
- Samples that were recovered from areas near or close to identified contaminated sampling locations (i.e. contamination “hot spots”) were avoided as these contaminants may affect nearby samples. Hot spots are usually highlighted in the audit report;
- In cases where no Australian map grid (AMG) reference points were given for sampling locations, approximate AMG points were calculated using a commercially available map of Melbourne, Australia [277];
- It was ensured that all results, entered into the database, were produced by a laboratory that was accredited by the National Association of Testing Authorities (NATA) registered for the analyses undertaken;
- Laboratory results from the audit report were compared to NEPM background ranges [278] and in the absence of NEPM criteria ANZECC B guidelines [279] were used. If constituents were found to be higher than guideline values and the audit report had referred to them as being “contaminated” then these data were not to be entered into the database. Conversely, in cases where the constituent levels were higher than the guideline values and the audit report did not mention that the elevated result was due to contamination then the result was included in the database. In most cases, the constituent was found to be lower than the

guideline value and was entered into the database provided that it had not been affected by contamination;

- Constituent concentrations that were reported as being less than a certain concentration or below the method detection/reporting limit of the laboratory were assumed to be zero, to provide consistent results. A value equal to half the detection limit could not be used because various laboratories use different detection/reporting limits.

The information entered into the database was obtained from audit reports that were conducted in two main operation regions of EPAV, namely: the “West Metro” region and “Yarra” region. The West Metro region entails audit reports that were conducted in the western metropolitan suburbs of Melbourne, Australia while the Yarra region entails audit reports that were conducted in the northern and eastern metropolitan suburbs of Melbourne. Due to the number of audit reports present at EPAV and time constraints on this project not all reports were included in the database. However, the number that was included is sufficient to ensure that representative sampling could be made.

3.1.2 Statistical Analysis of Data

The database was set up so that data entered for samples recovered from a certain geological unit can be grouped together. This was done to ensure that statistical analyses performed on the data would correctly represent the soils of a given geological unit and not combine data pertaining to soils that were taken from two or more different geological units.

The statistical analyses conducted on the raw data extracted from the database in the first instance included the calculation of the mean, standard deviation, minimum, maximum and “count” (i.e. the number of reports entered into the database). In addition to these statistics, the 95% upper confidence limit (95% UCL) was calculated using the statistical “student t” method [280]. On close examination of these statistics it was noticed that some of the data appeared to be skewed to the right (i.e. the right tail of the distribution is much longer than the left tail due to a small number of larger constituent concentrations) and that there appeared to be a number of outliers that were causing the skewness in the dataset. These outliers may have resulted for any of three reasons: (i)

the data were not normally distributed and have resulted in values that are highly variable due to the nature of the soil; (ii) some soil samples may have contained contamination which has resulted in extreme outlier values; or (iii) some soil samples contained naturally elevated soil constituents which can not be identified as naturally occurring and appear as outliers. The cause of the outliers is impossible to identify without further analyses on the soil samples. The latter was clearly not possible since the study was based on a desktop survey of data contained in environmental audit reports.

Due to the outlier issue it was decided that a better method of dealing with these outliers was to use a statistical method that is more resistant to change, so that outliers have little influence over the final outcome [280]. A very simple strategy that achieves this involves the use of the median values instead of the mean values. The median value in each case gives the central value or 50th percentile as compared to the mean that produces a skewed central value. However, using the median value alone does not provide any indication of spread and so the quartiles were also calculated. The first quartile (Q1) is the 25th percentile and the third quartile (Q3) is the 75th percentile. Subtracting Q3 from Q1 measures the spread of the data which is referred to as the interquartile range (IQR) [280]. Using this simple statistical method also allows for the identification of suspected outliers by identifying values that fall at least $1.5 \times \text{IQR}$ above Q3 or below Q1. This method of outlier identification was applied to the dataset to identify the presence of outliers. Once the outliers were identified it was then a matter of deciding either to leave the outliers in the dataset or to delete them. It was ultimately found that the inclusion or exclusion of outliers from that dataset was of no consequence because the median was being used as the central value, it no longer mattered whether the outliers were included or excluded in the dataset. Nonetheless, if a comparison was to be made between the median and mean then the outliers would need to be removed. For the sake of this comparison the outliers were removed from the dataset. The removal of the outliers results in a more conservative dataset that tends to underestimate the natural soil constituent concentrations rather than overestimate them. Overall, this provides a more reliable dataset than one that includes data derived from potentially contaminated soil samples.

3.2 Arsenic Sorption

The materials and methods associated with the experiments conducted to determine the sorption of arsenic are presented in this section. In particular, Section 3.2.1 presents the materials and methods used in experiments to determine the effect of soil type on the sorption of arsenic. Section 3.2.2 presents the materials and methods used in experiments designed to study the temporal sorption of arsenic.

3.2.1 Effect of Soil Type on the Sorption of Arsenic

Four different soil types were obtained from the National Measurement Institute. These types comprised a clay loam (S1), light clay (S2), sand (S3) and silt loam (S4). Each of the soil types was determined using the Northcote bolus manipulation [80] that is an agronomical soil classification system. In this method, a sample of soil sufficient to comfortably fit into the palm of the hand is moistened with water, a little at a time, and kneaded until the ball of soil just fails to stick to the fingers. More soil or water is added to attain this condition that is known as the “sticking point,” and approximates field moisture capacity for that soil. Kneading and moistening is continued until there is no apparent change in the soil ball, usually a working time of 1 to 2 min. The behaviour of the bolus and the ribbon produced by shearing (pressing out) between the thumb and forefinger characterizes the texture. Nineteen grades of texture are commonly recognized and may be defined by the behaviour of the moist bolus.

Other parameters were also measured to characterize each of the four soil types. The moisture content [281] of the soil was measured by weighing 10 g of soil into a metallic crucible and placing the soil into an oven at 106°C for 1 h. The soil was then reweighed and the moisture content was calculated using equation (3.1):

$$\% \text{ Moisture} = \frac{\text{Weight undried sample} - \text{Weight dried sample}}{\text{Weight undried sample}} \times 100\% \quad (3.1)$$

Electrical conductivity (EC) and pH [282-283] were also measured on each of the four soil types to further characterize the soils. The EC measurements were conducted on a conductivity meter (Orion 160) and pH measurements were conducted on a reference pH meter (Radiometer PHM93). Each of the four soil types was prepared for measurement by allowing the soil samples to dry overnight. The samples were then

ground to a fine powder with mortar and pestle and 10 g of each soil sample was weighed and placed into a 100 mL screw cap plastic container. A 50 mL aliquot (or portion) of Milli Q water was added to the container and the container and its contents were tumbled for 1 h on a rotary tumbler. The pH and EC were then measured on each of the solutions before these settled. The pH meter used was pre-calibrated using commercially available pH buffer solutions of pH 4, 7 and 10 (Merck Pty Ltd).

Total organic carbon (TOC) was determined by preparing a sucrose calibration standard that involved weighing 0.0594 g of sucrose into a 250 mL Erlenmeyer flask [284]. This standard contains 25 mg carbon, corresponding to 2.5% carbon for a 1.0 g soil sample. Five standards were prepared with quantities of 0, 5, 15, 25, 50 mg of carbon. The soil samples were left to dry overnight after which they were ground to a fine powder with a mortar and pestle. A 0.8 g sample of each soil was weighed into four separate 250 mL Erlenmeyer flasks. Sodium dichromate (10 mL, 0.5 M, $\text{Cr}_2\text{Na}_2\text{O}_7 \cdot 2\text{H}_2\text{O}$, 99.99%, Sigma Chemical Company) was added to each of the standards and soils with each one being gently swirled to ensure all soil particles were wetted. After 10 min with occasional swirling, 20 mL of concentrated sulfuric acid (H_2SO_4 , 97%, Sigma Chemical Company) was carefully added with gentle swirling. After a further 30 min with occasional swirling, 170 mL of milli Q water was added and mixed thoroughly. The samples were set aside to cool and particles were allowed to settle. In cases where the supernatant was not clear the samples were centrifuged for 15 min at 3000 r.p.m. The absorbance of the standards and sample soil supernatant was determined using an UV/VIS absorption spectrophotometer (HST UV1201) at 600 nm with milli Q water set at zero. A standard curve was plotted of the absorbance of the standard sucrose assay against the known content of carbon. The TOC was determined for each of the four soil type absorbencies using the standard curve.

A preliminary experiment was conducted to determine the sorption of total arsenic (As^{Tot}) onto four soil types – S1, S2, S3 and S4. The experiment initially involved spiking each of the soil types at various arsenic concentrations using a $1000 \mu\text{g mL}^{-1}$ arsenic trioxide (As_2O_3 , 99.99%, Perkin Elmer Australia) solution. The spiking was conducted by adding a quantity of As_2O_3 into the soil sample using an auto-pipette. Each soil type was spiked at six different As_2O_3 concentrations (0, 1, 2, 3, 4 and 5 mg L^{-1} in solution). Six reagent blank spikes were also prepared and consisted of samples containing no soil that were spiked at the same arsenic concentrations as those

used in the soil samples. A summary indicating the number of samples spiked and the spiking concentration for each of the four soil types is presented in Table 3.1.

Table 3.1. Spiked levels of As₂O₃ used in S1, S2, S3 and S4 for total arsenic extraction.

System	Sample Number	Spiked Level in solution / mg L ⁻¹	Spiked Level in soil / mg kg ⁻¹	Volume 1000 mg mL ⁻¹ As ₂ O ₃ added / mL
1	Reagent Blank 1	0	0	0
	Replicates 1 - 7	0	0	0
2	Reagent Blank 2	1	10	0.02
	Replicates 8 - 14	1	10	0.02
3	Reagent Blank 3	2	20	0.04
	Replicates 15 - 21	2	20	0.04
4	Reagent Blank 4	3	30	0.06
	Replicates 22 - 28	3	30	0.06
5	Reagent Blank 5	4	40	0.08
	Replicates 29 - 35	4	40	0.08
6	Reagent Blank 6	5	50	0.10
	Replicates 36 - 42	5	50	0.10

The As^{Tot} was then extracted from the soil using a method adapted from USEPA method 3050 [285]. Samples were prepared by discarding all non-soil material, such as stones, rock and vegetation, that could not be broken up and mixed if they were larger than 5 mm diameter. The samples were homogenized by thoroughly mixing and breaking up any lumps. A 2 g sample of each soil type was weighed into a 50 mL graduated plastic centrifuge tube. To each sample 6 mL HNO₃ (13.5M, analytical grade) and 2 mL HCl, (11.4M, high purity, Mallinckrodt Chemical Company, U.S.A.) was added. Precautions were taken incase a vigorous reaction occurred; acids were added slowly and in small amounts. The samples were allowed to stand inside a fume cabinet for at least 15 min or enough time to ensure that any vigorous reactions ended. The lid was then replaced and the samples were placed into a boiling water bath for 1 h. The tubes were removed from the boiling water and milli Q water was added up to the 15 mL mark. The lid was replaced tightly and each sample was agitated using a vortex mixer (Ratek Instrument VM1) for up to 30 s. The tubes were then placed in a steam bath for 15 min, after which time each tube was shaken for 30 s on vortex and then replaced in the steam bath for a further 2 h. Samples which frothed to near the top of the tube were shaken on the vortex mixer every 15 min. It was important that the steam bath was boiling vigorously when samples were being digested to ensure that the

digesting process was working in the approved manner. The solutions were made up to the 20 mL mark with Milli Q water and mixed by shaking. All samples were then centrifuged for 10 min at 1500 r.p.m. The As^{Tot} content of each sample was determined using an ICP-AES, Perkin Elmer, Optima 4300 DV with CETAC Technologies ASX – 500 model No. 510 auto-sampler). The ICP-AES used an Rf power of 1400 W, outer gas flow of 15 L min^{-1} , intermediate gas flow of 0.5 L min^{-1} , nebulizer gas flow of 0.65 L min^{-1} using argon gas, sample flow rate of 1.5 mL min^{-1} , instrument operating pressure was at normal atmospheric pressure (760 mm Hg) and the temperature was maintained at 21°C .

Total Fe and Al were also extracted from the soil samples using the same method described above [285]. The extracted Fe and Al concentrations were obtained from the preliminary As_2O_3 spiking experiment for the samples which did not contain any spiked As_2O_3 . The extracted Fe and Al were also used to characterize each of the soil types.

An additional As^{Tot} soil sorption test method was also conducted using the four soil types – (S1, S2, S3 and S4), however, a different spiking method was used for this experiment. A 10 mg L^{-1} stock solution of arsenic trioxide (As_2O_3 , 99.8%, Hopkin & Williams Limited) solution was made up in a 1 L volumetric flask with analytical grade milli Q water. A 2 g sample of each of the soil types (each conducted in duplicate) was weighed into a 50 mL graduated plastic centrifuge tube and made up to the 20 mL mark with the As_2O_3 stock solution. Each of the samples was mixed for 30 min on a rotating mixer and then left to soak for 168 h. Each sample was centrifuged for 15 min at 3000 r.p.m. after which the supernatant solution was decanted and discarded. The soil samples were washed with 20 mL of milli Q water, mixed for 5 min on a rotating mixer and then centrifuged for 15 min at 3000 r.p.m. The same washing procedure was repeated a second time. The soil samples were then extracted using the method adapted from USEPA method 3050 [285] to determine the As^{Tot} sorbed by the soil. The extraction and determination (using ICP-AES) procedure are both described above.

3.2.2 Temporal Studies of the Sorption of Arsenic

A temporal As^{Tot} soil sorption test method was also conducted using soil type - S2. A 10 mg L^{-1} stock solution of As_2O_3 solution was made up in a 1 L volumetric flask and made up to the mark with analytical grade milli Q water. Samples (2 g) of type S2 soil

were weighed into four separate 50 mL graduated plastic centrifuge tubes and each made up to the 20 mL mark with the As_2O_3 stock solution. Each of the samples was mixed for 30 min on a rotating mixer and then left to soak for 0.5, 24, 48 or 168 h. Each sample was then centrifuged for 15 min at 3000 r.p.m. after which the supernatant solution was decanted and discarded. The soil samples were washed with 20 mL of milli Q water, mixed for 5 min on a rotating mixer and then centrifuged for 15 min at 3000 r.p.m. The same washing procedure was repeated a second time. The soil samples were then extracted using the method adapted from USEPA method 3050 [285] to determine the As^{Tot} sorbed by the soil. The extraction and determination (using ICP-AES) procedure are both described in Section 3.2.1.

3.3 Bioavailability using Geophagy Method

An experiment was conducted to estimate the proportion of As^{Tot} that would be potentially made available (i.e. bioavailable) to the human body. The bioavailability method used in this experiment is adapted from the geophagy digestion or “gut” simulation method [134-135] that has been used in the past to determine the nutrients made available to humans from eating clay. The bioavailability experiment was conducted on the same four soil types as specified previously in Section 3.2 – S1, S2, S3 and S4. The experiment involved spiking each of the soil types at various arsenic concentrations using a $1000 \mu\text{g mL}^{-1}$ As_2O_3 (99.99%, Perkin Elmer Australia) aqueous solution. The spiking was conducted by adding a quantity of As_2O_3 into the soil sample using an auto-pipette. Each soil type was spiked using six different As_2O_3 solutions (0, 1, 2, 3, 4 and 5 mg L^{-1}) with each concentration conducted in seven replicates. Six reagent blank spikes were also prepared and consisted of samples containing no soil that were spiked at the same As_2O_3 concentrations as those used in the soil samples. A summary indicating the number of samples spiked and the spiking concentration for each of the four soil types is presented in Table 3.2.

The bioavailable As^{Tot} was then extracted from the soil using the adapted geophagy “gut” simulation method [134-135]. Samples were prepared by discarding all non-soil material, such as, stones, rock and vegetation that was larger than 5 mm diameter and that could not be broken up and mixed. Any large matter that remained in the samples was broken up and the samples were homogenized by thoroughly mixing. A 0.5 g sample of each soil type was weighed into a 50 mL graduated plastic centrifuge tube.

Each sample was made up to the 50 mL mark with an aqueous stock solution of 0.1 M HCl (Mallinckrodt Chemical Company, U.S.A.). The samples were placed into a rotating shaker and mixed for 6 h at 200 r.p.m. All samples were then centrifuged for 10 min at 3000 r.p.m. The As^{Tot} content of each sample was determined using ICP-AES (Perkin Elmer Optima 4300 DV with CETAC Technologies ASX – 500 model No. 510 auto-sampler). The operating conditions of the ICP-AES were the same as those described in Section 3.2.1.

The relative bioavailability was calculated using equation (3.2):

$$\text{Relative Bioavailability \%} = \frac{\text{Bioavailable Extractable As}^{\text{Tot}}}{\text{Total Extractable As}^{\text{Tot}}} \times 100\% \quad (3.2)$$

3.4 Speciation Investigations

In order to investigate, both qualitatively and quantitatively, the speciation of arsenic in environmental samples, a number of techniques have been explored. These are described in the following sections.

Table 3.2. Spiked levels of As₂O₃ used in S1, S2, S3 and S4 for bioavailable arsenic extraction.

System	Sample Number	Spiked Level in solution / mg L ⁻¹	Spiked Level in soil / mg kg ⁻¹	Volume 1000 mg mL ⁻¹ As ₂ O ₃ added / mL
1	Reagent Blank 1	0	0	0
	Replicates 1 - 7	0	0	0
2	Reagent Blank 2	1	100	0.05
	Replicates 8 - 14	1	100	0.05
3	Reagent Blank 3	2	200	0.10
	Replicates 15 - 21	2	200	0.10
4	Reagent Blank 4	3	300	0.15
	Replicates 22 - 28	3	300	0.15
5	Reagent Blank 5	4	400	0.20
	Replicates 29 - 35	4	400	0.20
6	Reagent Blank 6	5	500	0.25
	Replicates 36 - 42	5	500	0.25

3.4.1 Electrospray Mass Spectrometry of Phosphorus and Arsenic Species

Investigations were performed to explore the utility of ESI-MS for the characterization of arsenic species in solution. Parallel investigations were also undertaken on phosphorus species as a benchmark, since the chemistries of arsenic and phosphorus are closely related and phosphorus chemistry is better characterized in the literature [286-288]. Aqueous stock solutions of the sodium salts of arsenate, arsenite and phosphate were made up at concentrations of 20 mg L⁻¹ in three separate 1 L volumetric flasks. Each of the volumetric flasks was made up to the mark with analytical grade Milli-Q water. The arsenate and arsenite stock solutions were made up using di-sodium hydrogen arsenate heptahydrate (Na₂HAsO₄·7H₂O, 98.0%, Sigma Chemical Company) and sodium meta arsenite (NaAsO₂, 99.0%, Sigma Chemical Company) respectively. Anhydrous di-sodium hydrogen orthophosphate (Na₂HPO₄, 98 to 100.5%, BDH Chemicals Ltd) was used for the phosphate stock solution.

Each of the stock solutions was further diluted to 1 mg L⁻¹ with Milli-Q water for use in the ESI-MS. The 1 mg L⁻¹ aqueous solutions of arsenate, arsenite and phosphate were individually injected directly into the ESI-MS using a 50 µL glass syringe with a stainless steel needle. Mass analysis was performed using a Micromass Platform II 8326E Electrospray Mass-Spectrometer using a Windows NT version 3.51 running on a personal computer. The software used was the Masslynx NT, version 2.22. The ESI-MS source temperature was 20°C, turbo pressure 1.0 x 10⁻⁶ mBar; nitrogen was used as the nebulizing gas (10 L h⁻¹). The electrospray potential was set to 3 kV in both positive and negative ion modes and the extraction cone voltage was usually 30 V unless stated otherwise. It has been demonstrated that lower cone voltages (i.e. ≤ 30 V) are required to preserve dissolved-phase interactions [289]. The 50 µL aliquots were introduced into a mobile phase of 90% v/v tetrahydrofuran (THF, 99.0%, Sigma Chemical Company) at a flow rate of 20 µL min⁻¹. Mass spectral acquisition was usually performed from m/z = 0 to m/z = 250 in 10 s.

3.4.2 Computer Modelling of ESI-MS Identified Phosphorus and Arsenic Species

The equilibrium geometries and relative energies of all relevant phosphorus and arsenic species identified in the ESI-MS spectra (see Table 4.7) were calculated under high level density functional theory (DFT); namely B3LYP, using the diffuse basis set 6-

311+G** [290]. This level of calculation was chosen since the individual calculated energies have been employed to determine the energies for postulated reactions involving a number of these species and it is therefore important for the effects of electron correlation to be taken into account. The diffuse basis set was chosen since most of the species under investigation are anionic for which a description of electron distributions far away from atomic positions should be accommodated [290]. The software used was Spartan '04 Windows (Version 1.0.1, Wavefunction Inc., 18401 Von, Irvine CA 92612 USA). All calculations were performed on standard laptop computers (Toshiba Satellite Pro and P20). From the calculations, a variety of additional information on these species may be obtained, including, molecular structures, formation energies, bond angles, bond lengths, conventional space-filling volume and area, weight, energy of the highest occupied molecular orbital (E_{HOMO}), energy of the lowest unoccupied molecular orbital (E_{LUMO}), dipole, electrostatic charge structures, electrostatic potential energy maps, HOMO structures and LUMO structures (see Table 4.7, Chart 4.1, 4.2, 4.4 and 4.5). The output files for these calculations are available on the attached CD.

3.4.3 Selective Organic Phase Extraction of As^{III} from Soil

The arsenic speciation method utilized in this investigation was chosen because it was desirable to quantitatively speciate all of the arsenic present in selected soil samples using a simple procedure. The method involves extracting the arsenic from the soil with concentrated hydrochloric acid and to speciate using solvent extractions. The method works on the premise that As^{III} can be selectively extracted into an organic phase from a strongly acidic phase and is then back-extracted into water for analysis [29,264-265]. It has been shown that inorganic arsenic in solution is most stable in its hydrolysed form [263], however, in the presence of an excess of hydrochloric acid, chlorination of arsenic will occur, yielding arsenic trichloride and arsenic pentachloride. It has also been shown that arsenic trichloride is a covalent molecule while arsenic pentachloride most likely exists as the complex ions, $[\text{AsCl}_4]^+$ or $[\text{AsCl}_6]^-$ [263]. The arsenic trichloride can be extracted into an organic phase such as chloroform or benzene, while As^V is excluded owing to its ionic properties. The As^{III} contained in the organic phase can be easily recovered by back extraction with water, since inorganic arsenic is most stable in solution in its hydrolysed form. When the As^{III} comes into contact with water, hydrolysis occurs, excluding the arsenic from the organic phase [32].

This arsenic speciation method was first implemented to standardize an arsenite sample and then used to determine the amount of As^{III} sorbed onto soil at different pH levels.

3.4.3.1 Method for the Standardisation of Arsenite Sample

Three separate aqueous stock solutions were made-up containing the following arsenic species: (i) $76.7 \text{ mg L}^{-1} \text{As}^{\text{III}}$ as NaAsO_2 , (ii) $55.1 \text{ mg L}^{-1} \text{As}^{\text{V}}$ as $\text{Na}_2\text{AsO}_4 \cdot 7\text{H}_2\text{O}$, and (iii) 50% v/v mixture of the As^{III} and As^{V} stock solutions. Analytical grade milli-Q water was used to dilute each of the solutions. Determination of As^{III} was conducted in the following way. A 10 mL aliquot of each of the stock solutions was transferred into three separate 100 mL separating funnels and 80 mL of 10 M HCl (high purity, Mallinckrodt Chemical Company, U.S.A.) was then added to each separating funnel to adjust the acid concentration to greater than 9 M. This was followed by extraction of the As^{III} into chloroform with $4 \times 10 \text{ mL}$ washings. At that stage the strongly acidic aqueous phase (i.e. top layer) was discarded. The As^{III} was then back-extracted from the organic phase into $2 \times 20 \text{ mL}$ aliquots of water and diluted to 100 mL. Each of the three samples were analyzed using an ICP-AES, Perkin Elmer Optima 4300 DV with CETAC Technologies ASX – 500 model No. 510 auto-sampler). The ICP-AES analysis used an Rf power of 1400 W, outer gas flow of 15 L min^{-1} , intermediate gas flow of 0.5 L min^{-1} , nebulizer gas flow of 0.65 L min^{-1} using argon gas, sample flow rate of 1.5 mL min^{-1} , instrument operating pressure at normal atmospheric pressure (760 mm Hg) and the temperature was maintained at 21°C .

The As^{Tot} was also determined by running the three aqueous stock solutions individually through the ICP-AES. The concentration of As^{V} was calculated by subtracting the As^{III} concentration from the As^{Tot} . A percent difference from the As^{Tot} was calculated by taking the difference of As^{Tot} from As^{III} and then dividing by the As^{Tot} concentration. The percent difference is the amount of arsenic which most likely relates to the oxidative impurities present in the sample container.

3.4.3.2 Method for Arsenite Sorbed onto Soil at Different pH Values

The first part of this experiment involves allowing the sorption of arsenic onto soil samples. This was achieved using the same three stock solutions that were prepared in

Section 3.4.3.1. The pH of the stock solution was adjusted by pouring 50 mL of the NaAsO₂ aqueous stock solution into 5 separate beakers and adjusting the pH in each of the beakers to pH values of approximately 2, 4, 6.5, 9 and 12 respectively using 0.1 to 1.0 M H₂SO₄ and 0.1 to 1.0 M NaOH. Where appropriate, throughout this work, pH measurements were made repeatedly to ensure that the pH of the medium remained constant.

A 5 g soil sample (light clay - S2) was placed into six separate plastic 50 mL centrifuge tubes. Five of these centrifuge tubes containing the pre-weighed soil sample were made up to the 50 mL mark using the pH-adjusted stock solutions. The sixth centrifuge tube was made up to the 50 mL mark with analytical grade milli-Q water (blank H₂O). The contents of each of the six tubes was mixed on a rotating mixer for 30 min and then left to soak for 7 days. The samples were centrifuged for 15 min at 3000 r.p.m. and decanted. The supernatant liquid from the decanting was retained for later use. Each soil sample was washed with 20 mL milli-Q water, mixed for 5 min on a rotating mixer, centrifuged for 15 min at 3000 r.p.m. and decanted. The washing procedure was repeated a second time.

The next part of the experiment involved the extraction of As^{Tot} from the soil. This involved treating each of the six samples with a 20 mL aliquot of 10 M HCl, and shaking it vigorously for 30 min. Each sample tube was centrifuged for 5 min at 3000 r.p.m. and poured into a 100 mL volumetric flask. The As^{Tot} extraction procedure was repeated two more times (i.e. another 2 × 20 mL of 10 M HCl). The soil sample was then washed into filter paper (Whatman 44) with milli-Q water and diluted to the 100 mL mark. The concentration of the As^{III} species was determined in each sample by taking a 10 mL aliquot of the As^{Tot} extract and transferring it to a 100 mL separating funnel where 80 mL of 10 M HCl was added. The As^{III} was extracted with 4 × 10 mL washings of chloroform. The acidic aqueous phase was discarded. The As^{III} was then back-extracted from the organic phase using 2 × 20 mL aliquots of milli-Q water and diluted to the 100 mL mark in a volumetric flask. Each of the 6 samples was then analysed by ICP-AES.

The final part of the experiment involved determining the As^{III} concentration in the supernatant liquid for each of the six samples. The As^{III} concentration was determined by taking a 10 mL aliquot of each of the supernatant liquids and transferring each

aliquot to a 100 mL separating funnel. To each of the tubes, 80 mL of 10 M HCl was added. The As^{III} was extracted using 4 × 10 mL washings of chloroform. The acidic aqueous phase was discarded. The As^{III} was back-extracted from the organic phase using 2 × 20 mL aliquots of milli-Q water and diluted to the 100 mL mark in a volumetric flask. Each of the supernatant liquid samples was then analysed by ICP-AES.

The whole procedure was repeated two more times, changing the original 76.7 mg L⁻¹ As^{III} as NaAsO₂ aqueous stock solution to: (i) the previously prepared aqueous stock solution of 55.1 mg L⁻¹ As^V as Na₂AsO₄·7H₂O; and (ii) the previously prepared aqueous stock solution containing 50% v/v mixture of the As^{III} and As^V stock solutions.

In Sections 3.2, 3.3 and 3.4, where time and resources permitted, replicates and reference soil material were used for QA/QC purposes. Results for QA/QC have been included on the appended CD. The preparation of fresh stock solutions of particular arsenic species was carried out for each experimental section in order to minimize possible transformation of arsenic between different forms.

4.0 Results and Discussion

4.1 Inorganic Background Soil Data

A summary of results for inorganic background soil data is presented in Appendix B. The summary comprises a table that includes the statistical data calculated for each constituent in each of the different geological units encountered in the environmental audit reports that were used to construct the database. The statistical results for six metals (As, Cr, Cu, Pb, Ni and Zn) within various geological units from the database are presented and discussed. The nine geological units include: Quaternary Aeolian (Qpw), Quaternary Coode Island Silt (Qpy), Quaternary Fluvial (Qrc), Quaternary Paludal (Qrm), Quaternary Newer Volcanics (Qvn), Silurian Anderson Creek Formation (Sla), Silurian Dargile Formation (Sud), Tertiary Brighton Group (Tpb), and Older Volcanics (Tvo).

4.1.1 Arsenic

In Figure 4.1, the median arsenic concentration has been summarised within the nine different geological units located within Melbourne, Australia¹. The data were obtained from the computer database software. The results in Figure 4.1 indicate the geological unit Sla has the highest median arsenic concentration at 6.4 mg kg⁻¹ with a maximum of 21.0 mg kg⁻¹. The second highest median arsenic concentration occurs in Sud at 6.0 mg kg⁻¹ with a maximum of 20.0 mg kg⁻¹. Both of these geological units formed in the Silurian age in a sedimentary marine environment and mainly consist of siltstone and sandstone [291]. Researchers [7,292] suggest that sedimentary rocks are the parent materials of many different soils and that during the formation of sedimentary rocks, arsenic is carried down by precipitation of iron hydroxides and sulfides. These researchers also indicated that arsenic concentrations in soil derived from sedimentary rocks may contain 20 to 30 mg kg⁻¹ of arsenic. Other sources [71] suggest that sandstones and limestones often contain arsenic concentrations of anywhere between less than 1 to 20 mg kg⁻¹.

¹ Figures 4.1 to 4.6 are also represented in Appendix C for comparative purposes.

The other geological units referred to in Figure 4.1 all have lower median arsenic concentrations compared to Sla and Sud. These other units were formed during the Quaternary and Tertiary age in sedimentary non-marine and igneous extrusive environments and consist of various lithological descriptions [291]. The lowest median arsenic concentration is exhibited in Qvn and Qrc with both containing a median arsenic concentration that is either below detection limits or zero. The geological unit Qvn formed in an igneous extrusive environment mainly consisting of basalt with minor scoria and ash whereas Qrc formed in a sedimentary non-marine environment consisting of gully alluvium/colluvium including gravel, sand and silt [291]. Generally, arsenic has the ability to bind to sulfur ligands which means that it tends to be associated with sulfide-bearing mineral deposits as arsenic minerals or as trace constituents of other sulfide minerals [71]. In the case of Qvn and Qrc it appears that little or no sulfur is part of the composition of soils formed from these geological units and thus little or no arsenic is present in these soils.

There is relatively little difference in the concentration of arsenic in most rocks/soils unless the concentration has been altered by mineralisation [71]. It appears that the geological units presented in Figure 4.1 are clearly from non-mineralised areas, which may explain the relatively low arsenic concentrations.

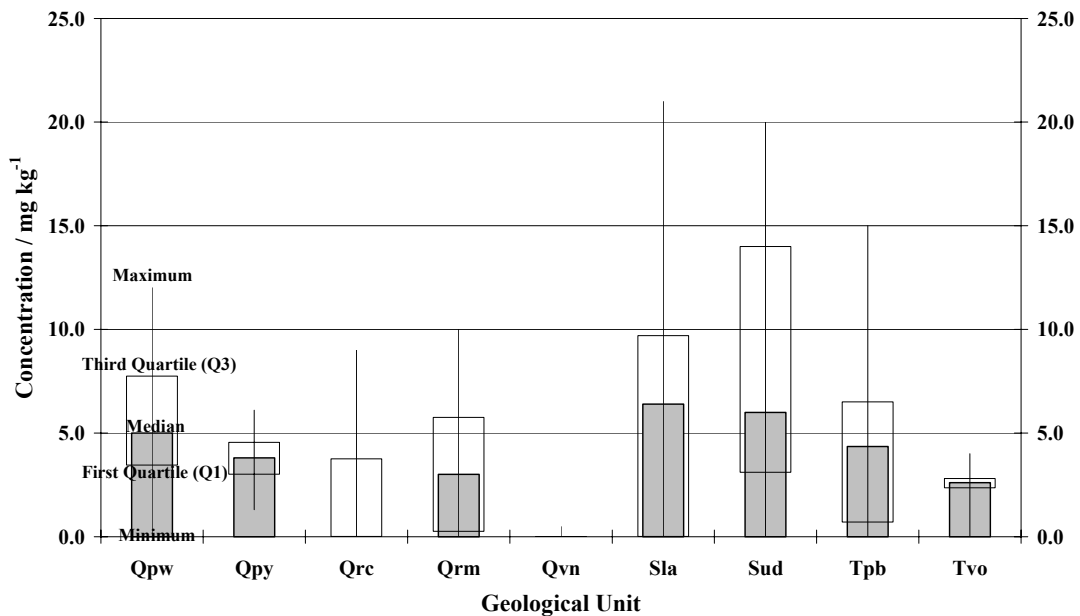


Figure 4.1. Summary statistics for arsenic in various geological units of Melbourne, Australia

4.1.2 Chromium

A summary of chromium concentrations obtained from the database software is presented for eight geological units located within Melbourne, Australia in Figure 4.2. The median chromium concentrations range from 30 mg kg⁻¹ in Qpw up to 51 mg kg⁻¹ in Qrc. The other geological units presented in Figure 4.2 all have fairly close median concentrations between approximately 30 to 40 mg kg⁻¹. However, the highest maximum chromium concentration is exhibited in Qvn with a maximum concentration of 89 mg kg⁻¹. The higher maximum in Qvn may be due to the fact that it is a basaltic igneous rock where it commonly substitutes for iron which has an ionic radius fairly close to that of chromium (III) [70]. Basaltic igneous rocks, similar to Qvn, can exhibit chromium concentrations that range between 40 to 600 mg kg⁻¹ whereas sedimentary rocks like limestones and sandstones exhibit concentrations of approximately 10 to 35 mg kg⁻¹ respectively [293].

Another reason for the higher maximum chromium concentration in Qvn may be due to the fact that Qvn is made up from a significant proportion of basaltic clays. Research conducted by McGrath and Loveland [294] have shown that clay-rich soils contain higher concentrations of chromium compared to soils composed of coarse loamy, sandy and peaty soils. The median chromium concentrations reported by McGrath and Loveland [294] in topsoils of England and Wales classified by soil texture class are as follows: clay (59.0 mg kg⁻¹), fine loamy (43.5 mg kg⁻¹), fine silty (48.0 mg kg⁻¹), coarse silty (39.3 mg kg⁻¹), coarse loamy (27.4 mg kg⁻¹), sandy (13.2 mg kg⁻¹) and peaty soil (12.2 mg kg⁻¹).

4.1.3 Copper

Figure 4.3 presents a summary of copper concentrations obtained from the database software in nine geological units located within Melbourne, Australia. The median copper concentrations range from 3 mg kg⁻¹ in Tvo up to 18 mg kg⁻¹ in both Sud and Qrc. These values appear to be relatively low compared to some of the literature values [295-296]. For example, the literature indicates copper concentrations ranging from 30 to 160 mg kg⁻¹ for basic igneous basalts, 4 to 30 mg kg⁻¹ for acid igneous granites, 30 to 150 mg kg⁻¹ for shales/clays, 5 to 20 mg kg⁻¹ for volcanic rocks, 5 to 20 mg kg⁻¹ for sandstone/limestone with a general average soil copper concentration of 20 to 30

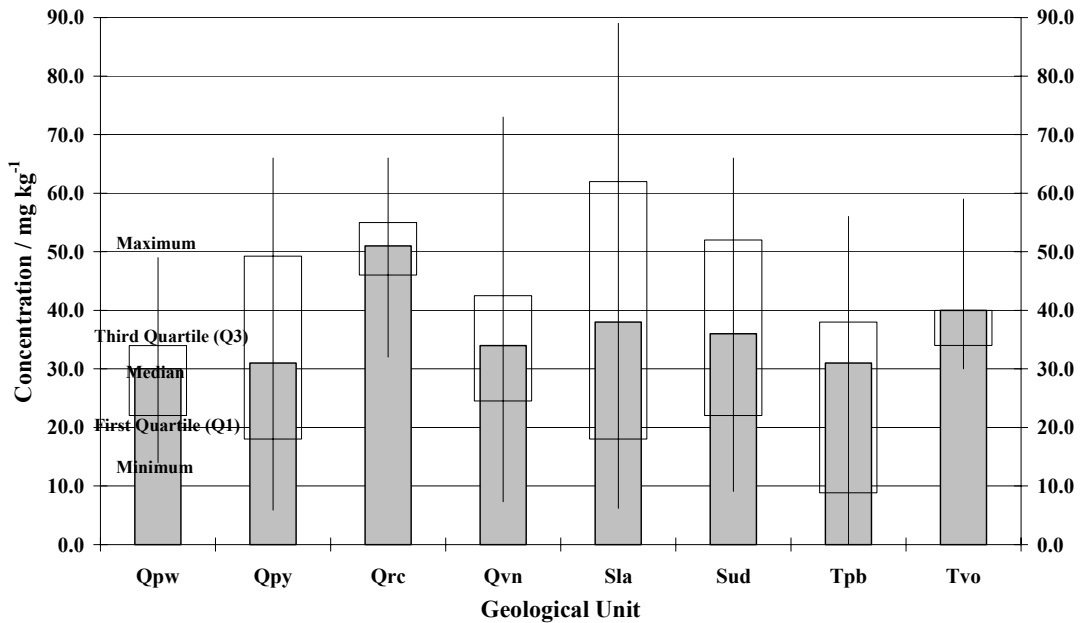


Figure 4.2. Summary statistics for chromium in various geological units of Melbourne, Australia

mg kg⁻¹ [295-296]. The mechanism for copper forming in igneous rocks is controlled by the process of differentiation during crystallisation where compounds crystallise in layers due to their melting points. The general order of crystallisation is magnesium silicates, iron/calcium minerals, followed by alkali aluminium silicates and quartz. The remaining liquid in the crystallisation process is saturated with sulfide which forms an immiscible copper sulphide rich layer [297-298]. In silicate clays and mafic rocks (i.e. rocks rich in Hg (II) and Fe (II)) Cu (II) can replace Mg (II), Fe (II), Zn (II), Ni (II) and Mn (II) by the process of isomorphous substitution [299].

4.1.4 Lead

In Figure 4.4 the median lead concentration obtained from the database software for eight geological units within Melbourne, Australia are presented. The median lead concentrations range from 6.3 mg kg⁻¹ in Qrc up to 20 mg kg⁻¹ in Sud. On comparison with literature values, lead concentrations tend to rise with increasing silica content from ultrabasic (basalt) to acid igneous (granite) rocks [300-301]. Sedimentary rocks like shales and mudstones have been reported to have an average lead concentration of

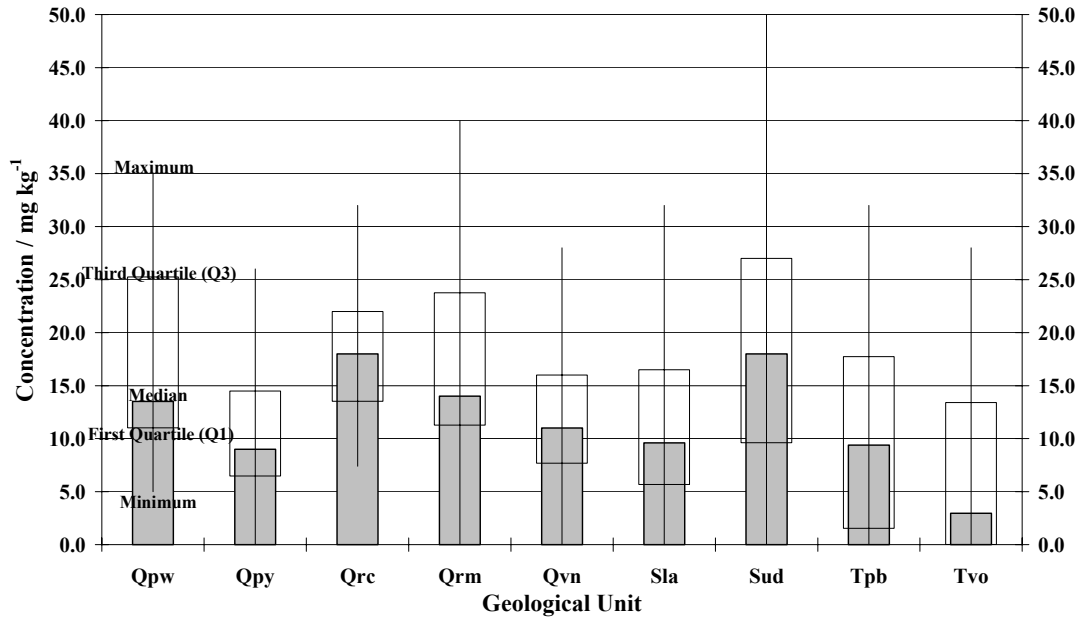


Figure 4.3. Summary statistics for copper in various geological units of Melbourne, Australia

approximately 23 mg kg⁻¹ while sandstones have an average of approximately 10 mg kg⁻¹ and limestones are reported to have an average of 71 mg kg⁻¹ [300-301]. These values are in general consistent with the data shown in Figure 4.4 that include the data for Qvn, that is an igneous extrusive alkaline basalt [291]. The Qvn basalt appears to contain less silica than some of the other geological parent materials, which suggests it may have a relatively low lead concentration. The Sud basalt, on the other hand, consists of siltstone with thin-bedded sandstone suggesting a higher content of silica that may consequently result in a higher concentration of lead. However, this is not consistent with the literature lead concentration found for limestone which suggests a lead concentration of 10 mg kg⁻¹ [300-301].

4.1.5 Nickel

A summary of median nickel concentrations has been made in Figure 4.5 for eight different geological units. The highest median nickel concentration (40 mg kg⁻¹) was exhibited in Qrc which is a Quaternary aged sedimentary deposit formed in a non-marine environment consisting of fluvial: gully alluvium and colluvium: gravel, sand and silt [291]. The lowest median nickel concentration (12.7 mg kg⁻¹) is exhibited in

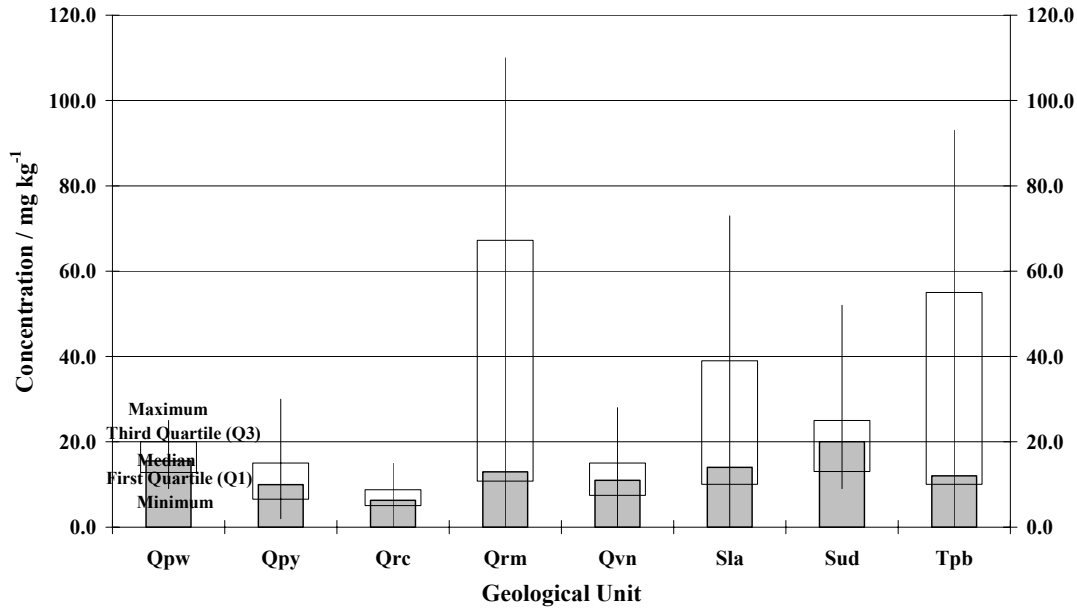


Figure 4.4. Summary statistics for lead in various geological units of Melbourne, Australia

Tpb, which is a Tertiary aged geological unit formed in a sedimentary non-marine environment consisting of fluvial: gravel, sand and silt [291]. Generally, the geological units containing clay have higher median nickel concentrations than those soils derived from sandstone, siltstone and sandy parent materials. These results are consistent with data presented by Cannon [293] who has stated that the order of increasing nickel content in various parent materials is sandstone (2 mg kg^{-1}), granitic igneous (8 mg kg^{-1}), limestone (20 mg kg^{-1}), black shales (50 mg kg^{-1}), shales/clays (68 mg kg^{-1}), basaltic igneous (140 mg kg^{-1}) and ultramafic igneous (2000 mg kg^{-1}). Data from McGrath and Loveland [294] are also consistent indicating that the median nickel concentration increases according to the following soil textures: peaty (6.6 mg kg^{-1}), sandy (7.5 mg kg^{-1}) coarse loamy (15.8 mg kg^{-1}), coarse silty (22.4 mg kg^{-1}), fine silty (28.2 mg kg^{-1}), fine loamy (25.3 mg kg^{-1}) and clay (38.2 mg kg^{-1}). Other researchers have reported average nickel concentrations between 20 and 40 mg kg^{-1} [59,302-303], however, many do not classify their results by soil or parent geology type.

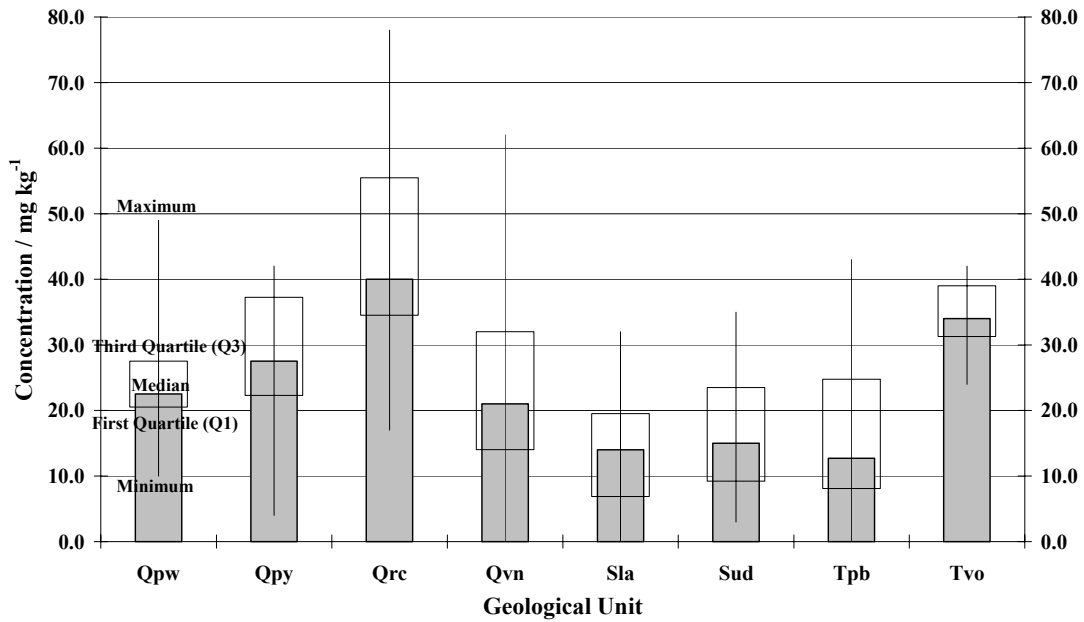


Figure 4.5. Summary statistics for nickel in various geological units of Melbourne, Australia

4.1.6 Zinc

The median zinc concentrations in nine geological units of Melbourne, Australia range from 19 to 42 mg kg⁻¹ and the concentrations are summarised in Figure 4.6. The highest zinc concentration occurs in Qpw which is a Quaternary Pleistocene aged material which formed in a sedimentary non-marine environment consisting of Aeolian dune deposits: sand, clay and calcareous sand [291]. The lowest median zinc concentration is exhibited in Tvo, which is a Tertiary aged material formed in an igneous extrusive environment consisting of tholeiitic and minor alkaline basalts [291]. Median zinc concentrations do not vary greatly within the nine geological units and appear to have relatively low concentrations compared to literature values. Mean zinc contents vary from 40 mg kg⁻¹ in acid rocks (granites) to 100 mg kg⁻¹ in basaltic rocks [304]. In sedimentary rocks, the highest zinc contents are found in shales and clayey sediments (80 to 120 mg kg⁻¹), whereas sandstones, limestones and dolomites generally have lower contents, ranging from 10 to 30 mg kg⁻¹ [296]. The results summarised in Figure 4.6 appear to be consistent with literature values for sandy materials like sandstones and limestones [296], however, results for clayey sediments appear to be lower than expected [296].

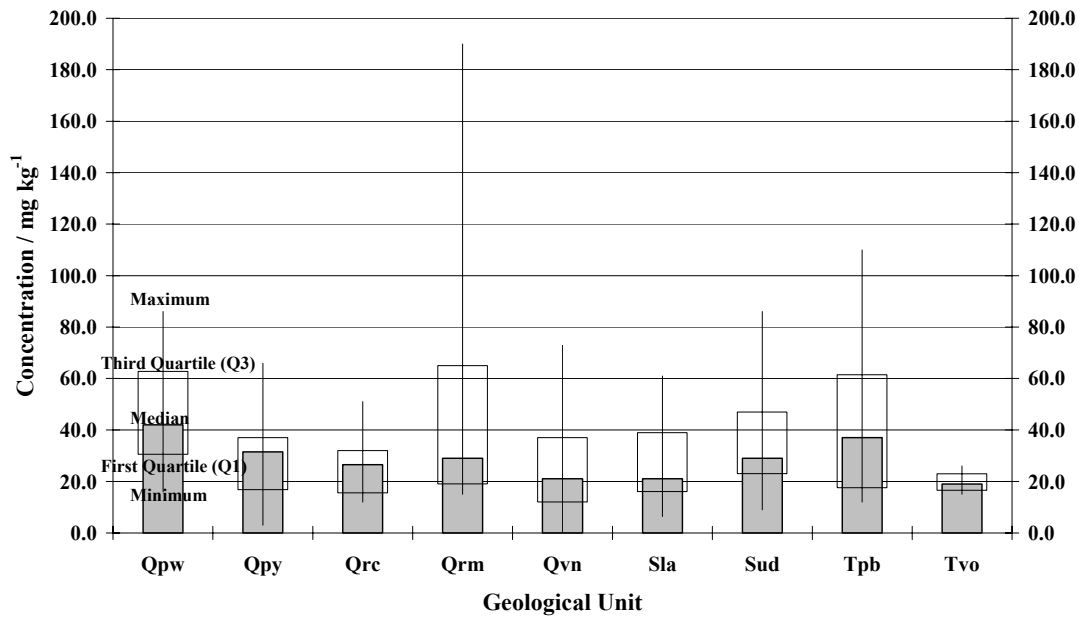


Figure 4.6. Summary statistics for zinc in various geological units of Melbourne, Australia

4.2 Arsenic Sorption

Each of the four soil types used in the experiments was characterised using the methods described in Section 3.2.1. The four soils were characterised in terms of “bolus” texture [80] (including approximate clay and silt content), colour (based on visual observation), pH [285,305], electrical conductivity (EC) [283,305], moisture content [306], total organic carbon (TOC) [307] and the extracted Fe and Al concentration [285]. The “bolus” texture [80] classification system has been defined in terms of clay, silt and sand particle size, which is discussed and compared to other soil classification systems in Section 2.2. These chemical and physical properties were studied in order to determine the influence of arsenic sorption/release for each of the soils.

The results presented in Table 4.1 reveal that the light clay (S2) has the highest clay content, followed by silt loam (S4), clay loam (S1) and sand (S3). The same trend was observed for pH and EC with each of these parameters exhibiting a direct proportionality to the clay content. It appears that soils with a high clay content are likely to contain exchangeable cations which means that the soil is able to conduct electricity more efficiently, resulting in higher EC values [308-309]. For the same reason, pH in a high clay content soil is also influenced by the cations that are present,

e.g. in soils depleted of basic cations (i.e. sodium carbonate or calcium carbonate), aluminium becomes increasingly soluble because of the decreasing pH and is absorbed in preference to hydrogen on the permanent charge leaving hydrogen ions in solution which ultimately results in lower pH values [310]. Similar observations have been shown by others in that the soil EC depends on the soil porosity, soil moisture content, concentration of dissolved electrolytes in the soil, soil temperature, the amount and composition of colloids and the cation exchange capacity [309]. According to Domsch and Giebel [311] the EC primarily reflects soil moisture content and cation exchange capacity with the latter essentially depending on clay content and soil organic matter. These observations appear to be consistent with the results presented in Table 4.1, however, in the present case soil moisture content is not directly related to the soil clay composition possibly because the soil moisture content in these soils is fairly similar.

The extractable Fe and Al concentrations in the four soil types were also considered (Table 4.1). Soil types S1 and S4 have the highest concentration of extractable Fe and Al, followed by soil type S2 that still has high concentrations of extractable Fe and Al, followed lastly by soil type S3 that has extremely low concentrations of extractable Fe and Al. It appears that the extractable Fe and Al concentration is not related to the clay content, pH or EC. However, the results in Table 4.1 indicate a general trend with the extractable Fe and Al concentration increasing with an increase in moisture content and TOC.

Table 4.1. Soil type characterisation.

Soil Type	S1	S2	S3	S4
Bolus Texture Grade	Clay Loam	Light Clay	Sand	Silt Loam
Clay Content / %	10-15	35-40	<5	25
Silt Content / %				>25
Colour	Grey/brown	Light brown	Yellow/brown/grey	Dark brown
pH at 20°C	6.14	8.16	5.83	7.63
EC / mS cm⁻¹	0.24	0.53	0.05	0.52
Moisture Content / %	6.9	1.7	0.2	3.8
TOC / %	6.36	3.23	0.07	6.18
Extracted Fe / mg L⁻¹	3800	1600-2200	6.9	2500-4000
Extracted Al / mg L⁻¹	4800	1300-1400	12-14	1100-1600

4.2.1 The Effect of Soil Type on As₂O₃ Sorption

A number of experiments were conducted to determine the effect of soil type on As₂O₃ sorption. In the first instance a preliminary study was conducted and this is discussed in Section 4.2.1.1. Further analyses were conducted in Section 4.2.1.2 which involved altering the spiking method to allow a greater exposure time for the soil to sorb As₂O₃.

4.2.1.1 Preliminary Study on the Effect of Soil Type on As₂O₃ Sorption

Having characterized each of the four soil types it was possible to determine in a preliminary sense, the effect of soil type on the sorption of As₂O₃. Each of the soil types was spiked with As₂O₃ in replicate as described in Section 3.2.1. At each of the six different spiking levels, the recoverable total arsenic, As^{Tot}, was determined for the blank sample, As^{Blk}, as well as the average total arsenic concentration, As^{Ave}, calculated from seven replicates for each of the four soil types. The standard deviation, As^{St. Dev.}, and the adjusted sample concentration, As^{Adj}, (i.e. As^{Ave} minus the background concentration) were calculated. In addition, the percentage of arsenic sorbed by each soil type, As^{Tot}(sorb), was calculated using Equation 4.1.

$$\%As^{Tot}(\text{sorb}) = \frac{As^{Blk} - As^{Adj}}{As^{Blk}} \times 100 \quad (4.1)$$

The average percentage of total arsenic sorbed by each soil type was also calculated by averaging each of the %As^{Tot}(sorb) values in each of the six systems. The average percentage %As^{Tot}(sorb) values clearly show that each of the soil types sorbs a different amount of As₂O₃ with S1, S2 and S4 having a %As^{Tot}(sorb) of approximately 19.6%, 2.9% and 38.2% respectively. For soil type S3 the value of %As^{Tot}(sorb) is below the method detection limit. The results for each of the soil types are presented in Table 4.2 and are represented graphically in Figures 4.7 to 4.10 with each discussed in detail below².

Figure 4.7 is a plot of the recoverable As^{Tot} concentration versus the spiked As₂O₃ concentration for soil type S1 and the corresponding blank which contains no soil. It can be seen that when S1 and the blank are spiked at the same concentration, the clay

² Figures 4.7 to 4.10 are also represented in Appendix C for comparative purposes.

Table 4.2. Effect of soil type on As₂O₃ sorption.

System		Spiked [As ₂ O ₃]	Recoverable As ^{Tot} in S1	Recoverable As ^{Tot} in S2	Recoverable As ^{Tot} in S3	Recoverable As ^{Tot} in S4
1	As ^{Blk} / mg L ⁻¹	0	0.01	ND	0.01	ND
	As ^{Ave} / mg L ⁻¹	0	0.59	0.53	0.04	0.11
	As ^{St. Dev.} / mg L ⁻¹		0.08	0.07	0.02	0.05
	As ^{Adj} / mg L ⁻¹		ND	ND	ND	ND
	%As ^{Tot} (sorb)		ND	ND	ND	ND
2	As ^{Blk} / mg L ⁻¹	1	0.85	1.04	0.91	1.06
	As ^{Ave} / mg L ⁻¹	1	1.43	1.53	1.15	0.57
	As ^{St. Dev.} / mg L ⁻¹		0.18	0.12	0.11	0.08
	As ^{Adj} / mg L ⁻¹		0.84	0.99	1.11	0.46
	%As ^{Tot} (sorb)		2.2	4.3	ND	56.8
3	As ^{Blk} / mg L ⁻¹	2	2.07	1.99	2.11	1.74
	As ^{Ave} / mg L ⁻¹	2	2.21	2.54	2.20	1.23
	As ^{St. Dev.} / mg L ⁻¹		0.09	0.06	0.05	0.09
	As ^{Adj} / mg L ⁻¹		1.62	2.01	2.16	1.12
	%As ^{Tot} (sorb)		21.7	ND	ND	35.3
4	As ^{Blk} / mg L ⁻¹	3	3.15	3.05	3.07	2.99
	As ^{Ave} / mg L ⁻¹	3	2.94	3.54	3.25	2.15
	As ^{St. Dev.} / mg L ⁻¹		0.16	0.11	0.08	0.13
	As ^{Adj} / mg L ⁻¹		2.34	3.01	3.21	2.05
	%As ^{Tot} (sorb)		25.5	1.5	ND	31.4
5	As ^{Blk} / mg L ⁻¹	4	4.26	3.91	4.06	4.13
	As ^{Ave} / mg L ⁻¹	4	3.71	4.55	4.28	2.82
	As ^{St. Dev.} / mg L ⁻¹		0.10	0.09	0.13	0.13
	As ^{Adj} / mg L ⁻¹		3.12	4.02	4.24	2.72
	%As ^{Tot} (sorb)		26.6	ND	ND	34.2
6	As ^{Blk} / mg L ⁻¹	5	5.16	4.87	5.02	5.33
	As ^{Ave} / mg L ⁻¹	5	4.61	5.45	5.29	3.66
	As ^{St. Dev.} / mg L ⁻¹		0.09	0.20	0.23	0.09
	As ^{Adj} / mg L ⁻¹		4.02	4.92	5.25	3.56
	%As ^{Tot} (sorb)		22.1	ND	ND	33.3
Average %As^{Tot}(sorb)			19.6	2.9	ND	38.2

Notes: As^{Tot} = total arsenic, As^{Blk} = arsenic concentration in blank, As^{Ave} = average of the total arsenic concentration in seven replicates, As^{Adj} = adjusted As^{Ave} (i.e. As^{Ave} minus background concentration), As^{Tot}(sorb) = total arsenic sorbed and ND = not detected.

loam has a lower As^{Tot} compared to that of the blank. In addition, as the concentration of the spike is increased the As^{Tot} concentration in the clay loam decreases compared to

the blank. These data suggest that the clay loam sorbs a proportion of the As_2O_3 and so during the extraction process not all As^{Tot} is released, as was the case of the blank.

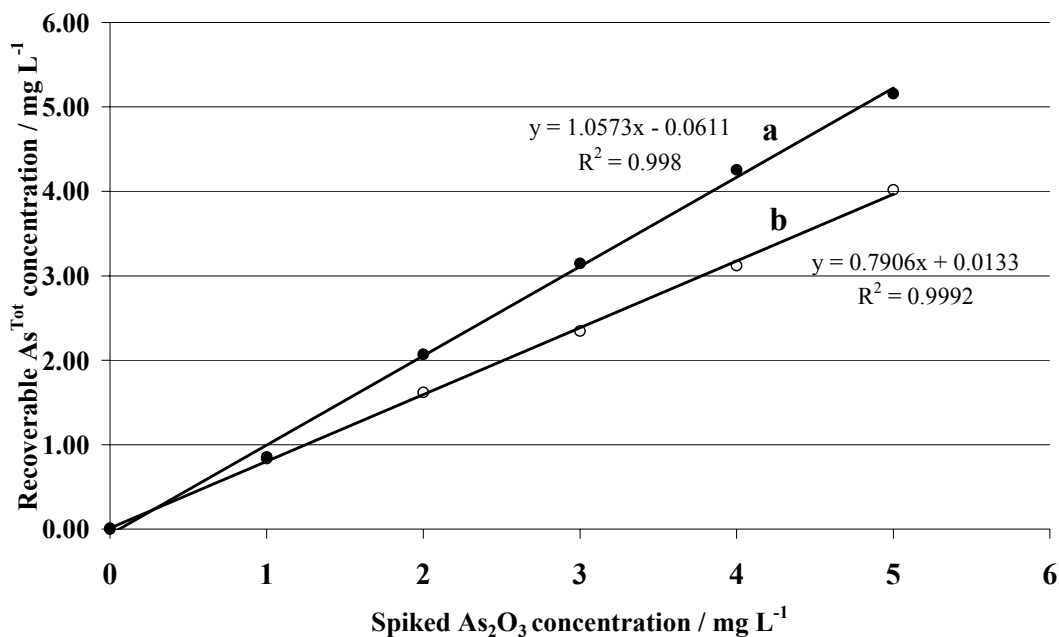


Figure 4.7. Recoverable As^{Tot} in: (a) blank and (b) soil type S1 versus the spiked As_2O_3 concentration (mg L^{-1}). Solid lines are plotted from the regression analysis.

Figure 4.8 is a plot of the recoverable As^{Tot} concentration versus the spiked As_2O_3 concentration for soil type S2 and the corresponding blank which contains no soil. In this case the light clay and blank show very similar recoverable As^{Tot} concentrations, which suggests that the light clay does not sorb or retain a significant amount of the As_2O_3 that was added. The calculated average % As^{Tot} (sorb) between the clay loam and the corresponding blank is 2.9% (see Table 4.2). This is an unexpected result considering that the light clay contains the highest clay content compared to the three other soils. This discrepancy may reflect the spiking method used for this part of the experiment. The spiking method consisted of adding a quantity of As_2O_3 to the soil sample using an auto pipette and allowing a short exposure time for the soil to sorb As_2O_3 . In this case the light clay appears to require more time for As_2O_3 to sorb onto its particles than was required in the other soil types.

The recoverable As^{Tot} concentration versus the spiked As_2O_3 concentration for soil type S3 and the corresponding blank which contains no soil has been plotted in Figure 4.9. In this case the sand and blank show similar recoverable As^{Tot} concentrations that

suggest the sand retains little of the As_2O_3 that was added. It is anticipated that the amount of As_2O_3 sorbed and subsequently retained by the sand would be extremely low

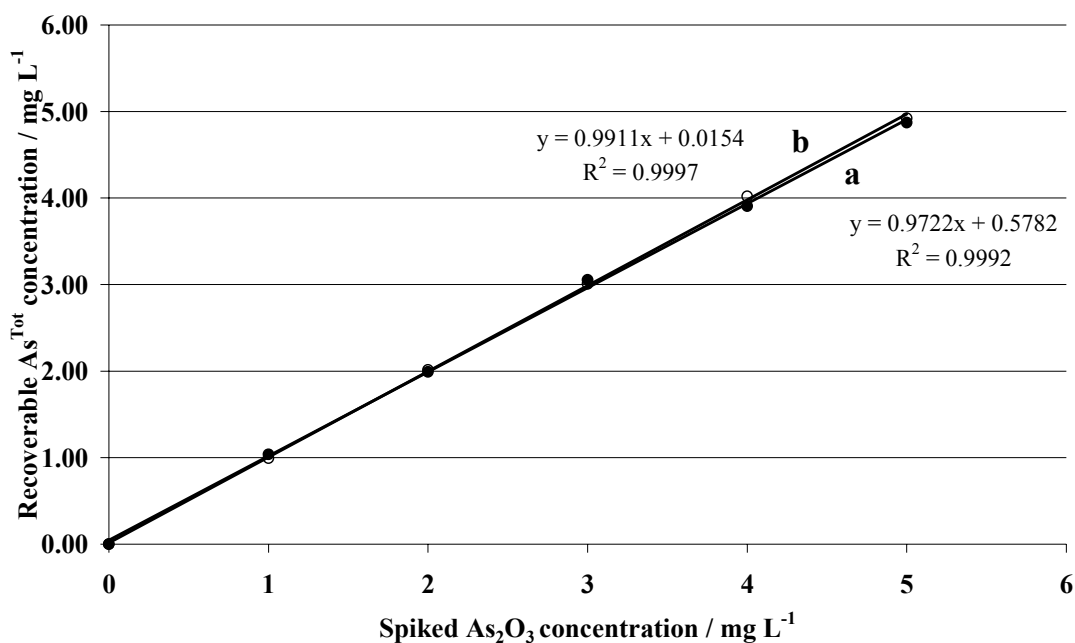


Figure 4.8. Recoverable As^{Tot} in: (a) blank and (b) soil type S2 versus the spiked As_2O_3 concentration (mg L^{-1}). Solid lines are plotted from the regression analysis.

which may be attributed directly to the repulsive interaction between the As_2O_3 and the negatively charged sand surface [312]. The composition of sand is such that it contains very little clay, silt and organic matter (as defined by the “bolus” texture [80] characterisation) that would allow the sorption of As_2O_3 . The average value of $\% \text{As}^{\text{Tot}}(\text{sorb})$ calculated for the case of sand is below the method detection limit.

In a similar manner to that of S1 (shown in Figure 4.7), Figure 4.10 is a plot of the recoverable As^{Tot} concentration versus the spiked As_2O_3 concentration for soil type S4 and the corresponding blank which contains no soil. It can be clearly seen that when S4 and the blank are spiked in the same manner, the silt loam has a lower As^{Tot} compared to that of the blank. As the level of the spike is increased, the recoverable As^{Tot} in the silt loam is decreased compared to the blank. Again, an explanation for this trend is that the silt loam sorbs a proportion of the As_2O_3 and that during the extraction process not all As^{Tot} is released, as in the case of the blank. According to the calculated average $\% \text{As}^{\text{Tot}}(\text{sorb})$ in Table 4.2, more As_2O_3 is sorbed by the silt loam (38.2%) compared to the clay loam (19.6%).

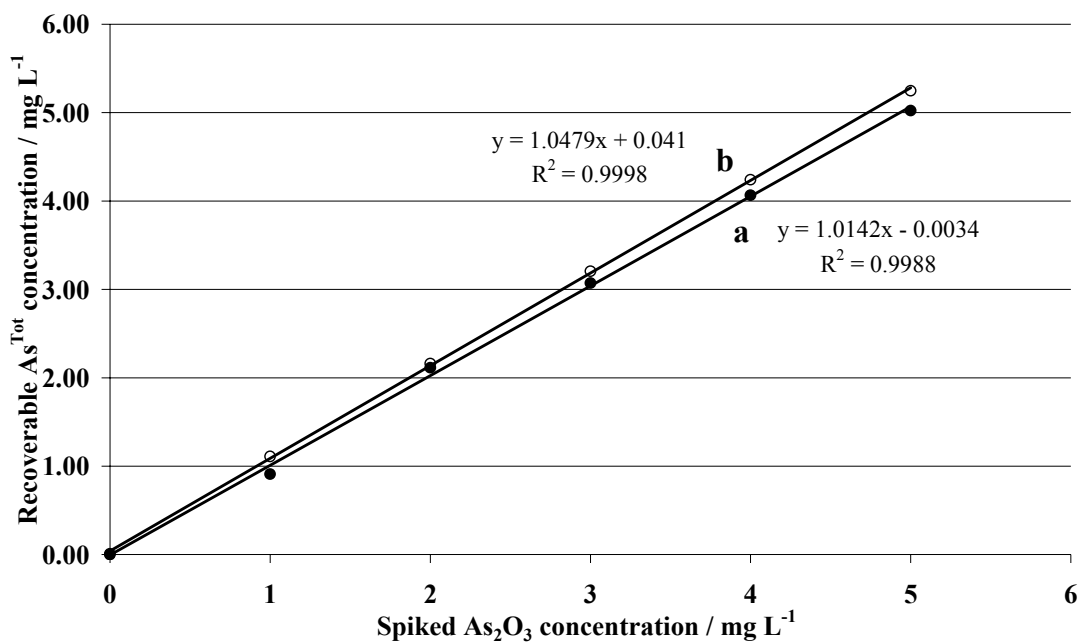


Figure 4.9. Recoverable As^{Tot} in: (a) blank and (b) soil type S3 versus the spiked As_2O_3 concentration (mg L^{-1}). Solid lines are plotted from the regression analysis.

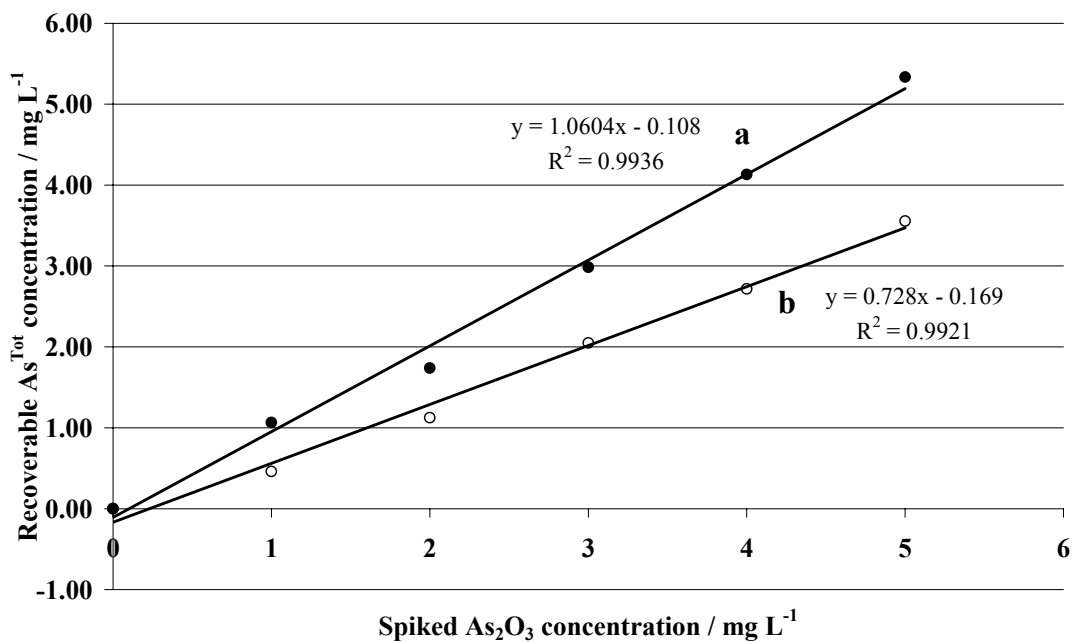


Figure 4.10. Recoverable As^{Tot} in: (a) blank and (b) soil type S4 versus the spiked As_2O_3 concentration (mg L^{-1}). Solid lines are plotted from the regression analysis.

From the data presented in Table 4.2 and Figures 4.7 to 4.10 it can be seen that the amount of As_2O_3 that is sorbed depends on the soil type. The extent of sorption is most likely related to the relative amount of clay, silt and sand which makes up the soil. Soils that have a high clay content have greater quantities of small soil particles which are generally less than 0.002 mm in diameter. These small soil particles provide a greater surface area that enables more As_2O_3 to be sorbed by the soil [313].

In a similar study to the current one, a study of three Californian arid-zone soils [314] indicated that a fine-loamy soil, which contained the highest surface area, percent clay, and levels of extractable Fe and Al, had the greatest arsenic sorption capacity. Other investigations [315-318] have also emphasised the importance of Fe(III) oxides in establishing the arsenic sorption capacity of soils. This general interpretation is supported by the investigations of Fordham and Norrish [317,319], who concluded that Fe(III) oxides such as $[\alpha]\text{-FeOOH}$ preferentially sorb As^{V} in soil, and by others [315-316,318], who found that the magnitude of As^{V} sorption in soil is in proportion to Fe(III) oxide content. The importance of iron oxide on arsenic sorption has been extensively reported in the literature and has shown to be consistent with the data presented in Table 4.2 of the current study. Soil type S4 was determined to have the highest arsenic sorption followed by S1, S2 and S3 that show a direct correlation to the extractable Fe and Al concentrations.

In the above case, the results for soil types S1, S3 and S4 appear to be consistent in that more As_2O_3 is sorbed by smaller clay soil particles and less As_2O_3 is sorbed by larger sand particles. The exception to this general trend was soil type S2 that has the highest clay content of the four soils but did not sorb the most As_2O_3 . It is possible that the spiking method adopted here that allows only a short exposure time for the soil to sorb As_2O_3 may have influenced the results obtained for S2 more than S1 and S4. As a result, further experiments were conducted to explore the reason for this discrepancy (see Section 4.2.1.2).

4.2.1.2 Further Analysis on the Effect of Soil Type on As_2O_3 Sorption

In order to investigate further the apparent discrepancy in results obtained for soil type S2 in Section 4.2.1.1 a series of additional experiments were embarked upon. These

experiments involved altering the spiking method to allow a greater exposure time for the soil to sorb As_2O_3 . The procedure for this modified As_2O_3 sorption method is described in Section 3.2.1. The results obtained using the modified As_2O_3 sorption technique indicated that the concentration of As_2O_3 sorbed by soil types S1, S2, S3 and S4 were 7.61, 8.40, 0.24 and 7.17 mg L^{-1} respectively at pH 2.3 and 20.3°C as presented in Figure 4.11.

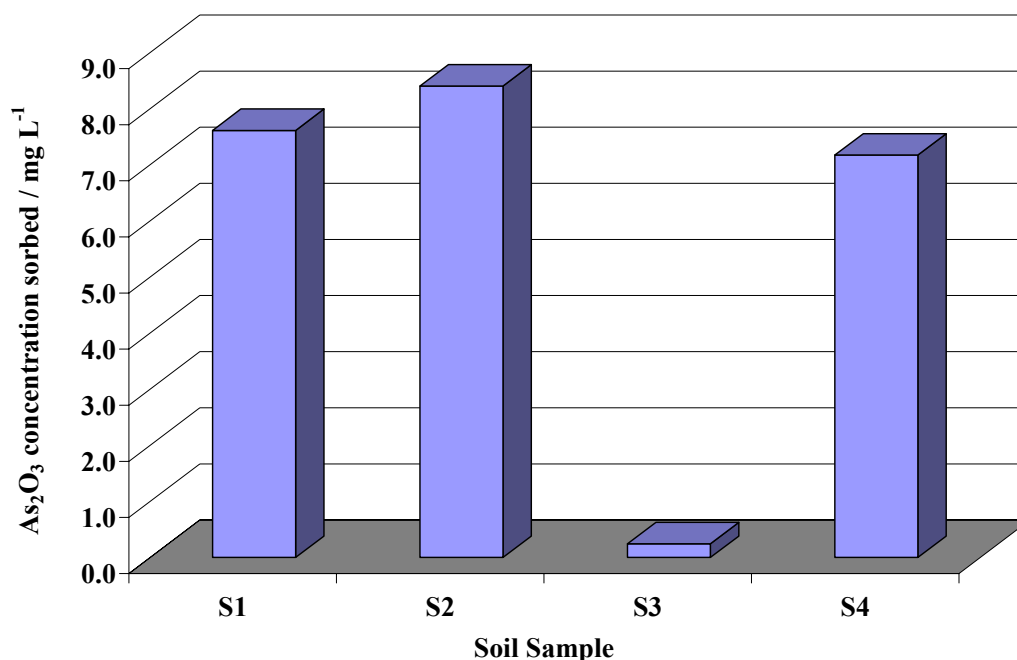


Figure 4.11. Average As_2O_3 sorbed in soil type S1, S2, S3 and S4 at pH 2.3 and 20.3°C

These results suggest that the modified spiking method made a significant difference to the sorption of As_2O_3 in all soil types, especially soil type S2. Soil types S1, S2, S3 and S4 using this method sorbed approximately 76 %, 84 %, 2.4 % and 72 % respectively of As_2O_3 which are significantly higher results than those obtained using the initial spiking method (see Section 4.2.1.1). These results generally appear to be more consistent with the notion that the amount of sorption is related to the relative amount of clay and silt that comprise the soil. When these results are compared to the soil characterisation data (see Table 4.1) it is evident that the As_2O_3 sorption of soil types S1, S2 and S4 correlate fairly well with the clay content, pH and EC values. In addition, soil type S3 which consists of mainly sand, has very low pH and EC values and sorbs far less As_2O_3 than the other three soil types. It is also noted that the soils with the higher As_2O_3 sorption qualities generally exhibited higher concentrations of extractable Fe and Al

concentrations, however, this relationship was not directly related as was the case in the preliminary experiment (Section 4.2.1.1).

4.2.2 Time Dependency of As_2O_3 Sorption on Soil

An experiment was conducted to determine the effect of time on the sorption of As_2O_3 by soil. For this experiment soil type S2 was selected and left to soak in an aqueous As_2O_3 solution (10 mg L^{-1}) for time periods 0, 0.5, 24, 48 and 168 h as described in Section 3.2.2. The results for this experiment indicate that the As_2O_3 sorption concentration starts at zero and increases rapidly to 4.74 mg L^{-1} (C_1) after approximately 30 min. After the first 30 min the As_2O_3 sorption process appears to slow down and As_2O_3 continues to be slowly sorbed, approaching a maximum sorption concentration (C_∞). From these observations it is suggested that the sorption process is in fact a two-step process as represented in Figure 4.12.

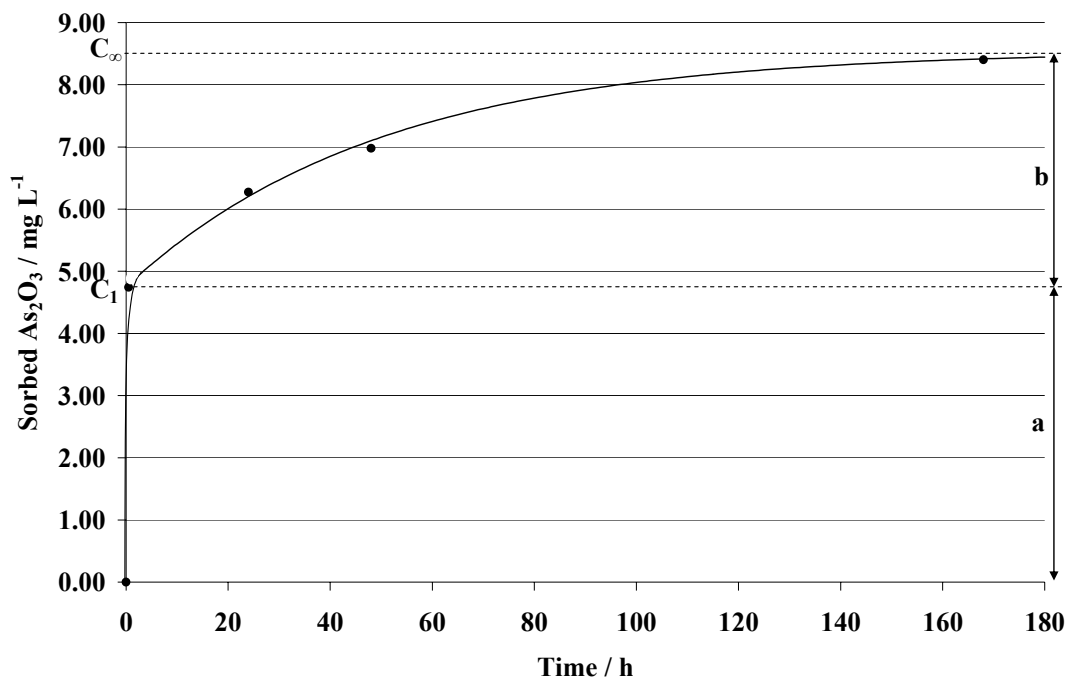


Figure 4.12. Plot of the sorbed As_2O_3 versus time showing: (a) the rapid first-step sorption process and (b) the slower second-step sorption process.

It was decided to test the slower second-step sorption process for first-order kinetic behaviour. In order to do this it was justifiably assumed that the first sorption process occurs instantaneously compared with the second process and so the latter process can

be treated kinetically as a separate process. The As_2O_3 sorption concentration after 30 min (i.e. C_1) was therefore subtracted from each concentration measured after 30 min in order to transpose the graph in preparation for kinetic analysis (see Figure 4.13).

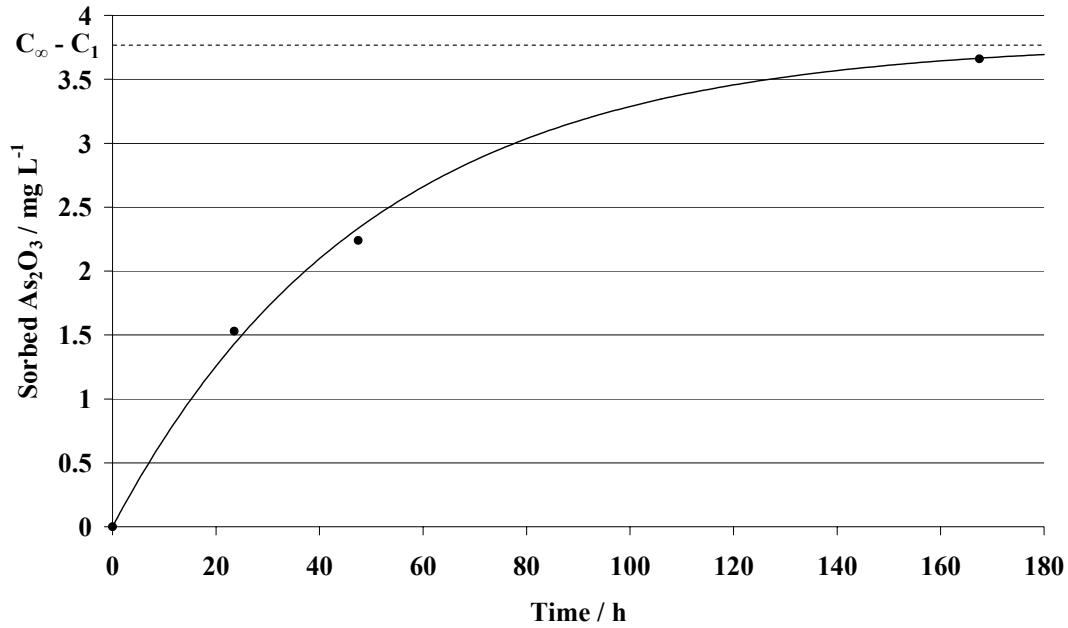


Figure 4.13. Plot of the As_2O_3 sorbed in the second-step sorption process versus time.

Assuming the rate of As_2O_3 sorption is proportional to the amount of As_2O_3 remaining in the solution at time t then:

$$\frac{dC}{dt} = -kC \quad 4.2$$

Where C is the concentration of As_2O_3 remaining in solution at time t , and k is a first-order rate constant. In particular: $C't = Ct - C_1$, where Ct is the concentration of sorbed As_2O_3 at time t . Therefore, $C = C_\infty - C_1 - C't$.

Equation 4.2 can be integrated between $t = 0$ and $t = t$ with corresponding limits of $(C_\infty - Ct)$ and $(C_\infty - C_1)$ as follows:

$$-k \int_0^t dt = \int_{C_\infty - C_1}^{C_\infty - Ct} \frac{dC}{C} \quad 4.3$$

$$-kt = \ln C \left| \begin{array}{l} C_{\infty} - Ct \\ C_{\infty} - C_1 \end{array} \right. \quad 4.4$$

$$-kt = \ln (C_{\infty} - Ct) - \ln (C_{\infty} - C_1) \quad 4.5$$

If the second-step sorption process follows first-order kinetics then, from Equation 4.5, a plot of $\ln (C_{\infty} - Ct)$ versus t will be a straight line of gradient $-k$, passing through a y-intercept of $\ln (C_{\infty} - C_1)$ as shown in Figure 4.14.

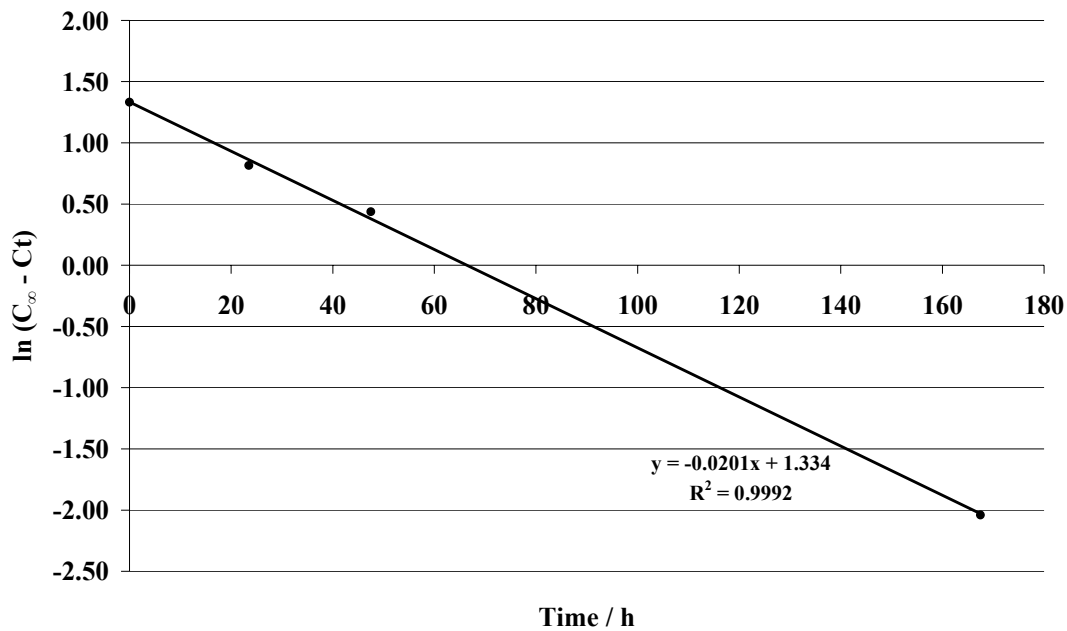


Figure 4.14. A plot of $\ln (C_{\infty} - Ct)$ for the second-step sorption process versus time. Solid lines are plotted for regression analysis.

In an alternative two-step soil sorption process, Grossl *et al.* [320] has proposed that the mechanism for oxyanion ($H_2AsO_4^-$ or $HCrO_4^-$) sorption on goethite is a two-step process resulting in the formation of an inner-sphere bidentate surface complex. The first step involves an initial ligand exchange reaction of the aqueous oxyanion with goethite, forming an inner-sphere monodentate surface complex. This first step produces relaxation signals associated with the fast relaxation time constant values. The succeeding step involves a second ligand exchange reaction, resulting in the formation of an inner-sphere bidentate surface complex. This step produces the signal associated with the slow relaxation time constant values. Other researchers [321-323] have also

reported the formation of inner-sphere bidentate binuclear complexes with the sorption of HAsO_4^{2-} on iron oxide surfaces analogous to the HPO_4^{2-} anion [324]. It would appear that these results [320] are consistent with the results presented in Figure 4.12 of the current study.

Raven *et al.* [95] and Fuller *et al.* [103] also reported the slow sorption kinetics of arsenate on ferrihydrite after an initial rapid sorption of 5 min. It was suggested [95] that the different relative reaction rates at low and high initial arsenic concentrations for arsenate sorption could relate to Extended X-ray Absorption Fine Structure (EXAFS) results [322,325-326], which have provided evidence that, at low surface coverage, arsenate is retained mainly by the formation of monodentate complexes on the iron oxide surface, and at high surface coverage arsenate binds to the surface mainly by the formation of bidentate binuclear and bidentate mononuclear complexes. It is possible that formation of the bidentate complexes at high surface coverage is slower than the predominantly monodentate reactions at low surface coverage. Raven *et al.* [95] indicated that the arsenic sorption kinetic data were generally best described by the parabolic diffusion equation. The results suggest that the reactions between arsenic and ferrihydrite were diffusion-controlled. Fuller *et al.* [103] reported that the time dependence of arsenate sorption on ferrihydrite could be described by a general model for diffusion into a sphere if a subset of surface sites located near the exterior of aggregates is assumed to attain equilibrium rapidly. Orthophosphate diffusion (analogous to H_2AsO_4^-) into ferrihydrite particles has been verified by electron microprobe analysis [327], however, the diffusion of arsenic into ferrihydrite particles has not been verified.

In a similar experiment [328], it was shown that the removal of As^{V} , from solution to soil, increases with time and attains saturation in approximately 35 min for hematite and approximately 60 min for feldspars with removal occurring rapidly in the initial stages and decreasing with time. The sorption of As^{V} onto hematite/feldspar was determined using mathematical modelling based on first-order kinetics. The same observation was reported by Smith *et al.* [329] who indicated that various soils were able to remove As^{V} rapidly and attain equilibrium in 1 h and that after the initial rapid removal, sorption of As^{V} continued at a slow and steady rate for the 72 h investigation. Other researchers have also reported similar findings for As^{V} sorption [316] and As^{III} sorption [315,330].

4.3 Bioavailability of Arsenic

The bioavailability of As^{Tot} was determined in each of the four soil types as described in Section 3.4. The method used was adapted from the geophagy digestion method [134-135] that has been used in the past to determine the nutrients made available to humans from eating clay. The results for the bioavailability experiment are presented in Table 4.3.

The results indicate that as the concentration of the As_2O_3 spike increases, the $\% As^{Bioavailability}$ also increases until it reaches a maximum value. Each soil type has different physical and chemical properties (shown in Table 4.1) which controls the amount of As^{Tot} bound by the soil. Clearly, the amount of As^{Tot} that is not tightly bound by the soil is the amount of As^{Tot} that is bioavailable. This applies for soil types S1, S2, S3 and S4 with the $\% As^{Bioavailability}$ approaching approximately 32%, 80%, 100% and 60% respectively. These results show that the composition of soils greatly affects the $\% As^{Bioavailability}$ which means that a 100% $As^{Bioavailability}$ does not occur in the case of many soils. Studies investigating the sorption of soluble arsenic ingested by humans suggest that close to 100% of soluble arsenic is sorbed from the gastrointestinal tract [16,123]. However, arsenic in soils generally exists as mineral forms or soil-arsenic complexes that will be incompletely solubilised during transit through the gastrointestinal tract. Research indicates that arsenic must be dissolved in order to be completely sorbed [124] which means that far less sorption of arsenic will occur from soil.

It is noted in System 1 of Table 4.3, where no As_2O_3 spike was added, that the results do not fit well with the rest of the data. Two plausible explanations for this irregularity are: (i) the total and bioavailable arsenic concentrations presented in Table 4.2 and Table 4.3 respectively are measured at very low concentrations which are close to the limit of the ICP-AES detection limit. These values may not be reliable for data analysis purposes and ultimately may affect the calculated $\% As^{Bioavailability}$; and (ii) that the arsenic present is the background concentration which may exist as a different species to that of As_2O_3 . This may affect the $\% As^{Bioavailability}$ calculation and, as a result, System 1 data (from Table 4.3) were not used in data analyses.

The results in Table 4.3 indicate that the sorption process is not an equilibrium process because the calculated ratio (R) of the % As^{Bioavailability} to the % As^{Non-bioavailability} varies with the concentration of the As₂O₃ spike. If these ratios were partition coefficients they would be expected to remain constant. In particular, the relationship between % As^{Bioavailability} versus the concentration of As₂O₃ spike, s, is derived in Equations 4.6 and 4.7.

Let $b = \% \text{As}^{\text{Bioavailability}}$

$$\text{Then } b/(s - b) = K \quad (4.6)$$

$$\text{whence } b = [K/(1 + K)] s \quad (4.7)$$

Thus a plot of % As^{Bioavailability} versus s should give a straight line with slope equal to $K/(1 + K)$.

A plot of % As^{Bioavailability} versus s for the four soil types has been presented in Figure 4.15. A linear relationship is not obtained (see Figure 4.15) suggesting that the amount of As₂O₃ tightly bound to the soil is less than that which occurs at lower spiked concentrations. This could be due to competition for sorption sites on the soil at higher As₂O₃ concentrations.

Moreover, tangents at $s = 0$ on the plot of % As^{Bioavailability} versus s can be used to estimate the values of the partition coefficients. The calculated tangent $m = K/(1 + K)$, so that $K = m/(1 - m)$.

The estimated tangent and the calculated partition coefficient at $s = 0$ are shown in Table 4.4.

A study conducted by Oomen *et al.* [133] compared five *in vitro* digestion models using three different soil types to assess the bioaccessibility of As, Pb and Cd. One of the digestive models evaluated (called the ‘SBET’ method) is similar to the geophagy digestion method [134-135] in that they both simulate a stomach (gastric) digestion system that does not take into account the intestinal compartment. These methods are quite significant for bioavailability studies because they provide an extremely simple

Table 4.3. Bioavailability results.

System	Sample	Spiked [As ₂ O ₃]	GEOPHAGY EXTRACTION			
			S1	S2	S3	S4
1	As ^{Ave} / mg L ⁻¹	0	0.03	0.02	0.03	0.12
	As ^{St. Dev.} / mg L ⁻¹		0.01	0.01	0.02	0.05
	% As ^{Bioavailability}		4.4	3.8	68.6	~ 100
2	As ^{Ave} / mg L ⁻¹	1	0.18	0.70	1.07	0.09
	As ^{St. Dev.} / mg L ⁻¹		0.02	0.02	0.01	0.06
	% As ^{Bioavailability}		12.8	45.7	93.4	15.0
	% As ^{Non-bioavailability}		87.2	54.3	6.6	85.0
	R		0.147	0.843	14.08	0.177
3	As ^{Ave} / mg L ⁻¹	2	0.43	1.54	2.14	0.53
	As ^{St. Dev.} / mg L ⁻¹		0.02	0.04	0.03	0.05
	% As ^{Bioavailability}		19.6	60.5	97.3	43.4
	% As ^{Non-bioavailability}		80.4	39.5	2.7	56.6
	R		0.244	1.534	35.65	0.768
4	As ^{Ave} / mg L ⁻¹	3	0.75	2.47	3.20	1.06
	As ^{St. Dev.} / mg L ⁻¹		0.02	0.04	0.05	0.05
	% As ^{Bioavailability}		25.4	69.8	98.5	49.2
	% As ^{Non-bioavailability}		74.6	30.2	1.5	50.8
	R		0.340	2.307	67.52	0.969
5	As ^{Ave} / mg L ⁻¹	4	1.08	3.41	4.23	1.64
	As ^{St. Dev.} / mg L ⁻¹		0.02	0.06	0.05	0.14
	% As ^{Bioavailability}		29.1	75.0	98.7	58.2
	% As ^{Non-bioavailability}		70.9	25.0	1.3	41.8
	R		0.411	2.998	75.69	1.391
6	As ^{Ave} / mg L ⁻¹	5	1.44	4.30	5.25	2.32
	As ^{St. Dev.} / mg L ⁻¹		0.05	0.06	0.05	0.15
	% As ^{Bioavailability}		31.3	78.9	99.3	63.3
	% As ^{Non-bioavailability}		68.7	21.1	0.7	36.7
	R		0.456	3.745	152.3	1.722

Notes: As^{Ave} = Average As₂O₃ concentration in seven replicates, As^{St. Dev.} = standard deviation for As^{Ave}, % As^{Bioavailability} = percentage As₂O₃ bioavailability which is calculated by dividing As^{Ave} from Table 4.2 by As^{Ave} from this table, % As^{Non-bioavailability} = 100 - % As^{Bioavailability} and R (Ratio) = % As^{Bioavailability} divided by % As^{Non-bioavailability}

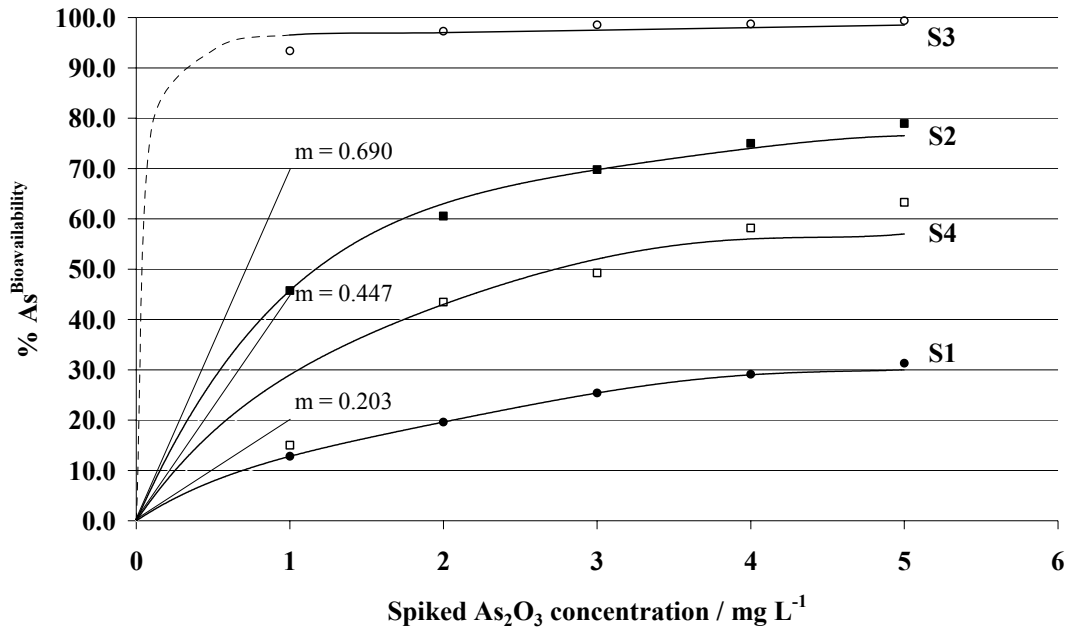


Figure 4.15. A plot of % $As^{Bioavailability}$ versus the spiked As_2O_3 concentration ($mg L^{-1}$).

Table 4.4. Table of estimated partition coefficients.

Soil Type	Tangent at $s = 0$	Estimated Partition Coefficient
S1	0.203	0.255
S2	0.690	2.228
S4	0.447	0.809

extraction process that can be performed quickly, inexpensively and in large batches [40,133]. This can not be achieved for some of the more complicated models that simulate the full gastrointestinal system of the human body [133]. Oomen *et al.* [133] found that the combination of a low pH in the stomach compartment and the absence of an intestinal compartment probably results in higher bioaccessibility values (i.e. more conservative), especially in the case of Pb and Cd. However, the results for arsenic are more consistent with values from the other research groups who used the other four, more complex, gastrointestinal digestion models. It was concluded that arsenic appears to show less difference in bioaccessibility between gastric and gastrointestinal digestion models. The bioaccessibility values are in many cases lower than 50%, indicating that

reduction of bioavailability by a decreased bioaccessibility can be significant. Bioaccessibility also appears to depend on contaminant and soil type, supporting the hypothesis that site-specific approaches are required [40,133,331]. This is in agreement with the current study which indicates that the soil type has a significant effect on the % As^{Bioavailability} (see Table 4.3) and that % As^{Bioavailability} can be far less than the conservative assumption of 100%.

4.4 Speciation Investigations

Several methods have been employed to investigate the speciation of phosphorus and arsenic under a variety of conditions. A particular focus of these investigations is to delineate the relationship between species both within and between the different sets of conditions (*gaseous/in vacuo*, solution, soil). The methods employed involve ESI-MS, supported by high-level computational chemistry, and a wet chemistry technique for isolating As^{III} species from As^V. These studies have been conducted with a view to delineating both qualitative and quantitative aspects of arsenic speciation.

4.4.1 Electrospray Mass Spectrometry

These experiments (described in Section 3.4) were conducted to investigate the potential of ESI-MS to identify and characterise phosphorus (benchmark) and arsenic species that originate from aqueous solutions of dissolved salts. In this regard, the starting species introduced into the instrument were the disodium salts of HPO₄²⁻ and HAsO₄²⁻.

4.4.1.1 Phosphate Speciation

Figure 4.16 shows the phosphorus species detected. These are tabulated together with their relative abundance in Table 4.5. Two out of the five major peaks obtained in the phosphorus spectrum are attributed to the monomeric species PO₃⁻ and H₂PO₄⁻. These are of most interest in the current study for benchmarking to arsenic. The remaining peaks are attributed to polymeric species that are more characteristic of phosphorus rather than arsenic chemistry [332]. Such species are of less importance for the present comparative study³. Notably, the ‘starting’ species HPO₄²⁻ does not appear in the

³ By analogy with the subsequent arsenic results it is assumed that the peak assigned to PO₃⁻ at *m/z* = 78.9 is not the cyclic P₃O₉³⁻ trimer.

spectrum having been converted into PO_3^- and H_2PO_4^- . A postulated mechanism for this is depicted in Equations 4.8 and 4.9:

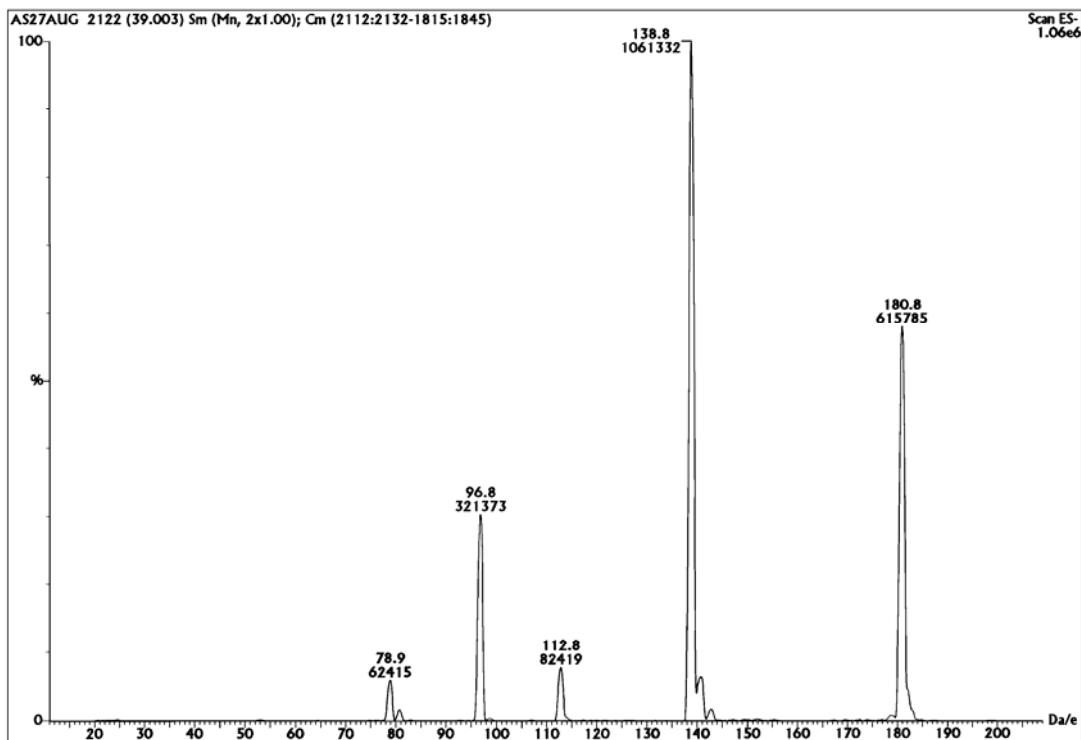


Figure 4.16. The ESI-MS difference spectrum obtained between anhydrous disodium hydrogen orthophosphate (Na_2HPO_4) in water and the background THF/water. The spectrum was recorded in electrospray negative mode at cone voltage 30 V with 90% THF/water carrier solvent. Peaks were assigned as follows: $m/z = 78.9$, PO_3^- ; $m/z = 96.8$, H_2PO_4^- ; $m/z = 112.8$, $\text{NaP}_4\text{O}_{12}^{3-}$; $m/z = 138.8$, $\text{NaH}_2\text{P}_3\text{O}_{10}^{2-}$; and $m/z = 180.8$, $\text{Na}_2\text{P}_4\text{O}_{12}^{2-}$.

Note that the above mechanism requires H_3O^+ to be present in the instrument for the reaction to take place. Therefore, the same aqueous sample of Na_2HPO_4 was run in the *positive electrospray mode* to test for the presence of H_3O^+ . The spectrum shown in Figure 4.17 reveals that H_3O^+ was indeed present as water/hydronium ion clusters, $(\text{H}_2\text{O})_n\text{H}_3\text{O}^+$. It may be observed that the peaks form a regular pattern corresponding to the sequential addition of one water molecule to H_3O^+ [333-338] up to a total of 25

adducted H₂O molecules (n = 1 to 25). The peaks also form a characteristic [333-334] curve-like pattern with the relative abundance tending to decrease as m/z increases in the range investigated.

Table 4.5. Phosphorus and arsenic species identified in the ESI-MS spectra together with their relative abundance.

System	Species	Observed m/z	Calculated m/z	Relative Abundance
Na₂HPO₄	PO ₃ ⁻	78.9	79.0	5.9
	H ₂ PO ₄ ⁻	96.8	97.0	30.3
	NaP ₄ O ₁₂ ³⁻	112.8	113.0	7.8
	NaH ₂ P ₃ O ₁₀ ²⁻	138.8	139.0	100.0
	Na ₂ P ₄ O ₁₂ ²⁻	180.8	180.9	58.0
Na₂HAsO₄.7H₂O	AsO ₃ ⁻	122.8	122.9	16.4
	H ₂ AsO ₄ ⁻	140.9	140.9	100.0
NaAsO₂	AsO ₄ ³⁻	45.9	46.3	13.1
	*HAsO ₃ ²⁻	60.8	62.0	100.0
	AsO ₂ ⁻	106.7	106.9	97.5
	AsO ₃ ⁻	122.6	122.9	16.8
	H ₂ AsO ₃ ⁻	124.7	124.9	87.2
	H ₂ AsO ₄ ⁻	140.5	140.9	54.9

* Does not correspond exactly with the calculated m/z

4.4.1.2 Arsenic Speciation

Figure 4.18 shows the arsenic species detected using ESI-MS when an aqueous solution of Na₂HAsO₄.7H₂O was injected into the instrument. These species are also tabulated together with their relative abundance in Table 4.5. In this case, the two major peaks obtained in the arsenic spectrum are attributed to the monomeric species AsO₃⁻ and H₂AsO₄⁻ that may be taken as being analogous to the monomeric phosphorous species already mentioned in Section 4.4.1.1. Although, the formation of polymeric phosphorous species is well established in the literature, *vide supra*, this is not the case for arsenic and, correspondingly, no such species are observed. The ‘originating’

species, HAsO_4^{2-} , does not appear in the spectrum, having been converted into AsO_3^- and H_2AsO_4^- in an analogous manner as depicted by the phosphorous chemistry. These results are consistent with previous negative ion ESI-MS results for As^{V} [339]. Thus a postulated mechanism for the conversion is depicted in Equations 4.10 and 4.11:



Again, the test for H_3O^+ was conducted using the aqueous $\text{Na}_2\text{HAsO}_4 \cdot 7\text{H}_2\text{O}$ and was found to be almost identical to the spectrum of the aqueous sample of Na_2HPO_4 (see Figure 4.17), which indicated the presence of H_3O^+ as expected.

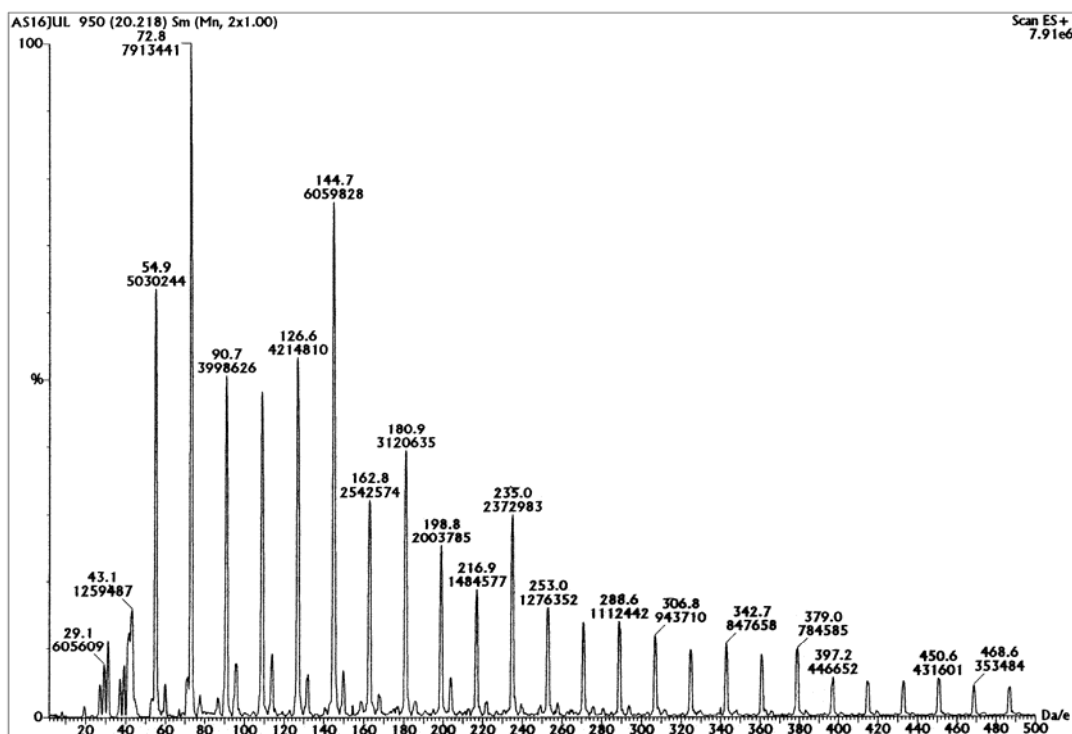


Figure 4.17. The ESI-MS spectrum of anhydrous di-sodium hydrogen orthophosphate (Na_2HPO_4) in water showing the water/hydronium ion clusters that form in electrospray positive mode. The spectrum was recorded at cone voltage 70 V with 90% THF/water carrier solvent. Peaks were assigned as shown in Table 4.6.

Table 4.6. Water/hydronium clusters identified in the ESI-MS spectra.

Observed m/z	Calculated m/z	Assigned Peaks
19.0	19.0	H ₃ O ⁺
37.0	37.0	(H ₂ O)H ₃ O ⁺
54.9	55.1	(H ₂ O) ₂ H ₃ O ⁺
72.8	73.1	(H ₂ O) ₃ H ₃ O ⁺
90.7	91.1	(H ₂ O) ₄ H ₃ O ⁺
108.8	109.1	(H ₂ O) ₅ H ₃ O ⁺
126.6	127.1	(H ₂ O) ₆ H ₃ O ⁺
144.7	145.1	(H ₂ O) ₇ H ₃ O ⁺
162.8	163.1	(H ₂ O) ₈ H ₃ O ⁺
180.9	181.2	(H ₂ O) ₉ H ₃ O ⁺
198.8	199.2	(H ₂ O) ₁₀ H ₃ O ⁺
216.9	217.2	(H ₂ O) ₁₁ H ₃ O ⁺
235.0	235.2	(H ₂ O) ₁₂ H ₃ O ⁺
253.0	253.2	(H ₂ O) ₁₃ H ₃ O ⁺
271.0	271.2	(H ₂ O) ₁₄ H ₃ O ⁺
288.6	289.2	(H ₂ O) ₁₅ H ₃ O ⁺
306.8	307.3	(H ₂ O) ₁₆ H ₃ O ⁺
324.8	325.3	(H ₂ O) ₁₇ H ₃ O ⁺
342.7	343.3	(H ₂ O) ₁₈ H ₃ O ⁺
361.0	361.3	(H ₂ O) ₁₉ H ₃ O ⁺
379.0	379.3	(H ₂ O) ₂₀ H ₃ O ⁺
397.2	397.3	(H ₂ O) ₂₁ H ₃ O ⁺
415.0	415.4	(H ₂ O) ₂₂ H ₃ O ⁺
433.0	433.4	(H ₂ O) ₂₃ H ₃ O ⁺
450.6	451.4	(H ₂ O) ₂₄ H ₃ O ⁺
468.6	469.4	(H ₂ O) ₂₅ H ₃ O ⁺

A similar investigation was conducted for an aqueous solution of NaAs^{III}O₂ (sodium meta arsenite) that was injected into the instrument. Figure 4.19 shows the spectrum that was recorded. In this case, the spectrum is not as clear as the spectrum obtained for arsenate and, consequently, only a limited number of peaks could be confidently assigned. These are tabulated together with their relative abundance in Table 4.5. The

peaks of particular interest are peaks obtained at $m/z = 106.7$ and $m/z = 124.7$ which are assigned as $\text{As}^{\text{III}}\text{O}_2^-$ and $\text{H}_2\text{As}^{\text{III}}\text{O}_3^-$ respectively. It is interesting to note in this case that the ‘originating’ species, AsO_2^- , does appear in the spectrum. This is in contrast to the originating species of the phosphate and arsenate systems, *vide supra*. A postulated mechanism for the reaction of the trivalent arsenic species is depicted in Equation 4.12:

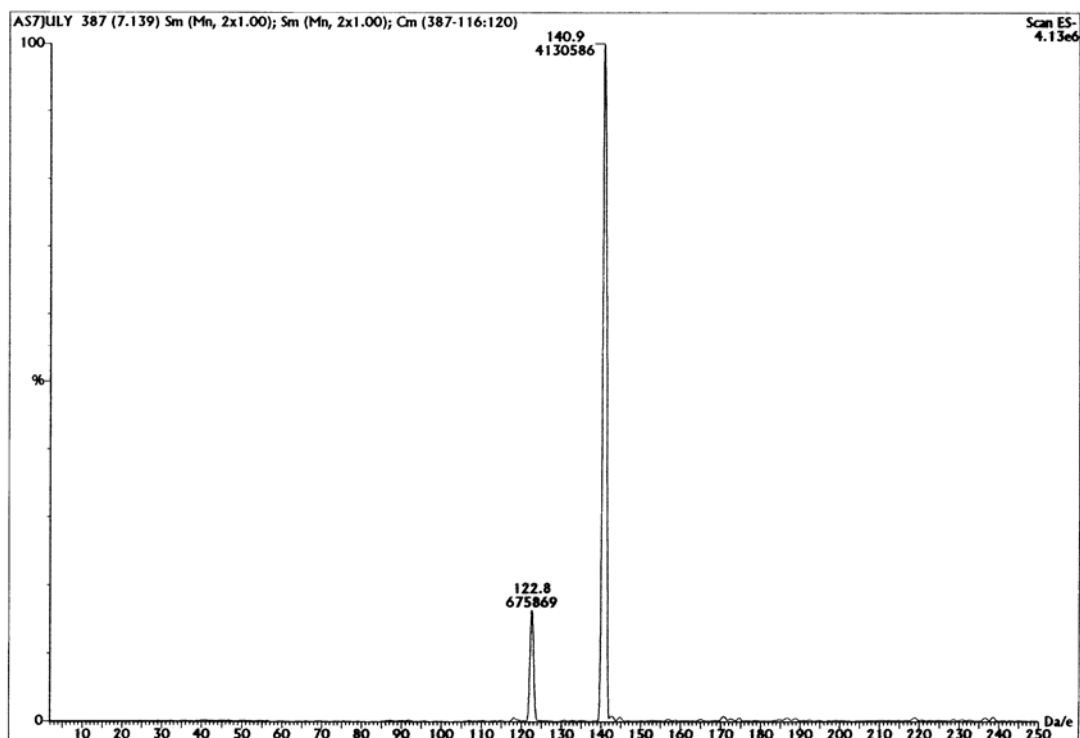


Figure 4.18. The ESI-MS difference spectrum obtained between di-sodium hydrogen arsenate heptahydrate ($\text{Na}_2\text{HAsO}_4 \cdot 7\text{H}_2\text{O}$) in water and the background THF/water. The spectrum was recorded in electrospray negative mode at cone voltage 30 V with 90% THF/water carrier solvent. Peaks were assigned as follows: $m/z = 122.8$, AsO_3^- ; and $m/z = 140.9$, H_2AsO_4^- .

Also, the peak observed at $m/z = 60.8$ is clearly a peak of interest since it has the highest relative abundance. However, the assignment of this peak is unclear, as it does not correspond precisely with any calculated m/z values for recognized arsenic species. However, it exhibits an m/z that is close to the calculated m/z of $\text{HAS}^{\text{III}}\text{O}_3^{2-}$ ($m/z = 62.0$). It is conceivable that “exotic” species, including radical species, are present. For example, the hydrogen atom of the latter species could be abstracted to give the radical

dianion ($\text{As}^{\text{III}}\text{O}_3\text{'}^{2-}$) (for which $m/z = 61.5$ – and is closer to the experimental value). However, it is beyond the scope of this thesis to pursue such species further.

Other peaks assigned at $m/z = 45.9$ ($\text{As}^{\text{V}}\text{O}_4^{3-}$), 122.6 ($\text{As}^{\text{V}}\text{O}_3^-$), 124.7 ($\text{H}_2\text{As}^{\text{V}}\text{O}_3^-$) and $m/z = 140.5$ ($\text{H}_2\text{As}^{\text{V}}\text{O}_4^-$) appear to provide evidence of the formation of oxidative contaminants or products. Such species may have been produced in the bottle containing the solid sample or in the aqueous stock solution. The former situation would appear to be more likely considering that As^{III} is susceptible to aerobic oxidation. However, As^{III} may persist in aerated water due to slow oxidation kinetics [340]. It is also possible that oxidation of As^{III} could have taken place on entering the ESI-MS ionisation chamber. However, a low cone voltage was used (i.e. 30 V) to reduce the likelihood of such oxidation. It has been demonstrated that lower cone voltages (i.e. ≤ 30 V) tend to preserve dissolved-phase speciation [341]. In light of the above findings, it is possible that ESI-MS may prove to be a suitable method to routinely assay the “oxidative purity” of such samples.

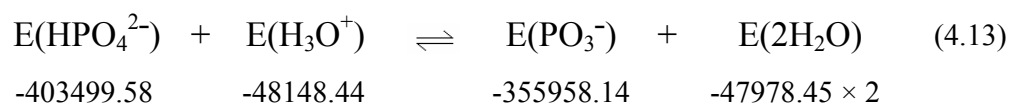
4.4.2 Computer Modelling of Phosphate, Arsenate and Arsenite

All species detected by the ESI-MS were modelled by high-level density functional calculations (see Section 3.4). The primary imperative is to provide supporting evidence for the reaction mechanisms proposed in Section 4.4.1 in terms of the relative energies of the species involved and the calculated reaction energies. However, in the course of these calculations, a considerable amount of further information on these species has been obtained and documented in this thesis (see Section 4.4.2.2).

4.4.2.1 Energies of Species and Reaction Energies

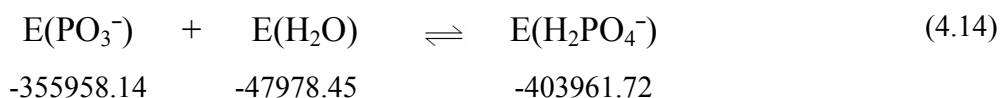
The calculated energies for each of the species detected in the ESI-MS experiments are given in Table 4.7. The reaction energies were calculated in each case for the phosphate, arsenate and arsenite systems by subtracting the reactant energies from the product energies.

In the case of the phosphate system, the suggested mechanism consists of the two processes that are represented by Equations 4.8 and 4.9. The reaction energy for each of these equations has been calculated as indicated below:



Reaction energy for Equation 4.13

$$= (-355958.14 - 95956.90) - (-403499.58 - 48148.44) = -267.02 \text{ kcal mol}^{-1}$$



Reaction energy for Equation 4.14

$$= (-403961.72) - (-355958.14 - 47978.45) = -25.13 \text{ kcal mol}^{-1}$$

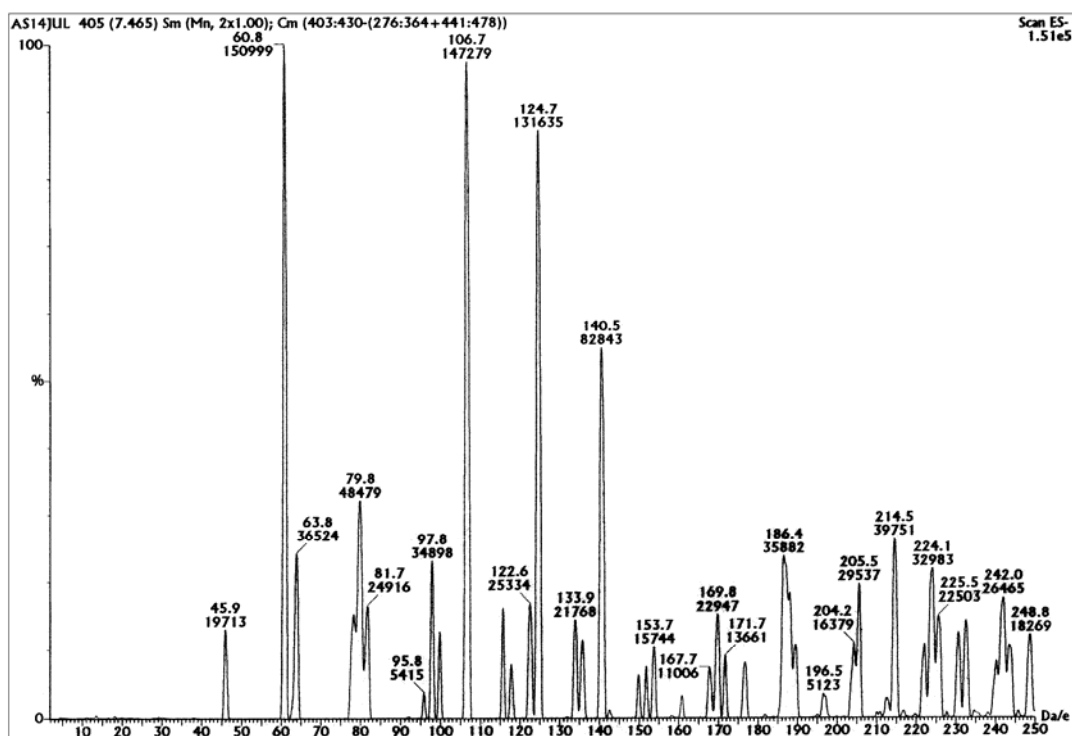


Figure 4.19. The ESI-MS difference spectrum obtained between sodium arsenite (NaAsO_2) in water (pH 7.5) and the background THF/water. The spectrum was recorded in electrospray negative mode at cone voltage 30 V with 90% THF/water carrier solvent. Peaks were assigned as follows: $m/z = 45.9$, AsO_4^{3-} ; $m/z = 60.8$, HAsO_3^{2-} ; $m/z = 106.7$, AsO_2^- ; $m/z = 122.6$, AsO_3^- ; $m/z = 124.7$, H_2AsO_3^- ; and $m/z = 140.5$, H_2AsO_4^- .

In Equation 4.13, the negative reaction energy, $-267.02 \text{ kcal mol}^{-1}$, indicates that the reaction favours the right hand side, i.e. the formation of the products PO_3^- and H_2O . The reaction proceeds further as shown in Equation 4.14 which, similarly, has the negative reaction energy, $-25.13 \text{ kcal mol}^{-1}$, favouring the formation of the product H_2PO_4^- . These results support the postulated mechanism for the formation of the monomeric phosphate species detected in the ESI-MS spectrum.

Using the phosphate system as a benchmark, analogous reaction energy calculations were carried out for the arsenate system. Thus using analogous calculations to those depicted in Equations 4.10 and 4.11, the calculated reaction energies for the arsenate system are $-265.10 \text{ kcal mol}^{-1}$ and $-22.30 \text{ kcal mol}^{-1}$ respectively. These reaction energies support the postulated reaction mechanism for the formation of the arsenic species detected in the ESI-MS spectrum. The magnitudes are also very similar to those for the phosphorous system. It is also of interest to note that when the relative energies of the phosphorus and arsenic species are compared it is evident that both AsO_3^- and H_2AsO_4^- are more stable than their phosphorous analogues, PO_3^- and H_2PO_4^- .

Similar reaction energy calculations were carried out for the arsenite system. The postulated mechanism is shown in Equation 4.12. Here, the calculated reaction energy is $-70.84 \text{ kcal mol}^{-1}$. Similar to the other systems already discussed, this reaction energy indicates that the equation favours the formation of the product H_2AsO_3^- , hence supporting the postulated mechanism.

Estimates for the equilibrium constants for reactions 4.3, 4.5 and 4.6 may be obtained in each case by taking the ratio of the relative energies of product to reactant. For example, a ratio for the energy of the two monomeric phosphate species detected in the ESI-MS was calculated by dividing the energy of H_2PO_4^- by the energy of PO_3^- as shown in Equation 4.15. The ratio gives a constant (K) equal to 1.13 indicating that the H_2PO_4^- species is slightly favoured over the PO_3^- species within the ESI-MS environment.

$$\frac{E(\text{H}_2\text{PO}_4^-)}{E(\text{PO}_3^-)} = \frac{-403961.72}{-355958.14} = 1.13 \quad (4.15)$$

Similarly, an energy ratio calculation was made for the two arsenate species detected in the ESI-MS (see Equation 4.16). In this case a value of $K = 1.03$ suggests that the H_2AsO_4^- species is slightly favored over the AsO_3^- species.

$$\frac{E(\text{H}_2\text{AsO}_4^-)}{E(\text{AsO}_3^-)} = \frac{-1592719.36}{-1544718.61} = 1.03 \quad (4.16)$$

The above estimates for the relative equilibrium constants (1.13 compared to 1.03 for phosphorous and arsenic respectively) reflect the relative abundances of the phosphorus species ($30.3/5.9 = 5.14$) compared to the arsenic species ($54.9/16.8 = 1.13$), Table 4.5. It must be born in mind, however, that this comparison is complicated by the presence of polymeric species in the case of phosphorus, presumably derived from PO_3^- .

4.4.2.2 Geometries

As part of the species energy and reaction energy calculations a number of geometries and other molecular information emerged for each of the phosphorus and arsenic species detected in the ESI-MS. These are clearly of interest and are presented, and compared to reported crystallographic data, in Table 4.7.

A feature of the computed PO_3^- species is that it forms a trigonal planar structure that is perfectly symmetrical with all bond angles at 120° and all bond lengths at 1.503 \AA . This might be, naively, unexpected - when one considers the valence bond representation where PO_3^- is represented with two double $\text{P}=\text{O}$ bonds and one single $\text{P}-\text{O}$ bond, see Chart 4.1. Therefore, the computed structure suggests that PO_3^- is a resonance structure with delocalised electrons, where the double and single bonds effectively average out. Thus the three computed $\text{P}-\text{O}$ (hybrid) bond lengths of 1.503 \AA are very close to the computed $\text{P}=\text{O}$ and $\text{P}-\text{O}^-$ bond lengths (both 1.500 \AA) of the *trans* isomer of the H_2PO_4^- species (that is also a monoanion⁴) and are essentially an average (1.500 \AA) of the computed $\text{P}=\text{O}$ and $\text{P}-\text{O}^-$ bond lengths of 1.513 \AA and 1.491 \AA respectively for the *cis* isomer of H_2PO_4^- , Table 4.7. The possibility of *cis* and *trans* isomers for the latter species and the implications of this are discussed in more detail

⁴ It is found that, for phosphorus and arsenic species, the $\text{P}(\text{As})-\text{O}$ bond lengths increase with an increase in charge. This is discussed further in the text.

later. This resonance is also reflected in the electrostatic potential energy map, Chart 4.1, as discussed later.

The AsO_3^- species is entirely analogous to PO_3^- in terms of its perfect trigonal symmetry and delocalised electrons, Chart 4.2. Thus the three bond lengths in AsO_3^- are identical at 1.655 Å. They are also considerably longer than the corresponding bond lengths in PO_3^- . Furthermore, the three As-O (hybrid) bond lengths of 1.655 Å are almost identical to the As=O and As-O⁻ bond lengths (both 1.654 Å) for the *trans* isomer of the H_2AsO_4^- species and are essentially an average (1.655 Å) of the computed P=O and P-O⁻ bond lengths of 1.644 Å and 1.665 Å respectively for the *cis* isomer of H_2AsO_4^- , Table 4.7.

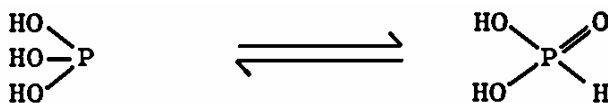
The computed geometries for the species HXO_4^{2-} (X = P, As) show distorted tetrahedral geometries with O-X-O angles ranging from 102.19 – 116.13° and 102.01 – 116.60° respectively, Table 4.7. These compare favourably with the crystallographic data [342] for these species of 102.7 – 114.2° and 102.7 – 113.7° respectively. The comparative X-OH, X=O and the X-O⁻ bond lengths in the computed species tend to be longer than the crystallographic values. This is particularly pronounced for X-OH. This is perhaps, not unexpected, given that the computed values are *in vacuo* and the crystallographic geometries are subject to crystal packing forces such as intermolecular hydrogen bonding. This argument is also true with respect to angles. In this regard, the computed structures for HXO_4^{2-} have a plane of symmetry that is broken in the crystal structures as reflected in the values for angles O=X-O⁻ and O⁻-X-OH in Table 4.7. For example, the computed values for the two O=P-O⁻ angles in HPO_4^{2-} are both identically 116.13°, whereas the corresponding angles in the crystal structure are 112.2° and 114.2°.

The computed geometries for the species H_2XO_4^- (X = P, As) also show distorted tetrahedral geometries, with O-X-O angles, including both *cis* and *trans* isomers, ranging from 100.91 – 126.25° and 100.00 – 128.67° respectively, Table 4.7. The upper values represent considerable distortion of the O=X-O⁻ angles in all cases and reflect the presence of strong intramolecular hydrogen bonds in the computed structures, as indicated in Chart 4.3. Notably, in the crystal structure of $\text{H}_2\text{XO}_4^{2-}$ the range of O-X-O angles is 106.5 – 115.5° [342] and 105.1 – 116.5° [343] respectively. The relief in distortion is probably due to the presence of competing intermolecular hydrogen bonding in the crystal structure. The computed X-OH, X=O and the X-O⁻ bond lengths

in the monoanions are shorter than in the previous HXO_4^{2-} dianions. This bond length dependency on formal charge has also been observed experimentally upon going from the dianion to the neutral H_3PO_4 [342]. For this reason the bond lengths and angles for the latter species have also been included in Table 4.7. The computed P-OH bond lengths are longer than in the crystal structure. Again, this is attributed to the presence of crystal packing forces, particularly intermolecular hydrogen bonding, in the latter case.

The two arsenite species, $\text{As}^{\text{III}}\text{O}_2^-$ and $\text{H}_2\text{As}^{\text{III}}\text{O}_3^-$, detected in the ESI-MS, exhibit interesting computed geometries as depicted in Chart 4.4. The AsO_2^- species forms a linear structure with equivalent As-O bond lengths of 1.721 Å. This appears to be elongated with respect to both the As=O and As-O⁻ bonds in $\text{H}_2\text{As}^{\text{V}}\text{O}_4^-$. However, it should be realized that arsenic species in the +III oxidation state are intuitively expected to exhibit a contraction of bond lengths with increasing oxidation state. Like PO_3^- and AsO_3^- , *vide supra*, AsO_2^- displays a delocalised electron configuration where the double and single bonds are effectively averaged out.

The H_2AsO_3^- species forms an interesting pyramidal shape, Chart 4.4, analogous to the shape of H_3PO_3 , that is proposed to be in equilibrium with its tetrahedral tautomer [287], i.e.:



In the latter structure, a proton has transferred from an oxygen atom to the phosphorus atom. Here, the tetrahedral structure is computed to be 11.11 kcal mol⁻¹ more stable than the pyramidal. This is consistent with the tetrahedral structure being reported [286-287] as the favoured equilibrium species. In this regard the pyramidal tautomer of the arsenic species is computed to be 27.68 kcal mol⁻¹ more stable than the tetrahedral, Table 4.7. Therefore, whereas the tetrahedral species is the more stable for phosphorus, the pyramidal is the more stable for arsenic. It is clear from the HOMO representation of the pyramidal structure of H_2AsO_3^- , Chart 4.4, that a lone pair is available to receive a proton from one of the hydroxyl groups. This is also true for phosphorus (not represented here).

It should be pointed out that, for H_2AsO_3^- , a structure that is intermediate in energy between the pyramidal and the tetrahedral may also be satisfactorily computed, Table 4.7. This has an unusual T-shaped structure with the O-H groups *cis* to one another, Chart 4.5. The *trans* configuration is also possible but is higher in energy than the other three isomers. For the phosphorous analogues, only the *trans*-T-shaped structure can be computed and this is considerably higher in energy than the pyramidal and the tetrahedral ($-35668.5 > -356705.2 > -356716.3 \text{ kcal mol}^{-1}$). The *cis* configuration tends to revert to the pyramidal upon refinement and is therefore postulated not to exist.

The bond lengths and angles for the four arsenic isomers of H_2AsO_3^- (pyramidal, *cis*-T-shaped, tetrahedral and *trans*-T-shaped) are given Table 4.7. The respective As-OH bond lengths are 1.901, 2.022, 1.853 and 2.019/2.053 Å. Notably the pyramidal and tetrahedral bond lengths are shorter than those in the *cis/trans* isomers suggesting that flattening out the structures brings about an elongation of this type of bond. The respective As-O bond lengths are 1.683, 1.664, 1.667 and 1.651 Å and, as observed previously, are shorter than the As-OH bonds. The bond lengths of $\text{H}_2\text{As}^{\text{III}}\text{O}_3^-$ are also observed to be elongated with respect to similar types of bonds in the monoanionic $\text{H}_2\text{As}^{\text{V}}\text{O}_4^-$ species. This is consistent with the notion that, for the same type of bond, a lower oxidation state results in bond lengthening. The As=O bond length in the tetrahedral isomer is 1.657 Å. This is consistent with corresponding bond lengths in other arsenic species. The As-H bond length in the tetrahedral isomer is 1.536 Å. From the data in Table 4.7 it is possible to estimate that the average bond lengthening *in vacuo* compared to the crystal structure data (where crystal packing forces are in effect) is approximately 3.5%. This would result in a “corrected” As-H distance of 1.48 Å that is comparable to the sum of the respective covalent radii, 1.49 Å [344]. Notably, in the H_3PO_3 tetrahedral analogue this hydrogen is not considered to be available and the species is considered to be dibasic only [286-287]. This is also expected to be the case for arsenic. Indeed, the LUMO representation of the tetrahedral H_2AsO_3^- shows this hydrogen to be non-acidic.

The O-As-OH bond angles for the pyramidal, *cis*-T-shape, tetrahedral and *trans*-T-shape isomers are 100.23°, 94.04°, 103.81° and 94.71/94.42° respectively with the T-shaped isomers exhibiting smaller bond angles as a result of their flattened structure, *vide supra*. The OH-As-OH bond angles for the pyramidal, *cis*-T-shape and *trans*-T-

shape isomers are 98.59° , 171.93° and 170.87° with the T-shaped structures showing larger bond angles compared to the pyramidal isomer. The O=As-O⁻ and O=As-OH bond angles in the tetrahedral isomer are observed to be slightly less distorted with respect to similar types of bonds in the monoanionic H₂As^VO₄⁻ species. Attempts to find crystal structure information for the arsenite species proved to be unsuccessful. This has also been noted by others [345] for the H₃AsO₃ species. However, crystal structure information was reported for an AsO₂OH fragment present in a (C₃H₁₂N₂)₂[H₂As₆Mo₄O₂₂].2H₂O [345] structure. In that particular fragment species the reported crystal structure distance for an As-O bond is 1.801 Å. This is longer than the modelled H₂AsO₃⁻ species but would appear to be consistent with the expected elongation of dianion species compared to monoanion and neutral species, *vide supra*, see Table 4.7.

4.4.2.3 Electrostatic potential energy calculations

The electrostatic potential energy maps were also calculated for each of the phosphorus and arsenic species, along with calculated energies for the highest occupied molecular orbital (E_{HOMO}) and lowest unoccupied molecular orbital (E_{LUMO}). Both qualitative and graphical representations are provided. The E_{HOMO} and E_{LUMO} values are given in Table 4.7 and the electrostatic potential energy maps along with the HOMO and LUMO graphics are presented in Charts 4.1, 4.2, 4.4 and 4.5.

The E_{HOMO} is of particular interest because it gives an indication of the reactivity of the species of interest, with higher E_{HOMO} values indicating more reactivity [346]. It has been reported that the value of E_{HOMO} could be a first approximation to the nucleophilicity of the compound [346-347]. Generally speaking, the HOMO of these phosphorus and arsenic species are likely to form bonds with the LUMO of other species that might be present (i.e. possibly in soil or water). The calculated LUMO energy of the phosphorus and arsenic species also provide useful information because any further electrons that enter the system will be accommodated in the LUMO, the energetically most accessible unfilled molecular orbital. Hence, the LUMO may be thought of as demarking the location of positive charge in a molecule [290]. It has also been suggested that the E_{LUMO} could also be a first approximation to the electrophilicity of the compound [346-347].

Table 4.7. Geometries and further information for phosphorus and arsenic species.

	PO₃⁻ Modelled	HPO₄²⁻ Modelled	HPO₄²⁻ Crystal Structure [342]	trans H₂PO₄⁻ Modelled	cis H₂PO₄⁻ Modelled	H₂PO₄⁻ Crystal Structure [342]	H₃PO₄ Crystal Structure [342]
Bond Angle / °							
O=X-O ⁻	120.00	116.13	112.2, 114.2	126.25	125.93	115.5	
O=X-OH		102.19	102.7	106.80, 106.66	107.52	110.4, 108.4	112.0, 113.2, 113.0
O ⁻ -X-OH		102.80	106.9, 107.5	106.65, 106.80	105.95	107.2, 108.5	
OH-X-OH				100.91	101.35	106.5	105.6, 107.3, 104.9
X-O-H		102.31		106.72	106.25		
O=X=O	120.00						
O ⁻ -X-O ⁻		113.89	112.5				
H-X-O ⁻							
H-X-OH							
Bond Length / Å							
X-OH		1.783	1.618	1.680	1.679	1.572, 1.556	1.545, 1.548, 1.545
O-H		0.962		0.963	0.962		
X=O	1.503	1.537	1.535	1.500	1.491	1.504	1.496
X-O ⁻	1.503	1.548	1.522, 1.529	1.500	1.513	1.515	
X-H							
O ⁻ - - H (H bonding)							
Energy / kcal mol⁻¹	-355958.14	-403499.58		-403961.72	-403960.78		
ΔE(E_{cis} - E_{trans}) / kcal mol⁻¹				0.94			
CPKVOLUME / Å³	49.02	61.15		63.06			
CPKAREA / Å²	72.26	88.99		91.48			
WEIGHT / g mol⁻¹	78.971	95.978		96.986			
E_{HOMO} / kcal mol⁻¹	-51.44	91.46		-56.60			
E_{LUMO} / kcal mol⁻¹	76.70	175.40		78.48			
DIPOLE / Debye	0	5.85		5.69			

X denotes the element phosphorus or arsenic for the respective phosphorus or arsenic species

Table 4.7 (Cont...). Geometries and further information for phosphorus and arsenic species.

	AsO₃⁻ Modelled	HAsO₄²⁻ Modelled	HAsO₄²⁻ Crystal Structure [342]	trans H₂AsO₄⁻ Modelled	cis H₂AsO₄⁻ Modelled	H₂AsO₄⁻ Crystal Structure [343]	H₃AsO₄ Crystal Structure [343]
Bond Angle / °							
O=X-O ⁻	120.00	116.60	113.0, 113.7	128.62	128.67	116.5	
O=X-OH		102.16	102.7	104.87, 107.46	107.87	107.8, 109.7	114.4, 115.0, 113.7
O ⁻ -X-OH		102.01	107.0, 107.7	107.49, 104.92	104.31	111.1, 105.1	
OH-X-OH				100.00	100.37	106.2	99.7, 102.8, 109.8
X-O-H				103.91, 104.08	103.58	109, 100	126, 104, 115
O=X=O	120.00						
O ⁻ -X-O ⁻		114.06	111.9				
H-X-O ⁻							
H-X-OH							
Bond Length / Å							
X-OH		1.940	1.728	1.833, 1.832	1.833	1.703, 1.715	1.690, 1.698, 1.705
O-H		0.964		0.965	0.965		0.92, 1.29, 0.79
X=O	1.655	1.690	1.654	1.654	1.644	1.656	1.644
X-O ⁻	1.655	1.699	1.669, 1.662	1.654	1.665	1.658	
X-H							
O ⁻ - - H (H bonding)		2.851					
Energy / kcal mol⁻¹	-1544718.61	-1592261.97		-1592719.36	-1592718.23		
ΔE(E_{cis} - E_{trans}) / kcal mol⁻¹					1.13		
CPKVOLUME / Å³	52.81	65.64		67.59			
CPKAREA / Å²	77.08	94.97		97.69			
WEIGHT / g mol⁻¹	122.919	139.926		140.934			
E_{HOMO} / kcal mol⁻¹	-60.02	74.97		-62.69			
E_{LUMO} / kcal mol⁻¹	61.50	167.35		70.39			
DIPOLE / Debye	0	5.77		5.28			

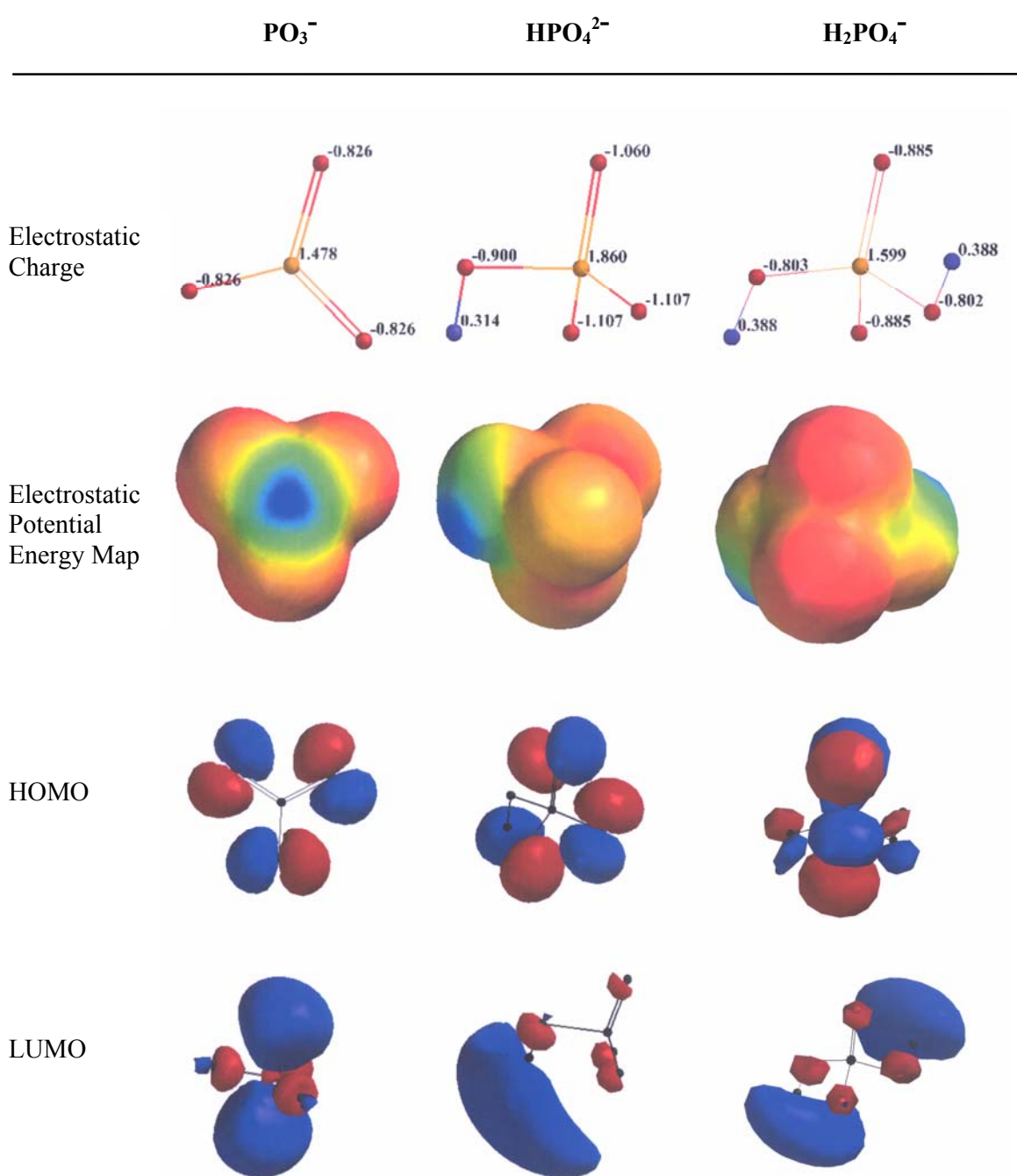
X denotes the element phosphorus or arsenic for the respective phosphorus or arsenic species

Table 4.7 (Cont...). Geometries and further information for phosphorus and arsenic species.

	AsO₂⁻ Modelled	Pyramidal H₂AsO₃⁻ Modelled	Tetrahedral H₂AsO₃⁻ Modelled	cis H₂AsO₃⁻ Modelled	trans H₂AsO₃⁻ Modelled	HAsO₃²⁻ Crystal Structure [345]
Bond Angle / °						
O=X-O ⁻	180.00		124.99			
O=X-OH			109.03			
O ⁻ -X-OH		100.23	103.81	94.04	94.71, 94.42	
OH-X-OH		98.59		171.93	170.87	
X-O-H		102.83	103.02	106.53	103.37, 103.93	
O=X=O						
O ⁻ -X-O ⁻						
H-X-O ⁻			109.61			
H-X-OH			97.47			
Bond Length / Å						
X-OH		1.901	1.853	2.022	2.019, 2.053	
O-H		0.967	0.965	0.966	0.967, 0.965	
X=O	1.721		1.657			
X-O ⁻	1.721	1.683	1.667	1.664	1.651	1.801
X-H			1.536			
O ⁻ - - H (H bonding)		2.533	2.540	2.523	2.531	
Energy / kcal mol⁻¹	-1497458.98	-1545508.27	-1545480.59	-1545483.10	-1545479.01	
ΔE(E_{cis} - E_{trans}) / kcal mol⁻¹					4.09	
CPKVOLUME / Å³	45.69			62.04		
CPKAREA / Å²	67.89			90.89		
WEIGHT / g mol⁻¹	106.920			124.935		
E_{HOMO} / kcal mol⁻¹	-7.53	-34.67	-53.28	-40.44	-35.06	
E_{LUMO} / kcal mol⁻¹	62.46	91.04	86.53	53.37	52.77	
DIPOLE / Debye	0	2.36	4.43	1.56	2.42	

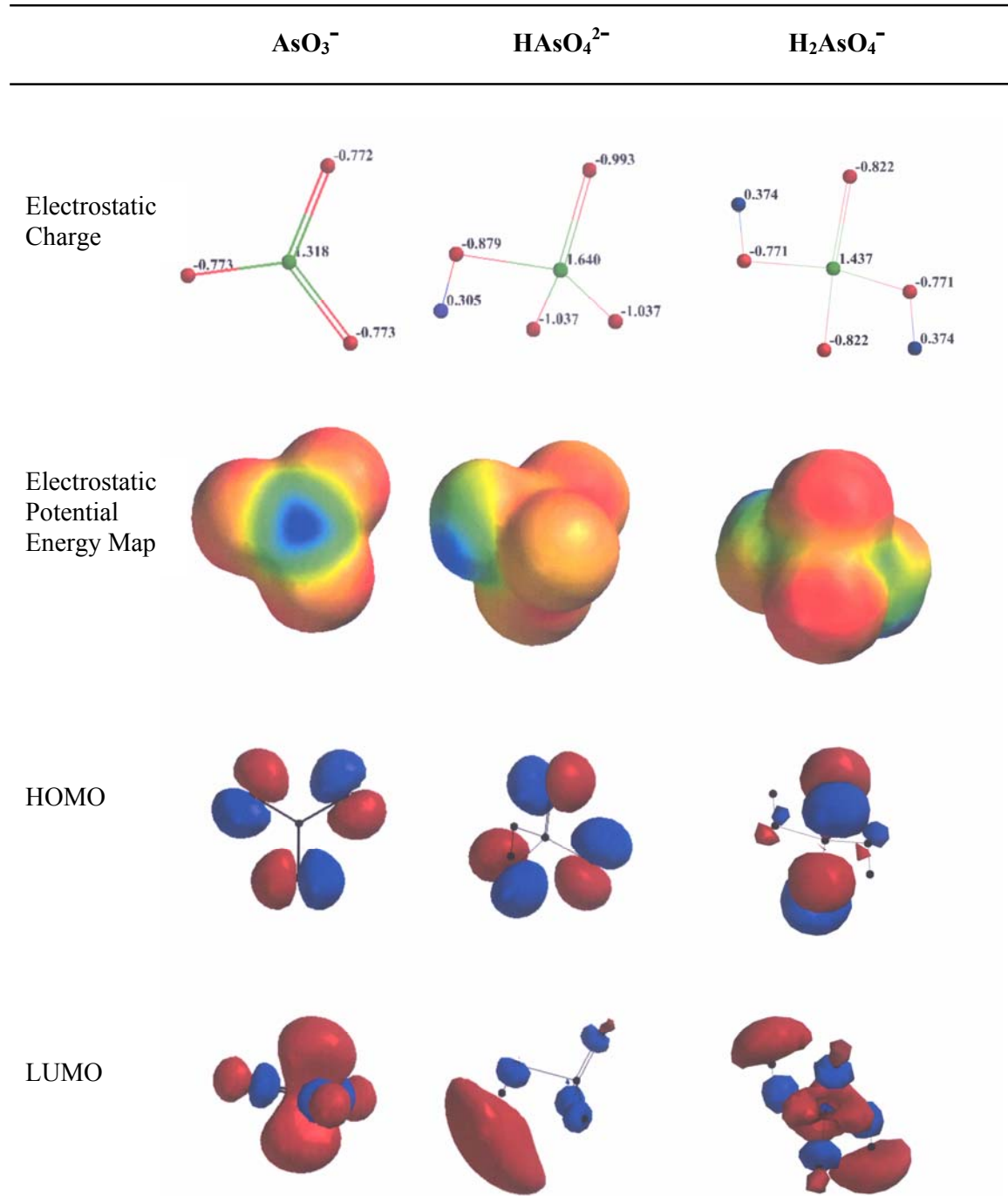
X denotes the element phosphorus or arsenic for the respective phosphorus or arsenic species

Chart 4.1. Electrostatic potential energy structures for PO_3^- , HPO_4^{2-} and H_2PO_4^- species



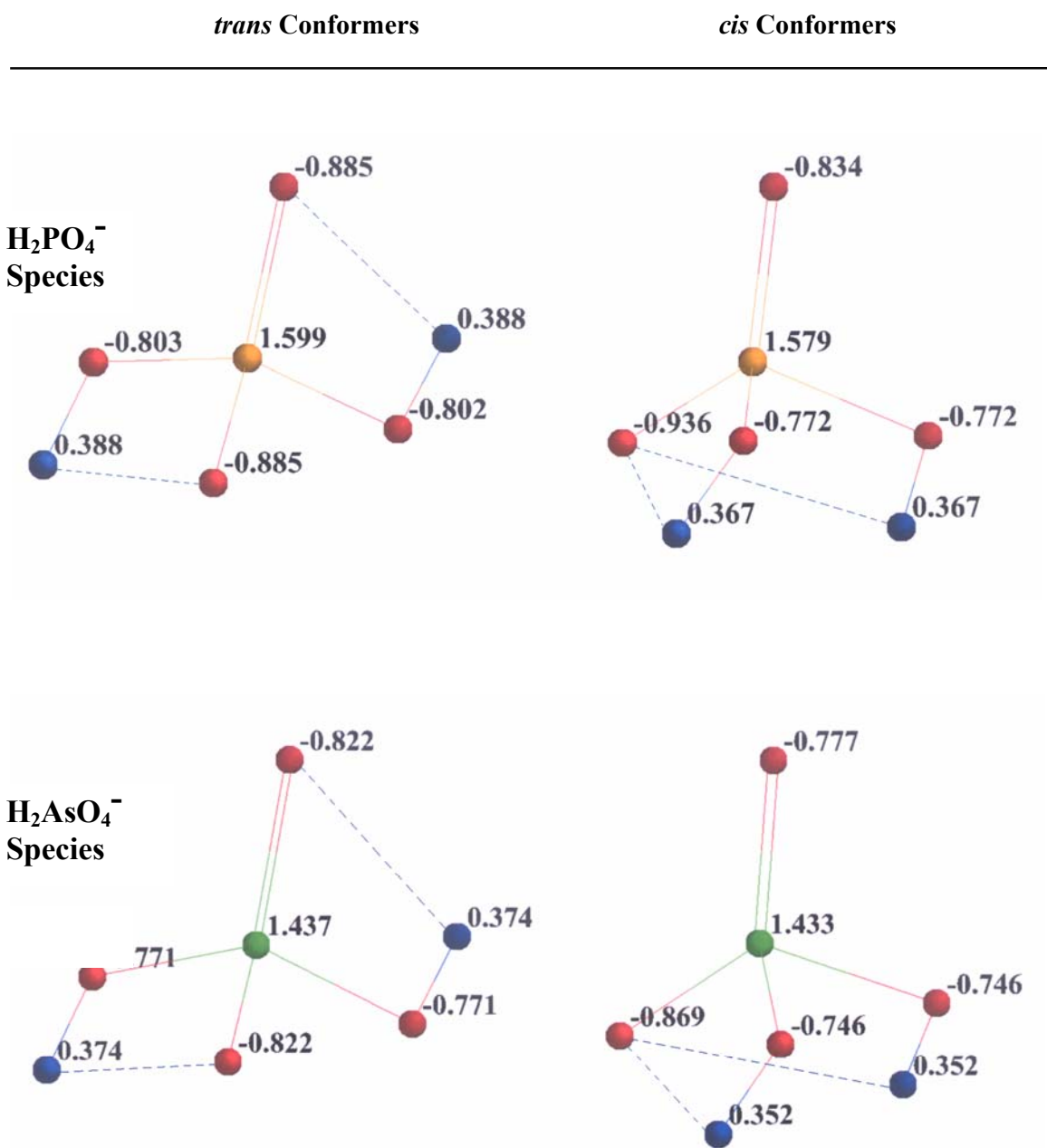
Notes: For electrostatic charge structures: phosphorus atom, yellow; oxygen atom, red; and hydrogen atom, blue.

Chart 4.2. Electrostatic potential energy structures for AsO_3^- , HAsO_4^{2-} and H_2AsO_4^- species



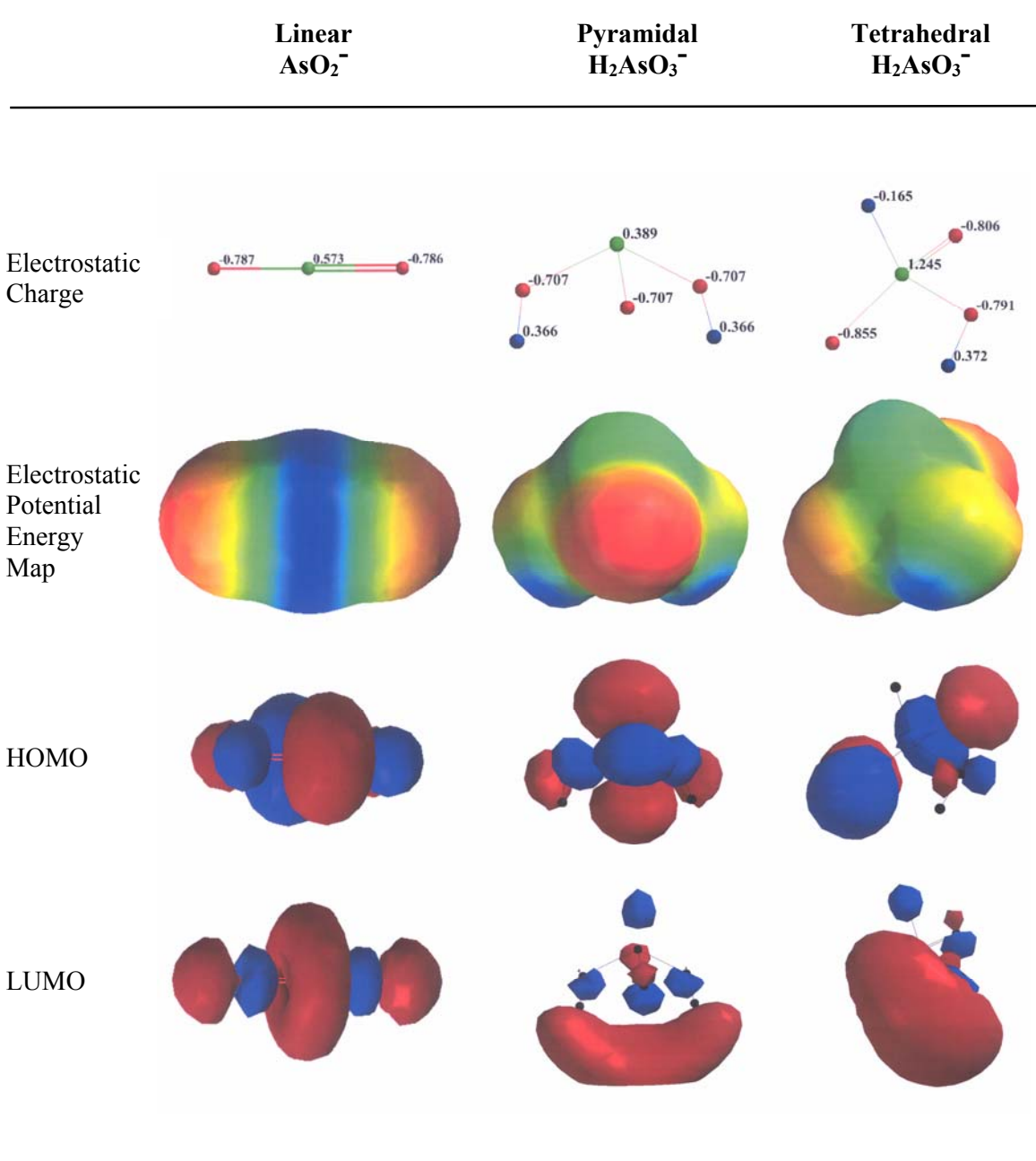
Notes: For electrostatic charge structures: arsenic atom, green; oxygen atom, red; and hydrogen atom, blue.

Chart 4.3. H_2PO_4^- and H_2AsO_4^- conformers



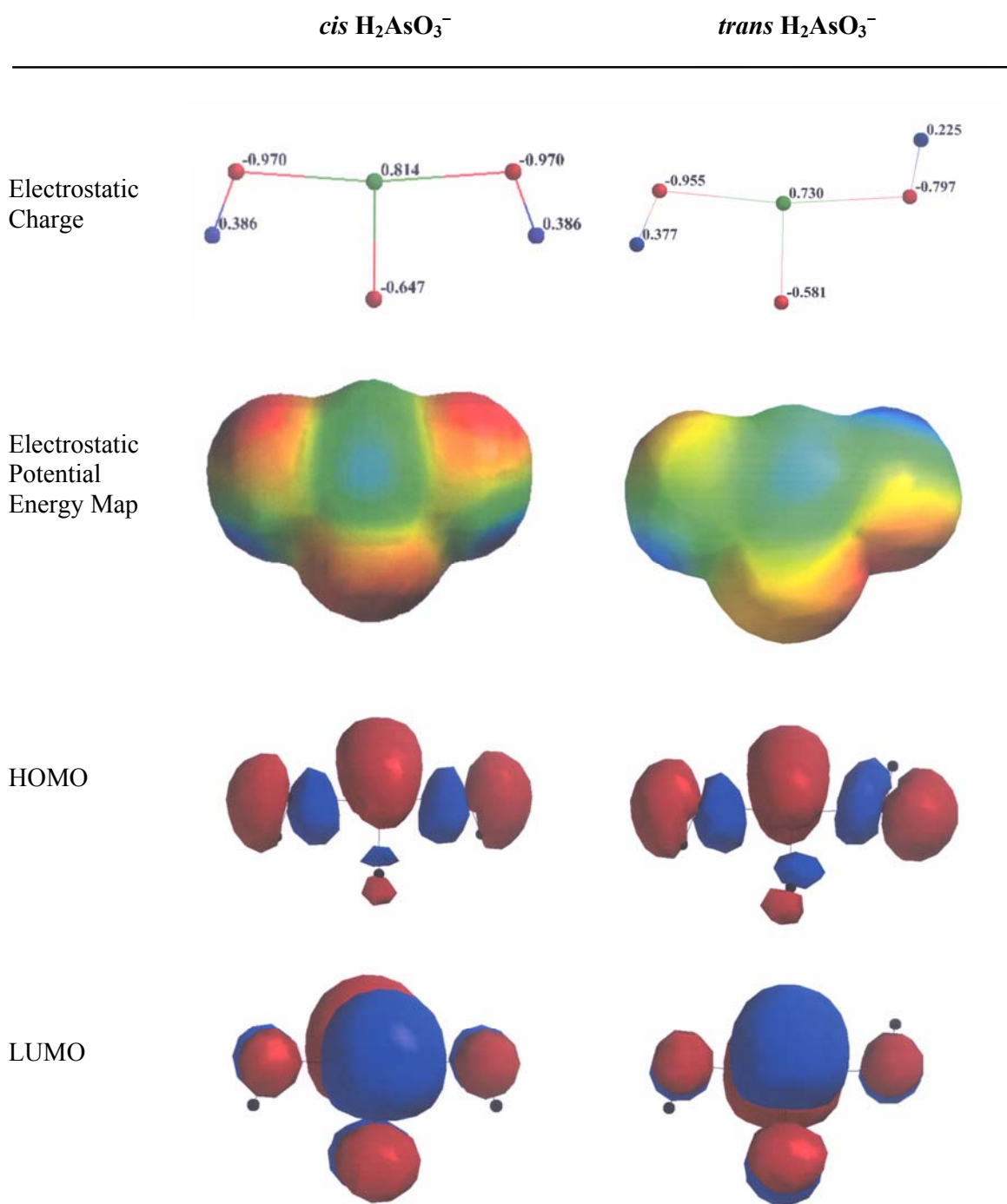
Notes: For electrostatic charge structures: phosphorus atom, yellow; arsenic atom, green; oxygen atom, red; and hydrogen atom, blue. Blue dotted lines represent hydrogen bonding.

Chart 4.4. Electrostatic potential energy structures for AsO_2^- , pyramidal H_2AsO_3^- and tetrahedral H_2AsO_3^- Species



Notes: For electrostatic charge structures: arsenic atom, green; oxygen atom, red; and hydrogen atom, blue.

Chart 4.5. Electrostatic potential energy structures for *cis* and *trans* H₂AsO₃⁻ species



Notes: For electrostatic charge structures: arsenic atom, green; oxygen atom, red; and hydrogen atom, blue.

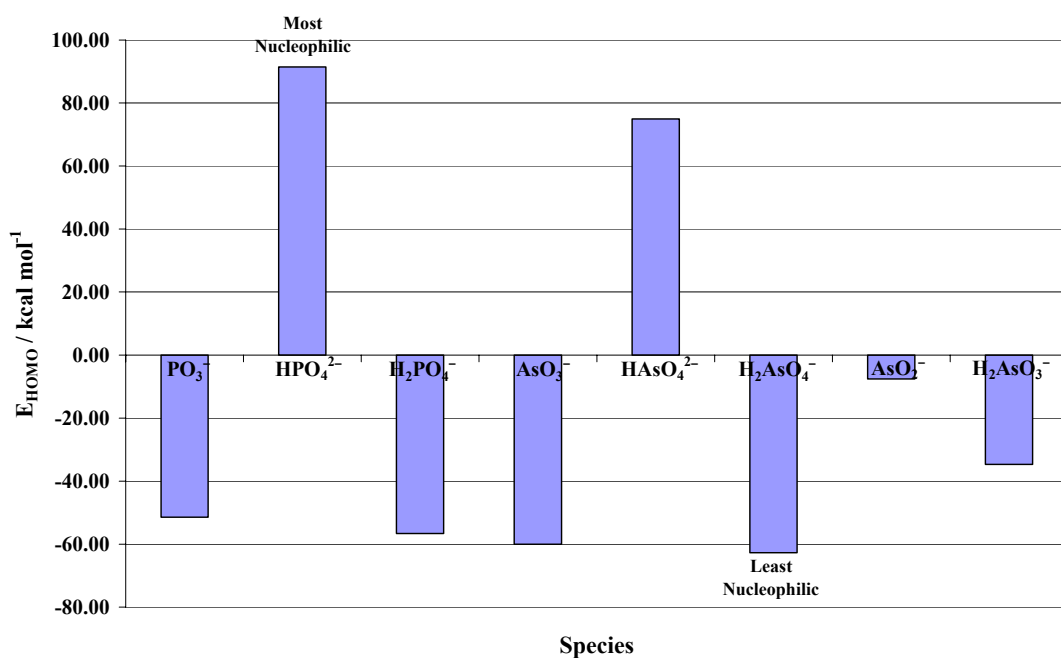


Figure 4.20. Relative computed E_{HOMO} values.

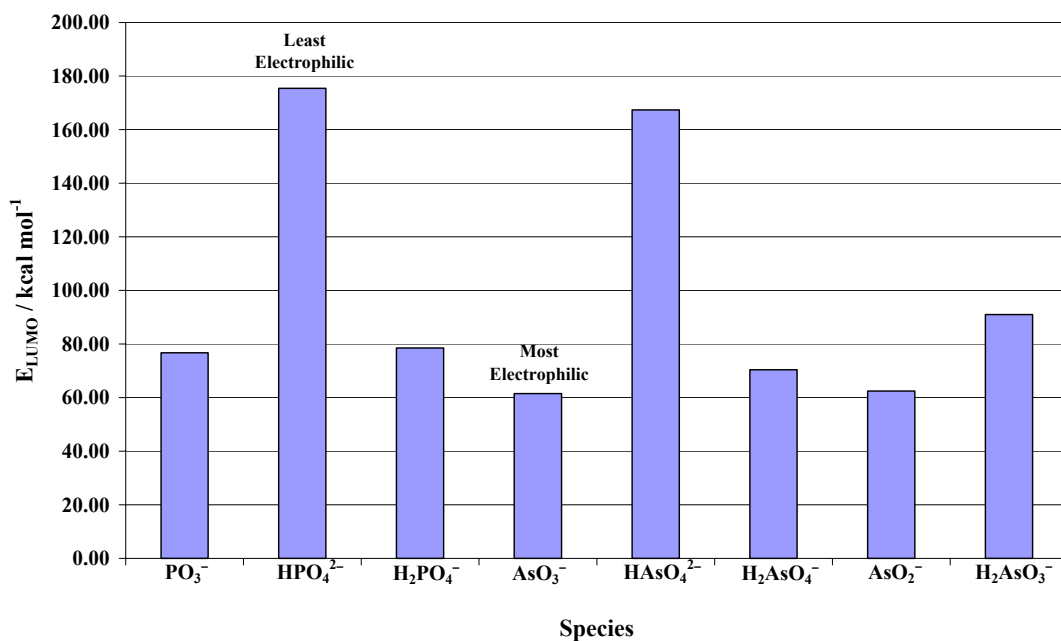


Figure 4.21. Relative computed E_{LUMO} values.

The order of highest to lowest E_{HOMO} for the phosphorus and arsenic species investigated are: $\text{HPO}_4^{2-} > \text{HAsO}_4^{2-} > \text{AsO}_2^- > \text{H}_2\text{AsO}_3^- > \text{PO}_3^- > \text{H}_2\text{PO}_4^- > \text{AsO}_3^- > \text{H}_2\text{AsO}_4^-$ which indicates that the HPO_4^{2-} and HAsO_4^{2-} are the most reactive phosphorus and arsenic species respectively (see Table 4.7). This is consistent with the reactions

that are observed in the ESI-MS. The relative E_{HOMO} values for all species detected by ESI-MS are shown in Figure 4.20. Similarly, the relative E_{LUMO} values are shown in Figure 4.21.

The electrostatic potential energy maps for the $\text{PO}_3^-/\text{HPO}_4^{2-}/\text{H}_2\text{PO}_4^-$ species, the $\text{AsO}_3^-/\text{HASO}_4^{2-}/\text{H}_2\text{AsO}_4^-$ species, the AsO_2^- /pyramidal H_2AsO_3^- / tetrahedral H_2AsO_3^- and the *cis* and *trans* H_2AsO_3^- species respectively are presented in Charts 4.1, 4.2, 4.4 and 4.5. These maps give the electrostatic potential at locations on a particular surface, most commonly a surface of electron density corresponding to overall molecular size [290]. Colours are used in the electrostatic potential energy maps to designate values of the potential. Colours close to red represent large negative values of potential, while colours close to blue represent large positive values. Orange, yellow and green represent intermediate values of potential. The electrostatic potential energy maps serve to quickly characterise various regions in a molecule as electron rich or electron poor, or neither rich nor poor [290]. In the planar PO_3^- and AsO_3^- species the areas near the surface oxygen atoms are shown in red indicating large negative potential values associated with electron rich areas. Whereas, the central phosphorus or arsenic atoms are shown in blue which represent a positive potential value associated with an electron poor area. The electrostatic potential energy maps for PO_3^- and AsO_3^- species are of particular interest because they clearly illustrate the delocalised electron configuration.

As expected, the tetrahedral HXO_4^{2-} and H_2XO_4^- species display negative potential values (i.e. electron rich areas) on the oxygen atoms and exhibit positive potential values (i.e. electron poor areas) on the X and hydrogen atoms. In the H_2XO_4^- species, it is of interest to compare the effect of *cis/trans* isomerism on the electrostatics, Chart 4.3. For both phosphorus and arsenic *trans* isomers the intramolecular H-bonding arrangement results in an effective delocalisation of electrons over the $\text{O}=\text{X}-\text{O}^-$ bond. This is reflected in the fact that the $\text{X}=\text{O}$ and the $\text{X}-\text{O}^-$ bond lengths are identical in these isomers, Table 4.7. This is not the case for the *cis* isomers. This is consistent with the *trans* isomers being more stable than the *cis* by approx. 1 kcal mol^{-1} . This is an example of where an alternative intramolecular hydrogen bonding arrangement within a molecule can result in additional stabilization.

The AsO_2^- and H_2AsO_3^- species exhibit interesting structures and electrostatic potential energy maps. In the case of AsO_2^- the structure has a linear shape with a delocalised

electron configuration that leads to electron rich areas located at either end of the molecule and an electron poor area in the middle. The isomeric H_2AsO_3^- species display pyramidal, tetrahedral and unusual planar T-shape structures that, as expected, exhibit electron rich areas on the oxygen atoms and electron poor areas on the hydrogen atoms and the central arsenic atoms.

4.4.3 Extraction of Arsenite from Soil

The quantification of arsenite in soil was performed using a chloroform extraction technique [32] that is described in Section 3.4.3. The technique was first used to quantify the purity of the arsenite sample utilized in experimental work (see Section 4.4.3.1) and then used to determine the amount of As^{III} sorbed onto soil at different pH (see Section 4.4.3.2).

4.4.3.1 Standardisation of Arsenite Sample

An examination of the ESI-MS spectrum (Section 4.4.1.2) of an aqueous solution of the arsenite “standard” that was made up, suggested the presence of oxidative impurities. These were, originally, thought to have formed either in the ESI-MS ionisation chamber or in the aqueous stock solution after being made up. However, both of these ideas were subsequently dismissed for the reasons discussed in Section 4.4.1.2. It was concluded that the presence of these impurities originated with the supplied arsenite salt. In order to quantify the amount of As^{III} present and to gain more insight into the nature of such purported oxidative processes, the chloroform extraction technique was implemented as follows:

Three different aqueous stock solutions containing the following arsenic species: (i) As^{III} as NaAsO_2 ; (ii) As^{V} as $\text{Na}_2\text{AsO}_4 \cdot 7\text{H}_2\text{O}$; and (iii) 50% v/v mixture of As^{III} and As^{V} stock solutions were prepared. The As^{Tot} was determined in each case. The measured As^{III} and As^{Tot} were compared to calculated As^{III} and As^{Tot} concentrations as shown in Table 4.8. The results indicate that the aqueous stock solution of NaAsO_2 contained 65.9 mg L^{-1} as As^{III} and 76.7 mg L^{-1} as As^{Tot} . It is noted, in these results, that the concentration of As^{III} is approximately 14% lower than the As^{Tot} concentration. This is consistent with the likelihood of oxidative impurities suggested by the ESI-MS. The calculated concentration, of both As^{III} and As^{Tot} , assuming a pure aqueous stock

solution of NaAsO₂ is 83.6 mg L⁻¹. The fact that this is higher than the 76.7 mg L⁻¹ measured for As^{Tot} reflects the presence of such (oxidized) species in the salt. The identity of such possible contaminants can be deduced from the ESI-MS as given in Table 4.5. Such contaminants would be expected to be of a higher molecular weight (MW) than the NaAsO₂ and this would result in a lower value of the measured As^{Tot} – as observed. The following calculations have been made to support the theory that the oxidative impurities have a higher molecular weight:

The concentration of As^{III} in the first aqueous stock solution was determined to be 0.0659 g L⁻¹ (Section 4.4.3.1, Table 4.8) which means that the required mass of pure NaAsO₂ to give such an answer can be calculated as follows:

$$\begin{aligned} \text{Mass}(\text{NaAsO}_2) &= 0.0659 \text{ g As}^{\text{III}} \times [\text{MW}(\text{NaAsO}_2)/\text{MW}(\text{As})] \\ &= 0.1143 \text{ g as NaAsO}_2 \end{aligned} \quad (4.17)$$

However, the mass of NaAsO₂ actually added to the stock solution was 0.1450 g, so the mass of the oxidative impurities can be calculated by subtracting the amount calculated in Equation 4.17 from the actual mass added:

$$\text{Mass of oxidative impurity} = 0.1450 - 0.1143 = 0.0307 \text{ g} \quad (4.18)$$

The effective molecular weight of the oxidative impurities can be calculated by using the concentration difference between the measured As^{Tot} and As^{III} (i.e. 0.0108 g L⁻¹ - values shown in Table 4.8) as follows:

$$\text{MW}(\text{Oxidative impurities}) = \text{MW}(\text{As}) \times 0.0307 \text{ g} / 0.0108 \text{ g} = 213.2 \text{ g mol}^{-1} \quad (4.19)$$

Thus, it can be seen from Equation 4.19 that the effective molecular weight of the oxidative impurities is in the vicinity of 213.2 g mol⁻¹ that may correspond to the Na₃AsO₄ species with a molecular weight of 207.89 g mol⁻¹. This is in good agreement with the ESI-MS results that suggests that the dominant oxidative species present is the AsO₄³⁻ species.

The chloroform extraction method results for the aqueous Na₂AsO₄·7H₂O solution show virtually no As^{III} is present. The As^{Tot} in this case is 55.1 mg L⁻¹. The calculated

concentrations for As^{III} and As^{Tot} of 0 mg L^{-1} and 54.3 mg L^{-1} respectively, are therefore consistent with the experimental values. An estimation of the error associated with the data presented in Table 4.8 has been calculated using the 95% confidence limit (i.e. $t_{0.05,6} = 1.943$) of the arithmetic average concentration based on experimental data used in Section 4.2.1 (see Table 4.2) that are based on seven replicates. The maximum error calculated was $\pm 0.2 \text{ mg L}^{-1}$ without dilution or $\pm 2 \text{ mg L}^{-1}$ with dilution.

The 50% v/v mixture of As^{III} and As^{V} stock solution also indicated consistent results compared to the NaAsO_2 solution which also exhibited lower than expected As^{III} and As^{Tot} concentrations. The results for the aqueous stock solution of NaAsO_2 (from Table 4.8) were subsequently used to standardise the NaAsO_2 sample for further calculations made in quantitative experimental work.

Table 4.8. Purity of Arsenite sample.

Species in aqueous stock solution	Measured stock solution conc.		Percent difference from As^{Tot} / %	Calculated stock solution conc.	
	As^{III} / mg L^{-1}	As^{Tot} / mg L^{-1}		As^{III} / mg L^{-1}	As^{Tot} / mg L^{-1}
As^{III} as NaAsO_2	65.9	76.7	14.1	83.6	83.6
As^{V} as $\text{Na}_2\text{AsO}_4 \cdot 7\text{H}_2\text{O}$	0.2	55.1		0	54.3
50% v/v As^{III} and As^{V} stock solutions	33.3	65.5		41.8	69.0

Note: Estimated error calculation based on 95% confidence level for seven replicates: $\pm 2 \text{ mg L}^{-1}$

4.4.3.2 Arsenite Sorbed onto Soil at Different pH Values

The method for this experiment is described in Section 3.4.3.2 and the results are presented in Table 4.9. This experiment was conducted in order to provide insight into the behaviour of As^{III} species when taken up in soil. A number of aspects are of interest: (i) the nature of the species in the soil (a light clay), (ii) possible redox processes that might occur, and (iii) the pH dependency of such processes.

The chloroform extraction technique was used to determine the amount of As^{III} sorbed onto soil type S2 at different pH values. The concentration of any As^{V} present was calculated in each case by subtracting As^{III} from As^{Tot} . The supernatant concentrations

of As^{III} and As^{Tot} were determined in order to undertake mass balance calculations to trace all As^{III} and As^{Tot} species. A number of checks and balances have been included in the results (Table 4.9) which include a sum of the S2 extracted As^{Tot} and supernatant liquid As^{Tot} to monitor As^{Tot} in the system. In addition, a blank H_2O was also run for each of the systems to ensure that the technique worked correctly. The results of this experiment are considered as three separate systems:

System 1

In System 1 of Table 4.9, S2 was soaked in aqueous stock solutions of NaAsO_2 that were each adjusted to five different pH values. It was expected that the amount of As^{III} sorbed onto the soil and subsequently extracted from the soil would be reflected in the amount of As^{III} added in the aqueous stock solutions. Any As^{III} that was not sorbed and extracted was expected to remain in the supernatant liquid as As^{III} . However, the results reveal that only a portion of As^{III} is sorbed and extracted from the soil, ranging from approximately 17 to 33 % depending on the pH. It was assumed that the remaining As^{III} (approximately 67 to 83 %) would stay in the supernatant liquid as As^{III} . Interestingly, this assumption proved to be incorrect. An explanation for the observed results is that when the aqueous stock solution of NaAsO_2 is allowed to soak with the soil, some of the As^{III} is sorbed by the soil onto specific sorption sites while the rest is oxidised by the soil. Some of the oxidised As^{III} (i.e. As^{V}) is also sorbed by the soil, however, approximately 32 to 59 % of the As^{V} remains in the supernatant liquid. The amount of sorption and oxidation that takes place is influenced by the pH of the system. Generally, when the pH is high the percent As^{III} sorbed and extracted by the soil is highest. The opposite is observed for oxidation, with more As^{III} being oxidised at lower pH, as reflected in the soil extract and the supernatant.

Some of the data from System 1 of Table 4.9 have been plotted to show the percent As^{III} (Figure 4.22) and percent As^{V} (Figure 4.23) sorbed and extracted from the soil. Figure 4.22 indicates that in the NaAsO_2 system the maximum As^{III} sorption and extraction from soil takes place at $\text{pH} \sim 7.6$ and has a minimum sorption and extraction at $\text{pH} \sim 2.8$. The sorption and extraction of As^{III} at pH greater than approximately 10.5 appears to increase again, however, this does not appear to be representative since at extremely high pH the clay lattice may become damaged or destroyed. In the HAsO_4^{2-} system the maximum As^{III} sorption and extraction occurs at $\text{pH} \sim 9.7$ and has a minimum sorption

and extraction at $\text{pH} < 2$. In the system that contains 50% v/v mixture of As^{III} and As^{V} stock solutions the maximum As^{III} sorption and extraction occurs at $\text{pH} \sim 9.5$ and has a minimum sorption and extraction also at $\text{pH} < 2$. In Figure 4.23, the NaAsO_2 system shows that the maximum and minimum As^{V} sorption and extraction occur at $\text{pH} \sim 3.2$ and $\text{pH} \sim 7.6$ respectively. For the $\text{H}_2\text{AsO}_4^{2-}$ system the maximum and minimum As^{V} sorption and extraction occur at $\text{pH} < 2$ and $\text{pH} \sim 10.2$ respectively.

According to Oscarson *et al.* [348] the oxidation of As^{III} by Fe^{III} (e.g. goethite) should be favorable at low pH values. At low pH, any As^{V} oxyanions produced from the oxidation of As^{III} in solution can be sorbed selectively by goethite and enriched in the solid phase [108]. However, the oxidation of As^{III} on goethite would not be expected to occur at high pH [349]. These observations made by others appear to fit well with the current study, suggesting that Fe^{III} could oxidize the As^{III} to As^{V} . It is not likely that oxygen present in the system is responsible for the oxidation of As^{III} . It has been shown that As^{III} in distilled de-mineralized water exposed to air is very stable and that no oxidation of As^{III} was observed after 37 days [350]. Eary and Schramke [351] reported a half-life of 1 year for As^{III} oxidation in distilled water by atmospheric oxygen. Spectroscopic evidence [108] indicates that the goethite surface plays an important role in oxidation either as a catalyst or as a direct oxidant that may be responsible for the observed results of System 1 in Table 4.9.

Other As^{III} oxidants that could be present in the soil of the current study are manganese oxides, as birnessite, which is one of the most common Mn oxides in terrestrial and aquatic environments [19-20,352]. Scott and Morgan [353] described the mechanism of As^{III} oxidation by birnessite as a surface reaction with three steps: (i) As^{III} adsorption, (ii) oxidation of As^{III} to As^{V} , and (iii) desorption of As^{V} . These three steps appear to be similar to the observed process that has taken place in the systems of the current study. This notion is also considered plausible bearing in mind that the S2 soil contains total manganese concentrations ranging between 26 to 38 mg kg^{-1} based on a relatively weak total extraction using 10 M HCl. Unlike iron oxides, manganese oxides are capable of As^{III} oxidation over a wide pH range in natural waters [353]. The oxidation of As^{III} to As^{V} by oxygen is favored by high pH values, whereas low pH values favor the oxidation of As^{III} by Fe and Mn oxides in solution [108] that is likely to be the case with the results from System 1 (Table 4.9).

Examples of the proposed redox reactions that could be responsible for the results of System 1, Table 4.9, are suggested in the following oxidation equations that can occur at both low and high pH values. The standard electrode potential (E°) values have been included along with the standard Gibbs free energy of formation (ΔG°) values. For Equations 4.22 and 4.25 the ΔG° values suggest that the equations proceed spontaneously, indicated by a negative value.

Oxidation at low pH



Oxidation at high pH



System 2

In System 2 of Table 4.9, an analogous experiment to System 1 was conducted with the aqueous stock solution containing Na_2HAsO_4 instead of NaAsO_2 . The results here also proved to be very interesting from a redox and speciation point of view, with between approximately 18 to 29 % of arsenic sorbed and extracted from the soil as As^{III} . From the ESI-MS spectrum, it was anticipated that there would be no As^{III} species present in the aqueous stock solution that was made up from $\text{Na}_2\text{HAsO}_4 \cdot 7\text{H}_2\text{O}$. In addition to the As^{III} sorbed and extracted from the soil, between approximately 29 to 40 % arsenic was sorbed and extracted as As^{V} . The arsenic that was not sorbed and extracted from the soil remained in the supernatant liquid as both As^{III} (between approximately 1 to 5 %)

Table 4.9. Amount of As^{III} sorbed onto soil at different pH values.

System	Species	pH	S2 Extracted					Supernatant liquid					S2 Ext. As ^{Tot} + super. As ^{Tot} / mg L ⁻¹
			As ^{III}		As ^V		As ^{Tot}	As ^{III}		As ^V		As ^{Tot}	
			/ mg L ⁻¹	/ %	/ mg L ⁻¹	/ %	/ mg L ⁻¹	/ mg L ⁻¹	/ %	/ mg L ⁻¹	/ %	/ mg L ⁻¹	
1	As^{III} as NaAsO₂	2.22	13.4	17.5	17.9	23.4	31.3	0.1	0.2	45.0	58.9	45.1	76.4
		3.94	15.3	20.5	19.2	25.7	34.5	1.2	1.6	39.0	52.2	40.2	74.7
		6.02	22.8	30.6	12.1	16.2	34.9	0.3	0.4	39.4	52.8	39.7	74.6
		10.20	22.0	29.4	14.6	19.6	36.6	0.2	0.3	37.9	50.7	38.1	74.7
		11.85	23.4	32.8	13.5	18.9	36.8	11.7	16.5	22.7	31.9	34.5	71.3
	Blank H₂O		0.4	na	0.5	na	0.9	0.4	na	nd	na	0.1	1.0
2	As^V as Na₂HAsO₄·7H₂O	2.26	9.7	18.8	20.8	40.4	30.5	0.3	0.6	20.7	40.2	21.0	51.5
		4.33	11.4	23.4	18.0	36.9	29.3	2.3	4.7	17.0	34.9	19.3	48.6
		6.77	11.8	22.8	17.9	34.5	29.7	1.3	2.5	20.8	40.2	22.1	51.9
		8.61	14.6	28.5	14.4	28.2	29.0	0.6	1.1	21.6	42.2	22.2	51.2
		11.44	9.5	18.4	15.1	29.4	24.6	0.6	1.2	26.3	51.0	26.8	51.4
	Blank H₂O		0.3	na	0.5	na	0.8	0.2	na	nd	na	0.1	0.9
3	50% v/v As^{III} & As^V stock solutions	1.94	13.1	20.6	16.2	25.4	29.3	2.1	3.3	32.3	50.7	34.4	63.7
		4.14	18.5	29.6	12.3	19.7	30.9	1.1	1.8	30.6	48.9	31.8	62.7
		6.57	19.3	30.9	11.9	19.0	31.2	0.2	0.4	31.2	49.8	31.4	62.7
		10.01	20.5	32.8	11.6	18.6	32.1	0.2	0.3	30.2	48.3	30.4	62.5
		11.67	16.4	27.1	14.4	23.9	30.8	16.2	26.8	13.4	22.2	29.5	60.3
	Blank H₂O		0.5	na	0.4	na	0.9	0.2	na	nd	na	0.1	1.0

Notes: na = not applicable, nd = not detected and estimated error calculation based on 95% confidence level for seven replicates: ± 2 mg L⁻¹

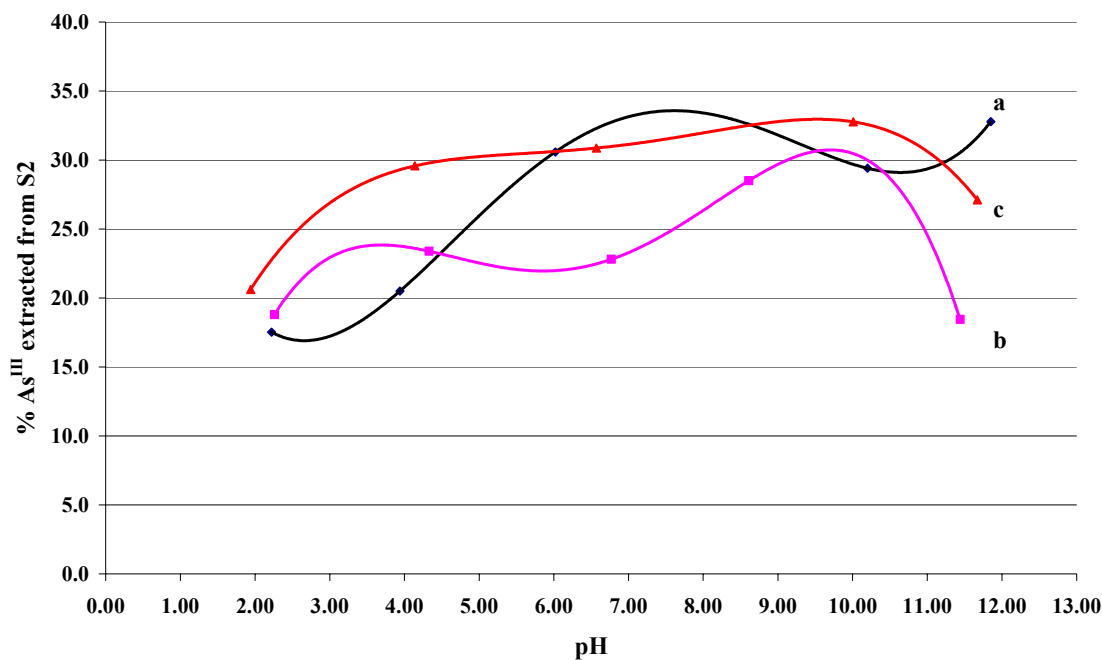


Figure 4.22. A plot of % As^{III} extracted from S2 versus pH: (a) As^{III} as NaAsO₂ species, (b) As^V as Na₂HAsO₄ species and (c) 50% v/v mixture of As^{III} and As^V stock solutions.

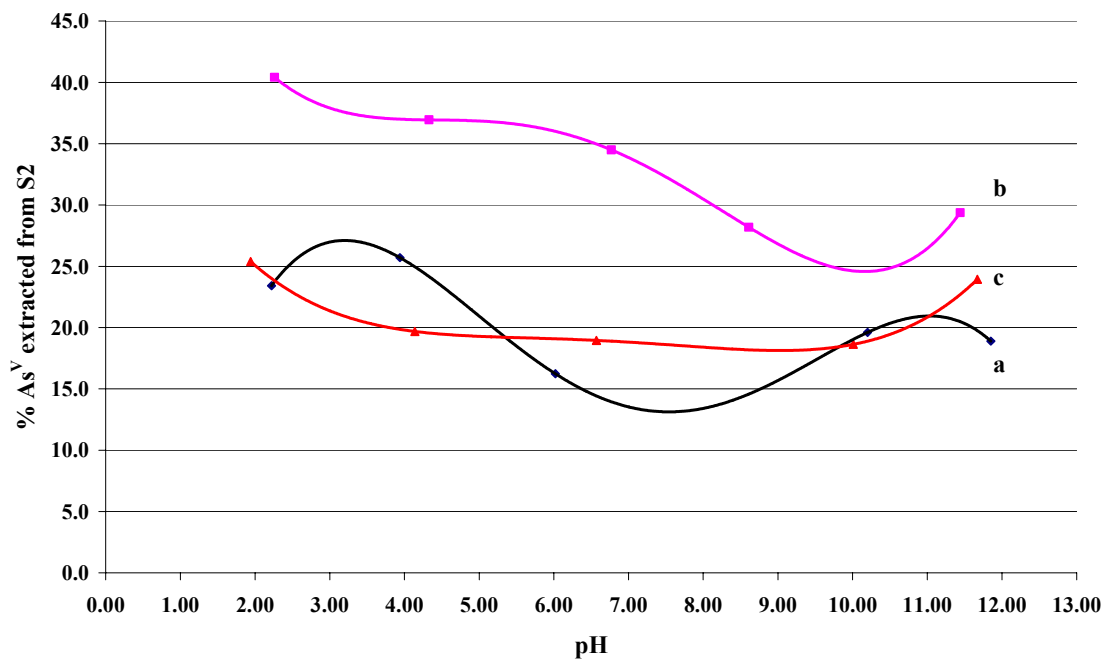


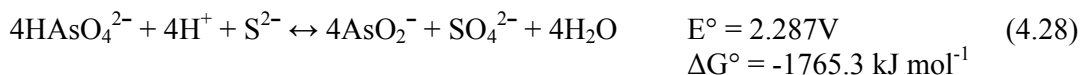
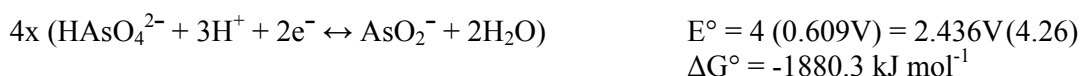
Figure 4.23. A plot of % As^V extracted from S2 versus pH: (a) As^{III} as NaAsO₂ species, (b) As^V as Na₂HAsO₄ species and (c) 50% v/v mixture of As^{III} and As^V stock solutions.

and As^V (between approximately 35 to 51 %). The detection of As^{III} sorbed and extracted from the soil suggests that something in the soil causes the As^V to be reduced to As^{III}. This phenomenon does not take place in the absence of soil as shown in the results in Table 4.8.

An explanation for the results of System 2, Table 4.9, is that under oxic conditions, arsenic is primarily found as As^V, which sorbs strongly to Fe and Al (hydr)oxides [322,326,354-356]. Surface-bound arsenic is released into solution under slightly reducing conditions through the reductive dissolution of the Fe (hydr)oxides [357-359]. Arsenate reduction to highly toxic As^{III} may accompany its release into solution [360-362].

Postulated reduction equations at low and high pH values, in the presence of Fe^{III} and sulfides, are suggested below. The E° and ΔG° values have been included to support the notion that the equations proceed spontaneously.

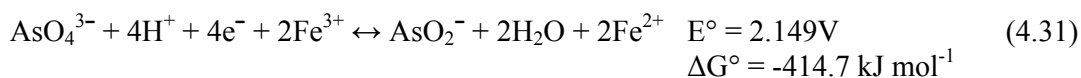
Reduction at low pH



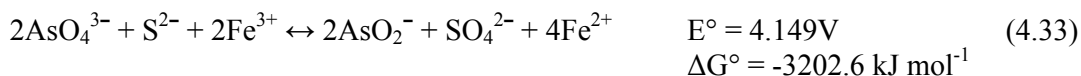
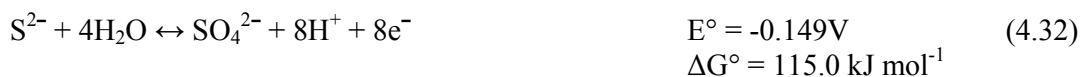
Reduction at high pH



Equation 4.29 and Equation 4.30 can be added together as follows:



If Equation 4.31 is multiplied by 2 it can be reduced using the following equation:



System 3

In System 3 of Table 4.9, the aqueous stock solution contained a 50% v/v mixture of As^{III} and As^V stock solutions. Not surprisingly, the results for System 3 are found to be consistent with those of System 1, in that, when the pH is high the percentage As^{III} sorbed and extracted by the soil is generally highest. The opposite is observed for oxidation, with more As^{III} being oxidised at lower pH, as reflected in the soil extract and more particularly in the supernatant.

In summary, both oxidative and reductive processes have been established as a result of exposure of As^{III}/As^V to a light clay in aqueous media over a range of pH values. It is evident that specific sorption sites on the light clay are able to sorb, oxidise/reduce and desorb As^{III}/As^V species in varying amounts according to the pH of the system. Generally, the maximum sorption and extraction of As^{III} occurs at an almost neutral pH for NaAsO₂ compared to a relatively basic pH for Na₂HAsO₄ species. On the other hand, the maximum sorption and extraction of As^V generally occurs at relatively low pH values.

5.0 Conclusions & Future Directions

5.1 Conclusions

A statistical analysis of data entered into a database revealed the relative abundances of metals and, in particular, arsenic within soils of various geological units. These units included the Quaternary Aeolian (Qpw, highest concentration of zinc, lowest concentration of chromium) the Quaternary Fluvial (Qrc, highest chromium and nickel concentrations, equal highest copper, lowest lead and equal lowest arsenic concentrations); the Quaternary Newer Volcanics (Qvn, equal lowest arsenic concentration); Silurian Anderson Creek Formation (Sla, highest arsenic concentration); Silurian Dargile Formation (Sud, highest lead and equal highest copper concentrations); Tertiary Brighton Group (Tpb, lowest nickel concentration) and Older Volcanics (Tvo, lowest copper and zinc concentrations).

A detailed review of the current literature has exposed a number of limitations in conducting comparisons between different inorganic background soil constituent data. Namely, issues associated with non-standardised sampling strategies (i.e. single versus bulked/composited samples), varying sampling depths, differing soil sampling intensities, sampling location strategies which vary randomly or systematically, and data obtained using different analytical techniques, were identified. In particular, it was found that most studies present chemical constituent data as a total concentration that provides limited information about the chemical species that are present and the bioavailability of those species. A particular limitation of inorganic background soil data in the literature includes the failure to relate the data to targeted geological regions.

Initial arsenic soil sorption experiments revealed that the average percentage As^{Tot} sorbed depends on the soil type. Thus clay loam, light clay and silt loam were found to sorb approximately 19.6%, 2.9% and 38.2% respectively, whereas the sand sorbed negligible arsenic, with concentrations below the method detection limit. A second sorption study that allowed for a longer exposure time revealed optimum arsenic sorption concentrations. Under these conditions the clay loam, light clay, sand and silt loam sorbed approximately 76 %, 84 %, 2.4 % and 72 % respectively. These results were found to relate to the clay content, pH and EC values. This is consistent with literature data confirming that the material substrate plays a vital role in the sorption of

arsenic (i.e. higher clay content soils sorb the most arsenic) with the pH of the system also playing a significant role in determining the amount of arsenic sorbed. The results of the current study also confirm that soils with higher arsenic sorption qualities generally exhibit higher concentrations of extractable Fe and Al. Iron present in these soils is likely to be in the form of iron (hydr)oxides that has been extensively identified in the literature as being a most suitable sorption material for arsenic.

The experimental results obtained in the present work revealed that the extent of sorption of arsenic in soils is highly dependent on the time of sorption. The concentration of sorbed arsenic increases rapidly in the first 30 min and then continues to increase more slowly thereafter, approaching a maximum sorption concentration. The sorption has been modelled using a two-step kinetic process.

An *in vitro* bioavailability technique was evaluated to assess its applicability in determining the relative bioavailability of arsenic when sorbed onto four different soil types. The technique demonstrated a clear differentiation in the relative bioavailabilities of the four soil types and illustrated the dependence of arsenic bioavailability on the physical and chemical properties of the soil. For the clay loam, light clay, sand and silt loam the relative arsenic bioavailability was determined to be approximately 32%, 80%, 100% and 60% respectively. The sorption process in these studies was not an equilibrium process since the ratio for the percentage arsenic bioavailability to the percentage arsenic non-bioavailability varied with the spiked concentration. The calculated ratios cannot be considered to be partition coefficients since they do not remain constant with various spike concentrations. A plot of the percentage arsenic bioavailability versus the concentration of arsenic delivered in the spike reveals that the bioavailability is limited in a non-linear way by the loading capacity of the soil. These plots also illustrate that different soil types result in different bioavailability profiles. A novel technique was implemented to estimate, for each soil type, the apparent partition coefficient that is obtained as the concentration of arsenic in the spike approaches zero. The apparent limiting partition coefficients for the clay loam, light clay and silt loam are 0.255, 2.228 and 0.809 respectively.

The observation that (except for sand) the maximum percentage bioavailability ranged from approximately 32 to 80 % is in contrast with a number of studies in the literature that assume that close to 100% of soluble arsenic is sorbed by the human

gastrointestinal tract. This tacit assumption is questionable given that arsenic in soil is expected to be incompletely extracted during transit through the gastrointestinal tract.

In a global sense, a simple gastric relative bioavailability technique provides a valuable estimation for the bioavailability characteristics of a given soil. Such a technique provides quick and readily available information on the relative bioavailability of arsenic in soils without the need for conducting ethically questionable, expensive and time-consuming *in vivo* bioavailability experiments. Simple models, like the one used in this study, rely on the fact that although arsenic is sorbed through the intestinal epithelium, the rate-controlling step in arsenic sorption is dissolution in the stomach. As a result, complicated gastrointestinal models do not necessarily estimate relative bioavailability better than the simpler gastric models.

Several techniques were employed to investigate and evaluate the speciation of phosphorus (as a benchmark) and arsenic under a variety of conditions, including gaseous/*in vacuo*, solution and soil. The utility of ESI-MS for the qualitative and quantitative assessment of arsenic and phosphorus speciation in solution was evaluated to identify and characterize these species. The technique demonstrated considerable potential for the study of both phosphorus and arsenic speciation, particularly for qualitative speciation analyses in solution. From the qualitative data, various postulates were formulated for the interaction between different species. For the speciation of phosphorus using ESI-MS, HPO_4^{2-} in the presence of hydronium ions was postulated to form PO_3^- and water. The continued reaction of PO_3^- to form H_2PO_4^- was also proposed to account for the experimental observations. A similar mechanism to that of phosphorus was also proposed to account for the experimental observations made on the analogous arsenic species. In this case, ESI-MS was also used to identify and characterise arsenite species in solution. From these results, a mechanism for the formation of the H_2AsO_3^- species from AsO_2^- in the presence of water was postulated. In the process of ESI-MS speciation analyses, a novel technique was developed to assay the “oxidative purity” of an aqueous arsenite sample. The ESI-MS results revealed that the supplied arsenite salt contained the following oxidative impurities: AsO_4^{3-} , AsO_3^- , H_2AsO_3^- and H_2AsO_4^- . The ESI-MS technique proved to be a most suitable technique for identification of such oxidative impurities in an aqueous sample and can be recommended to be used for this purpose in future investigations of this nature.

The species identified in ESI-MS were modelled using high-level density functional calculations with the aim of providing supporting evidence for the postulated reaction mechanisms. The reaction energies for the two phosphorus mechanisms were -267.02 and -25.13 kcal mol⁻¹ indicating an equilibrium shift to the right-hand side in both cases, favouring the PO₃⁻ and H₂PO₄⁻ species in their respective reactions. Using analogous calculations to those of phosphorus, the calculated reaction energies for the arsenate systems were -265.10 and -22.30 kcal mol⁻¹, with the equilibrium shift in both cases towards the right-hand side, favouring the AsO₃⁻ and H₂AsO₄⁻ species. For the arsenite system the calculated reaction energy was -70.84 kcal mol⁻¹, favouring the formation of the H₂AsO₃⁻ species. These novel, modelled reaction energy calculations proved in all cases to be a favourable method in supporting the postulated mechanisms arising from the ESI-MS results.

As part of the species energy and reaction energy calculations, a number of computer-generated geometries for the phosphorus and arsenic species were obtained and were found to compare favourably with reported crystallographic data. Along with these computer-generated geometries, structures for each of the identified ESI-MS phosphorus and arsenic species were also modelled. The computer-generated structures for XO₃⁻ (X = P, As) indicated perfect trigonal planar geometries with a delocalized electron configuration. For HXO₄²⁻ and H₂XO₄⁻ species the structures exhibited varying degrees of distorted tetrahedral geometries. In light of the computer-generated structures, it was discovered that the H₂XO₄⁻ species exhibited isomers, predicated on the existence of strong intramolecular hydrogen bonds, with the hydrogen atoms located in either *cis* or *trans* positions relative to each other. In the case of the arsenite species, computer structures for AsO₂⁻ and H₂AsO₃⁻ proved to be extremely interesting. The structure of AsO₂⁻ exhibited a linear geometry with a delocalized electron configuration. Whereas, the structure for H₂AsO₃⁻ exhibited four possible isomeric structures with increasing energies in the following order: pyramidal H₂AsO₃⁻ < *cis*-T-shaped (planar) H₂AsO₃⁻ < tetrahedral H₂AsO₃⁻ (with one hydrogen directly bonded to the central arsenic atom) < *trans*-T-shaped (planar) H₂AsO₃⁻. These isomers seem not to have been reported previously in the literature and represent significant finds with respect to arsenic speciation.

Modelled HOMO and LUMO data revealed the order of decreasing reactivity for the phosphorus and arsenic species investigated: HPO₄²⁻ > HAsO₄²⁻ > AsO₂⁻ > H₂AsO₃⁻

$>PO_3^- > H_2PO_4^- > AsO_3^- > H_2AsO_4^-$. It is postulated that the HOMO of each of these phosphorus and arsenic species is likely to form bonds with the LUMO of other species that might be present in the soil or water environments. In this regard, the more reactive species are likely to sorb to soil particles. This facilitates hypotheses to be proposed for the distribution of such species in solution and also provides insight into how these species may be taken up into a clay structure. The computer modelled calculations also yielded electrostatic potential energy maps for each of the phosphorus and arsenic species which serve to quickly characterise various regions within a molecular species as being electron rich, electron poor, or neither rich nor poor, based on a colour scale.

A novel technique was adopted to quantify the purity of an As^{III} sample and to determine the amount of As^{III} sorbed onto soil under different pH conditions. The technique is based on a previously reported speciation technique that utilizes the known preference of halogenated As^{III} to be extracted into chloroform. The purity of the As^{III} sample, using this technique, was demonstrated to be approximately 86 % with the remaining 14 % corresponding to the “oxidative impurities” that were qualitatively identified using ESI-MS. Using this extraction technique, the quantitative amount of As^{III} sorbed onto soil under different pH conditions was also measured in order to provide insight into the behaviour of As^{III} species when taken up by the soil. The results for an As^{III} sample revealed that approximately 17 to 33 % of As^{III} was sorbed and extracted by the soil with < 1 to 16.5 % As^{III} remaining in the supernatant liquid. The remainder of the As^{III} was oxidized (possibly by manganese oxides or by aerobic oxidation processes) to As^V and was either sorbed and extracted by the soil (~16 to 26 %) or remained oxidized in the supernatant liquid (~32 to 59 %). The sorption and oxidation characteristics taking place in the soil were found to be pH dependent, with higher As^{III} sorption taking place at higher pH. For the oxidation process, more As^{III} is oxidised at lower pH.

For the As^V system, approximately 18 to 29 % was sorbed and extracted as As^{III} , with approximately 1 to 5 % As^{III} remaining in the supernatant liquid. The remainder of the As^V was either sorbed and extracted by the soil (~28 to 40 %) or remained in the supernatant liquid (~35 to 51 %) as As^V . The detection of As^{III} in a soil soaked in an As^V solution suggests that the soil is capable of reducing some of the As^V into As^{III} . It was proposed that such a reduction could be facilitated by the presence of Fe^{III} and sulfides that are present in the soil. From these results it is evident that specific sorption

sites on the clay are able to sorb, oxidize/reduce and desorb $\text{As}^{\text{III}}/\text{As}^{\text{V}}$ species in varying amounts according to the pH of the system. It was found that the maximum sorption and extraction of As^{III} occurs at almost neutral pH and that the sorption and extraction of As^{V} occurs at a relatively low pH. These experimental results thus provide valuable information on the nature of the species in the soil, the possible redox processes taking place and the pH dependency of such processes.

5.2 Future Directions

The research has created new pathways that can be explored to continue the quest to elucidate the complex nature of arsenic sorption in, and bioavailability from, soils. It is anticipated that further research in the following areas could be undertaken in the future:

(i) The determination of the relationship between the kinetics described in Section 4.2 with the bioavailability (Section 4.3) and speciation (Section 4.4). Such work could provide valuable information as to whether arsenic is kinetically bioavailable to humans and also provide an insight into the speciation kinetics.

(ii) The determination of arsenic speciation using ESI-MS is a promising method that could be investigated further by the development of soil extraction techniques and by the optimization of instrumental parameters to enable the instrumental speciation to reflect, as accurately as possible, the actual speciation in the extract. In addition, it is envisaged that techniques involving ESI-MS could also be developed for the *quantitative* analysis of individual arsenic species derived from soil matrices.

(iii) A continuation of computer modelling investigations for phosphorus and arsenic species, especially those identified by ESI-MS, is an area of ongoing interest. The existence of various isomers is of particular interest since little is known about how this relates to their (environmental) chemistry and biochemistry. It is also desirable for such isomers to be isolated in the laboratory for experimental evaluation.

6.0 References

- [1] San Juan, C., (1994), Natural Background Soil Metal Concentrations in Washington State. Publication No. 94 – 115, October 1994. The United States Geological Survey and the Washington State Department of Ecology.
- [2] Duchaufour, P., (1977). *Pedology*. George Allen & Unwin, London.
- [3] Kabata-Pendias, A., Dudka, S., Chlopecka, A. and Gawinowska, T., (1992). Background levels and environmental influences on trace metals in soils of the temperate humid zone of Europe, In: *Biogeochemistry of trace metals*, Ed. Adriano, D. C., Lewis Publishers, U.S.A.
- [4] National Environment Protection (Assessment of Site Contamination) Measure 1999, Schedule B(1) – Guideline on Investigation Levels for Soil and Groundwater, Section 5.2 Background Variation, pp 7.
- [5] Australian and New Zealand Environment and Conservation Council (ANZECC) and National Health and Medical Research Council (NHMRC). (1992). *Australian and New Zealand Guidelines for the Assessment and Management of Contaminated Sites*.
- [6] McKeague, J. A. and Wolynetz, M. S., (1980). Background levels of minor elements in some Canadian soils, *Geoderma*, 24, 299-307.
- [7] Yan-Chu, H., (1994). Arsenic distribution in soils, In: *Arsenic in the environment, Part 1: Cycling and characterisation*, Ed. Nriagu, J. O., John Wiley & Sons, New York, pp 17-49.
- [8] Sadiq, M., Zaidi, T. H. and Main, A., (1983). Environmental behaviour of arsenic in soils: Theoretical, *Water, Air, Soil Pollut.*, 20 (4), 369-377.
- [9] Li, S. Z., Wang, W. X., Li, E. G. and Dun, S. Q., (1981). A preliminary study of the fixation of methanearsonate herbicides in Hutuo river drainage soils, China

Environ. Sci., 1, 41-45.

- [10] Li, X. G., (1982). Chemical forms and content of arsenic in some soils of China, Turang Xuebao, 19 (4), 360-366.
- [11] Koyama, T. and Shibuya, M., (1976). Soil-plant relation studies on arsenic. II. Correlation between easily extractable arsenate in soils and the response of rice plants, Nippon Dojo Hiriyogaku Zasshi, 47 (3), 93-98.
- [12] Norimoto, W., and Osamu, H., (1982). Adsorption of arsenite and arsenate by soils and charcoal, Kankyo Gijutsu, 11 (8), 565-571.
- [13] Xu, H., Allard, B. and Grimvall, A., (1988). Influence of pH and organic substances on the absorption of arsenic(V) on geological materials, Water, Air, Soil Pollut., 40 (3-4), 293-305.
- [14] Galba, J. and Polacek, S., (1973). Sorption of arsenates under kinetic conditions in selected soil types, Acta Fytotech., 28, 187-197.
- [15] Micheal, B. A. and Russell, J. L., (1976). Chemical distribution and gaseous evolution of arsenic-74 added to soils arsenic-74-labeled DSMA, Soil Sci. Soc. Am. J., 40 (5), 655-658.
- [16] Ruby, M. V., Davis, A., Schoof, R., Eberle, S. and Sellstone, C. M., (1996). Estimation of Lead and Arsenic Bioavailability Using a Physiologically Based Extraction Test, Environ. Sci. Technol., 30, 422-430.
- [17] Walsh, L. M. and Keeney, D. R., (1975). Behaviour and phytotoxicity of inorganic arsenicals in soils, ACS Symp. Ser. 7, 35-52.
- [18] Xie, Z. M., Zhu, Z. X., Yuan, K. N. and Huang, C. Y., (1989). Effect of birnessite (δ -MnO₂) on oxidation of arsenic(III) in soils, Huanjing Huaxue, 8 (2), 1-6.
- [19] Tournassat, C., Charlet, L., Bosbach, D. and Manceau, A., (2002). Arsenic(III)

- oxidation by birnessite and precipitation of manganese(II) arsenate, *Environ. Sci. Technol.*, 36, 493-500.
- [20] Oscarson, D. W., Huang, P. M., Defosse, C. and Herbillion, A., (1981). Oxidative power of Mn(IV) and Fe(III) oxides with respect to As(III) in terrestrial and aquatic environments, *Nature*, 191, 50-51.
- [21] Helgesen, H and Larsen, E. H., (1998). Bioavailability and speciation of arsenic in carrots grown in contaminated soil, *Analyst*, 123, 791-796.
- [22] Hayes, K. F. and Traina, S. J., (1998). In: *Soil Chemistry and Ecosystem Health*, Special Publication 52, Soil Science Society of America.
- [23] Huang, P. M. and Fujii, R., (1998). In: *Chemical Methods. Methods of Soil Analysis, Part 3, Book Series No. 5*, Soil Science Society of America.
- [24] Bissen, M. and Frimmel, F. H., (2000). Speciation of As(III), As(V), MMA and DMA in contaminated soil extracts by HPLC-ICP/MS, *Fresenius J. Anal. Chem.*, 367, 51-55.
- [25] Ferguson, and Gavis, (1972). A review of the arsenic cycle in natural waters, *Water Res.*, 6 (11), 1259-1274.
- [26] Webb, J. L. (Ed.), (1976). *Enzyme and metabolic inhibitors*, Academic Press, New York.
- [27] Deuel, L. E. and Swoboda, A. R., (1972). Arsenic solubility in a reduced environment, *Soil Sci. Soc. Am. Pro.*, 36, 276-278.
- [28] Cullen, W. R. and Reimer, K. J., (1989). Arsenic speciation in the environment, *Chem. Rev.*, 89, 713-764.
- [29] Takamatsu, T., Aoki, H. and Yoshida, T., (1982). Determination of arsenate, arsenite, monomethylarsenate, and dimethylarsenate in soil polluted with arsenic, *Soil Sci.*, 133, 239-246.

- [30] Pohl, B., and Bächmann, K., (1986). *Fresenius J. Anal. Chem.*, 323, 859-865.
- [31] Bhumbla, D. K. and Keefer, R. F., (1994). Arsenic mobilization and bioavailability in soils, In: *Arsenic in the environment, Part 1: Cycling and characterisation*, Ed. Nriagu, J. O., John Wiley & Sons, New York, pp 51-82.
- [32] Chappell, J., Chiswell, B. and Olszowy, H., (1995). Speciation of arsenic in a contaminated soil by solvent extraction, *Talanta*, 42 (3), 323-329.
- [33] Pongratz, R., (1998). Arsenic speciation in environmental samples of contaminated soil, *Sci. Tot. Environ.*, 224, 133-141.
- [34] Pantsar-Kallio, M. and Manninen, P. K. G., (1997). Speciation of mobile arsenic in soil samples as a function of pH, *Sci. Tot. Environ.*, 204, 193-200.
- [35] Landrum, P. F., Hayton, W. L., *et al.*, (1992), *Bioavailability: Physical, Chemical and Biological Interactions*, Session 6, Chapter 3, Synopsis of discussion session on the kinetics behind environmental bioavailability, Thirteenth Pellston Workshop, Pellston, Michigan, August 17-22, Lewis Publishers.
- [36] Newman, M. C. and Jagoe, C. H., (1992), *Bioavailability: Physical, Chemical and Biological Interactions*, Session 3, Chapter 1, Ligands and the bioavailability of metals in aquatic environments, Thirteenth Pellston Workshop, Pellston, Michigan, August 17-22, Lewis Publishers.
- [37] Benson, W. H. and Alberts, J. J., (1992), *Bioavailability: Physical, Chemical and Biological Interactions*, Session 3, Chapter 2, Synopsis of discussion session on the bioavailability of inorganic contaminants, Thirteenth Pellston Workshop, Pellston, Michigan, August 17-22, Lewis Publishers.
- [38] Peijnenburg, W. J. G. M., Posthuma, L., Eijsackers, H. J. P. and Allen H. E., (1997), A Conceptual Framework for Implementation of Bioavailability of Metals for Environmental Management Purposes, *Ecotoxicol. Environ. Saf.*, 37,

163-172.

- [39] Ruby, M. V., Schoof, W. B., Brattin, W., Goldade, M., Post, G., Harnois, M., Mosby, D. E., Casteel, S. W., Berti, W., Carpenter, M., Edwards, D., Cragin, D. and Chappell, W., (1999). Advances in Evaluating the Oral Bioavailability of Inorganics in Soil for Use in Human Health Risk Assessment, *Environ. Sci. Technol.*, 33, 3697-3705.
- [40] Williams, T. M., Rawlins, B. G., Smith, B. and Breward, N., (1998). *In-Vitro* Determination of Arsenic Bioavailability in Contaminated Soil and Mineral Beneficiation Waste from Ron Phibun, Southern Thailand: A Basis for Improved Human Risk Assessment, *Environ. Geochem. Health.*, 20, 169-177.
- [41] Ruby, M. V., Davis, A., Link, T. E., Schoof, R., Chaney, R. L., Freeman, G. B. and Bergstrom, P., (1993). Development of an *in vitro* screening test to evaluate the *in vivo* bioaccessibility of ingested mine-waste lead, *Environ. Sci. Technol.*, 27 (13), 2870-2877.
- [42] Ng, J. C., Kratzmann, S. M., Qi, L., Crawley, H., Chiswell, B. and Moore, M. R., (1998). Speciation and absolute bioavailability: risk assessments of arsenic-contaminated sites in a residential suburb in Canberra, *Analyst*, 123, 889-892.
- [43] Das, A. K., Chakraborty, R., Cervera, M. L. and de la Guardia, M., (1995). Metal speciation in solid matrices, *Talanta*, 42, 1007-1030.
- [44] de la Guardia, M., (1996). Non-Chromatographic Methods for the Element Speciation by Atomic Spectrometry, In: *Element Speciation in Bioinorganic Chemistry*, Ed. Caroli, S., Wiley-Interscience.
- [45] Kot, A. and Namiesnil, J., (2000). The role of speciation in analytical chemistry, *Trends Anal. Chem.*, 19 (2-3), 69-79.
- [46] Templeton, D. M., Ariese, F., Cornelis, R., Danielsson, L. G., Huntan, H., Van Leeuwen, H. P., (2000). Guidelines for terms related to chemical speciation and fractionation of elements. Definitions, structural aspects, and methodological

- approaches (IUPAC Recommendations 2000), *Pure Appl. Chem.*, 72 (8), 1453-1470.
- [47] Bradley, R. I., (1980). Trace Elements in Soils around Llechryd, Dyfed, Wales, *Geoderma*, 24, 17-23.
- [48] Davies, B. E., (1985). Baseline Survey of Metals in Welsh Soils, *Environmental Geochemistry and Health*, I. Thornton, Ed., London, p 16-17.
- [49] McGrath, S. P., (1987). Computerized Quality Control, Statistics and Regional Mapping of the Concentrations of Trace and Major Elements in the Soils of England and Wales, *Soil Use and Management*, 3, 31-38.
- [50] McGrath, S. P., Cunliffe, C. H. and Pope, A. J., (1985). Lead, Zinc, Cadmium, Copper, Nickel Concentrations in the Topsoils of England and Wales, *Environmental Geochemistry and Health*, I. Thornton, Ed., London, p 16-17.
- [51] Archer, F. C. and Hodgson, J. H., (1987). Total and Extractable Trace Element Contents of Soils in England and Wales, *J. Soil Sci.*, 38, 421-431.
- [52] Thornton, I., (1991). Metal contamination of soils in urban areas, In *Soils in the urban environment*, Ed. Bullock, P., Blackwell Scientific Publications, 1991, Chapter 4, pp 47-75.
- [53] Aubert, M. and Pinta, M., (1977). Trace Elements in Soils, Amsterdam: Elsevier, pp 395.
- [54] Chen, T. B., Wong, J. W. C., Zhou, H. Y. and Wong, M. H., (1996). Assessment of Trace Metal Distribution and Contamination in Surface Soils of Hong Kong, *Environ. Pollut.*, 96 (1), 61-68.
- [55] Bini, C., Dall'Aglio, M., Ferretti, O. and Gragnani, R., (1988). Background Levels of Microelements in Soils of Italy, *Environ. Geochem. Health*, 10 (2), 63-69.

- [56] Angelone, M. and Bini, C., (1992). Trace Elements Concentrations in Soils and Plants of Western Europe, Printed in Biogeochemistry of Trace Metals, Ed. Domey C. Adriano, Lewis Publishers, Chapter Two, pp 19-60.
- [57] Aller, A. J. and Deban, L., (1989). Total and Extractable Contents of Trace Metals in Agricultural Soils of the Valderas Area, Spain, *Sci. Total Environ.*, 79, 253-270.
- [58] Shacklette, H. T., Hamilton, J. C., Boerngen, J. C. and Bowles, J. M., (1971). Elemental Composition of Surficial Material in the United States, U.S. Geol. Surv. Prof. Pap., 574D.
- [59] Vinogradov, A. P., (1959). The Geochemistry of Rare and Dispersed Chemical Elements in Soils, 2nd Edition, Consultants Bureau, New York, N.Y.
- [60] Tiller, K. G., de Vries, M. P. C., Spouncer, L. R., Smith, L. H., and Zarcinas, B., (1976). Environmental pollution of the Port Pirie region, Metal contamination of home gardens with city and then vegetable produce, *CSIRO Division of Soils Div. Rep. No. 15*.
- [61] Smith, L. H. and Tiller, K. G., (year unknown). Unpublished work referred to in Tiller, K. G., (1992), Urban Soil Contamination in Australia, *Aust. J. Soil Res.*, 30, 937-957.
- [62] Tiller, K.G., (1992). Urban Soil Contamination in Australia, Table 4 'Background' Concentrations of Heavy Metals in Urban Soils from Non-industrial Sites, *Aust. J. Soil Res.*, 30, 944-957.
- [63] Olszowy, H., Torr, P., and Imray, P., (1995). Trace Element Concentrations in Soils from Rural and Urban Areas of Australia, *Contaminated Sites Monograph Series No. 4*, South Australian Health Commission, pp 1-11.
- [64] Lawrie, R. A., Keneally, J. P. and Stevens, M. L., (1992). Background Trace Elements in Soils around Sydney, Fourth National Soils Conference – Soil Protection and Productivity, Adelaide, South Australia, pp 19-23.

- [65] Torr, P., and Alphen, M., (1993). Background Urban Levels of Heavy Metals in Surface Soils, *Contaminated Sites Monograph Series No. 4*, South Australian Health Commission, pp 65-87.
- [66] Davis, A., Sherwin, D., Ditmars, R. and Hoenke, A., (2001). An Analysis of Soil Arsenic Records of Decision, *Environ. Sci. Technol.*, 35 (12), 2401-2406.
- [67] Davies, B. E., (1992). Trace Metals in the Environment: Retrospect and Prospect, In *Biogeochemistry of Trace Metals*, Ed. Adriano, D. C., Lewis Publishers, Chelsea, MI., U.S.A.
- [68] Alloway, B. J., (1995), The Origins of Heavy Metals in Soils. In: *Heavy Metals in Soils*, Ed. Alloway, B. J., Blackie Academic & Professional, 1995. Chapter 3, pp 38-57.
- [69] Dragun, J. and Chekiri, K., (2005). *Elements in North American Soils*, Amherst Scientific Publishers, Amherst, Massachusetts, U.S.A.
- [70] McGrath, S. P., (1995). Chromium and Nickel, Chapter 7, In: *Heavy Metals in Soils*, Ed. Alloway, B. J., Blackie Academic & Professional, pp 152-178.
- [71] O'Neill, P., (1995). Arsenic, Chapter 5, In: *Heavy Metals in Soils*, Ed. Alloway, B. J., Blackie Academic & Professional, London, pp 105-121.
- [72] Lottermoser, B., (1997). Heavy metal pollution of Australian soils, *Search*, 28 (3), 91-93.
- [73] U.S. Department of Agriculture, Natural Resources Conservation Service, (2003). *National Soil Survey Handbook*, Title 430-VI [Online – www.soils.usda.gov/technical/handbook].
- [74] Unified Soil Classification System, USCS, (2000), American Society for Testing and Materials, D2487-00 Standard Classification of Soils for Engineering

Purposes.

- [75] Holtz, R.D. and Kovacs, W.D. (1981). An Introduction to Geotechnical Engineering, Chapter 3, Prentice Hall.

- [76] American Association of State Highways and Transportation (AASHTO) (1978). Standard specifications for transportation materials and methods of sampling and testing. AASHTO Designation: M 145-73, 12th ed. Washington, D.C.: AASHTO.

- [77] Federal Aviation Administration (FAA) (1967). Airport Paving. Washington D.C.: FAA.

- [78] American Society for Testing and Materials, (2002). D422-63(2002) Standard Test Method for Particle-Size Analysis of Soils.

- [79] Lambe, T. W., and Whitman, R. V., (1969). Soil Mechanics, Massachusetts Institute of Technology, John Wiley & Sons, New York, NY.

- [80] Northcote, K. H., (1971). A Factual Key for the Recognition of Australian Soils, 3rd Edition, Rellim Technical Publications.

- [81] Singh, D.B., Prasad, G. and Rupainwar, D.C., (1996). Adsorption technique for the treatment of As(V)-rich effluents, Colloids Surfaces A: Physicochem. Eng. Aspects 111, 49-56.

- [82] Singh, D. B., Gupta, G. S., Rupainwar, D. C. and Prasad, G., (1993). J. Environ. Sci. Health, Part 1, 28, 1813.

- [83] Genc-Fuhrman, H., Tjell, J. C. and McConchie, D., (2004). Adsorption of Arsenic from Water Using Activated Neutralized Red Mud, Environ. Sci. Technol., 38, 2428-2434

- [84] Matis, K. A., Zouboulis, A. I., Zamboulis, D. and Valtadorou, V., (1999). Sorption of As(V) by Goethite Particles and Study of their Flocculation, Water,

Air, and Soil Pollution, 111, 297-316.

- [85] Genc, H., Tjell, J. C., McConchie, D. and Schuiling, O., (2003). Adsorption of arsenate from water using neutralized red mud, *J. Colloid Interface Sci.*, 264(2), 327-334.
- [86] Zeng, L., (2003). A method for preparing silica-containing iron(III) oxide adsorbents for arsenic removal, *Water Research*, 37, 4351-4358
- [87] Singh, D.B., Prasad, G., Rupainwar, D.C. and Singh, V.N., (1988). As(III) Removal from Aqueous Solution by Adsorption, *Water, Air & Soil Pollut.*, 42, 337-386.
- [88] Mckay, G., El Geundi, M. and Nassar, M. M., (1988). External mass transport processes during the adsorption of dyes onto bagasse pith, *Water Res.*, 22, 1527-1533.
- [89] Gupta, G.S., Prasad, G. and Singh, V.N., (1988). *J. Environ. Sci. Health*, A23, 205.
- [90] Stumm, W., (1992). *Chemistry of the Solid Water Interface*, Wiley & Sons, New York.
- [91] Altundogan, H. S., Altundogan, S., Tumen, F. and Bildik, M., (2000). Arsenic removal from aqueous solutions by adsorption on red mud, *Waste Manage.*, 20, 761-767.
- [92] Arai, Y., Elzinga, E. J. and Sparks, D., (2001). X-ray Absorption Spectroscopic Investigation of Arsenite and Arsenate Adsorption at the Aluminum Oxide–Water Interface, *J. Colloid Interface Sci.*, 235, 80-88.
- [93] Goldberg, S. and Johnston C. T., (2001). Mechanisms of Arsenic Adsorption on Amorphous Oxides Evaluated Using Macroscopic Measurements, Vibrational Spectroscopy, and Surface Complexation Modeling, *J. Colloid Interface Sci.*, 234, 204-216.

- [94] Yang, J. K., Barnett, M., Jardine, P. M. and Casteel, S. W., (2002). Adsorption, Sequestration, and Bioaccessibility of As(V) in Soils, *Environ. Sci. Technol.*, 36, 4562-4569
- [95] Raven, K. P., Jain, A., Loeppert, R. H., (1998). Arsenite and Arsenate Adsorption on Ferrihydrite: Kinetics, Equilibrium, and Adsorption Envelopes, *Environ. Sci. Technol.*, 32, 344-349.
- [96] Prasad, G., (1994). In *Arsenic in the Environment, Part I: Cycling and Characterization*, Nriagu, J. O. (Ed.), Removal of Arsenic(V) from aqueous system by adsorption onto some geological materials, Wiley and Sons, New York.
- [97] Stumm, W., (1987). *Aquatic Surface Chemistry – Chemical Processes at the Particle-Water Interface*, Wiley and Sons, New York.
- [98] Zhang, J. and Stanforth, R., (2005). Slow Adsorption Reaction between Arsenic Species and Goethite (α -FeOOH): Diffusion or Heterogeneous Surface Reaction Control, *Langmuir*, 21, 2895-2901
- [99] Jain, A., Raven, K. P. and Loeppert, R. H., (1999). Arsenite and Arsenate Adsorption on Ferrihydrite: Surface Charge Reduction and Net OH⁻ Release Stoichiometry, *Environ. Sci. Technol.*, 33, 1179-1184.
- [100] Arai, Y., Sparks, D. L. and Davis, J. A., (2004). Effects of Dissolved Carbonate on Arsenate Adsorption and Surface Speciation at the Hematite-Water Interface, *Environ. Sci. Technol.*, 38, 817-824.
- [101] Sun, X. H. and Doner, H. E., (1996). An Investigation of Arsenate and Arsenite Bonding Structures on Goethite by FTIR, *Soil Sci.*, 161, 865.
- [102] Cornell, R. M. and Schwertmann, U., (2003). *The Iron Oxides: Structure, Properties, Reactions, Occurrence and Uses*, 2nd ed., Wiley-VCH: Weinheim, Germany.

- [103] Fuller, C. C., Davis, J. A. and Waychunas, G. A., (1993). Surface chemistry of ferrihydrite: Part 2. Kinetics of arsenate adsorption and coprecipitation, *Geochim. Cosmochim. Acta*, 57, 2271-2282.
- [104] O'Reilly, S. E., Strawn, D. G. and Sparks, D. L., (2001). Residence time effects on arsenate adsorption/desorption mechanisms on goethite, *Soil Sci. Soc. Am. J.*, 65, 67-78.
- [105] Waltham, C. A. and Eick, M. J., (2002). Kinetics of arsenic adsorption on goethite in the presence of sorbed silicic acid, *Soil Sci. Soc. Am. J.*, 66, 818-826.
- [106] Woolson, E. A., Axley, J. H. and Kearney, P. C., (1971). *Soil Sci. Soc. Am. Proc.*, 35, 101.
- [107] Wauchope, R. D., and McDowell, L. L., (1984). *J. Environ. Qual.*, 13, 499.
- [108] Sun, X. and Doner, H. E., (1998). Adsorption and oxidation of arsenite on goethite, *Soil Sci.*, 163 (4), 278-287.
- [109] Theis, T. L., Iyer, R. and Ellis, S. K., (1992). Evaluating a new granular iron oxide for removing lead from drinking water, *J. Am. Water Works Assoc.*, 84, 101-105.
- [110] Anderson, P. and Benjamin, M. M., (1985). Effects of silicon on the crystallization and adsorption properties of ferric oxides, *Environ. Sci. Technol.*, 19, 1048-1053.
- [111] Swedlund, P. J. and Webster, J. G., (1999). Adsorption and polymerization of silicic acid on ferrihydrite, and its effect on arsenic adsorption, *Water Res.*, 33 (16), 3413-3422.
- [112] Manning, B. A. and Goldberg, S., (1996). *Clay Clay Miner.*, 44 (5), 609-623.
- [113] Gao, Y. and Mucci, A., (2001). Acid base reactions, phosphate and arsenate

complexation, and their competitive adsorption at the surface of goethite in 0.7 M NaCl solution, *Geochim. Cosmochim. Acta.*, 65 (14), 2361-2378.

- [114] Wilkie, J. A. and Hering, J. G., (1996). Adsorption of arsenic onto hydrous ferric oxide: effects of adsorbate/adsorbent ratios and co-occurring solutes, *Colloids Surf., A*, 107, 97-110.
- [115] Holm, T. R., (2002). Effects of CO₃²⁻/bicarbonate, Si, and PO₄³⁻ on arsenic sorption to HFO, *J. Am. Water Works Assoc.*, 94 (4), 174-181.
- [116] Redman, A. D., Macalady, D. L. and Ahmann, D., (2002). Natural Organic Matter Affects Arsenic Speciation and Sorption onto Hematite, *Environ. Sci. Technol.*, 36, 2889-2896.
- [117] Gene, H. and Tjell, J. C., (2003). *J. Phys. IV*, 107, 537-540.
- [118] Gregor, J., (2001). Arsenic removal during conventional aluminium-based drinking-water treatment, *Water Res.*, 35 (7), 1659-1664.
- [119] Edwards, M., (1994). *J. Am. Water Works Assoc.*, 86 (9), 64-78.
- [120] Bajpai, S. and Chaudhuri, M., (1999). Removal of Arsenic from Ground Water by Manganese Dioxide-Coated Sand, *J. Environ. Engin.*, 125 (8), 782-784.
- [121] Kanel, S. R., Manning, B., Charlet, L. and Choi, H., (2005). Removal of Arsenic(III) from Groundwater by Nanoscale Zero-Valent Iron, *Environ. Sci. Technol.*, 39, 1291-1298.
- [122] Tseng, W. P., (1977). Effects and dose-response relationships of skin cancer and blackfoot disease with arsenic, *Environ. Health Perspect.*, 19, 109-119.
- [123] U.S. EPA. (1992). Relative absorption factors for risk assessment. U.S. Environmental Protection Agency, Exposure Assessment Group, Washington, DC.

- [124] Freeman, G. B., Schoof, R. A., Ruby, M. V., Davis, A. O., Dill, J. A., Liao, S. C., Lapin, C. A. and Bergstrom, P. D., (1996). Bioavailability of arsenic in soil and house dust impacted by smelter activities following oral administration in *Cynomolgus* monkeys, *Fund. Appl. Toxicol.*, 28 (2), 215-222.
- [125] Sarkar, D., and Datta, R., (2003). New initiatives: A modified *in-vitro* method to assess bioavailable arsenic in pesticide-applied soil, *Environ. Pollut.*, 126, 363-366.
- [126] Basta, N. T., Rodriguez, R. R and Casteel, S. W., (2002). Bioavailability and risk of arsenic exposure by the soil ingestion pathway, Chapter 5, In *Environmental Chemistry of Arsenic*, Edi. Frankenberger, W. T., Marcel Dekker Inc., New York.
- [127] Davis, A., Ruby, M. V., Bloom, M., Schoof, R., Freeman, G. and Bergstrom, P. D., (1996). Mineralogic Constraints on the Bioavailability of Arsenic in Smelter-Impacted Soils, *Environ. Sci. Technol.*, 30, 392-399.
- [128] Davis, A., V. Ruby, M. V. and Bergstrom, P. D., (1992). Bioavailability of Arsenic and Lead in Soils from the Butte, Montana, Mining District, *Environ. Sci. Technol.*, 26, 461-468.
- [129] Rodriguez, R. R., Basta, N. T., Casteel, S. and Pace, L., (1999). *An In Vitro* Gastrointestinal Method to Estimate Bioavailable Arsenic in Contaminated Soils and Solid Media, *Environ. Sci. Technol.*, 33, 642-649.
- [130] Freeman, G. B., Johnson, J. D., Killinger, J. M., Liao, S. C., Davis, A. O., Ruby, M. V., Chaney, R. L., Lovre, S. C., Bergstrom, P. D. (1993). *Fundam. Appl. Toxicol.*, 21, 83-88.
- [131] Freeman, G. B., Johnson, J. D., Liao, S. C., Feder, P. I., Davis, A. O., Ruby, M. V., Schoof, R. A., Chaney, R. L. and Bergstrom, P. D., (1994). *Toxicology*, 91, 151-163.
- [132] Sarkar, D., and Datta, R., (2003). New initiatives: A modified *in-vitro* method

to assess bioavailable arsenic in pesticide-applied soil, *Environ. Pollut.*, 126, 363-366.

- [133] Oomen, A. G., Hack, A., Minekus, M., Zeijdner, E., Cornelis, C., Schoeters, G., Verstraete, W., Van De Wiele, T., Wragg, J., Rempelberg, C. J. M., Sips, A. J. A. M. and Van Wijnen, J. H., (2002). Comparison of five *in vitro* digestion models to study the bioaccessibility of soil contaminants, *Environ. Sci. Technol.*, 36, 3326-3334.
- [134] Hunter, J. M., (1973). Geophagy in Africa and in the United States: A culture-nutrient hypothesis, *Geographical Review*, 63 (2), 170-195.
- [135] Drover, D. P. and Borrell, W., (1980). Analysis of two edible clays from East Sepik, Papua New Guinea, *Science in New Guinea*, 7 (1), 6-11.
- [136] Lake, D.L., Kirk, P.W.W. and Lester, J.N., (1984). Fractionation, characterisation, and speciation of heavy metals in sewage sludge and sludge-amended soils: A review, *J. Environ. Qual.*, 13, 175-183.
- [137] Gong, Z., Lu, X., Ma, M., Watt, C. and Le, C., (2002). Arsenic speciation analysis, *Talanta*, 58, 77-96.
- [138] Zhang, H., Davison, W., Miller, S. and Tych, W., (1995). In situ high resolution measurements of fluxes of Ni, Cu, Fe and Mn and concentrations of Zn and Cd in porewaters by DGT, *Geochim. Cosmochim. Acta*, 59, 4181-4191.
- [139] Zhang, H., Davison, W., Knight, B. and McGrath, S., (1998). In situ measurements of solution concentrations and fluxes of trace metals in soils using DGT, *Environ. Sci. Technol.*, 32, 704-710.
- [140] Hooda, P. S., Zhang, H., Davison, W. and Edwards, A. C., (1999). Measuring bioavailable trace metals by diffusive gradients in thin films (DGT): soil moisture effects on its performance in soils, *Eur. J. Soil Sci.*, 50, 285-294.
- [141] Zhang, H., Zhao, F., Sun, B., Davison, W. and McGrath, S. P., (2001). A new

method to measure effective soil solution concentration predicts copper availability to plants, Environ. Sci. Technol., 35, 2602-2607.

- [142] Jones, A. D., Supplement 5: Partition Equilibria: Henry's Law and Octanol-water Partition Equilibria important concepts for environmental chemistry, Review Materials for Chemistry 402, The Pennsylvania State University.
- [143] IUPAC Compendium of Chemical Terminology, Second Edition (1993). 65, 2385.
- [144] Perin, G., Fabris, R., Manente, S., Rebello Wagener, A., Hamacher, C. and Scotto, S., (1997). A five-year study on the heavy-metal pollution of Guanabara Bay sediments (Rio De Janeiro, Brazil) and evaluation of the metal bioavailability by means of geochemical speciation, Water Res., 31, 3017-3028.
- [145] Hansch, C. and Fujita, T., (1964). p - σ - π Analysis. A Method for the correlation of biological activity and chemical structure, J. Am. Chem. Soc., 86, 1616-1625.
- [146] Leo, A., Hansch, C. and Elkins, D., (1971). Partition Coefficients and their Uses, Chem. Rev., 71, 525-616.
- [147] Hansch, C. and Leo, A., (1979). Substituent Constants for Correlation Analysis in Chemistry and Biology, Wiley, New York.
- [148] Chou, J. T. and Jurs, P. C., (1979). Computer-assisted computation of partition coefficient from molecular structures using fragment constants. J. Chem. Inf. Comput. Sci., 19, 172-178.
- [149] Leo, A., (1990). In Comprehensive Medicinal Chemistry, Hansch, C. (Ed), Pergamon: Oxford, 4, 295-319.
- [150] Rekker, R. F. (1977). The Hydrophobic Fragment Constant, Elsevier: New York.
- [151] Suzuki, T. and Kudo, Y., (1990). Automatic log P estimation based on combined

additive modeling methods, *J. Comput.-Aided Mol. Des.*, 4, 155-198.

- [152] Klopman, G. and Wang, S., (1991). A Computer Automated Structure Evaluation (CASE) Approach to Calculation of Partition Coefficient, *J. Comput. Chem.*, 12, 1025-1032.
- [153] Klopman, G, Li, J., Wang, S. and Dimayuga, M., (1994). Computer Automated log P Calculations Based on an Extended Group Approach, *J. Chem. Inf. Comput. Sci.*, 34, 752-781.
- [154] Broto, P., Moreau, G. and Vanduycke, C., (1984). Molecular structures: perception, autocorrelation descriptor and SAR studies, *Eur. J. Med. Chem.*, 19, 71-78.
- [155] Ghose, A. K. and Crippen, G. M., (1986). Atomic Physicochemical Parameters for Three-Dimensional Structure-Directed Quantitative Structure-Activity Relationships. I. Partition Coefficients as a Measure of Hydrophobicity, *J. Comput. Chem.*, 7, 565-577.
- [156] Ghose, A. K., Pritchett, A. and Crippen, G. M., (1988). Atomic Physicochemical Parameters for Three-Dimensional Structure-Directed Quantitative Structure-Activity Relationships. III. Modelling Hydrophobic Interactions, *J. Comput. Chem.*, 9, 80-90.
- [157] Klopman, G. and Iroff, L. D., (1981). Calculation of Partition Coefficients by the Charge Density Method, *J. Comput. Chem.*, 2, 157-160.
- [158] Bodor, N., Gabanyi, Z. and Wong, C. K., (1989). A New Method for the Estimation of Partition Coefficient, *J. Am. Chem. Soc.*, 111, 3783-3786.
- [159] Wang, R., Fu, Y. and Lai, L., (1997). A New Atom-Additive Method for Calculating Partition Coefficients, *J. Chem. Inf. Comput. Sci.*, 37 (3), 615-621.
- [160] Liang, J. and Schoenau, J. J., (1996). Speciation in metal contaminated soils as revealed by an ion exchange resin membrane fractionation procedure, *Commun.*

Soil Sc. Plant Anal., 27 (18 – 20), 3013-3026.

- [161] Lebourg, A., Sterckeman, T., Ciesielski, H. and Proix, N., (1998). Trace metal speciation in three unbuffered salt solutions used to assess their bioavailability in soil, *J. Environ. Qual.*, 27, 584-590.
- [162] Conder, J. M., Lanno, R. P. and Basta, N. T., (2001). Assessment of metal availability in smelter soil using earthworms and chemical extractions, *J. Environ. Qual.*, 30 (4), 1231-1238.
- [163] Corbisier, P., Van der Lelie, D., Borremans, B., Provoost, A., De Lorenzo, V., Brown, N. L., Lloyd, J. R., Hobman, J. L., Csoregi, E., Johansson, G. and Mattiasson, B., (1999). Whole cell- and protein-based biosensors for the detection of bioavailable heavy metals in environmental samples, *Anal. Chim. Acta*, 387, 235-244.
- [164] Agemian, H. and Chau, A. s., (1976). Evaluation of extraction techniques for the determination of metals in aquatic sediments, *Analyst*, 101, 761-767.
- [165] Tessier, A., Campbell, P. G. and Bisson, M., (1979). Sequential extraction procedure for the speciation of particulate trace metals, *Anal. Chem.*, 51, 844-851.
- [166] Gatehouse, S., Russel, D.W. and van Moort, J.C., (1977). Sequential soil analysis in exploration geochemistry, *J. Geochem. Explor.*, 8, 483-494.
- [167] Sposito, G., Lund, L.J. and Chang, A.C., (1982). Trace metal chemistry in arid-zone field soils amended with sewage sludge: I. Fractionation of Ni, Cu, Zn, Cd, and Pb in solid phases, *Soil. Sci. Soc. Am. J.*, 46, 260-264.
- [168] Miller, W.P., and McFee, W.W., (1983). Distribution of Cd, Zn, Cu, and Pb in soils of industrial northwestern Indiana, *J. Environ. Qual.*, 12, 29-33.
- [169] Bermond, A., Yousfi, I. and Ghestem, J., (1998). Kinetic approach to the chemical speciation of trace metals in soils, *Analyst*, 123, 785-789.

- [170] Marin, B., Valladon, M., Polve, M. and Monaco, A., (1997). Reproducibility testing of a sequential extraction scheme for the determination of trace metal speciation in a marine reference sediment by inductively coupled plasma-mass spectrometry, *Anal. Chim. Acta*, 342, 91-112.
- [171] Psenner, R., Pucsko, R. and Sager, M., (1984). *Arch. Hydro-biol. Suppl.*, 70, 111-115.
- [172] Shuman, L.M. and Hargrove, W.L., (1985). Effect of tillage on the distribution of manganese, copper, iron, and zinc in soil fractions, *Soil. Sci. Soc. Am. J.*, 49, 1117-1121.
- [173] Kersten, M. and Forstner, U., (1986). Chemical fractionation of heavy metals in anoxic estuarine and coastal sediments, *Water Sci. Technol.*, 18, 121-130.
- [174] Zeien, H. and Brummer, G.W., (1989). *Mitt. Dt. Bodenkundl. Ges.*, 59, 505-510.
- [175] Hirner, A.V., Kritsotakis, K. and Tobschall, H.J., (1990). Metal-organic associations in sediments. Comparison of unpolluted recent and ancient sediments and sediments affected by anthropogenic pollution, *Appl. Geochem.*, 5, 491-505.
- [176] Chester, R. and Huges, M. J., (1967). A chemical technique for the separation of ferro-manganese minerals, carbonate minerals and adsorbed trace elements from pelagic sediments, *Chem. Geol.*, 2, 249-262.
- [177] Ho, M. D. and Evans, G. J., (1997). Operational speciation of cadmium, copper, lead and zinc in the NIST standard reference material 2710 and 2711 (Montana soil) by the BCR sequential extraction procedure and flame atomic absorption spectrometry, *Anal. Commun.*, 34, 363-364.
- [178] Adriano, D. C., (2001). *Trace Elements in Terrestrial Environments*, 2nd Edition, Springer, New York.

- [179] Wenzel, W. W., Kirchbaumer, N., Prohaska, T., Stingeder, G., Lombi, E. and Adriano, D. C., (2001). Arsenic fractionation in soils using an improved sequential extraction procedure, *Anal. Chim. Acta*, 436, 309-323.
- [180] Shiwatana, J., McLaren, R. G., Chanmekha, N. and Samphao, A., (2001). Fractionation of arsenic in soil by a continuous-flow sequential extraction method, *J. Environ. Qual.*, 30 (6), 1940-1949.
- [181] Johnston, S. E. and Barnard, W. M., (1979). Comparative effectiveness of fourteen solutions for extracting As from four western New York soils, *Soil Sci. Soc. Am. J.*, 43, 304.
- [182] Polyak, K. and Hlavay, J., (1999). Environmental mobility of trace metals in sediments collected in the Lake Balaton, *Fresenius J. Anal. Chem.*, 363, 587-593.
- [183] Marin, A., Lopez-Gonzalvez, A., and Barbas, C., (2001). Development and validation of extraction methods for determination of zinc and arsenic speciation in soils using focused ultrasound: Application to heavy metal study in mud and soils, *Anal. Chim. Acta*, 442, 305-318.
- [184] Szpunar, J., (2000). Bio-inorganic speciation analysis by hyphenated techniques, *Analyst*, 15, 963-988.
- [185] Guerin, T., Astruc, A., and Astruc, M., (1999). Review Speciation of arsenic and selenium compounds by HPLC hyphenated to specific detectors: a review of the main separation techniques, *Talanta*, 50, 1-24.
- [186] Timberbaev, A. R., (2000). Review Element speciation analysis by capillary electrophoresis, *Talanta*, 52, 573-606.
- [187] Kolbl, G., Kalcher, K, and Irgolic, K., (1993). Ion chromatography determination of selenite and selenate-specific detection by flame and graphite furnace atomic absorption spectrometry, *Anal. Chim. Acta*, 284, 301-310.

- [188] Szpunar-Lobinska, J., Witte, C., Lobinski, R., and Adams, F., (1995). Fresenius J. Anal. Chem., 351, 351.
- [189] Beauchemin, D., Siu, K., McLaren, J., Berman, S., (1989). Determination of arsenic species by high-performance liquid chromatography-inductively coupled plasma mass spectrometry, J. Anal. At. Spectrom., 4 (3), 285-289.
- [190] Cai, Y., Cabanas, M., Fernandez-Turiel, J., Abalos, M., and Boyona, J., (1995). On-line preconcentration of selenium(IV) and selenium(VI) in aqueous matrices followed by liquid chromatography-inductively coupled plasma mass spectrometry determination, Anal. Chim. Acta, 314, 183.
- [191] Li, K., Li, S. F. Y., (1995). Speciation of selenium and arsenic compounds in natural waters by capillary zone electrophoresis after on-column preconcentration with field-amplified injection, Analyst, 120, 361-366.
- [192] Naidu, R., Smith, J., McLaren, R. G., Stevens, D. P., Sumner, M. E. and Jackson, P. E., (2000). Application of capillary electrophoresis to anion speciation in soil water extracts: II. Arsenic, Soil Sci. Soc. Am. J., 64, 122.
- [193] Tomlinson, M. J., Lin, L. and Caruso, J. A., (1995). Plasma mass spectrometry as a detector for chemical speciation studies, Analyst, 120, 583-589.
- [194] Morita, M., Uehiro, T. and Fuwa, K., (1981). Determination of arsenic compounds in biological samples by liquid chromatography with inductively coupled argon plasma-atomic emission spectrometric detection, Anal. Chem., 53, 1806.
- [195] Tye, C. T., Haswell, S. J., O'Neill, P. and Bancroft, K. C. C., (1985). High performance liquid chromatography with hydride generation/atomic absorption spectrometry for the determination of arsenic species with application to some water samples, Anal. Chim. Acta, 169, 195.

- [196] Morita, M. and Shibata, Y., (1987). Speciation of arsenic compounds in marine life by high performance liquid chromatography combined with inductively coupled argon plasma atomic emission spectrometry, *Anal. Sci.*, 3, 575.
- [197] Maitani, T., Uchiyama, S. and Saito, Y., (1987). Hydride generation-flame atomic-absorption spectrometry as an arsenic detector for high-performance liquid chromatography, *J. Chromatogr. A*, 391, 161-168.
- [198] Shiomi, K., Orii, M., Yamanaka, H. and Kikuchi, T., (1987). *Nippon Suisan Gakkaishi*, 53, 103.
- [199] Heitkemper, D., Creed, J., Caruso, J. and Fricke, F. L., (1989). Speciation of arsenic in urine using high-performance liquid chromatography with inductively coupled plasma mass spectrometric detection, *J. Anal. At. Spectrom.*, 4 (3), 279-284.
- [200] Ricci, G. R., Shepard, L. S., Colovos, G. and Hester, N. E., (1981). Ion chromatography with atomic absorption spectrometric detection for determination of organic and inorganic arsenic species, *Anal. Chem.*, 53 (4), 610-613.
- [201] Brinckman, F. E., Jewett, K. L., Iverson, W. P., Irgolic, K. J., Ehrhardt, K. C. and Stockton, R. A., (1980). Graphite furnace atomic absorption spectrophotometers as automated element-specific detectors for high-pressure liquid chromatography: The determination of arsenite, arsenate, methylarsonic acid and dimethylarsinic acid, *J. Chromatogr. A*, 191, 31-46.
- [202] Kurosawa, S., Yasuda, K., Tagushi, M., Yamazaki, S., Toda, S., Morita, M., Uehiro, T. and Fuwa, K., (1980). *Agric. Biol. Chem.*, 44, 1993.
- [203] Iadevaia, R., Aharonson, N. and Woolson, E. A., (1980). *J. Assoc. Off. Anal. Chem.*, 63, 742.

- [204] Roychowdhury, S. B. and Koropchak, J. A., (1990). Thermospray enhanced inductively coupled plasma atomic emission-spectroscopy detection for liquid chromatography, *Anal. Chem.*, 62 (5), 484-489.
- [205] Spall, W. D., Lynn, J. G., Andersen, J. L., Valdez, J. G. and Gurley, L. R., (1986). High-performance liquid chromatographic separation of biologically important arsenic species utilizing on-line inductively coupled argon plasma atomic emission spectrometric detection, *Anal. Chem.*, 58, 1340.
- [206] Branch, S., Bancroft, K. C. C., Ebdon, L. and O'Neill, P., (1989). *Anal. Proc.*, 26, 73.
- [207] Shibata, Y. and Morita, M., (1989). Speciation of arsenic by reverse-phase high performance liquid chromatography-inductively coupled plasma mass spectrometry, *Anal. Sci.*, 5, 107.
- [208] Beauchemin, D., Bednas, M. E., Berman, S. S., McLaren, J. W., Siu, K. W. M. and Sturgeon, R. E., (1988). Identification and quantitation of arsenic species in a dogfish muscle reference material for trace elements, *Anal. Chem.*, 60 (20), 2209-2212.
- [209] Francesconi, K. A., Micks, P., Stockton, R. A., and Irgolic, K. J., (1985). Quantitative determination of arsenobetaine, the major water-soluble arsenical in three species of crab, using high pressure liquid chromatography and an inductively coupled argon plasma emission spectrometer as the arsenic-specific detector, *Chemosphere*, 14 (10), 1443.
- [210] Stocktan, R. A., and Irgolic, K. J., (1979). *Int. J. Environ. Anal. Chem.*, 6, 313.
- [211] Nisamaneepong, W., Ibrahim, M., Gilbert, W., and Caruso, J. A., (1984). *J. Chromatogr. Sci.*, 22, 473.
- [212] Low, G.K.-C., Batley, G. E., and Buchanan, S. J., (1986). Application of column switching in high-performance liquid chromatography to arsenic speciation

analysis with inductively coupled argon plasma spectrometric detection, *J. Chromatogr.*, 368, 423.

- [213] Wangkarn, S. and Pergantis, S. A., (2000). High-speed separation of arsenic compounds using narrow-bore high-performance liquid chromatography on-line with inductively coupled plasma mass spectrometry, *J. Anal. At. Spectrom.*, 15, 627-633.
- [214] Do, B., Robinet, S., Pradeau, D. and Guyon, F., (2001). Speciation of arsenic and selenium compounds by ion-pair reversed-phase chromatography with electrothermic atomic absorption spectrometry: Application of experimental design for chromatographic optimisation, *J. Chromatogr. A*, 918, 87-98.
- [215] Manning, B. A. and Martens, D. A., (1997). Speciation of Arsenic(III) and Arsenic(V) in Sediment Extracts by High-Performance Liquid Chromatography-Hydride Generation Atomic Absorption Spectrophotometry, *Environ. Sci. Technol.*, 31 (1), 171-177.
- [216] Howard, A. G. and Hunt, L. E., (1993). Coupled photooxidation-hydride AAS detector for the HPLC of arsenic compounds, *Anal. Chem.*, 65, 2995-2998.
- [217] Capelo, J., Lavilla, I. and Bendicho, C., (2001). Ultrasonic Extraction Followed by Sonolysis-Ozonolysis as a Sample Pretreatment Method for Determination of Reactive Arsenic toward Sodium Tetrahydroborate by Flow Injection-Hydride Generation AAS, *Anal. Chem.*, 73, 3732-3736.
- [218] Carrero, P., Malave, A., Luis Burguera, J., Burguera, M. and Rondon, C., (2001). Determination of various arsenic species by flow injection hydride generation atomic absorption spectrometry: investigation of the effects of the acid concentration of different reaction media on the generation of arsines, *Anal. Chim. Acta*, 438, 195-204.
- [219] Shraim, A., Chiswell, B. and Olszowy, H., (2000). Use of perchloric acid as a reaction medium for speciation of arsenic by hydride generation-atomic absorption spectrometry, *Analyst*, 125, 949-953.

- [220] Ebdon, L., Hill, S. and Ward, R. W., (1987). Directly coupled chromatography-atomic spectroscopy. Part 1. Directly coupled gas chromatography-atomic spectroscopy. A review, *Analyst*, 111, 1113-1138.
- [221] Blais, J.-S., Momplaisir, G.-M., and Marshall, W. D., (1990). Determination of arsenobetaine, arsenocholine, and tetramethylarsonium cations by HPLC thermochemical hydride generation-atomic absorption spectrometry, *Anal. Chem.*, 62 (11), 1161-1166.
- [222] Bermejo-Barrera, P., Barciela-Alonso, C., Ferron-Novais, M and Bermejo-Barrera, A., (1995). Speciation of arsenic by the determination of total arsenic and arsenic(III) in marine sediment samples by electrothermal atomic absorption spectrometry, *J. Anal. At. Spectrom.*, 10, 247-252.
- [223] Chausseau, M., Roussel, C., Gilon, N. and Mermet, J. M., (2000). Optimization of HPLC-ICP-AES for the determination of arsenic species, *Fresenius' J. Anal. Chem.*, 366, 476-480.
- [224] Weeger, W., Lievremont, D., Perret, M., Lagarde, F., Hubert, J. C., Leroy, M. and Lett, M. C., (1999). Oxidation of arsenite to arsenate by a bacterium isolated from an aquatic environment, *Biometals*, 12, 141-149.
- [225] Rauret, G., Rubio, R. and Padro, A., (1991). *Fresenius' J. Anal. Chem.*, 340, 157.
- [226] Rubio, R., Padro, A., Alberti, J. and Rauret, G., (1992). *Mikrochim. Acta*, 109, 39-44.
- [227] Gettar, R. T., Garavaglia, R. N., Gautier, E. A. and Batistoni, D. A., (2000). Determination of inorganic and organic anionic arsenic species in water by ion chromatography coupled to hydride generation-inductively coupled plasma atomic emission spectrometry, *J. Chromatogr. A*, 884, 211-221.

- [228] Do, B., Alet, P., Pradeau, D., Poupon, J., Guilley-Gaillet, M. and Guyon, F., (2000). On-line reversed-phase liquid chromatography hydride generation emission spectrometry: speciation of arsenic in urine of patients intravenously treated with As_2O_3 , *J. Chromatogr. B*, 740, 179-186.
- [229] Thompson, J. J., and Houk, R. S., (1986). Inductively coupled plasma mass spectrometric detection for multielement flow injection analysis and elemental speciation by reversed-phase liquid chromatography, *Anal. Chem.*, 58 (12), 2541-2548.
- [230] Yehl, P., and Tyson, J. F., (1997). Towards Speciation of Arsenic in a Standard Reference River Sediment by High-performance Ion Chromatography Coupled With Plasma Source Mass Spectrometry, *Anal. Commun.*, 34 (2), 49-51.
- [231] Geiszinger, A., Goessler, W., Kuehnelt, D., Francesconi, K. and Kosmus, W., (1998). Determination of Arsenic Compounds in Earthworms, *Environ. Sci. Technol.*, 32 (15), 2238-2243.
- [232] Byrdey, F. A. and Caruso, J. A., (1995). Trace metals speciation by HPLC with plasma source mass spectrometry detection, *Environ. Health Perspect. Suppl.*, 103 (1), 21.
- [233] Vela, N. P. and Caruso, J. A., (1993). The potential of LC-ICP-MS for trace metal speciation, *J. Anal. At. Spectrom.*, 8, 787-794.
- [234] Zybin, A., Schaldach, G., Berndt, H. and Niemax, K., (1998). Metal speciation in the ppt range by HPLC and diode laser atomic absorption spectrometry in a flame, *Anal. Chem.*, 70, 5093-5096.
- [235] Van Holderbeke, M., Zhao, Y., Vanhaecke, F., Moens, L., Dams, R. and Sandra, P., (1999). Speciation of six arsenic compounds using capillary electrophoresis-inductively coupled plasma mass spectrometry, *J. Anal. At. Spectrom.*, 14, 229-234.

- [236] Magnuson, M.L., Creed, M. T. and Brockhoff, C. A., (1997). Speciation of Arsenic Compounds in Drinking Water by Capillary Electrophoresis with Hydrodynamically Modified Electroosmotic Flow Detected Through Hydride Generation Inductively Coupled Plasma Mass Spectrometry With a Membrane Gas-Liquid Separator, *J. Anal. At. Spectrom.*, 12, 689-695.
- [237] Prange, A. and Schaumlöffel, D., (1999). Determination of element species at trace levels using capillary electrophoresis-inductively coupled plasma sector field mass spectrometry, *J. Anal. At. Spectrom.*, 14, 1329-1332.
- [238] Le, X. C., Lu, X., Ma, M., Cullen, W. R., Aposhian, H. V. and Zheng, B., (2000). Speciation of Key Arsenic Metabolic Intermediates in Human Urine, *Anal. Chem.*, 72, 5172-5177.
- [239] Le, X. C. and Ma, M., (1998). Short-Column Liquid Chromatography with Hydride Generation Atomic Fluorescence Detection for the Speciation of Arsenic *Anal. Chem.* 70, 1926-1933.
- [240] Bohari, Y., Astruc, A., Astruc, M. and Cloud, J., (2001). Improvements of hydride generation for the speciation of arsenic in natural freshwater samples by HPLC-HG-AFS, *J. Anal. At. Spectrom.*, 16, 774-778.
- [241] Vilano, M., Padro, A. and Rubio, R., (2000). Coupled techniques based on liquid chromatography and atomic fluorescence detection for arsenic speciation, *Anal. Chim. Acta*, 411, 71-79.
- [242] Corr, J. J. and Larsen, E. H., (1996). Arsenic speciation by liquid chromatography coupled with ionspray tandem mass spectrometry, *J. Anal. At. Spectrom.*, 11, 1215-1224.
- [243] Shibata, Y. and Morita, M., (1989). Exchange of comments on identification and quantitation of arsenic species in a dogfish muscle reference material for trace elements, *Anal. Chem.*, 61, 2116-2118.

- [244] Corr, J. J., (1997). Measurement of Molecular Species of Arsenic and Tin Using Elemental and Molecular Dual Mode Analysis by Ionspray Mass Spectrometry, *J. Anal. At. Spectrom.*, 12, 537-546.
- [245] Pergantis, S. A., Winnik, W. and Betowski, D., (1997). Determination of Ten Organoarsenic Compounds Using Microbore High-performance Liquid Chromatography Coupled With Electrospray Mass Spectrometry-Mass Spectrometry, *J. Anal. At. Spectrom.*, 12, 531-536.
- [246] Inoue, Y., Date, Y., Sakai, T., Shimizu, N., Yoshida, K., Chen, H., Kuroda, K. and Endo, G., (1999). Identification and quantification by LC-MS and LC-ICP MS of arsenic species in urine of rats chronically exposed to dimethylarsinic acid (DMAA), *Appl. Organomet. Chem.*, 13, 81-89.
- [247] Florencio, M. H., Duarte, M. F., De Bettencourt, A. M. M., Gomes, M. L. and Vilas, L. F., (1997). Electrospray Mass Spectra of Arsenic Compounds, *Rapid Commun. Mass Spectrom.*, 11, 469-473.
- [248] Pedersen, S. N. and Francesconi, K. A., (2000). Liquid chromatography electrospray mass spectrometry with variable fragmentor voltages gives simultaneous elemental and molecular detection of arsenic compounds, *Rapid Commun. Mass Spectrom.* 14, 641-645.
- [249] McSheehy, S. and Szpunar, J., (2000). Speciation of arsenic in edible algae by bi-dimensional size-exclusion anion exchange HPLC with dual ICP-MS and electrospray MS/MS detection, *J. Anal. At. Spectrom.*, 15, 79-87.
- [250] Mcsheehy, S., Pohl, P., Lobinski, R. and Szpunar, J., (2001). Investigation of arsenic speciation in oyster test reference material by multidimensional HPLC-ICP-MS and electrospray tandem mass spectrometry (ES-MS-MS), *Analyst*, 126, 1055-1062.
- [251] Gallagher, P. A., Wei, X., Shoemaker, J. A., Brockhoff, C. A. and Creed, J. T., (1999). Detection of arsenosugars from kelp extracts *via* IC-electrospray

ionization-MS-MS and IC membrane hydride generation ICP-MS, *J. Anal. At. Spectrom.*, 14, 1829-1834.

- [252] Pergantis, S. A., Wangkarn, S., Francesconi, K. A. and Thomas-Oates, J. E., (2000). Identification of Arsenosugars at the Picogram Level Using Nano-electrospray Quadrupole Time-of-Flight Mass Spectrometry, *Anal. Chem.*, 72 (2), 357-366.
- [253] Madsen, A. D., Goessler, W., Pedersen, S. N. and Francesconi, K. A., (2000). Characterization of an algal extract by HPLC-ICP-MS and LC-electrospray MS for use in arsenosugar speciation studies, *J. Anal. At. Spectrom.* 15, 657-662.
- [254] Gallagher, P. A., Shoemaker, J. A., Wei, X., Brockhoff-Schwegel, C. A. and Creed, J. T., (2001). Extraction and detection of arsenicals in seaweed via accelerated solvent extraction with ion chromatographic separation and ICP-MS detection, *Fresenius' J. Anal. Chem.*, 369, 71-80.
- [255] Wang, J. and Marshall, W. D., (1994). Metal speciation by supercritical fluid extraction with on-line detection by atomic absorption spectrometry, *Anal. Chem.*, 66, 3900-3907.
- [256] Deng, B. and Chan, W., (2001). Metal speciation using capillary electrophoresis – inductively coupled plasma atomic emission spectrometry and polytetrafluoroethylene capillaries, *Electrophoresis*, 22, 2186-2191.
- [257] Barnowski, C., Jakubowski, N., Stuewer, D., and Broekaert, J. A. C., (1997). Speciation of chromium by direct coupling of ion exchange chromatography with inductively coupled plasma mass spectrometry, *J. Anal. At. Spectrom.*, 12, 1155-1161.
- [258] Kalcher, K., Lintschinger, J., Gossler, W., Kolbl, G. and Novic, M., (1995). *Fresenius' J. Anal. Chem.*, 351, 604.
- [259] Tomlinson, M. J. and Caruso, J. A., (1996). Speciation of chromium using thermospray nebulization as sample introduction into inductively coupled

- plasma mass spectrometry, *Anal. Chim. Acta*, 322 (1), 1-9.
- [260] Pantsar-Kallio, M. and Manninen, P. K. G., (1996). Speciation of chromium in aquatic samples by coupled column ion chromatography-inductively coupled plasma-mass spectrometry, *Anal. Chim. Acta*, 318 (3), 335-343.
- [261] Forehand, T. J., Dupuy, A. E. and Tal, H., (1976). Determination of arsenic in sandy soils, *Anal. Chem.*, 48 (7), 999-1001.
- [262] Beard, H. C. and Lyerly, L. A., (1961). Separation of arsenic from antimony and bismuth by solvent extraction, *Anal. Chem.*, 33 (12), 1781-1782.
- [263] Greenwood, N. N. and Earnshaw, A., (1984). *Chemistry of the Elements*, Pergamon Press, Oxford, pp 650-665.
- [264] Holak, W. and Specchio, J. J., (1991). Determination of total arsenic, As(III) and As(V) in foods by atomic absorption spectrometry, *At. Spectrosc.*, 12 (4), 105-108.
- [265] Maher, W. A., (1981). Determination of inorganic and methylated arsenic species in marine organisms and sediments, *Anal. Chim. Acta*, 126, 157-165.
- [266] Maher, W. A., (1984). Mode of occurrence and speciation of arsenic in some pelagic and estuarine sediments, *Chem. Geol*, 47, 333-345.
- [267] Hansen, S. H., Larsen, E. h., Pritzl, G. and Cornett, C., (1992). Separation of Seven Arsenic Compounds by High-performance Liquid Chromatography With On-line Detection by Hydrogen-Argon Flame Atomic Absorption Spectrometry and Inductively Coupled Plasma Mass Spectrometry, *J. Anal. At. Spectrom.*, 7, 629-634.
- [268] Hirner, A. V., (1992). Trace element speciation in soils and sediments using sequential chemical extraction methods, *Int. J. Environ. Anal. Chem.*, 46, 77-85.
- [269] Foster, A. L., Brown, G. E. (Jr.), Tingle, T. N. and Parks, G. A., (1998).

Quantitative arsenic speciation in mine tailings using X-ray absorption spectroscopy, *Am. Mineral.*, 83, 553-568.

- [270] Larsen, E. H., (1995). *Fresenius' J. Anal. Chem.*, 352, 582.
- [271] Vergara Gallardo, M., Bohari, Y., Astruc, A., Potin-Gautier, M. and Astruc, M., (2001). Speciation analysis of arsenic in environmental solids Reference Materials by high-performance liquid chromatography–hydride generation–atomic fluorescence spectrometry following orthophosphoric acid extraction, *Anal. Chim. Acta*, 441, 257-268.
- [272] Demesmay, C. and Ollé, M., (1997). Application of microwave digestion to the preparation of sediment samples for arsenic speciation, *Fresenius J. Anal. Chem.*, 357, 1116.
- [273] Thomas, P., Finnie, J. K. and Williams, J. G., (1997). Feasibility of Identification and Monitoring of Arsenic Species in Soil and Sediment Samples by Coupled High-performance Liquid Chromatography - Inductively Coupled Plasma Mass Spectrometry, *J. Anal. Atom. Spectrom.*, 12, 1367-1372.
- [274] Garcia-Manyes, S., Jimenez, G., Padro, A., Rubio, R. and Rauret, G., (2002). Arsenic speciation in contaminated soils, *Talanta*, 58, 97-109.
- [275] Pizarro, I., Gomez, M., Camara, C. and Palacios, M. A., (2003). Arsenic speciation in environmental and biological samples Extraction and stability studies, *Anal. Chim. Acta*, 495, 85-98.
- [276] Diomides, C. J., (2000). Background Soil Quality Study for the Western Suburbs of Melbourne, Masters Thesis completed at Victoria University.
- [277] Melway, Greater Melbourne, Street Directory (1999). Melway Publishing Pty Ltd.
- [278] National Environment Protection (Assessment of Site Contamination) Measure 1999, Schedule B (1), Table 5-A – Soil Investigation Levels - Background

Ranges, pp 9.

- [279] ANZECC/NHMRC (1992). Guidelines for the Assessment and Management of Contaminated Sites, Table 2 – Environmental Soil Quality Guidelines, pp 40-41.
- [280] Moore, D. S. and McCabe, G.P., (1993). Introduction to the Practice of Statistics, Second Edition, W. H. Freeman and Company, New York.
- [281] Preparation and Determination of Moisture Content in Soils, (1998). National Measurement Institute (NMI), Method VL237, Issue 2.
- [282] Rayment, G. E. and Higginson, F. R., (1992). Australian Laboratory Handbook of Soil and Water Chemical Company Methods. Soil pH, Reed International Books Australia Ltd, Melbourne, Australia, pp 17-23.
- [283] Attiwell, S. and Worrall, R., (1996). “Soil Sub-Sampling.” Draft Public Interest Project 479, Australian Government Analytical Laboratories (AGAL), Perth, Western Australia.
- [284] Rayment, G. E. and Higginson, F. R., (1992). Australian Laboratory Handbook of Soil and Water Chemical Company Methods. Organic carbon, Reed International Books Australia Ltd, Melbourne, Australia, pp 29-37.
- [285] Edgell, K., (1988). USEPA Method Study 37 - SW-846 Method 3050 Acid Digestion of Sediments, Sludges, and Soils. EPA Contract No. 68-03-3254.
- [286] Corbridge, D. E. C., (1974). The Structural Chemistry of Phosphorus, Elsevier Scientific Publishing Company, Amsterdam, Netherlands.
- [287] Corbridge, D. E. C., (1980). Studies in Inorganic Chemistry 2 – Phosphorus, An Outline of its Chemistry, Biochemistry and Technology, 2nd Edi., Elsevier Scientific Publishing Company, Amsterdam, Netherlands.
- [288] Emsley, J. and Hall, D., (1976). The Chemistry of Phosphorus, Environmental, organic, inorganic, biochemical and spectroscopic aspects, Harper & Row Ltd,

London.

- [289] Ross, A. R. S, Ikonomou, M. G., Thompson, J. A. J and Orians, K. J., (1998). Determination of Dissolved Metal Species by Electrospray Ionization Mass Spectrometry, *Analyt. Chem.*, 70, 2225.
- [290] Hehre, W. J., (2003). *A Guide to Molecular Mechanics and Quantum Chemical Calculations*, Wavefunction, Inc., 18401 Von Karman Ave., Suite 370, Irvine, CA 92612, U.S.A., ISBN 1-890661-19-X.
- [291] Geological Survey of Victoria, (1997). 1:250000 Geological Map Series, Melbourne Sheet, Second Edition.
- [292] Zou, B. J., (1986). Arsenic in Soil, *Turangxue Jinzhan*, 14 (2), 8.
- [293] Cannon, H. L., (1978). Report of the workshop at South Seas Plantation, Captiva Island, Florida, *Geochemistry and the Environment*, 3, 17-31.
- [294] McGrath, S. P. and Loveland, P. J., (1992). *The Soil Geochemical Atlas of England and Wales*, Blackie Academic and Professional, London.
- [295] Adriano, D. C., (1986). *Trace Elements in the Terrestrial Environment*, Springer-Verlag, New York.
- [296] Kabata-Pendias, A. K. and Pendias, H., (1984). *Trace Elements in Soils and Plants*, CRC Press, Inc. Boca Taton, Florida.
- [297] Cox, D. P., (1979). In: *Copper in the Environment, Part I: Ecological Cycling*, Ed. Nriagu, J. O., Wiley, New York, pp. 19-42.
- [298] Baker, D. E. and Senft, J. P., (1995). Copper, Chapter 8, In: *Heavy Metals in Soils*, Ed. Alloway, B. J., Blackie Academic & Professional, London, pp. 179-205.
- [299] McBride, M. B., (1981). In: *Copper in Soils and Plants*, Ed. Loneragan, J. F.,

- Robson, A. D. and Graham, R. D., Academic Press, New York, , pp. 25-45.
- [300] Davies, B. E., (1995). Lead, Chapter 9, In: Heavy Metals in Soils, Ed. Alloway, B. J., Blackie Academic & Professional, London, pp. 206-223.
- [301] Nriagu, J. O., (1978). In: The Biogeochemistry of Lead, Ed. Nriagu, J. O., Elsevier Biomedical Press, Amsterdam, pp. 18-88.
- [302] Ure, A. M. and Berrow, M. L., (1982). In: Environmental Chemistry, Vol. 2, Chapter 3, Royal Society of Chemistry, London.
- [303] Berrow, M. L. and Reaves, G. A., (1986), Total chromium and nickel contents of Scottish soils, *Geoderma*, 37, 15-27.
- [304] Kiekens, L, (1995). Zinc, Chapter 13, In: Heavy Metals in Soils, Ed. Alloway, B. J., Blackie Academic & Professional, London, pp. 284-305.
- [305] Rayment, G. E. and Higginson, F. R., (1992). Australian Laboratory Handbook of Soil and Water Chemical Company Methods. Soil pH, Reed International Books Australia Ltd, Melbourne, Australia, pp. 17-23.
- [306] Preparation and Determination of Moisture Content in Soils (1998). National Measurement Institute (NMI), Method VL237, Issue 2.
- [307] Rayment, G. E. and Higginson, F. R., (1992). Australian Laboratory Handbook of Soil and Water Chemical Company Methods. Organic carbon, Reed International Books Australia Ltd, Melbourne, Australia, pp. 29-37.
- [308] Hartsock, N. J., Mueller, T. G., Thomas, G. W., Barnhisel, R. I., Wells, K. L. and Shearer, S.A., (2000). Soil Electrical Conductivity Variability. In. P.C. Robert et al. (ed.) Proc. 5th international conference on precision Agriculture. ASA Misc. Publ., ASA, CSSA, and SSSA, Madison, WI.

- [309] McNeill, J. D., (1980). Electrical conductivity of soils and rocks (Geonics Ltd., Mississauga, Ontario, Canada, Technical Note TN-5). In: Precision Agriculture, 5, 389-409.
- [310] FitzPatrick, E. A., (1980), Soils. Their formation, classification and distribution, Chapter 4, Longman Inc., New York.
- [311] Domsch, H. and Giebel, A. (2004). Estimation of Soil Textural Features from Soil Electrical Conductivity Recorded Using the EM38, Precision Agriculture, 5, 389–409
- [312] Sabhapondit, A., Borthakur, A. and Haque, I., (2003). Adsorption behaviour of Poly(n,N-dimethylacrylamide-co-Na 2-acrylamido-2-methylpropanesulfonate) on sand surface, J. Appl. Polym. Sci., 91, 2482.
- [313] Gupta, G. S., Prasad, G. and Singh, V. N., (1988). Removal of chrome dye from carpet effluents using coal. II, Environ. Technol. Lett., 9, 1413-1422.
- [314] Manning, B. A., and Goldberg, S., (1997). Arsenic(III) and Arsenic (V) Adsorption on three California Soils, Soil Sci., 162 (12), 886-895.
- [315] Elkhatib, E. A., Bennett, O. L. and Wright, R. J., (1984). Arsenite sorption and desorption in soils, Soil Sci. Soc. Am. J., 48, 1025-1030.
- [316] Livesey, N. T. and Huang, P. M., (1981). Adsorption of arsenate by soils and its relation to selected chemical properties and anions, Soil. Sci., 131, 88-94.
- [317] Fordham, A. W., and Norrish, K., (1979). Arsenate-73 uptake by components of several acid soils and its implications for phosphate retention, Aust. J. Soil Res., 17, 307-316.
- [318] Jacobs L. W., Syers, J. K. and Keeney, D. R., (1970). Arsenic sorption by soils, Soil Sci. Soc. Am. Proc., 34, 750-754.

- [319] Fordham, A. W. and Norrish, K., (1974). Direct measurement of the composition of soil components which retain added arsenate, *Aust. J. Soil Res.*, 12, 165-172.
- [320] Grossl, P. R., Eick, M., Sparks, D. L., Goldberg, S. and Ainsworth, C. C., (1997). Arsenate and Chromate Retention Mechanisms on Goethite. 2. Kinetic Evaluation Using A pressure – Jump Relaxation Technique, *Environ. Sci. Technol.*, 31, 321-326.
- [321] Sun, X. and Doner, H. E., (1996). An investigation of arsenate and arsenite bonding structures on goethite by FTIR, *Soil Sci.*, 161, 865-872.
- [322] Waychunas, G. A., Rea, B. A., Fuller, C. C. and Davis, J. A., (1993). Surface chemistry of ferrihydrite: Part 1. EXAFS studies of the geometry of coprecipitated and adsorbed arsenate, *Geochim. Cosmochim. Acta*, 57, 2251-2269.
- [323] Lumsdon, D. G., Fraser, A. R., Russell, J. D. and Livesey, N. T., (1984). New infrared band assignments for the arsenate ion adsorbed on synthetic goethite ($[\alpha]$ -FeOOH), *J. Soil Sci.*, 35, 381-386.
- [324] Parfitt, R. L., Russell, J. D. and Farmer, V. C., (1976). Confirmation of the surface structures of goethite ($[\alpha]$ -FeOOH) and phosphated goethite by infrared spectroscopy, *J. Chem. Soc. Faraday Trans. I*, 172, 1082-1087.
- [325] Manceau, A., (1995). *Geochim. Cosmochim. Acta*, 59, 3647-3653.
- [326] Fendorf, S. E., Eick, M. J., Grossl, P. and Sparks D. L., (1997). Arsenate and chromate retention mechanisms on goethite. 1. Surface structure. *Environ. Sci. Technol.*, 31, 315-320.
- [327] Willett I. R., Chartres, C. J. and Nguyen, T. T., (1988). *J. Soil Sci.*, 39, 275-282.
- [328] Prasad, G. (1994), Removal of Arsenic(V) from Aqueous Systems by Adsorption onto some Geological Materials, In: *Arsenic in the Environment*,

Part 1, Ed. Nriagu. J., Wiley, New York, pp. 133-154.

- [329] Smith, E., Naidu, R. and Alston, A. M., (1999). Chemistry of Arsenic in Soils: I. Sorption of Arsenate and Arsenite by Four Australian Soils, *J. Environ. Qual.*, 28, 1719-1726.
- [330] Pierce, M. L. and Moore, C. B., (1980). Adsorption of arsenite and arsenate on amorphous iron hydroxide from dilute aqueous solutions, *Environ. Sci. Technol.*, 14, 214-216.
- [331] Davis, A., Ruby, M. V., Bloom M., Schoof, R., Freeman, G. and Bergstrom, P. D., (1996). Mineralogic Constraints on the Bioavailability of Arsenic in Smelter-Impacted Soils, *Environ. Sci. Technol.*, 30, 932-399.
- [332] Cotton, F. A. and Wilkinson, G., (1988). *Advanced Inorganic Chemistry*, 5th Ed., Wiley, Canada.
- [333] Ledman, D. W., and Fox, R. O., (1997). Water Cluster Calibration Reduces Mass Error in Electrospray Ionization Mass Spectrometry of Proteins, *J. Am. Soc. Mass Spectrom.*, 8, 1158-1164.
- [334] Konig, S. and Fales, H. M., (1998). Formation and Decomposition of Water Clusters as Observed in a Triple Quadrupole Mass Spectrometer, *J. Am. Soc. Mass Spectrom.*, 9, 814-822.
- [335] Chowdhury, S. K. and Chait, B. T., (1991). Method for the Electrospray Ionization of Highly Conductive Aqueous Solutions, *Anal. Chem.*, 63 (15), 1660-1664.
- [336] Wei, S., Shi, Z. and Castleman, A. W. (Jr), (1991). Mixed Cluster Ions as Structure Probe: Experimental Evidence for Clathrate Structure of $(\text{H}_2\text{O})_{20}\text{H}^+$ and $(\text{H}_2\text{O})_{21}\text{H}^+$, *J. Chem. Phys.* 94 (4), 3268-3270.
- [337] Nagashima, U., Shinohara, H., Nishi, N. and Tanaka, H., (1985). Enhanced Stability of Ion-clathrate Structures for Magic Number Water Cluster, *J. Chem.*

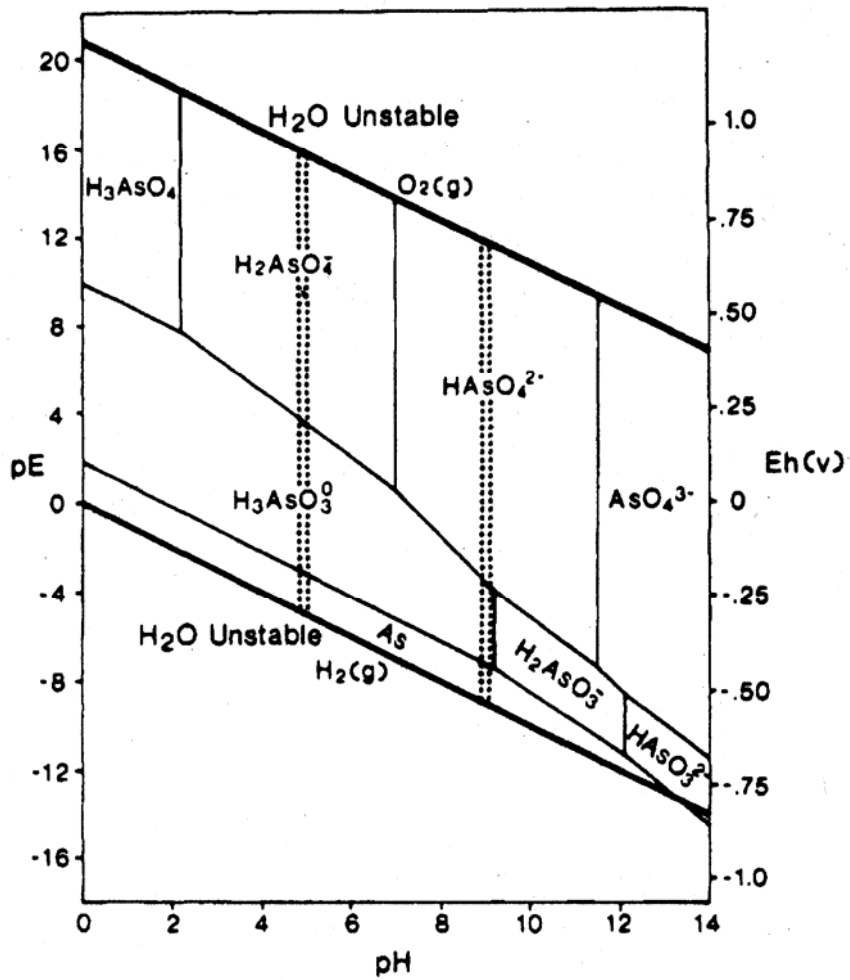
Phys. 84 (1), 209-214.

- [338] Lau, Y. K., Ikuta, S. and Kebarle, P., (1982). Thermodynamics and Kinetics of the Gas-Phase Reactions: $\text{H}_3\text{O}^+(\text{H}_2\text{O})_{n-1} + \text{H}_2\text{O} = \text{H}_3\text{O}^+(\text{H}_2\text{O})_n$, J. Am. Chem. Soc. 104, 1462-1469.
- [339] Florncio, M. H., Duarte, M. F., De Bettencourt, A. M. M., Gomes, M. L. and Vilas Boas, L. F., (1997). Electrospray Mass Spectra of Arsenic Compounds, Rapid Commun. Mass Spectrom., 11, 469-473.
- [340] Driehaus, W., Seith, R. and Jekel, M., (1995). Oxidation of Arsenate(III) with Manganese Oxides in Water Treatment, Wat. Res., 29 (1), 297-305.
- [341] Ross, A. R. S, Ikonomou, M. G., Thompson, J. A. J and Orians, K. J., (1998), Determination of Dissolved Metal Species by Electrospray Ionization Mass Spectrometry, Anal. Chem., 70, 2225.
- [342] Baur, W. H. and Khan, A. A., (1970). On the Crystal Chemistry of Salt Hydrates. VI. The Crystal Structures of Disodium Hydrogen Orthoarsenate Heptahydrate and of Disodium Hydrogen Orthophosphate Heptahydrate, Acta Cryst., B26, 1548-1596.
- [343] Ratajczak, H., Barycki, J., Pietraszko, A, Baran, J., Debrus, S., May, M. and Venturini, J., (2000). Preparation and structural study of a novel nonlinear molecular material: the L-histidinium dihydrogenarsenate orthophosphate acid crystal, J. Mol. Struct., 526, 269-278.
- [344] Cotton, F. A. and Wilkinson, G., (1966). Advanced Inorganic Chemistry: A Comprehensive Text, 2nd Ed., John Wiley & Sons, United States of America, pp. 105.
- [345] Sokolov, M. N., Virovets, A. V., Dybtsev, D. N., Chubarova, E. V., Fedin, V. P. and Fenske, D., (2001). Phosphorus acid and arsenious acid ligands, Inorg. Chem., 40, 4816-4817.

- [346] Fleming, I., (1976). *Frontier Orbitals and Organic Chemical Reactions*, Chapter 2 – Molecular Orbitals and Frontier Orbitals, John Wiley & Sons, London, pp 5-32.
- [347] Yuriev, E. and Orbell, J. D., (1996). Modelling Steric Effects in DNA-Binding Platinum(II)-am(m)ine Complexes, *J. Cmput. -Aided Mol. Des.*, 10, 589-606.
- [348] Oscarson, D. W., Huang, P. M. and Liaw, W. K., (1980). The oxidation of arsenite by aquatic sediment. *J. Environ. Qual.*, 9, 700-703.
- [349] Scott, M. J., (1991). Kinetics of adsorption and redox processes on iron and manganese oxides: Reactions of As(III) and Se(IV) at goethite and birnessite surfaces. Environmental Quality Laboratory. EQL Report No. 33. California Institute of Technology, Pasadena, CA.
- [350] Tallman, D. E., and Shaikh, A. U., (1980). Redox stability of inorganic arsenic(III) and arsenic(V) in aqueous solution. *Anal. Chem.*, 52, 196-199.
- [351] Eary, L. E., and Schramke, J. A., (1990). Rates of inorganic oxidation reactions involving dissolved oxygen. In: *Chemical modeling of aqueous systems II*. D. C. Ed. Melchior and R. L. Basset, ACS Symp. Ser. 416, 379-396.
- [352] Moore, J. N., Walker, J. R. and Hayes, T. H., (1990). Reaction scheme for the oxidation of As(III) to As(V) by birnessite. *Clays Clay Miner.*, 38, 549-555.
- [353] Scott, M. J., and Morgan, J. J., (1995). Reactions at oxide surface. 1. Oxidation of As(III) by synthetic birnessite. *J. Environ. Qual.*, 29, 1898-1905.
- [354] Anderson, M. A., Ferguson, J. F. and Gavis, J., (1976). Arsenate adsorption on amorphous aluminum hydroxide. *J. Colloid Interface Sci.*, 54, 391-399.
- [355] Manning, B. A. and Goldberg, S., (1996). Modeling competitive adsorption of arsenate with phosphate and molybdate on oxide minerals. *Soil Sci. Soc. Am J.*, 60, 121-131.

- [356] Hiemstra, T. and Van Riemsdijk, W. H., (1999). Surface structural adsorption modeling of competitive binding of oxyanions by metal (hydr)oxides. *J. Colloid Interface Sci.*, 210, 182-193.
- [357] Cummings, D. E., Caccavo, F., Fendorf, S. and Rosenzweig, R. F., (1999). Arsenic mobilization by the dissimilatory Fe(III)-reducing bacterium *Shewanella* alga BrY. *Environ. Sci. Technol.*, 33, 723-729.
- [358] Nickson, R. T., McArthur, J. M., Ravenscroft, P., Burgess, W. G. and Ahmed, K. M., (2000). Mechanism of arsenic release to groundwater, Bangladesh and West Bengal. *Appl. Geochem.*, 15, 403-413.
- [359] Zobrist, J., Dowdle, P. R., Davis, J. A. and Oremland, R. S., (2000). Mobilization of arsenite by dissimilatory reduction of adsorbed arsenate. *Environ. Sci. Technol.*, 34, 4747-4753.
- [360] Nickson, R., McArthur, J., Burgess, W., Ahmed, K. M., Ravenscroft, P. and Rahman, M., (1998). Arsenic poisoning of Bangladesh groundwater. *Nature*, 395, 338.
- [361] Acharyya, S. K., Chakraborty, P., Lahiri, S., Raymahashay, B. C., Guha, S. and Bhowmik, A., (1999). Arsenic poisoning in the Ganges Delta. *Nature*, 401, 545.
- [362] Langner, H. W. and Inskeep, W. P., (2000). Microbial reduction of arsenate in the presence of ferrihydrite. *Environ. Sci. Technol.*, 34, 3131-3136.

APPENDIX A



Appendix A. A Pourbaix diagram for the As-H₂O system at 25°C. Total dissolved As species set at 50 ppb. The area within the vertical bars represents the common pE-pH domains for natural water [28].

APPENDIX B

Appendix B. A statistical summary for inorganic background soil quality data within Geological Groups.

	Qpw Arsenic	Qpw Cadmium	Qpw Chromium	Qpw Copper	Qpw Lead	Qpw Mercury	Qpw Nickel	Qpw Zinc	Qpy Antimony	Qpy Arsenic	Qpy Barium	Qpy Cadmium
Count	14	13	11	14	12	11	12	14	8	12	11	16
Minimum	0.0	0.0	14.0	5.0	9.0	0.0	10.0	16.0	0.0	1.3	9.0	0.0
First Quartile (Q1)	3.5	0.0	22.0	11.0	12.8	0.0	20.5	30.5	0.0	3.0	21.0	0.0
Median (M)	5.0	0.0	30.0	13.5	15.5	0.0	22.5	42.0	0.0	3.8	59.0	0.0
Third Quartile (Q3)	7.8	0.0	34.0	25.3	20.0	0.0	27.5	62.8	0.0	4.6	84.0	0.0
Maximum	12.0	0.0	49.0	35.0	25.0	0.1	49.0	86.0	0.0	6.1	114.0	0.0
IQR = Q3 - Q1 =	4.3	0.0	12.0	14.3	7.3	0.0	7.0	32.3	0.0	1.6	63.0	0.0
1.5 x IQR =	6.5	0.0	18.0	21.4	10.9	0.1	10.5	48.4	0.0	2.3	94.5	0.0
Outliers Q3+1.5IQR	14.2	0.0	52.0	46.6	30.9	0.1	38.0	111.1	0.0	6.9	178.5	0.0
Mean	5.29	0.00	28.91	17.79	16.42	0.02	25.25	46.00	0.00	3.78	56.55	0.00
St Dev	3.67	0.00	10.43	10.20	5.25	0.03	10.58	22.01	0.00	1.26	37.21	0.00
t Value (n - 1)	2.160	2.179	2.228	2.160	2.201	2.228	2.201	2.160	2.365	2.201	2.228	2.131
95th Percentile	7.41	0.00	35.91	23.67	19.75	0.04	31.97	58.70	0.00	4.59	81.54	0.00

Appendix B (Cont...). A statistical summary for inorganic background soil quality data within Geological Groups.

	Qpy Chromium	Qpy Copper	Qpy Lead	Qpy Mercury	Qpy Nickel	Qpy Soil pH	Qpy Tin	Qpy Zinc	Qrc Arsenic	Qrc Cadmium	Qrc Chromium	Qrc Copper	Qrc Lead
Count	20	20	19	16	18	9	9	16	11	11	9	11	10
Minimum	5.9	0.0	2.0	0.0	4.0	3.2	0.0	3.0	0.0	0.0	32.0	7.4	0.0
First Quartile (Q1)	18.0	6.5	6.5	0.0	22.3	6.4	0.0	16.8	0.0	0.0	46.0	13.5	5.0
Median (M)	31.0	9.0	10.0	0.0	27.5	7.7	0.0	31.5	0.0	0.0	51.0	18.0	6.3
Third Quartile (Q3)	49.3	14.5	15.0	0.0	37.3	8.3	0.0	37.0	3.8	0.0	55.0	22.0	8.8
Maximum	66.0	26.0	30.0	0.1	42.0	9.3	0.0	66.0	9.0	0.0	66.0	32.0	15.0
IQR = Q3 - Q1 =	31.3	8.1	8.5	0.0	15.0	1.9	0.0	20.3	3.8	0.0	9.0	8.5	3.8
1.5 x IQR =	46.9	12.1	12.8	0.0	22.5	2.9	0.0	30.4	5.6	0.0	13.5	12.8	5.6
Outliers Q3+1.5IQR	96.1	26.6	27.8	0.1	59.8	11.2	0.0	67.4	9.4	0.0	68.5	34.8	14.4
Mean	33.94	11.18	12.66	0.02	28.06	7.08	0.00	28.94	2.22	0.00	50.89	18.04	6.79
St Dev	19.92	7.01	8.17	0.03	11.22	1.89	0.00	16.83	2.98	0.00	9.73	7.02	4.29
t Value (n - 1)	2.093	2.093	2.101	2.131	2.110	2.306	2.306	2.131	2.228	2.228	2.306	2.228	2.262
95th Percentile	43.26	14.46	16.60	0.03	33.63	8.53	0.00	37.90	4.22	0.00	58.37	22.75	9.86

Appendix B (Cont...). A statistical summary for inorganic background soil quality data within Geological Groups.

	Qrc Mercury	Qrc Nickel	Qrc Soil pH	Qrc Tin	Qrc Zinc	Qrm Arsenic	Qrm Copper	Qrm Lead	Qrm Zinc	Qvn Antimony	Qvn Arsenic	Qvn Barium	Qvn Beryllium
Count	7	11	11	10	10	10	12	12	11	51	142	73	47
Minimum	0.0	17.0	6.6	0.0	12.0	0.0	0.0	0.0	15.0	0.0	0.0	7.5	0.0
First Quartile (Q1)	0.0	34.5	7.9	0.0	15.5	0.3	11.3	10.8	19.0	0.0	0.0	57.0	0.0
Median (M)	0.0	40.0	8.6	0.0	26.5	3.0	14.0	13.0	29.0	0.0	0.0	170.0	0.0
Third Quartile (Q3)	0.0	55.5	9.2	0.0	32.0	5.8	23.8	67.3	65.0	0.0	0.0	360.0	0.0
Maximum	0.0	78.0	9.4	0.0	51.0	10.0	40.0	110.0	190.0	0.0	0.5	760.0	0.0
IQR = Q3 - Q1 =	0.0	21.0	1.3	0.0	16.5	5.5	12.5	56.5	46.0	0.0	0.0	303.0	0.0
1.5 x IQR =	0.0	31.5	1.9	0.0	24.8	8.3	18.8	84.8	69.0	0.0	0.0	454.5	0.0
Outliers Q3+1.5IQR	0.0	87.0	11.0	0.0	56.8	14.0	42.5	152.0	134.0	0.0	0.0	814.5	0.0
Mean	0.00	44.73	8.45	0.00	26.20	3.50	18.33	37.47	57.82	0.00	0.01	231.03	0.00
St Dev	0.00	17.28	0.88	0.00	12.12	3.57	12.24	42.29	62.33	0.00	0.05	197.04	0.00
t Value (n - 1)	2.447	2.228	2.228	2.262	2.262	2.262	2.201	2.201	2.228	2.009	1.983	1.994	2.014
95th Percentile	0.00	56.34	9.04	0.00	34.87	6.05	26.11	64.34	99.69	0.00	0.02	277.01	0.00

Appendix B (Cont...). A statistical summary for inorganic background soil quality data within Geological Groups.

	Qvn Boron	Qvn Cadmium	Qvn Chromium	Qvn Cobalt	Qvn Copper	Qvn Lead	Qvn Manganese	Qvn Mercury	Qvn Molybdenum	Qvn Nickel	Qvn Selenium
Count	13	185	191	105	200	189	15	117	43	174	54
Minimum	0.0	0.0	7.3	0.0	0.0	0.0	0.0	0.0	0.0	0.0	0.0
First Quartile (Q1)	0.0	0.0	24.5	11.0	7.7	7.4	122.0	0.0	0.0	14.0	0.0
Median (M)	0.0	0.0	34.0	16.0	11.0	11.0	260.0	0.0	0.0	21.0	0.0
Third Quartile (Q3)	8.0	0.0	42.5	20.0	16.0	15.0	405.0	0.0	0.0	32.0	0.0
Maximum	19.0	0.0	73.0	30.0	28.0	28.0	560.0	0.0	0.0	62.0	0.0
IQR = Q3 - Q1 =	8.0	0.0	18.0	9.0	8.3	7.6	283.0	0.0	0.0	18.0	0.0
1.5 x IQR =	12.0	0.0	27.0	13.5	12.5	11.4	424.5	0.0	0.0	27.0	0.0
Outliers Q3+1.5IQR	20.0	0.0	69.5	33.5	28.5	26.4	829.5	0.0	0.0	59.0	0.0
Mean	4.19	0.00	35.02	15.26	11.75	11.35	260.67	0.00	0.00	23.24	0.00
St Dev	6.92	0.00	14.47	6.69	6.17	6.34	190.67	0.00	0.00	12.91	0.00
t Value (n - 1)	2.179	1.982	1.982	1.984	1.982	1.982	2.145	1.984	2.019	1.982	2.006
95th Percentile	8.37	0.00	37.09	16.55	12.61	12.26	366.27	0.00	0.00	25.18	0.00

Appendix B (Cont...). A statistical summary for inorganic background soil quality data within Geological Groups.

	Qvn Soil pH	Qvn Tin	Qvn Zinc	Sla Antimony	Sla Arsenic	Sla Cadmium	Sla Chromium	Sla Copper	Sla Lead	Sla Manganese	Sla Mercury	Sla Nickel
Count	124	67	199	11	40	23	45	43	27	9	22	38
Minimum	6.2	0.0	0.0	0.0	0.0	0.0	6.2	0.0	0.0	17.0	0.0	0.0
First Quartile (Q1)	7.6	0.0	12.0	0.0	0.0	0.0	18.0	5.7	10.0	20.0	0.0	6.9
Median (M)	8.3	0.0	21.0	0.0	6.4	0.0	38.0	9.6	14.0	23.0	0.0	14.0
Third Quartile (Q3)	8.9	0.0	37.0	9.4	9.7	0.0	62.0	16.5	39.0	25.0	0.0	19.5
Maximum	9.9	0.0	73.0	11.0	21.0	0.0	89.0	32.0	73.0	30.0	0.0	32.0
IQR = Q3 - Q1 =	1.3	0.0	25.0	9.4	9.7	0.0	44.0	10.9	29.0	5.0	0.0	12.7
1.5 x IQR =	2.0	0.0	37.5	14.1	14.5	0.0	66.0	16.3	43.5	7.5	0.0	19.0
Outliers Q3+1.5IQR	10.9	0.0	74.5	23.5	24.1	0.0	128.0	32.8	82.5	32.5	0.0	38.5
Mean	8.17	0.00	24.36	3.80	6.88	0.00	40.41	10.93	23.35	22.78	0.00	13.31
St Dev	0.89	0.00	15.46	4.93	6.08	0.00	25.40	8.48	19.72	3.99	0.00	8.42
t Value (n - 1)	1.983	1.997	1.982	2.228	2.023	2.074	2.016	2.019	2.056	2.306	2.080	2.027
95th Percentile	8.33	0.00	26.54	7.11	8.83	0.00	48.04	13.54	31.16	25.85	0.00	16.08

Appendix B (Cont...). A statistical summary for inorganic background soil quality data within Geological Groups.

	Sla Soil pH	Sla Zinc	Sud Arsenic	Sud Cadmium	Sud Chromium	Sud Copper	Sud Lead	Sud Mercury	Sud Nickel	Sud Zinc	Tpb Arsenic	Tpb Cadmium
Count	8	39	25	19	25	25	21	13	15	23	14	12
Minimum	5.2	6.4	0.0	0.0	9.1	0.0	9.0	0.0	3.0	9.0	0.0	0.0
First Quartile (Q1)	5.4	16.0	3.1	0.0	22.0	9.6	13.0	0.0	9.2	23.0	0.7	0.0
Median (M)	5.8	21.0	6.0	0.0	36.0	18.0	20.0	0.0	15.0	29.0	4.4	0.0
Third Quartile (Q3)	5.9	39.0	14.0	0.0	52.0	27.0	25.0	0.1	23.5	47.0	6.5	0.0
Maximum	6.0	61.0	20.0	0.0	66.0	50.0	52.0	0.2	35.0	86.0	15.0	0.0
IQR = Q3 - Q1 =	0.5	23.0	10.9	0.0	30.0	17.4	12.0	0.1	14.3	24.0	5.8	0.0
1.5 x IQR =	0.8	34.5	16.4	0.0	45.0	26.1	18.0	0.1	21.5	36.0	8.7	0.0
Outliers Q3+1.5IQR	6.7	73.5	30.4	0.0	97.0	53.1	43.0	0.2	45.0	83.0	15.2	0.0
Mean	5.65	26.98	8.57	0.00	36.20	19.12	22.14	0.05	16.96	37.25	4.86	0.00
St Dev	0.31	15.00	6.96	0.00	17.76	12.39	11.03	0.07	10.23	23.04	4.63	0.00
t Value (n - 1)	2.365	2.025	2.064	2.101	2.064	2.064	2.086	2.179	2.145	2.074	2.160	2.201
95th Percentile	5.91	31.85	11.45	0.00	43.53	24.24	27.16	0.08	22.62	47.22	7.54	0.00

Appendix B (Cont...). A statistical summary for inorganic background soil quality data within Geological Groups.

	Tpb Chromium	Tpb Copper	Tpb Lead	Tpb Mercury	Tpb Nickel	Tpb Zinc	Tvo Arsenic	Tvo Chromium	Tvo Copper	Tvo Mercury	Tvo Nickel	Tvo Zinc
Count	16	14	13	10	10	12	7	7	8	8	8	6
Minimum	0.0	0.0	0.0	0.0	0.0	12.0	0.0	30.0	0.0	0.0	24.0	15.0
First Quartile (Q1)	8.8	1.5	10.0	0.0	8.1	17.5	2.4	34.0	0.0	0.0	31.3	16.5
Median (M)	31.0	9.4	12.0	0.0	12.7	37.0	2.6	40.0	3.0	0.0	34.0	19.0
Third Quartile (Q3)	38.0	17.8	55.0	0.1	24.8	61.5	2.8	40.0	13.4	0.0	39.0	23.0
Maximum	56.0	32.0	93.0	0.2	43.0	110.0	4.0	59.0	28.0	0.0	42.0	26.0
IQR = Q3 - Q1 =	29.2	16.2	45.0	0.1	16.7	44.0	0.5	6.0	13.4	0.0	7.8	6.5
1.5 x IQR =	43.8	24.3	67.5	0.2	25.1	66.0	0.7	9.0	20.1	0.0	11.6	9.8
Outliers Q3+1.5IQR	81.8	42.1	122.5	0.3	49.8	127.5	3.5	49.0	33.5	0.0	50.6	32.8
Mean	25.99	10.74	30.54	0.06	17.01	46.25	2.41	39.57	8.64	0.00	34.13	19.83
St Dev	17.44	9.62	31.56	0.07	13.29	35.61	1.21	9.43	11.85	0.00	6.66	4.40
t Value (n - 1)	2.131	2.160	2.179	2.262	2.262	2.201	2.447	2.447	2.365	2.365	2.365	2.571
95th Percentile	35.28	16.29	49.61	0.11	26.52	68.88	3.53	48.29	18.54	0.00	39.70	24.45

Notes:

Qpw (also called Qpd) – Quaternary, Pleistocene: Description: Aeolian: Dune deposits: sand, clay, calcareous sand;
 Qpy - Quaternary, Pleistocene (Coode Island Silt): Paludal: lagoon deposits: black silt, clay;
 Qrc – Quaternary, Mostly Holocene: Fluvial: “gully” alluvium, colluvium: gravel, sand, silt;
 Qrm – Quaternary, Mostly Holocene: Paludal: lagoon and swamp deposits: silt, clay;
 Qvn – Quaternary/Tertiary, Holocene to Pliocene (Newer Volcanics): Extrusive: tholeiitic to alkaline basalts, minor scoria and ash;
 Sla – Silurian, Lower (Anderson Creek Formation): Marine: sandstone, thick to thin bedded, siltstone, minor conglomerate;
 Sud – Silurian, Upper (Dargile Formation): Marine: siltstone, thick bedded, sandstone;
 Tpb – Tertiary, Pliocene to Miocene (Brighton Group): Fluvial: gravel, sand, silt;
 Tvo – Tertiary, Eocene to Oligocene (Older Volcanics): Extrusive: tholeiitic and minor alkaline basalts.

APPENDIX C

For convenience of comparative viewing a compendium of figures for Figures 4.1 - 4.6 and 4.7 - 4.10 have been presented as Appendix C.

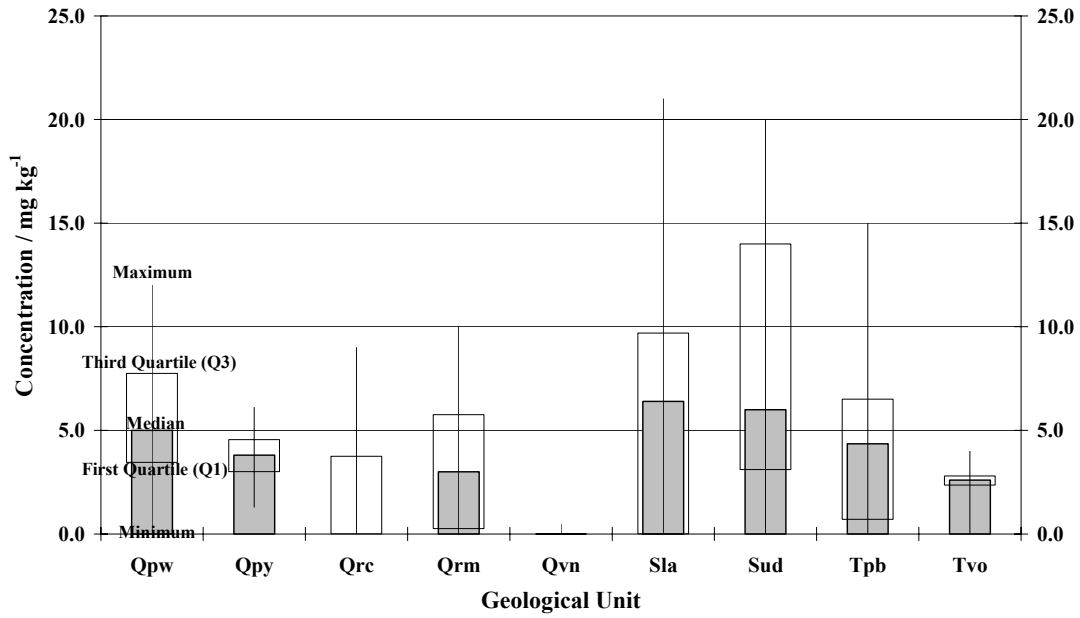


Figure 4.1. Summary statistics for arsenic in various geological units of Melbourne, Australia

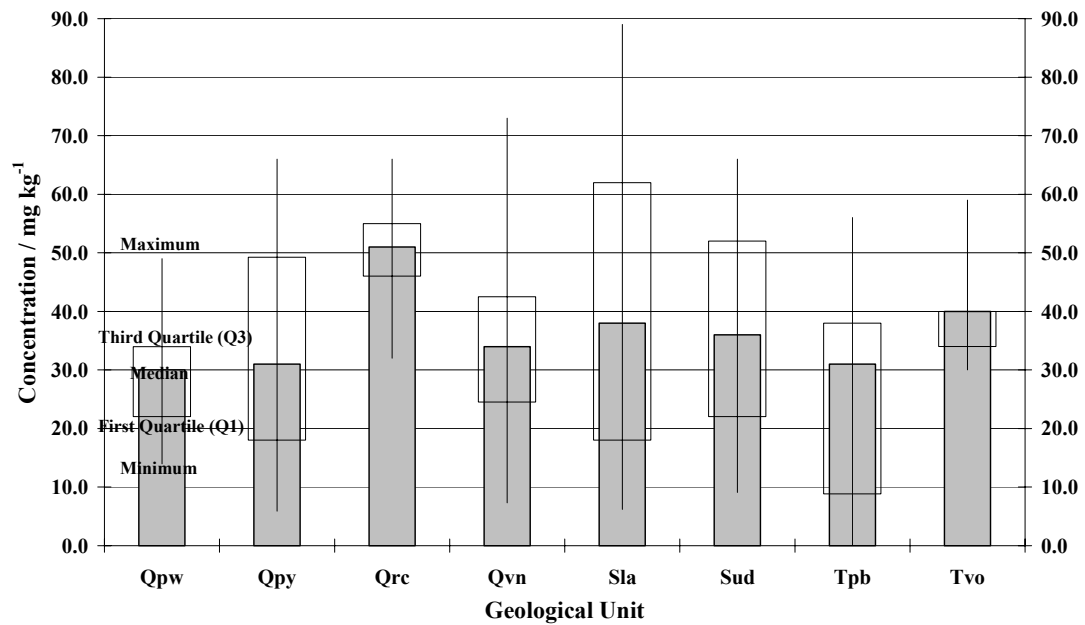


Figure 4.2. Summary statistics for chromium in various geological units of Melbourne, Australia

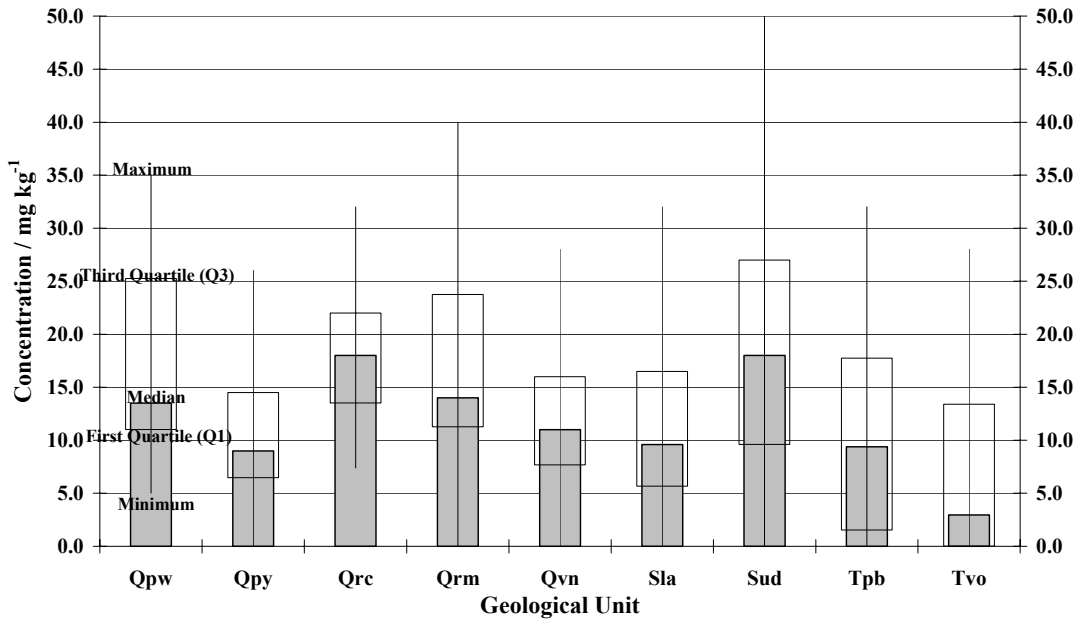


Figure 4.3. Summary statistics for copper in various geological units of Melbourne, Australia

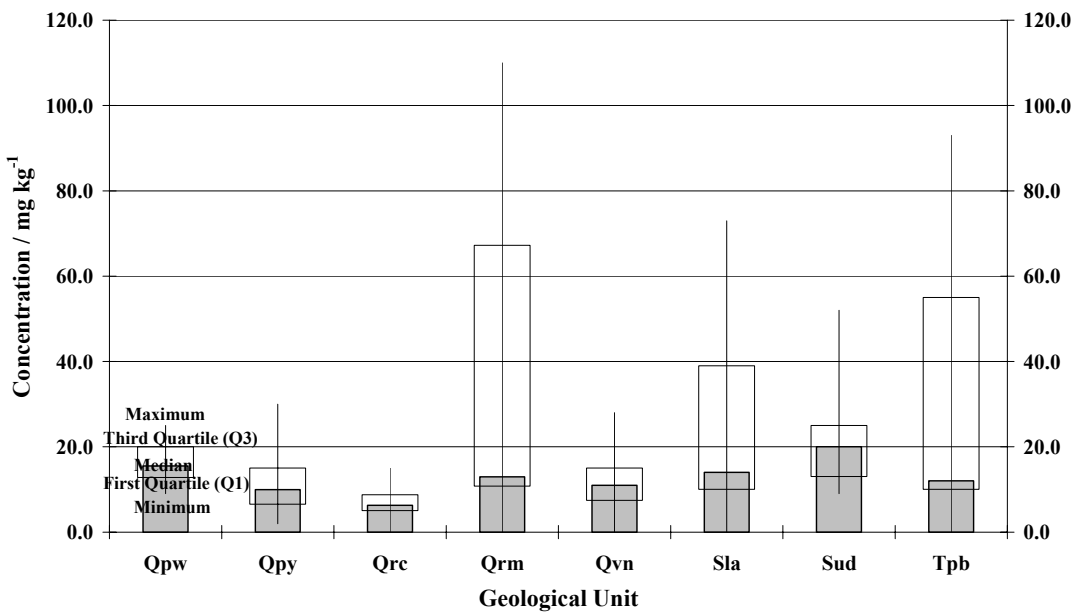


Figure 4.4. Summary statistics for lead in various geological units of Melbourne, Australia

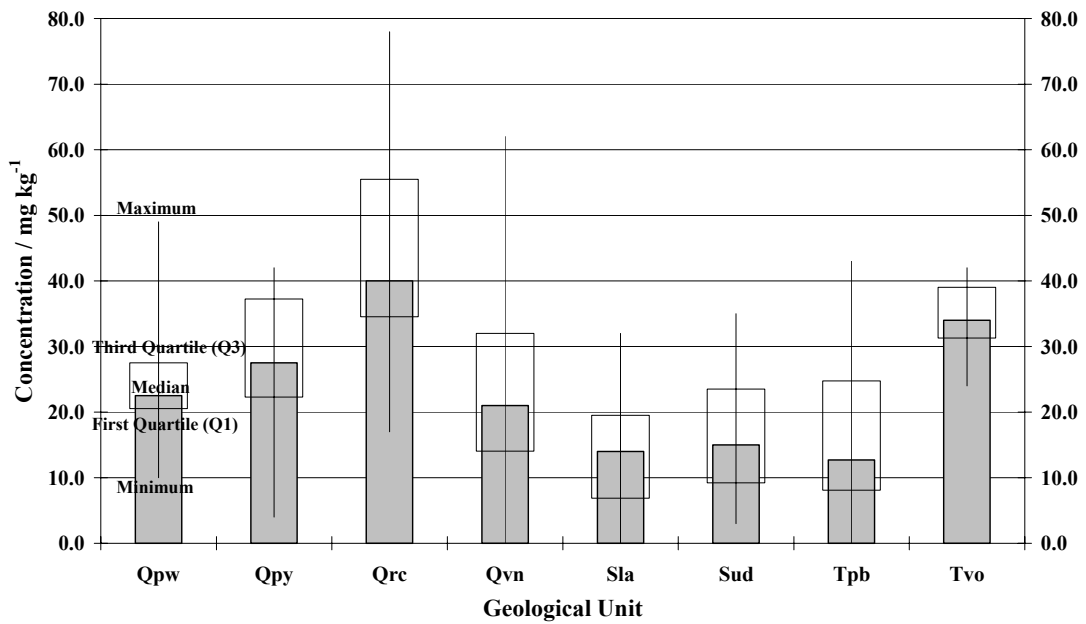


Figure 4.5. Summary statistics for nickel in various geological units of Melbourne, Australia

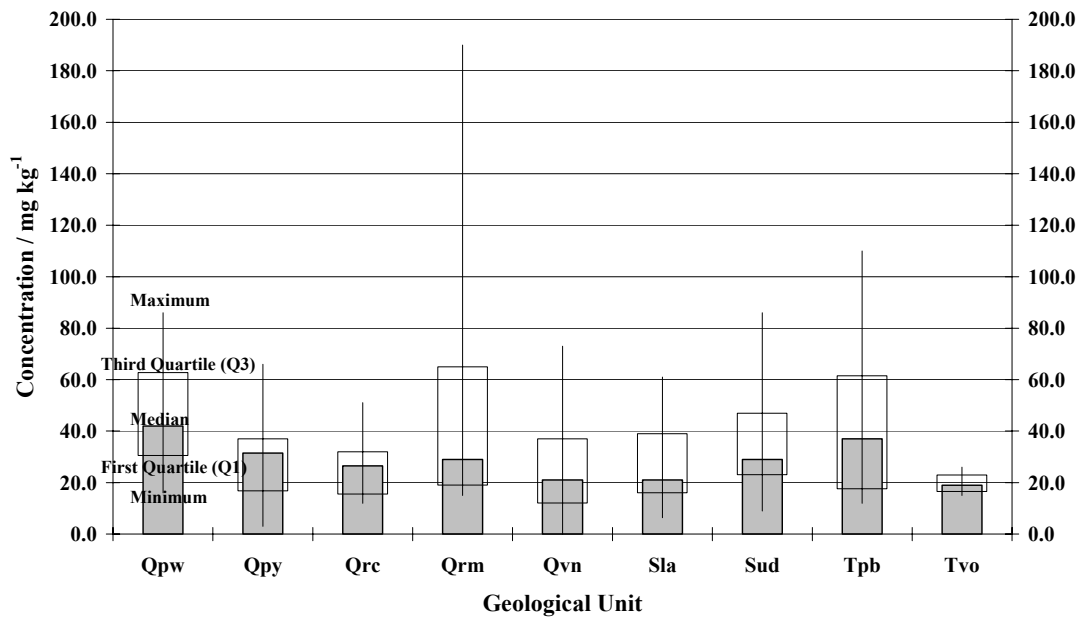


Figure 4.6. Summary statistics for zinc in various geological units of Melbourne, Australia

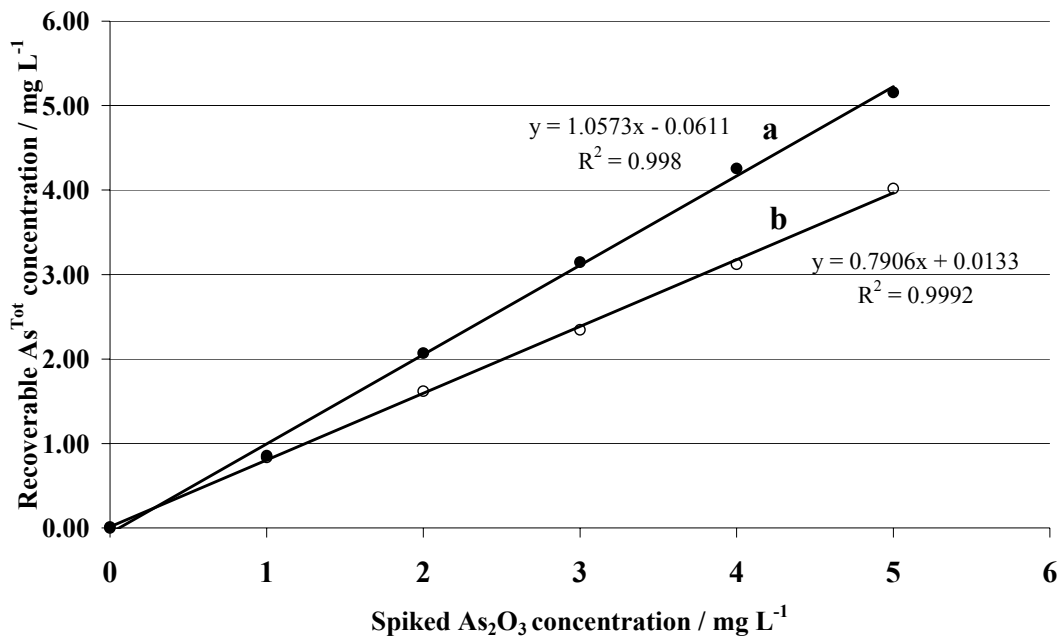


Figure 4.7. Recoverable As^{Tot} in: (a) blank and (b) soil type S1 versus the spiked As_2O_3 concentration (mg L^{-1}). Solid lines are plotted from the regression analysis.

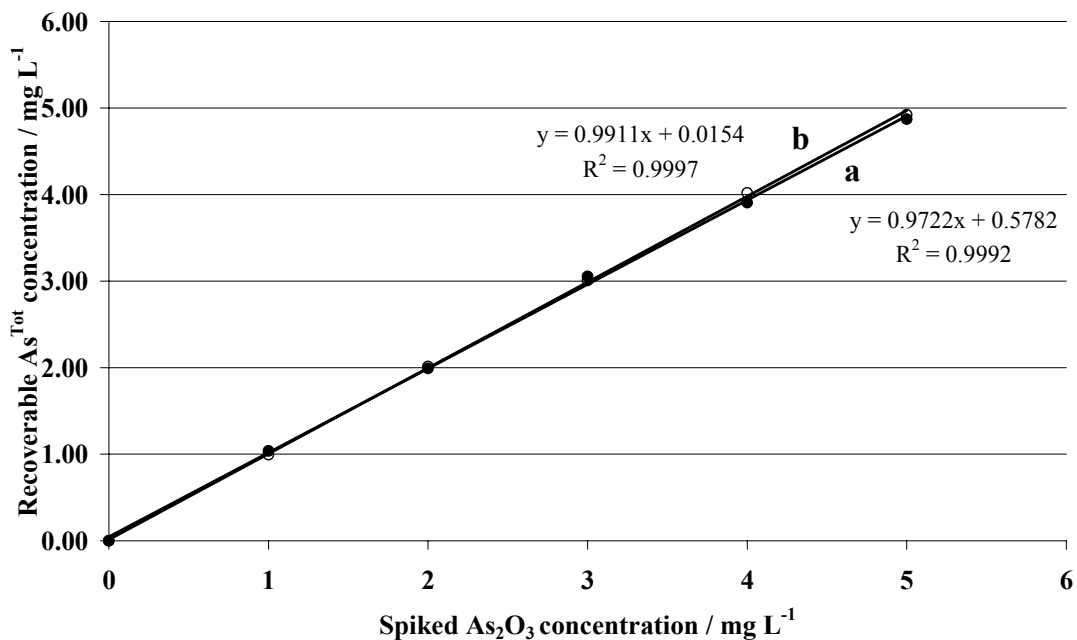


Figure 4.8. Recoverable As^{Tot} in: (a) blank and (b) soil type S2 versus the spiked As_2O_3 concentration (mg L^{-1}). Solid lines are plotted from the regression analysis.

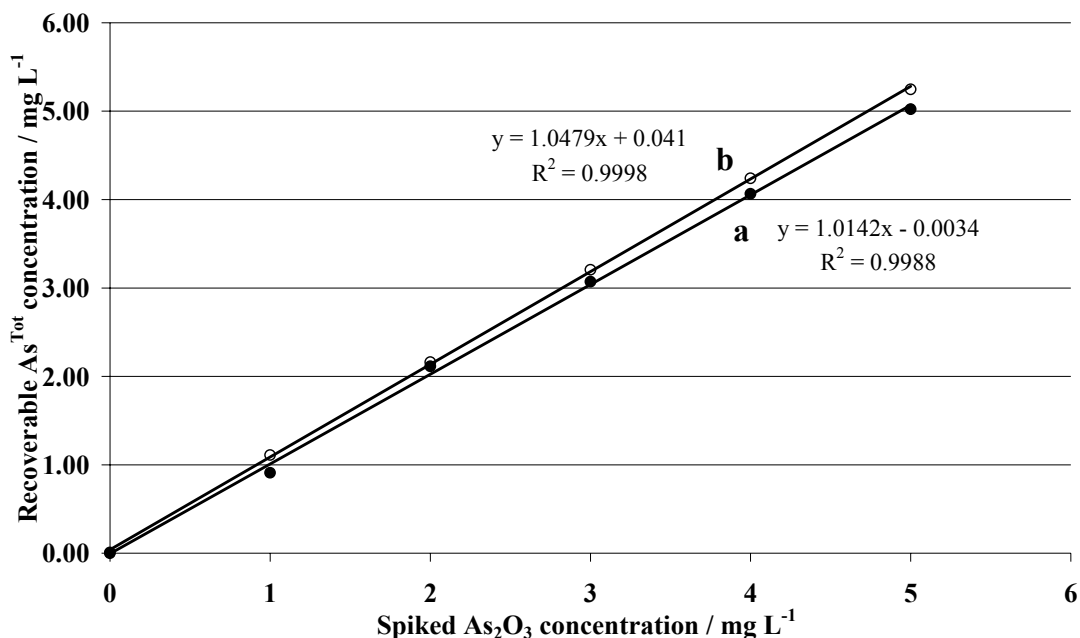


Figure 4.9. Recoverable As^{Tot} in: (a) blank and (b) soil type S3 versus the spiked As_2O_3 concentration (mg L^{-1}). Solid lines are plotted from the regression analysis.

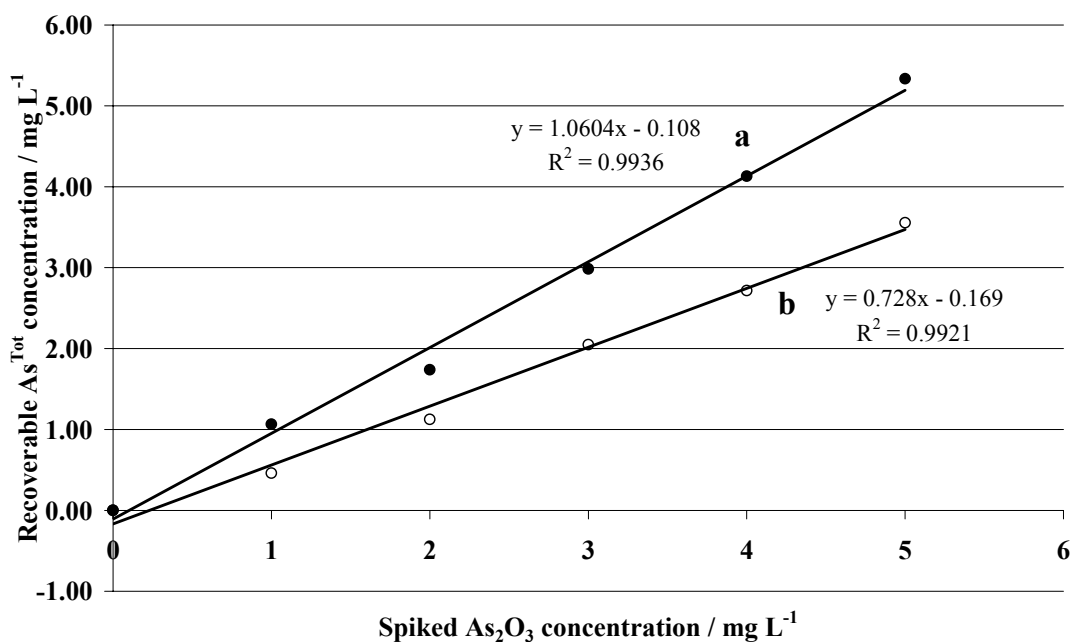


Figure 4.10. Recoverable As^{Tot} in: (a) blank and (b) soil type S4 versus the spiked As_2O_3 concentration (mg L^{-1}). Solid lines are plotted from the regression analysis.